



GESp-519
NASA-CR-72872

**DESIGN AND FABRICATION OF
BRAYTON CYCLE SOLAR HEAT RECEIVER
FINAL REPORT**

Edited by
I. Mendelson

July 1971

prepared for
NATIONAL AERONAUTICS AND SPACE ADMINISTRATION

**NASA Lewis Research Center
Contract NAS 3-10944
H. M. Cameron, Project Manager**

**NUCLEAR SYSTEMS PROGRAM
SPACE SYSTEMS
GENERAL ELECTRIC
CINCINNATI, OHIO 45215**



NOTICE

This report was prepared as an account of Government sponsored work. Neither the United States, nor the National Aeronautics and Space Administration (NASA), nor any person acting on behalf of NASA:

- A.) Makes any warranty or representation, expressed or implied, with respect to the accuracy, completeness, or usefulness of the information contained in this report, or that the use of any information, apparatus, method, or process disclosed in this report may not infringe privately owned rights; or
- B.) Assumes any liabilities with respect to the use of, or for damages resulting from the use of any information, apparatus, method or process disclosed in this report.

As used above, "person acting on behalf of NASA" includes any employee or contractor of NASA, or employee of such contractor, to the extent that such employee or contractor of NASA, or employee of such contractor prepares, disseminates, or provides access to, any information pursuant to his employment or contract with NASA, or his employment with such contractor.

Requests for copies of this report should be referred to:

National Aeronautics and Space Administration
Scientific and Technical Information Division
Attention: USS-A
Washington, D.C. 20546

FINAL REPORT

DESIGN AND FABRICATION OF
BRAYTON CYCLE SOLAR HEAT RECEIVER

Edited by
I. Mendelson

July 1971

NUCLEAR SYSTEMS PROGRAMS
SPACE SYSTEMS
GENERAL ELECTRIC COMPANY
Cincinnati, Ohio 45215

Prepared for
NATIONAL AERONAUTICS AND SPACE ADMINISTRATION

Contract NAS 3-10944

NASA Lewis Research Center
Cleveland, Ohio 44135
H. M. Cameron, Project Manager
Brayton Cycle Branch

ABSTRACT

A detail design and fabrication of a solar heat receiver using lithium fluoride as the heat storage material has been completed. A gas flow analysis was performed to achieve uniform flow distribution within overall pressure drop limitations. Structural analyses and allowable design criteria were developed for anticipated environments such as launch, pressure containment and thermal cycling. A complete heat receiver assembly was fabricated almost entirely from the refractory alloy, columbium-1% zirconium.

FOREWORD

This report describes the design and fabrication of a Brayton Cycle Solar Heat Receiver performed under NASA Contract NAS 3-10944. The work was conducted by General Electric Nuclear Systems Programs for the Space Power Systems Division, NASA-Lewis Research Center, under the direction of Mr. Harry M. Cameron, Project Manager.

CONTRIBUTING AUTHORS

W. H. Bennethum

J. A. Bond

R. A. Ekvall

A. A. Groh

J. Klekovic

M. D. Marvin

I. Mendelson

A. A. Salzarulo

W. R. Young

TABLE OF CONTENTS

	<u>Page No.</u>
1.0 SUMMARY AND CONCLUSIONS.	1
1.1 Summary	3
1.2 Conclusions	7
2.0 INTRODUCTION	9
3.0 DESIGN AND ANALYSIS.	13
3.1 Design Specifications	17
3.1.1 NASA Detail Specifications Summary	17
3.1.2 Structure Temperature Distributions.	21
3.2 Design Stress Criteria.	21
3.3 Gas System Design	23
3.3.1 Gas Flow Analysis.	23
3.3.2 Mechanical Design.	37
3.4 Shell Design.	45
3.4.1 Launch Conditions.	45
3.4.2 Thermal Stresses in Shell.	48
3.5 Top Closure	52
3.6 Aperture Assembly	59
3.6.1 Thermal Considerations	59
3.6.2 Structural Design.	63
3.6.3 Door Hinge and Bearings.	63
3.6.4 Flex Plate Support	64
3.7 Insulation.	64
3.8 Door Actuators.	71
3.8.1 Specification Development.	71
3.8.2 Actuator Design.	72
3.8.3 Linkage and Ball Bearings.	76
4.0 MATERIALS.	77
4.1 Refractory Raw Materials.	79
4.1.1 Specifications	80
4.1.2 Procurement Control.	80
4.1.3 Quality Assurance.	81
4.1.4 Material Control	81

TABLE OF CONTENTS (Continued)

	<u>Page No.</u>
4.2 Special Processes and Evaluations	83
4.2.1 Bimetallic Joint	83
4.2.2 Iron Titanate Coating.	91
4.2.3 Cb-1Zr Reducers.	96
4.2.4 Rivets	97
4.2.5 Top Closure.	97
4.2.6 Aperture Assembly.	98
5.0 WELDING DEVELOPMENT AND QUALIFICATION.	107
5.1 Qualification Plan.	109
5.2 Procedures.	111
5.3 Weld Development.	113
5.4 Qualification Results and Documentation	120
6.0 FABRICATION AND ASSEMBLY	121
6.1 Overall Sequence.	123
6.2 Gas System.	123
6.2.1 Welding.	123
6.2.2 Fabrication.	136
6.3 Shell Assembly.	167
6.4 Top Closure	167
6.5 Aperture Assembly	170
6.6 Final Assembly.	174
7.0 INSTRUMENTATION.	185
7.1 Thermocouple Alloy Selection.	187
7.2 Reference Junctions	190
7.3 Thermocouple Configuration and Installation	191
7.4 Pressure Taps	194
8.0 QUALITY CONTROL.	197
REFERENCES.	203
APPENDICES.	207
APPENDIX A. DESIGN CRITERIA FOR LOW CYCLE FATIGUE OF Cb-1Zr. .	207

TABLE OF CONTENTS (Continued)

	<u>Page No.</u>
APPENDIX B. DOOR ACTUATOR MAJOR COMPONENTS	219
APPENDIX C. WELD QUALIFICATION RESULTS AND DOCUMENTATION . . .	227
APPENDIX D. DISCREPANCY REPORT - POSTWELD ANNEAL OF BRAYTON CYCLE OUTLET MANIFOLD, GIRTH WELD NO. 1.	293

LIST OF ILLUSTRATIONS

<u>Figure No.</u>		<u>Page No.</u>
1	Gas System Weldment - Positioned for Assembly With Handling Fixture	5
2	Brayton Cycle Solar Heat Receiver - Installed in Shipping Fixture	6
3	Brayton Cycle Heat Receiver Assembly	16
4	Typical Calculated Transient Structure Temperatures.	22
5	Tensile Properties of Cb-1Zr	24
6	Larson-Miller Parameter Plot of 1% Creep Strengths of Cb-1Zr.	24
7	Estimated Coefficients of Expansion for Cb-1Zr . . .	25
8	Modulus of Elasticity Versus Temperature for Cb. . .	25
9	Total Hemispherical Emittance of Cb-1Zr Alloy. . . .	26
10	Solar Heat Receiver Assembly (Dwg. 47R199377, Sh.2).	29
11	Gas Tube Pressure Drop Versus Nozzle Orientation . .	33
12	Flow Maldistribution Versus $\Delta P/P$	34
13	$\Delta P/P$ Versus Outlet Manifold Diameter for In-Line Ducts With 2% Flow Maldistribution	35
14	$\Delta P/P$ Versus Outlet Manifold Diameter for Opposed Ducts With 2% Flow Maldistribution	36
15	Inlet Expansion and Outlet Contraction Losses. . . .	38
16	Coextruded Joint Schematic	40
17	Gas Tube Stress Versus Tube Extension Length	43
18	Gas Tube Stress Versus Shell-Tube Temperature Difference	44
19	Gas Tube Stress as a Function of Time.	46
20	Shock Spectrum for 100 Millisecond Half Sine Acceleration Pulse	47
21	Buckling Loads of Truncated Cones Due to Axial Compression.	49

LIST OF ILLUSTRATIONS (Continued)

<u>Figure No.</u>		<u>Page No.</u>
22	Membrane Stress Along the Meridian for 30 g Shock Load.	50
23	Hoop Stress for 30 g Shock Load	50
24	Bending Stress Along the Meridian for 30 g Shock Load.	51
25	Bending Stress in the Hoop Direction for 30 g Shock Load.	51
26	Temperature Distributions for Typical Thermal Cases	53
27	Membrane Stress Along the Meridian for Temperature Distribution A.	54
28	Hoop Stress for Temperature Distribution A.	54
29	Bending Stress Along the Meridian for Temperature Distribution A.	55
30	Bending Stress in the Hoop Direction for Temperature Distribution A.	55
31	Membrane Stress Along the Meridian for Temperature Distribution B.	56
32	Hoop Stress for Temperature Distribution B.	56
33	Bending Stress Along the Meridian for Temperature Distribution B.	57
34	Bending Stress in the Hoop Direction for Temperature Distribution B.	57
35	Top Closure Flex Plate Parameters	58
36	Aperture Assembly Heat Loss	61
37	Heat Flux Distribution in the Plane of the Aperture	62
38	Aperture Plate Temperature Distribution	62
39	Flex Plate Support Concept and Model.	65
40	Aperture Assembly Flexure Plate Parameters.	66
41	Effective Thermal Conductivity of Cb-1Zr Knurled Foil.	68

LIST OF ILLUSTRATIONS (Continued)

<u>Figure No.</u>		<u>Page No.</u>
42	Heat Flux Versus Number of Foil Layers.	69
43	Door Actuator Assembly (Dwg. No. 47E193580, Sh. 1).	73
44	Door Actuator Schematic and Wiring. (Dwg. No. 47E193580, Sh. 2)	74
45	Cooling Gas Flow Requirements	84
46	Sketch of a Longitudinal Full Section View of a Coextruded Joint.	84
47	Schematic Cb-1Zr/Stainless Steel/Hastelloy X Tran- sition Joint for Receiver Exit Header	85
48	Typical Coextruded Joint.	85
49	Typical Microstructure of Stainless Steel Portion of Co-Extruded Joints	88
50	Typical Microstructure of Cb-1Zr Portion of Co- Extruded Joints	89
51	Cb-1Zr Alloy Fin Specimen Coated with Iron Titanate.	93
52	Prototype Corrosion Loop Following Installation in the Test Chamber Spool Piece.	94
53	Close Up View of Corrosion Loop After Test.	95
54	Thermal Expansion of Aperture Cone Candidate Materials	100
55	Brayton Cycle Heat Receiver Weld Qualification Tests	110
56	Original Design Typical Boss-to-Manifold Joint. . .	114
57	Weld Qualification Test Specimen Illustrating GTA Tack Welds Used for Boss Positioning.	115
58	Internal Rotary GTA Welding Torch	116
59	Design of Tube-to-Manifold Weld Joints.	117
60	Special Water-Cooled Tube Welding Head.	119
61	Brayton Cycle Heat Receiver Fabrication Sequence. .	124

LIST OF ILLUSTRATIONS (Continued)

<u>Figure No.</u>		<u>Page No.</u>
62	Manifold Forming and Machining.	125
63	Manifold Welding.	126
64	Manifold Annealing, Final Welding and Machining . .	127
65	Heat Storage Tube Weld Sequence	128
66	Welding Chamber Installation, Side View	129
67	Welding Chamber Installation, End View.	130
68	Weld Chamber.	134
69	Manifold Sections - Forming and Inspection.	138
70	Inner and Outer Manifold Sections - Cleaned in Preparation for Girth Tacking	139
71	Inner Manifold Section - Being Loaded into Weld Chamber for Girth Tacking	140
72	Outer Manifold Section Set-up in Weld Chamber for Tack Welding of Girth Joints.	141
73	Tack Welding Girth Joint of Outer Manifold Section.	141
74	Machining for Circumferential Weld Joint on Inner Manifold Section.	142
75	Inlet and Outlet Manifold Being Set-up for Auto- matic TIG Welding	143
76	Inlet Manifold Set-up on Horizontal Boring Mill for Machining Boss Holes.	144
77	Inlet Manifold After Machining of 48 Boss Holes and Nozzle Opening.	145
78	Boss Alignment Fixture Locating a Boss on Inlet Manifold. Other Bosses Shown Have Been Tack Welded	146
79	Inlet and Outlet Manifolds Mounted on Rotating Weld Fixtures.	147
80	Outlet Manifold Illustrating Boss Location Where Welding Torch Failure Occurred.	149
81	Shell Support Rings for Inlet and Outlet Manifolds. Temporary Bridge Shown Tack Welded at Nozzle Cutout Location on Inlet Ring.	151

LIST OF ILLUSTRATIONS (Continued)

<u>Figure No.</u>		<u>Page No.</u>
82	Typical Manifold Support Tubes.	152
83	Welding Alignment Fixture for Outlet Manifold Support Tube.	152
84	Weld Alignment Fixture for Outlet Manifold Shell Ring.	153
85	Inlet Manifold - Typical Weldments Required During Fabrication	153
86	Inlet Manifold - Restraining Tie Bars Tack Welded to Halves for Post Weld Anneal	155
87	Typical Manifold Girth Joint Postweld Anneal Using Local Furnace	156
88	Outlet Manifold Prepared for Gas System Assembly. . .	158
89	Inlet Manifold Ready for Gas System Assembly.	159
90	LiF Heat Storage Tube From Third Batch Being Inspected for Envelope Conformance Using Contour Template Fixture	160
91	Heat Storage Tubes Loaded for Assembly Welding of Inlet Ferrules and Reducers	161
92	Close-up of Typical Automatic Weld Inlet Ferrule-to-Tube.	162
93	Typical Heat Storage Tube Assemblies.	163
94	Manifold Mounted on Rotating Weld Fixture	163
95	Gas System Set-up for Assembly Welding.	164
96	Completed Gas System.	166
97	Shell Assembly Panels - Before and After Installation of Reflectors	168
98	Cb-1Zr Top Closure Fabrication.	171
99	Aperture Assembly and Instrumentation	172
100	X-Ray Examination of Actuator Bellows Alignment . . .	173
101	Door Actuator and Typical Subassemblies	175

LIST OF ILLUSTRATIONS (Continued)

<u>Figure No.</u>		<u>Page No.</u>
102	Gas System Instrumentation-Typical Application Sequences	176
103	Gas Tube Instrumentation-Solar Heat Receiver.	178
104	Assembly of Shell, Reflectors and Gas System.	179
105	Aperture Structure, Doors and Linkage - Installation and Checkout.	181
106	Top Closure	182
107	Brayton Cycle Solar Heat Receiver - Installed in Shipping Fixture.	183
108	Thermocouple Junction Box - Solar Heat Receiver . . .	192
109	Gas System Instrumentation and Insulation	195
110	Gas System Showing Duct Instrumentation Features - Solar Heat Receiver	196

LIST OF TABLES

<u>Table No.</u>		<u>Page No.</u>
I	Receiver Design Conditions.	18
II	Short Time and Non-Cyclic Stress Criteria for Cb-1Zr. .	27
III	Tabulation of Gas Pressure Losses	39
IV	Door Actuator Performance and Design Data	75
V	NSP Material and Nondestructive Testing Specifications.	82
VI	Documentation of Quality Assurance Data for Cb-1Zr Alloy	82
VII	Sequence of Operations in Fabricating Coextruded Joints.	90
VIII	Typical Composition of <i>Refrasil</i>	104
IX	Brayton Cycle Heat Receiver Weld Qualification Tests. .	112
X	Fabrication Sequence, Brayton Cycle Heat Receiver . . .	131
XI	Rework Procedure for Outlet Manifold - Boss Weld Failure	150
XII	Weight Breakdown - Solar Heat Receiver.	184
XIII	Thermocouple Locations.	188

1.0 S U M M A R Y A N D C O N C L U S I O N S

Page intentionally left blank

1.0 S U M M A R Y A N D C O N C L U S I O N S

The General Electric Company, under Contract NAS 3-10944 to the National Aeronautics and Space Administration, has completed the design and fabrication of a solar heat receiver for use in a 10 KW_e Brayton cycle power system. The heat receiver functions as an absorber of the solar radiation incident on the mirror - collector, and as a heat exchanger to transfer heat into the Brayton System working fluid. Physically it is interposed between the recuperator and the turbine, receiving its gas flow from the recuperator at a temperature of 1564°R and delivering it to the turbine at 1960°R.

1.1 S U M M A R Y

A gas flow analysis was performed to study the pressure drop and flow distribution characteristics of the receiver and determine the following:

- 1) Manifold sizes required.
- 2) Flow restrictions required, if any, to achieve uniform flow.
- 3) Size of inlet and outlet nozzles.

Results of the analysis showed that the actual pressure drop was within the specified allowable (2% of inlet pressure). Each of the gas tubes was also provided with an orifice to assure uniform flow distribution.

Thermostructural analyses performed on all major components, including the shell, aperture assembly and top closure, revealed that thermal stresses were well within the allowable limits. The most significant inertial load requirement was the 20 g "half-sine" shock pulse of 100 millisecond duration. The shock spectrum approach was used to evaluate the inertial response. Results of the analysis showed a large factor of safety with respect to the applied load.

Mechanical design of the heat receiver incorporated six heat-rejection doors to protect the structure from overtemperature damage. These elec-

trically-actuated doors are designed to open when the cavity temperature has reached a temperature of 2140⁰R.

A very extensive refractory metal procurement and quality assurance effort was conducted during the course of the program. All structural material of the heat receiver was originally specified to be Cb-1Zr. The corrosion resistance, weldability, strength, fabricability, and availability of Cb-1Zr alloy made it a sound selection as the primary structural material. All Cb-1Zr material was ordered to GE-NSP specifications and control over procurement and documentation was governed by NSP Instructions. All material was 100% visually and ultrasonically inspected, and where appropriate, selected samples of each type of material were evaluated for stress-rupture strength, chemistry, grain size, and metallurgical structure.

Qualification for welding personnel was carried out for each unique joint type used in the heat receiver. Weld process qualification also included welding equipment, fixtures, and tooling required for each weld. The primary purpose of the weld qualification task was to identify problems with weld joint designs, welding procedures, or fixtures, prior to commitment of hardware. Results of the weld qualification trials required a change in either the joint design or welding procedure for five of the weld joints used in the heat receiver.

The lithium fluoride filled heat storage tubes were furnished by NASA-LeRC for incorporation into the design as well as assembly fabrication. The heat storage tube units were fabricated at the Lewis Research Center. Filling of the bellows cavity with lithium fluoride was accomplished at the Oak Ridge National Laboratory as described in Reference 1. The heat storage tubes as assembled with the gas system can be seen in Figure 1.

In addition to extensive Cb-1Zr weldment type assemblies, relatively large Cb-1Zr sheet metal type fabrications were designed and successfully completed. Some of the shell support panels, representative of the Cb-1Zr sheet metal type fabrications can be seen in Figure 2. This is a photograph of the completed heat receiver which was delivered to NASA LeRC in December 1969. A weight summary of the heat receiver is tabulated below.



Figure 1. Gas System Weldment - Positioned for Assembly with Handling Fixture. (P69-11-12A)



69-12-11AQ

Fig 2-

Brayton Cycle Solar Heat Receiver - Installed in
Shipping Fixture. (P69-12-11AQ)

WEIGHT SUMMARY - BRAYTON SOLAR HEAT RECEIVER

Gas System Assembly		1131
Gas Tubes (includes 266 pounds of LiF)	576	
Inlet Manifold	260	
Outlet Manifold	230	
Ducts (elbows and bimetallics)	35	
Foil Insulation and Thermocouples	30	
Shell Assembly (with reflectors)		230
Top Closure (with flex plates and bkts)		70
Aperture Assembly (less actuators)		175
Actuators (total of six)		133
Miscellaneous Hardware		35
Refractory Alloy	25	
Stainless Steel	10	
<u>Total Heat Receiver Weight</u>		<u>1174 Pounds</u>

1.2 CONCLUSIONS

The most significant conclusion from the program is the practicality of fabricating large complex structures from the refractory alloy Cb-1Zr. Development of new welding and fabrication procedures played a major role in making the heat receiver a reality.

Weight reductions are achievable in a number of areas as noted below.

- a) Since the weight of the manifolds represents a significant portion of the overall weight, system studies should be made to determine the validity of the 2% pressure drop limitation. If the pressure drop could be increased with relative impurity, the inlet and outlet manifold diameters could be decreased along with the wall thickness.
- b) The outlet manifold diameter and wall thickness were matched with those of the inlet manifold for manufacturing economy. Weight reductions are therefore achievable independent of changes in pressure drop limitations.

- c) The thermal stress allowable which was developed for Cb-1Zr is considered to be conservative. Any increase in the stress allowable resulting from additional low cycle fatigue test data, not now available would decrease the Cb-1Zr component weights, particularly the manifolds.
- d) The top closure could be replaced by a thin flexible membrane.
- e) Except for the torroidal transition section the wall thickness of the upper and lower shell support cones can be reduced. (Material procurement lag time imposed a relative inflexibility on design changes.)
- f) The door actuators are not flight type components (because of limitations in development funding). Weight reductions in both the actuators and their support structure could be significant.

Insulation of the heat receiver structure was identified as a formidable problem. Evaluation of several candidate insulation systems resulted in an interim solution. It is apparent that no really good solution currently exists for insulating large or complex refractory alloy structures, particularly where flight considerations are involved. The need for considerable development in this area is indicated if the performance potential of space power systems is to be realized.

To obtain larger emissivity values than that obtained by grit blasting, a coating needs to be developed which is compatible with the Cb-1Zr heat storage tubes for the anticipated operating range of 1700°F to 1800°F. Iron titanate, the emissivity coating originally contemplated was eliminated during the course of the program. Potential embrittlement of the Cb-1Zr heat storage tubes resulting from degradation of the iron titanate coating was considered an undue risk.

2.0 I N T R O D U C T I O N

Page intentionally left blank

2.0 I N T R O D U C T I O N

Space missions beyond those of the Apollo Program which successfully put man on the moon will require increased electrical power. The NASA Lewis Research Center has been actively engaged in developing Brayton cycle power systems for meeting these increased needs for space electrical power. Nuclear or solar heat sources can be used in conjunction with the Brayton power-conversion system. To evaluate a unique solar heat receiver concept, NASA-Lewis Research Center authorized Nuclear Systems Programs of the General Electric Company to design and fabricate a prototype solar heat receiver. Test evaluation of the heat receiver under simulated conditions would be accomplished by NASA in the Plum Brook Space Power Facility. A thirty-foot diameter parabolic reflector, a solar simulator energy source as well as the Brayton cycle power conversion machinery would all be involved in simulating the total power system operating in its space environment.

The heat receiver absorbs solar radiation from a mirror - collector and functions as a heat exchanger to transfer heat into the Brayton System working fluid. The basic heat exchanger portion of the receiver consists of a flux cone made up of forty-eight gas tubes symmetrically arranged around a center axis to form the frustrum of a cone. Surrounding each gas tube is a second tube containing lithium fluoride which acts as a thermal storage material. During the sun time, excess energy is absorbed to melt the heat storage material. During shade times, the heat storage material freezes as thermal energy continues to be transferred to the working fluid. Thus, the receiver transfers heat continuously to the working fluid which comes from the Brayton system recuperator and delivers heated gas to the turbine for specified maximum shade times.

A recent program (Reference 2) was conducted to determine the compatibility of several promising columbium-base alloys with lithium fluoride under the cyclic thermal conditions which simulate the sun-shade

cycle of a heat receiver, and to evaluate a design concept for containment of lithium fluoride in a manner which accommodates the 29% expansion upon melting. The compatibility tests indicated the columbium-base alloys Cb-1Zr, FS-85, and SCb-291 were corrosion resistant to lithium fluoride. The results of the compatibility study are described in a separate report. (Reference 3)

Earlier effort on the Sunflower Program, sponsored by NASA, produced the initial design information for solar heat receivers. In that program, lithium hydride was used as the heat storage material. Unfortunately, a basic characteristic of lithium hydride is its dissociation into free hydrogen and elemental lithium in the liquid state. This led to a later effort of design analysis, small scale experiments, and material corrosion tests, using lithium fluoride as the heat storage material. That program resulted in the basic design concept for heat receivers, engineering properties of lithium fluoride, and corrosion information with LiF at temperatures up to 1850°F.

Based on the results of this previous work, a preliminary design of a heat receiver, using LiF heat storage, has been evolved by NASA. The purpose of the effort described in this report was to provide for the detail design, fabrication, and delivery of an assembled heat receiver to NASA for subsequent testing.

3.0 DESIGN AND ANALYSIS

Page intentionally left blank

3.0 DESIGN AND ANALYSIS

The heat receiver is made up of four major assemblies: the gas system, shell support structure, aperture assembly, and the top closure as depicted in Figure 3. The gas system incorporates an inlet header, outlet header, and 48 tubes arranged in such a manner that the structure assumes the shape of a frustum of a cone. Each manifold is provided with a single gas flow duct. Surrounding each gas tube is a convoluted tube. The lithium fluoride is contained between the gas tubes and the convoluted tubes, but since by design the inner diameter of the convoluted tubes nearly touches the OD of the gas tube, almost all of the LiF is stored in the volume of the convolution.

The distribution of lithium fluoride along the length of the tube was patterned to fit the flux density at each locality. Since the flux decreases as the square of the distance from the mirror's focus, the lithium fluoride quantity per inch of tube length also decreases. Consequently, the diameter of the convolutions decreases along the length of the tube. The shell support provides an enclosure to reradiate incident energy which passes through the tube spacing and a structural support during the launch condition.

The conical cavity formed by the tubes is closed off at the base by the aperture assembly, and up above by the top closure. The aperture assembly contains the aperture, located in the focal plane of the mirror, which remains open during the entire sun-shade cycle. The aperture assembly also contains heat rejection doors, whose function is to open when the cavity temperature has reached 2140°R . This protects the structure from overtemperature damage. The door area is sufficiently large as to reradiate 95% of the incoming energy.

This section outlines the design bases, detail designs and analyses for these assemblies.

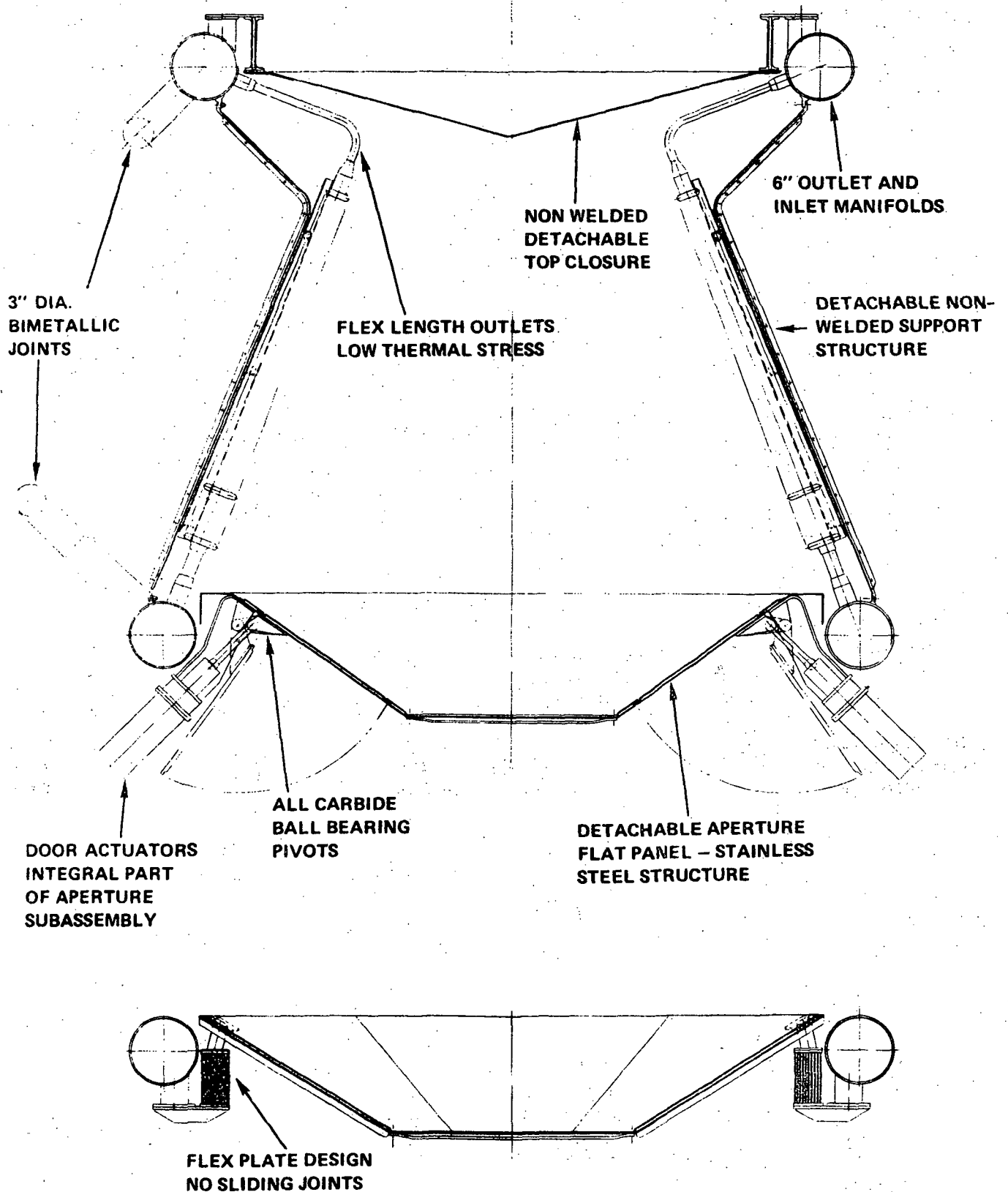


Figure 3. Brayton Cycle Heat Receiver Assembly.

3.1 DESIGN SPECIFICATIONS

The detail design specifications for the receiver are given under Exhibit "A" of NASA Contract NAS 3-10944. Pertinent portions of the specifications are paraphrased and summarized below for completeness. Table I is a listing of receiver design conditions.

3.1.1 NASA Detail Specifications Summary

Inlet Header - The inlet header shall be designed to act as the structural base of all receiver components; supporting static and dynamic loads imposed on the receiver as per environmental Specifications PI224-1 and PI224-2. The inlet header shall be furnished with mounting lugs by means of which the receiver will be attached to the other components of the Brayton system. The gas inlet shall be welded to a coextruded columbium-1Zr and 300 series stainless steel transition element. The free extremity of the transition element shall be designed to mate with recuperator exit duct. The inlet header shall provide means for attachment of the aperture assembly in a manner which will allow separation by nondestructive methods.

Gas Tubes - NASA shall furnish the contractor with at least 55 tube assemblies, filled with lithium fluoride, and coated with iron titanate. The contractor shall be responsible for providing the specified thermocouple instrumentation.

Exit Header - The exit header shall accommodate the gas flow from heat transfer tubes. The gas outlet of the exit header shall be welded to a coextruded columbium-1Zr and 300 series transition element. The free extremity of the transition element shall be designed to mate with the turbine inlet duct.

Top Closure - The top closure shall be welded or bolted to the exit header. It shall be designed to minimize aperture heat losses; that is, the design shall provide an optimum view factor with respect to the tubes and minimize the view factor with the aperture.

Gutters - "Gutters" shall be designed to reflect back onto the tubes sunlight that passes between the tubes. The gutters may be attached either to the headers or to the conical shell surrounding the tubes. The gutters shall be plasma sprayed with Iron Titanate - -200 to +325 Mesh, if detail thermal analysis shows such a requirement.

TABLE I
RECEIVER DESIGN CONDITIONS

Gas inlet temperature	1558°R Nominal Temperature
Gas exit temperature	1960°R Nominal Temperature
Gas inlet pressure	53.92 psia
Gas flow rate	1.607 lb/sec
Working fluid	Helium-xenon mixture with 83.8 moled, wt.
Gas pressure drop	2% of inlet pressure
Minimum sun time	60 minutes*
Maximum sun time	continuous*
Maximum shade time	40 minutes*
Mirror input	72.5 KW*
Maximum receiver wall temp.	2240°R*
Receiver output rate	40.4 KW*
(Continuous)	
Maximum radiant heat loss from receiver (excluding aperture)	2 KW*
Max. radiative heat rejection	70 KW
(from movable doors or louvers)	
Min. radiative heat rejection	0
from movable doors or louvers	
Operational design life	5 years
Aperture size	14 inch diameter ⁽¹⁾

* Reference only

(1) Aperture sized for test with Solar Simulator in which the light source produces a collimation half angle of 1°20' (sun ray half angle of 16' would result in 8 inch diameter aperture)

Aperture Assembly - The aperture consisting of a circular opening shall be cut into a detachable aperture plate, so that apertures of various sizes may be utilized. The maximum aperture diameter required is 14 inches.

The aperture assembly shall be capable of radiative heat rejection at variable rates from 0 to 70 KW by means of 6 doors whose position can vary from fully closed to fully open. The door area shall be sized so that if one of the doors should fail to open, the maximum required heat rejection should still occur without exceeding the temperature limitation stated below. The doors operating simultaneously must start to open when the receiver cavity's mean radiant temperature reaches 2130°R and be fully open when that temperature reaches 2200°R . At least 3 sensors shall be installed in different locations to obtain verifications of the mean radiant temperature. The actuating mechanism to open and close the doors in response to a signal provided by the appropriate temperature sensors, shall have a "manual" override for remote actuation from outside the vacuum chamber in which the receiver will be tested.

Joining - All components shall be joined by welding or brazing (except for the insulation and as otherwise specified) in accordance with approved specifications. The design of the junctions shall be such as to allow for differential thermal expansion and contraction (resulting from differences in temperature and thermal inertia of the components) without excessive stress build-up. The components to be joined by welding shall be brought into assembly position without causing detrimental strain in the components prior to welding.

Material Requirements - The receiver assembly shall be made from Cb-1Zr alloy. The exceptions noted below shall apply:

- a. The inlet-exit headers shall be provided with a Cb-1Zr to 300 series stainless steel transition joints to allow field welds to be made to the stainless steel recuperator and turbine.
- b. All components associated with the heat rejection mechanism which have the operational requirement to move relative to each other shall have their junction surfaces faced with an alloy which resists self welding in a vacuum environment at the temperatures to which the surfaces are exposed.

- c. Insulation if required to isolate receiver components from each other shall be furnished by the contractor.

Allowable Stresses - Design stresses shall be limited to the following values:

	<u>Operational Mode (Hot)</u>		
	<u>All Components Except Inlet-Header</u>	<u>Inlet-Header</u>	<u>Launch Mode (Cold)</u>
Tension (psi)	3,000	5,000	10,000
Compression (psi)	3,000	5,000	10,000
Shear (psi)	1,500	2,500	5,000

Thermocouple Instrumentation - All instrumentation shall be connected to one or at most two panels or bulkheads and be furnished with a terminal strip capable of connecting the thermocouple wire to another wire (probably copper) which will then lead to the chamber feedthrough. The contractor will furnish all instrumentation up to and including the terminal strip but will not be responsible for the instrumentation from the terminal strip to the readout equipment. The contractor shall supply a means for maintaining a constant temperature over the terminal strip so it can be used as the thermocouple junction temperature. All leads to the panel or bulkhead shall be attached in a manner to facilitate troubleshooting. Instrumentation shall be provided to meet the following requirements:

Six (6) equally spaced tubes shall be selected for temperature mapping. Twenty-four (24) thermocouples shall be installed on each tube in a manner to obtain the axial as well as circumferential temperature distribution for each tube. In addition, the following thermocouples shall be provided:

<u>Location</u>	<u>No. of Thermocouples</u>
Shell	9
Doors	6
Top Closure	3
Aperture Cone	10
Inlet Duct	3
Exit Duct	3
Door Actuators	12

Platinum-rhodium or tungsten 3% rhenium-tungsten 25% rhenium shall be used for all thermocouples attached to refractory surfaces. Chromel-alumel may be used on stainless steel components.

3.1.2 Structure Temperature Distributions

The temperature distributions throughout the structure were furnished by NASA for a variety of transient and steady-state operating conditions. These temperatures were used in the design and analysis of the receiver. Figure 4 is a typical temperature-time plot of calculation results provided by NASA.

3.2 DESIGN STRESS CRITERIA

Allowable stresses set forth in the specifications formed the basis of the design criteria. Additional criteria, patterned after those used in the ASME Nuclear Pressure Vessel Code (Reference 4), were formulated. Design stresses in the heat receiver were limited to prevent three different types of failure.

1. Bursting and gross distortion are prevented by the limits placed on primary stresses due to mechanical and pressure loadings. These stress limits were as set forth in the specifications.
2. Progressive distortion is prevented by the limits placed on primary plus secondary stresses. These limits assure shakedown to elastic action after a few repetitions of the loading.
3. Fatigue failure is prevented by the limits placed on peak stresses.

To clarify the stress categories mentioned above the following discussion is presented.

- a. Primary stress is a stress developed by the imposed loading which is necessary to satisfy the laws of equilibrium. The basic characteristic of a primary stress is that it is not self-limiting. Thus, exceeding the limitations on primary stresses can be expected to lead to short-term failures (whose prevention is entirely limited by the strain hardening of the material) or by excessive distortion due to creep.
- b. Secondary stress is a stress developed by self constraint of the structure. The basic characteristic of a secondary stress is that it is self-limiting since minor distortions of the structure can relieve the stress and prevent a further increase of the stress.

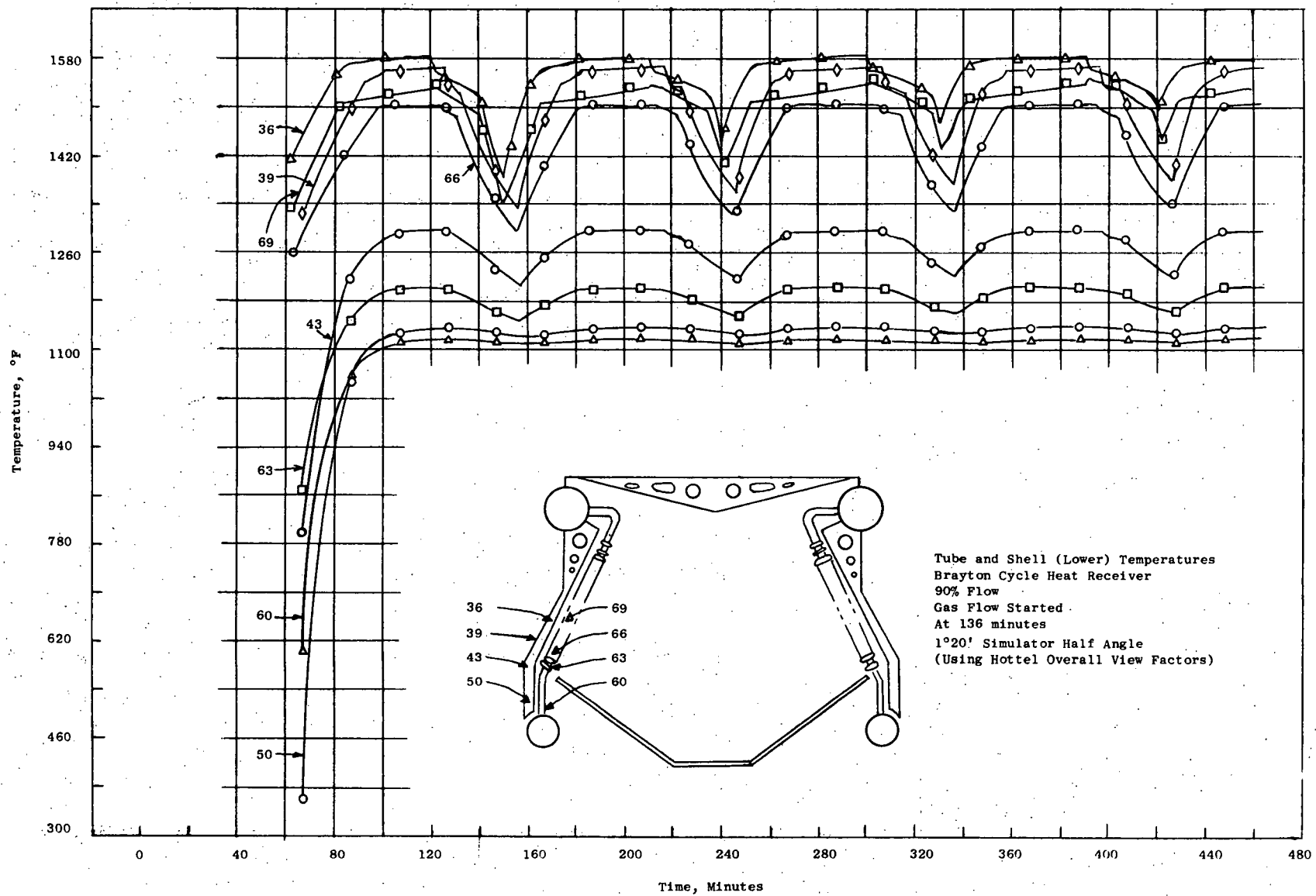


Figure 4. Typical Calculated Transient Structure Temperatures.

- c. Peak stress is the highest stress in the region under consideration. The basic characteristic of a peak stress is that it causes no significant distortion and is objectionable mostly as a possible source of a fatigue failure. The peak stress includes the sum of all the previous stresses plus stress concentration effects.

In addition to primary stress limits as delineated in the NASA Specifications, allowable stresses were established basically on the extent to which the applied stresses would be self-relieving. Material properties used for Cb-1Zr are as shown in Figures 5 through 9.

The basis and numerical values for short time and non-cyclic stress allowables are summarized in Table II. The stress allowable for inertial loading was set at 19,500 psi as is shown in the table.

The stress limit for thermal fatigue was set by low cycle fatigue behavior and is derived in Appendix A. Based on a total of 100 start-up cycles each of which would be characterized by large temperature excursions, a thermal stress allowable of 12,000 psi was established. The thermal stress allowable as developed in Appendix A is considered to be conservative. It is based on semi-empirical relationships and an increase in allowable stress could probably be achieved upon correlation with sufficient test data not now available.

3.3 GAS SYSTEM DESIGN

The term "gas system" as used in this report refers to the gas containment subassembly, which includes the inlet manifold, the 48 heat storage tubes and the outlet manifold. Figure 10 shows the gas system design. In operation, the Brayton cycle working fluid enters the receiver through the nozzle on the inlet manifold. The gas then flows through the 48 gas tubes where it is heated by the LiF stored in the bellows cavities. The heated gas is discharged from the gas tubes into the outlet manifold where it is collected and discharged at the outlet nozzle.

3.3.1 Gas Flow Analysis

Performance calculations for the receiver are based on the assumption that the gas flow is distributed uniformly in the gas tubes. If this is not the case, poor performance and/or high thermal stresses could result. It is apparent that if the pressure drop across the tubes is sufficiently

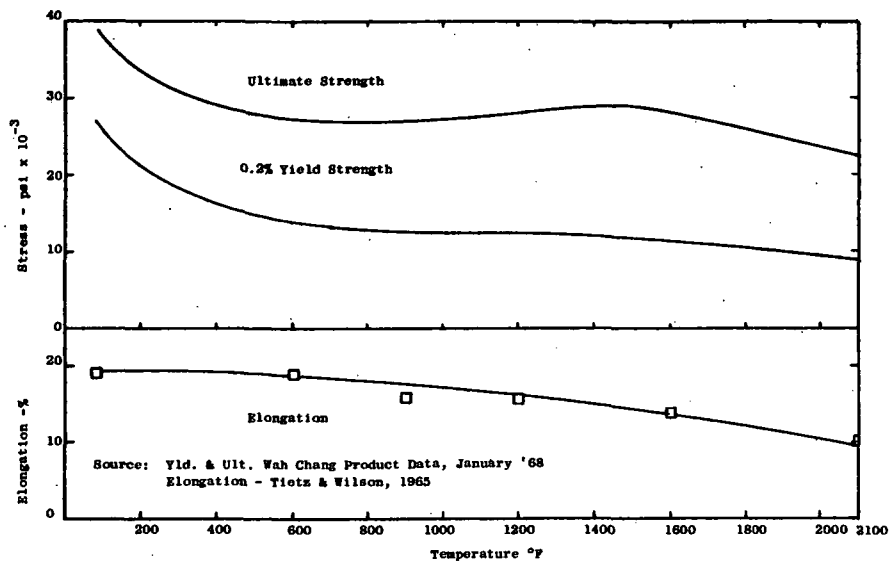


Figure 5. Tensile Properties of Cb-1Zr.

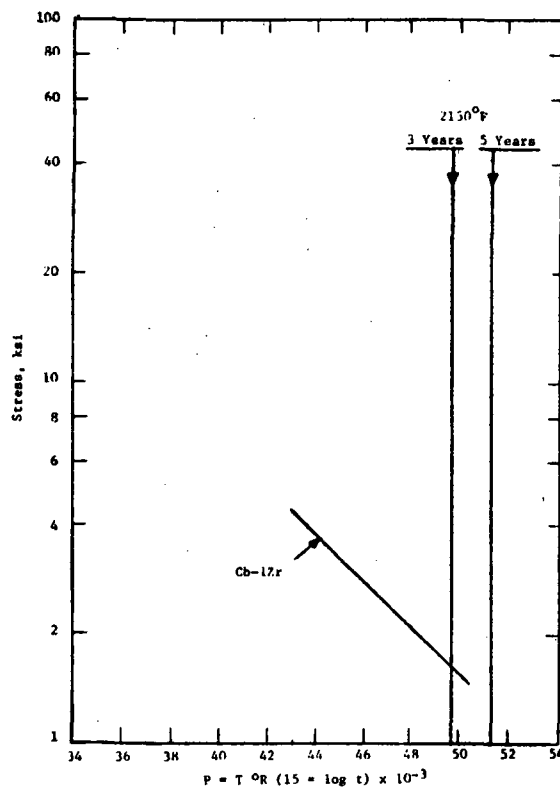


Figure 6. Larson-Miller Parameter Plot of 1% Creep Strengths of Cb-1Zr.

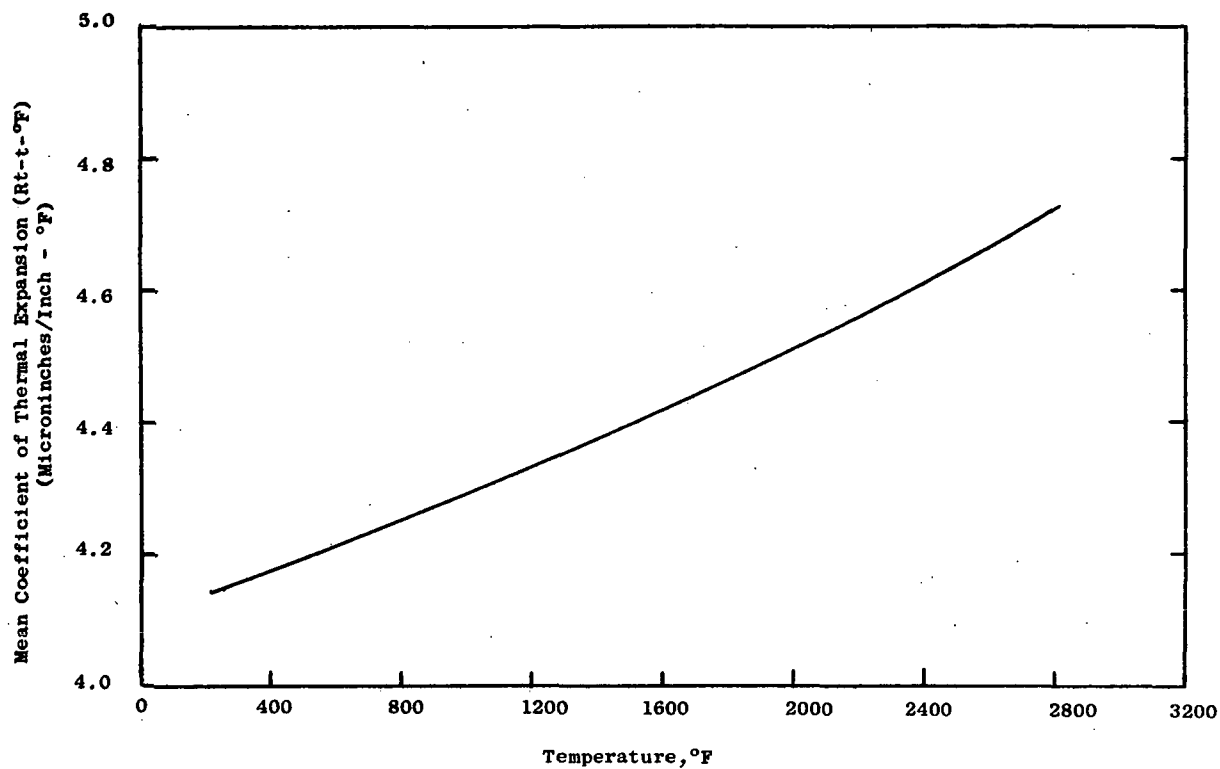


Figure 7. Estimated Coefficients of Expansion for Cb-1Zr.

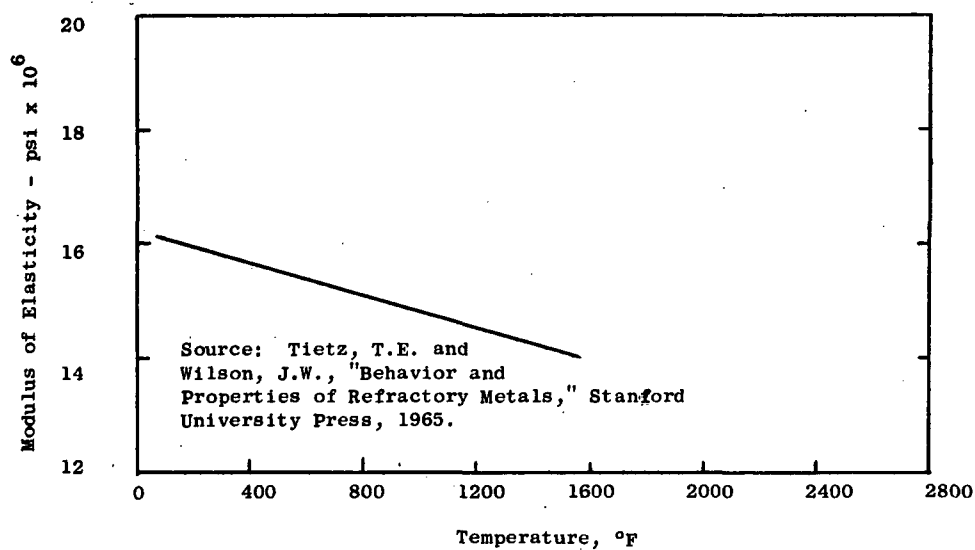


Figure 8. Modulus of Elasticity Versus Temperature for Cb.

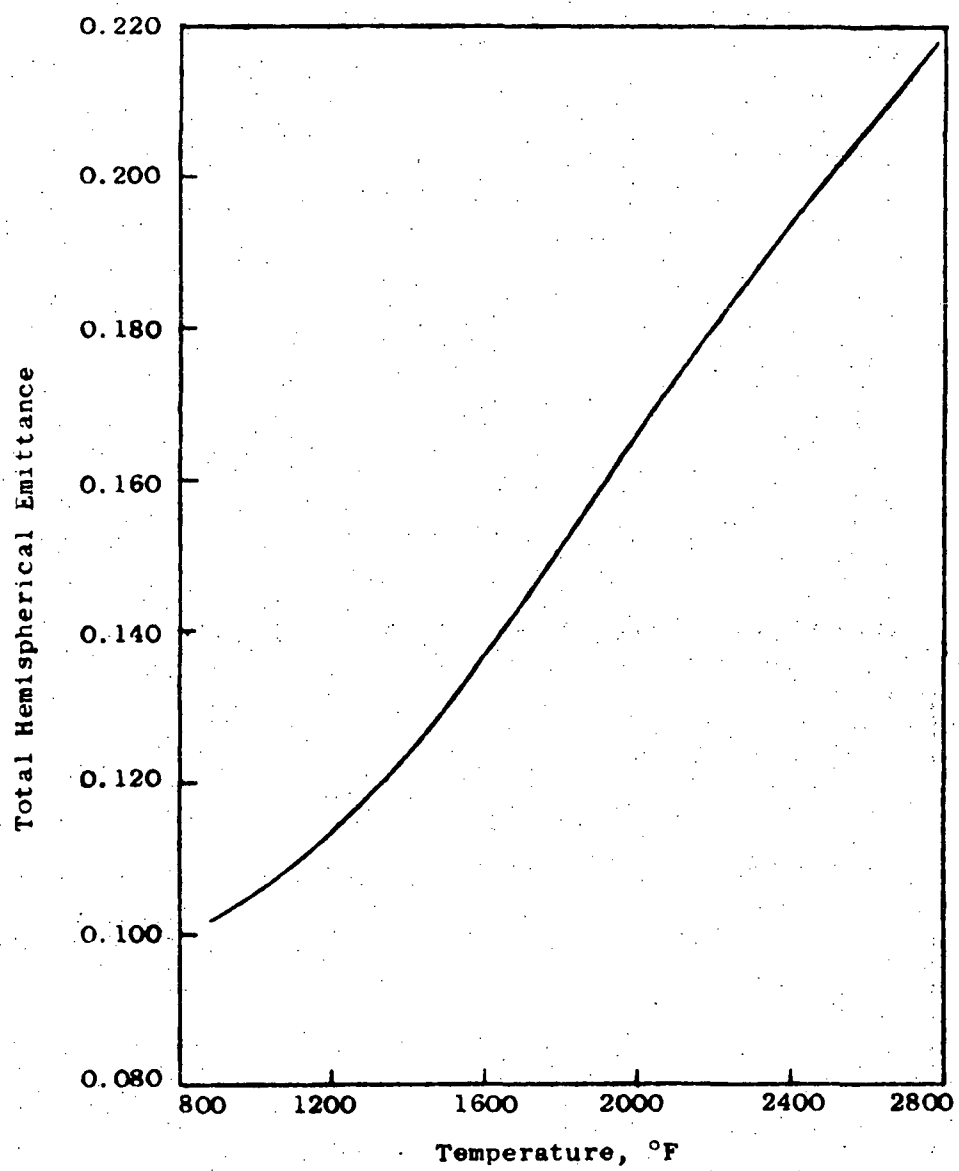
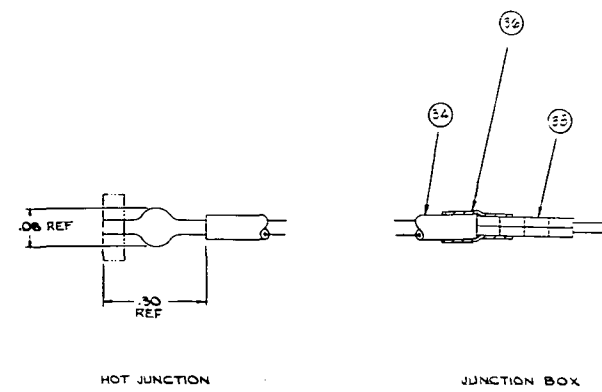


Figure 9. Total Hemispherical Emittance of Cb-1Zr Alloy.

TABLE II
SHORT TIME AND NON-CYCLIC
STRESS CRITERIA FOR Cb-1Zr

TEMPERATURE	RT	1800°F
YIELD (Psi)	27,000	10,500
ULTIMATE (Psi)	39,000	26,000
* S_m = Lower Value of:		
2/3 Yield	18,000	7,000
1/3 Ultimate	13,000	8,700
ALLOWABLE STRESS:		
BASIS	$1.5 S_m$	$3.0 S_m$ (No SCF)
VALUE	19,500	21,000
APPLICABILITY	INERTIAL LOADING (Primary Bending)	THERMAL STRESS Neglecting: (1) Cyclic Loading (2) Creep

* Per Section III ASME Nuclear Vessel Code.



TYP THERMOCOUPLE ROUTING SEE TABLE (ZONE E16)

- THERMOCOUPLE INSTALLATION & ROUTING**
1. T/C TO BE INSTALLED PER 03-0005-00-A UNLESS OTHERWISE NOTED - PAR. 3.6, 3.7, 3.8, 3.9 OF DWS 1423181G NOT APPLICABLE
 2. INSULATORS / LEADWIRE TO BE SECURED BY MEANS OF FOIL STRIPS TACKWELDED PER 03-0005-00-A SUCH THAT LEADWIRE/INSULATOR EXPANSION LOOPS COULD ALLOW EXPANSION OF EACH COMPONENT RELATIVE TO LEADWIRE EQUIV TO .005 IN./IN. CB-12F FOIL COATING TO BE USED ON CB-12F COMPONENTS & HIGHWIRE FOIL TO BE USED ON CB-12F COMPONENTS
 3. WHERE T/C ARE ROUTED AROUND CORNERS INSULATORS TO BE BROKEN INTO SHORT LENGTHS TO OBTAIN GRADUAL BENDS IN T/C LEADS
 4. WHERE SURF T/C ARE INSTALLED UNDER CB-12F FOIL INSULATION CARE MUST BE TAKEN TO PREVENT CONTACT BETWEEN FOIL & T/C LEADS
 5. T/C LEADS TO BE ROUTED AS FOLLOWS:
 - A) T/C 1 THRU 16, 18 THRU 25 TO BE ROUTED DOWN OUTBOARD SIDE OF RESPECTIVE INSTRUMENTED TUBE (TUBE NO. 12, 20, 28, 36, 44)
 - B) T/C 17 THRU 19 THRU 26 TO BE ROUTED DOWN OUTBOARD SIDE OF TUBE ADJACENT TO INSTRUMENTED TUBE (C/W LOOKING FROM INLET MANIFOLD TOWARD OUTLET MANIFOLD) TAKING CARE TO CLEAR REFLECTORS BETWEEN TUBES
 - C) T/C 26 THRU 31 THRU 38 TO BE ROUTED DOWN OUTBOARD SIDE OF TUBE ADJACENT TO INSTRUMENTED TUBE (C/W LOOKING FROM INLET MANIFOLD TOWARD OUTLET MANIFOLD) TAKING CARE TO CLEAR REFLECTORS BETWEEN TUBES
 - D) ALL OTHER T/C ROUTINGS TO BE ON OUTSIDE SURF. OF COMPLETELY ASSEMBLED HEAT RECIPIER ALONG INLET MANIFOLD TO THEIR RESPECTIVE JUNCTION BOXES
 - E) T/C 165, 166, 167 TO HAVE ENOUGH SLACK IN ROUTING SUCH THAT THEY WILL NOT INTERFERE WITH THE OPERATION OF THE DOORS

T/C NO.	WIRE
1-16	INVAR-CHROMEL
17-19	CHROMEL-ALUMEL
20-25	CHROMEL-ALUMEL
26-31	CHROMEL-ALUMEL
32-38	CHROMEL-ALUMEL
39-44	CHROMEL-ALUMEL
45-49	CHROMEL-ALUMEL
50-54	CHROMEL-ALUMEL
55-59	CHROMEL-ALUMEL
60-64	CHROMEL-ALUMEL
65-69	CHROMEL-ALUMEL
70-74	CHROMEL-ALUMEL
75-79	CHROMEL-ALUMEL
80-84	CHROMEL-ALUMEL
85-89	CHROMEL-ALUMEL
90-94	CHROMEL-ALUMEL
95-99	CHROMEL-ALUMEL
100-104	CHROMEL-ALUMEL
105-109	CHROMEL-ALUMEL
110-114	CHROMEL-ALUMEL
115-119	CHROMEL-ALUMEL
120-124	CHROMEL-ALUMEL
125-129	CHROMEL-ALUMEL
130-134	CHROMEL-ALUMEL
135-139	CHROMEL-ALUMEL
140-144	CHROMEL-ALUMEL
145-149	CHROMEL-ALUMEL
150-154	CHROMEL-ALUMEL
155-159	CHROMEL-ALUMEL
160-164	CHROMEL-ALUMEL
165-169	CHROMEL-ALUMEL
170-174	CHROMEL-ALUMEL
175-179	CHROMEL-ALUMEL
180-184	CHROMEL-ALUMEL
185-189	CHROMEL-ALUMEL
190-194	CHROMEL-ALUMEL
195-199	CHROMEL-ALUMEL
200-204	CHROMEL-ALUMEL
205-209	CHROMEL-ALUMEL
210-214	CHROMEL-ALUMEL
215-219	CHROMEL-ALUMEL
220-224	CHROMEL-ALUMEL
225-229	CHROMEL-ALUMEL
230-234	CHROMEL-ALUMEL
235-239	CHROMEL-ALUMEL
240-244	CHROMEL-ALUMEL
245-249	CHROMEL-ALUMEL
250-254	CHROMEL-ALUMEL
255-259	CHROMEL-ALUMEL
260-264	CHROMEL-ALUMEL
265-269	CHROMEL-ALUMEL
270-274	CHROMEL-ALUMEL
275-279	CHROMEL-ALUMEL
280-284	CHROMEL-ALUMEL
285-289	CHROMEL-ALUMEL
290-294	CHROMEL-ALUMEL
295-299	CHROMEL-ALUMEL
300-304	CHROMEL-ALUMEL
305-309	CHROMEL-ALUMEL
310-314	CHROMEL-ALUMEL
315-319	CHROMEL-ALUMEL
320-324	CHROMEL-ALUMEL
325-329	CHROMEL-ALUMEL
330-334	CHROMEL-ALUMEL
335-339	CHROMEL-ALUMEL
340-344	CHROMEL-ALUMEL
345-349	CHROMEL-ALUMEL
350-354	CHROMEL-ALUMEL
355-359	CHROMEL-ALUMEL
360-364	CHROMEL-ALUMEL
365-369	CHROMEL-ALUMEL
370-374	CHROMEL-ALUMEL
375-379	CHROMEL-ALUMEL
380-384	CHROMEL-ALUMEL
385-389	CHROMEL-ALUMEL
390-394	CHROMEL-ALUMEL
395-399	CHROMEL-ALUMEL
400-404	CHROMEL-ALUMEL
405-409	CHROMEL-ALUMEL
410-414	CHROMEL-ALUMEL
415-419	CHROMEL-ALUMEL
420-424	CHROMEL-ALUMEL
425-429	CHROMEL-ALUMEL
430-434	CHROMEL-ALUMEL
435-439	CHROMEL-ALUMEL
440-444	CHROMEL-ALUMEL
445-449	CHROMEL-ALUMEL
450-454	CHROMEL-ALUMEL
455-459	CHROMEL-ALUMEL
460-464	CHROMEL-ALUMEL
465-469	CHROMEL-ALUMEL
470-474	CHROMEL-ALUMEL
475-479	CHROMEL-ALUMEL
480-484	CHROMEL-ALUMEL
485-489	CHROMEL-ALUMEL
490-494	CHROMEL-ALUMEL
495-499	CHROMEL-ALUMEL
500-504	CHROMEL-ALUMEL
505-509	CHROMEL-ALUMEL
510-514	CHROMEL-ALUMEL
515-519	CHROMEL-ALUMEL
520-524	CHROMEL-ALUMEL
525-529	CHROMEL-ALUMEL
530-534	CHROMEL-ALUMEL
535-539	CHROMEL-ALUMEL
540-544	CHROMEL-ALUMEL
545-549	CHROMEL-ALUMEL
550-554	CHROMEL-ALUMEL
555-559	CHROMEL-ALUMEL
560-564	CHROMEL-ALUMEL
565-569	CHROMEL-ALUMEL
570-574	CHROMEL-ALUMEL
575-579	CHROMEL-ALUMEL
580-584	CHROMEL-ALUMEL
585-589	CHROMEL-ALUMEL
590-594	CHROMEL-ALUMEL
595-599	CHROMEL-ALUMEL
600-604	CHROMEL-ALUMEL
605-609	CHROMEL-ALUMEL
610-614	CHROMEL-ALUMEL
615-619	CHROMEL-ALUMEL
620-624	CHROMEL-ALUMEL
625-629	CHROMEL-ALUMEL
630-634	CHROMEL-ALUMEL
635-639	CHROMEL-ALUMEL
640-644	CHROMEL-ALUMEL
645-649	CHROMEL-ALUMEL
650-654	CHROMEL-ALUMEL
655-659	CHROMEL-ALUMEL
660-664	CHROMEL-ALUMEL
665-669	CHROMEL-ALUMEL
670-674	CHROMEL-ALUMEL
675-679	CHROMEL-ALUMEL
680-684	CHROMEL-ALUMEL
685-689	CHROMEL-ALUMEL
690-694	CHROMEL-ALUMEL
695-699	CHROMEL-ALUMEL
700-704	CHROMEL-ALUMEL
705-709	CHROMEL-ALUMEL
710-714	CHROMEL-ALUMEL
715-719	CHROMEL-ALUMEL
720-724	CHROMEL-ALUMEL
725-729	CHROMEL-ALUMEL
730-734	CHROMEL-ALUMEL
735-739	CHROMEL-ALUMEL
740-744	CHROMEL-ALUMEL
745-749	CHROMEL-ALUMEL
750-754	CHROMEL-ALUMEL
755-759	CHROMEL-ALUMEL
760-764	CHROMEL-ALUMEL
765-769	CHROMEL-ALUMEL
770-774	CHROMEL-ALUMEL
775-779	CHROMEL-ALUMEL
780-784	CHROMEL-ALUMEL
785-789	CHROMEL-ALUMEL
790-794	CHROMEL-ALUMEL
795-799	CHROMEL-ALUMEL
800-804	CHROMEL-ALUMEL
805-809	CHROMEL-ALUMEL
810-814	CHROMEL-ALUMEL
815-819	CHROMEL-ALUMEL
820-824	CHROMEL-ALUMEL
825-829	CHROMEL-ALUMEL
830-834	CHROMEL-ALUMEL
835-839	CHROMEL-ALUMEL
840-844	CHROMEL-ALUMEL
845-849	CHROMEL-ALUMEL
850-854	CHROMEL-ALUMEL
855-859	CHROMEL-ALUMEL
860-864	CHROMEL-ALUMEL
865-869	CHROMEL-ALUMEL
870-874	CHROMEL-ALUMEL
875-879	CHROMEL-ALUMEL
880-884	CHROMEL-ALUMEL
885-889	CHROMEL-ALUMEL
890-894	CHROMEL-ALUMEL
895-899	CHROMEL-ALUMEL
900-904	CHROMEL-ALUMEL
905-909	CHROMEL-ALUMEL
910-914	CHROMEL-ALUMEL
915-919	CHROMEL-ALUMEL
920-924	CHROMEL-ALUMEL
925-929	CHROMEL-ALUMEL
930-934	CHROMEL-ALUMEL
935-939	CHROMEL-ALUMEL
940-944	CHROMEL-ALUMEL
945-949	CHROMEL-ALUMEL
950-954	CHROMEL-ALUMEL
955-959	CHROMEL-ALUMEL
960-964	CHROMEL-ALUMEL
965-969	CHROMEL-ALUMEL
970-974	CHROMEL-ALUMEL
975-979	CHROMEL-ALUMEL
980-984	CHROMEL-ALUMEL
985-989	CHROMEL-ALUMEL
990-994	CHROMEL-ALUMEL
995-999	CHROMEL-ALUMEL

JUNCTION BOX NO.	AREA	ROW	T/C NUMBER
X	A	1	15
		2	16
		3	17
		4	18
		5	19
	B	6	20
		7	21
		8	22
		9	23
		10	24
C	A	11	25
		12	26
		13	27
		14	28
		15	29
	B	16	30
		17	31
		18	32
		19	33
		20	34
D	A	21	35
		22	36
		23	37
		24	38
		25	39
	B	26	40
		27	41
		28	42
		29	43
		30	44

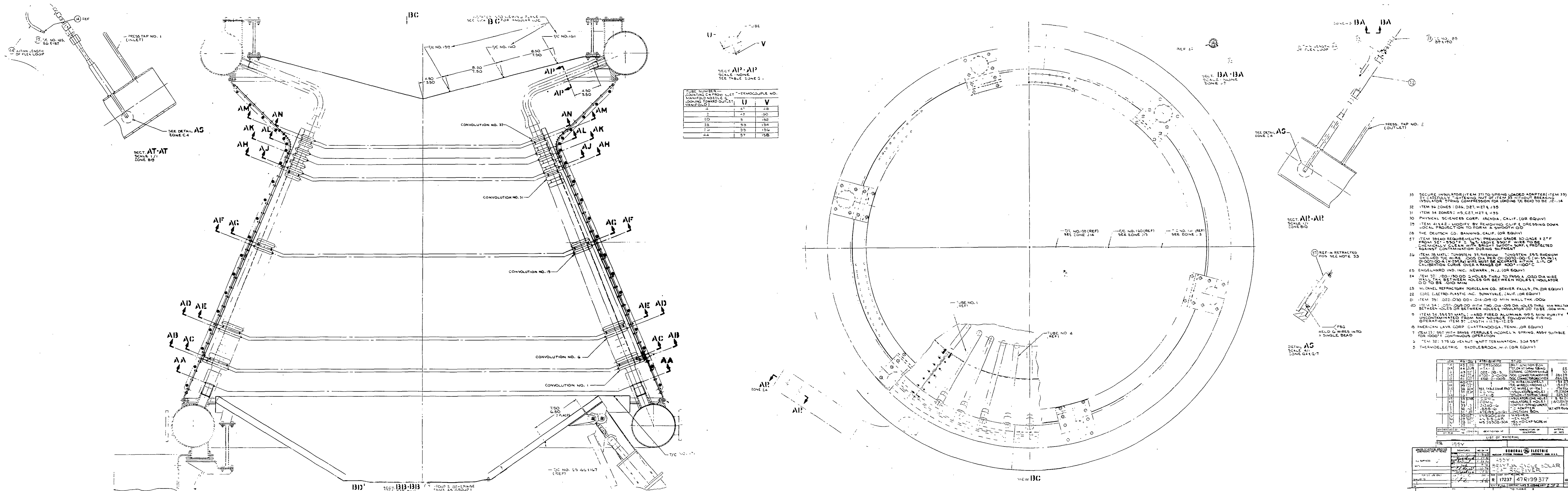


Figure 10. Solar Heat Receiver Assembly (Dwg. 47R199377, Sh. 2)

Page intentionally left blank

large relative to pressure variations in the manifolds, then the flow will be nearly uniform. However, the specification restricts the overall receiver pressure drop to less than 2% of the inlet pressure. Consequently, a gas flow analysis was performed to study the pressure drop and flow distribution characteristics of the receiver. This analysis was aimed at answering the following questions:

1. What manifold sizes are required?
2. How much flow restriction, if any, is required in the tubes to achieve uniform flow? Also, should the restrictions vary from tube-to-tube or should the same restriction be placed on all tubes?
3. What size should the inlet and outlet nozzles be?
4. How should the outlet nozzle be oriented with respect to the inlet manifold?

Before proceeding, the term "flow maldistribution" was defined and a limit placed on its magnitude. The flow maldistribution, λ , is defined as

$$\lambda = \frac{W_{\max} - W_{\min}}{W_{\text{ave}}} \quad (1)$$

where

W_{\max} = Maximum flow rate in any tube

W_{\min} = Minimum flow rate in any tube

W_{ave} = Flow rate per tube for uniform flow

Agreement was reached with NASA that the flow maldistribution should be limited to a maximum of 2%. The decision was also made at the outset, based on manufacturing considerations, that any flow restrictions (orifices) placed in the tubes should be of uniform size.

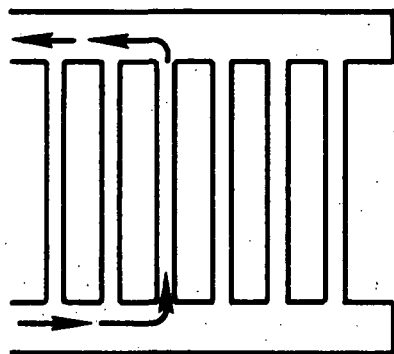
Flow Distribution - Pressure variations in the manifolds are a result of frictional losses and momentum effects. The problem of flow in manifolds is analyzed in some detail in Reference 5. In the inlet manifold, frictional effects contribute a negative pressure gradient while momentum effects (due to loss of fluid to the tubes) contribute a positive pressure gradient. Whether the pressure actually increases or decreases in the direction of flow depends upon the relative magnitudes of the two effects. For the inlet manifold size selected, the momentum

is the dominant term and the pressure rises in the flow direction. In the outlet manifold, the friction and momentum effects act in the same sense and the pressure decreases in the direction of flow. The resulting manifold-to-manifold pressure drop depends on the location of the outlet nozzle relative to the inlet nozzle as shown in Figure 11.

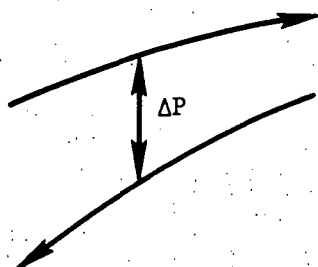
In Version I, the pressure variations in the two manifolds are such that ΔP (and hence, the tube flow) is fairly uniform. In Version II, the pressure curves diverge, causing flow maldistributions. The qualitative trends illustrated in Figure 11 were confirmed in the gas flow analysis.

The flow distribution analysis consisted of writing the equations describing the flow in the manifolds and gas tubes. These equations were programmed and solved numerically on a digital computer. For given inlet and outlet manifold sizes, the flow calculations were made for various flow restrictions in the gas tubes. The results are plotted in Figure 12 and show flow maldistributions as a function of $\Delta P/P$. As the tube flow resistance increases, $\Delta P/P$ increases and the flow maldistribution decreases. The information in Figure 12 was cross-plotted as follows. For a given inlet manifold diameter, the pressure drop for 2% flow maldistribution was plotted as a function of outlet manifold diameter as shown in Figure 13. For each inlet manifold diameter, the $\Delta P/P$ versus outlet manifold diameter curve has a minimum value. These curves do not include the manifold nozzle pressure losses, which are the major pressure drop. Consequently, the manifold and gas tube losses must be kept as small as possible in order that the 2% limit not be exceeded when the nozzle losses are added. The pressure drop for a "Version II" arrangement is shown in Figure 14. For the cases considered, the pressure drop for 2% flow maldistribution is higher than the corresponding Version I. Also, for outlet manifold diameters less than about 6 inches, the calculations indicated that flow reversals could occur. Fraas (Reference 6) discusses the circumstances under which flow reversals will occur.

Based on the results of the calculations, the Version I nozzle arrangement and a 6-inch inlet manifold were selected. Based primarily on manufacturing reasons, a 6-inch outlet manifold diameter was selected, even though the minimum ΔP occurs at about 7-inches. The difference in $\Delta P/P$ between the 6-inch and 7-inch outlet manifold diameters is only about 0.07% which is negligible.



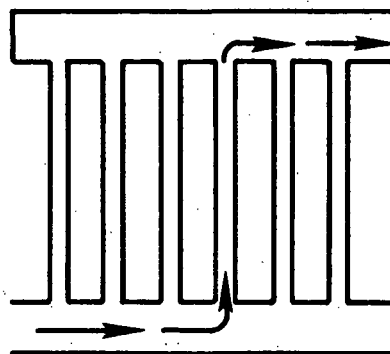
Inlet Manifold Pressure



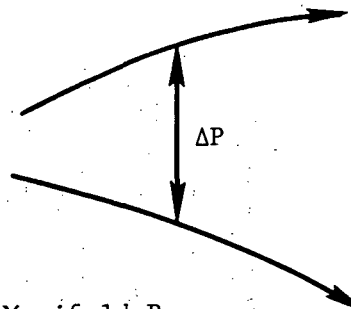
Outlet Manifold Pressure

Version I

Exit In-Line
With Entrance



Inlet Manifold Pressure



Outlet Manifold Pressure

Version II

Exit Opposite
Entrance

Figure 11. Gas Tube Pressure Drop vs. Nozzle Orientation.

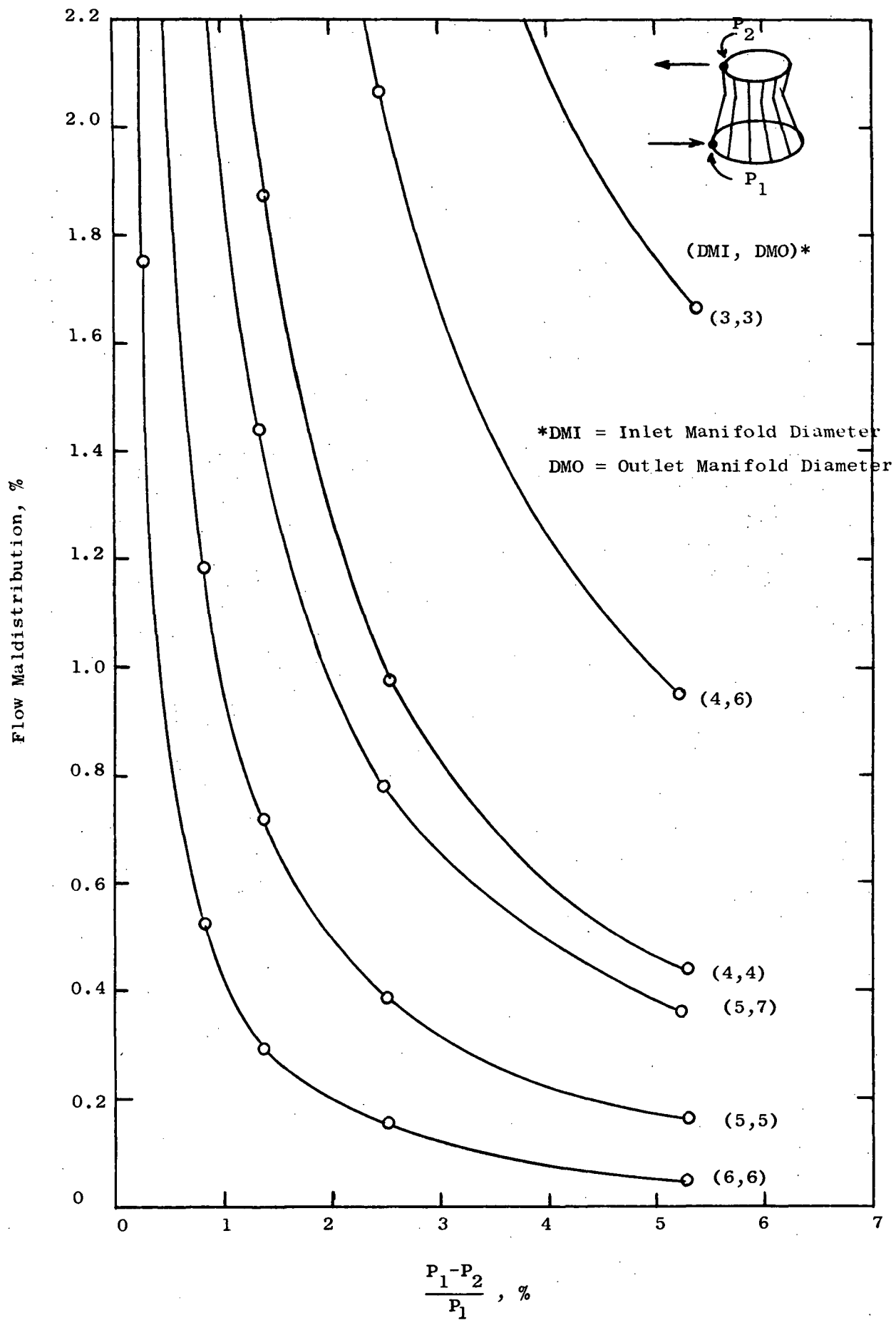


Figure 12. Flow Maldistribution vs. $\frac{\Delta P}{P}$.

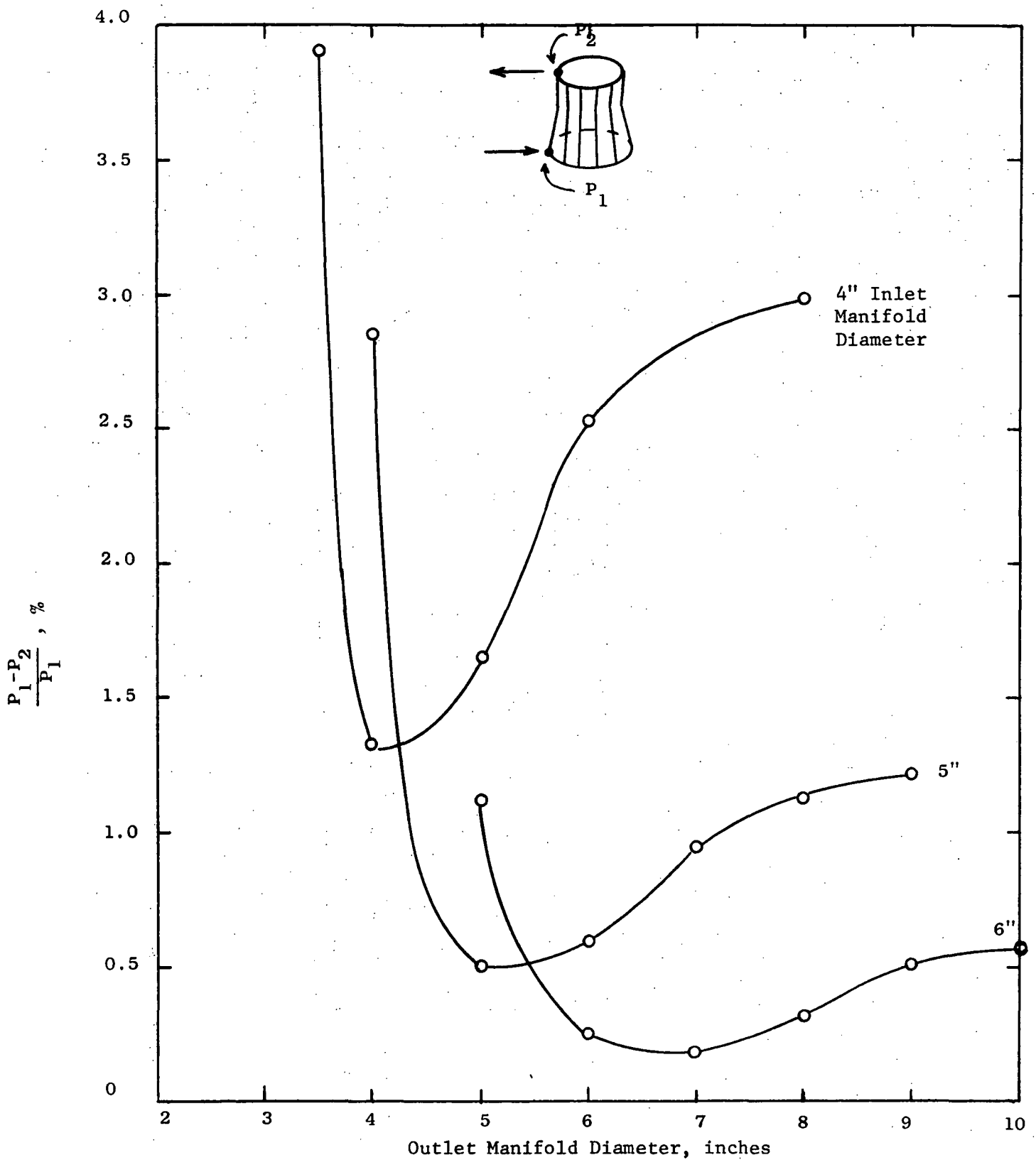


Figure 13. $\frac{\Delta P}{P}$ Versus Outlet Manifold Diameter for In-Line Ducts With 2% Flow Maldistribution.

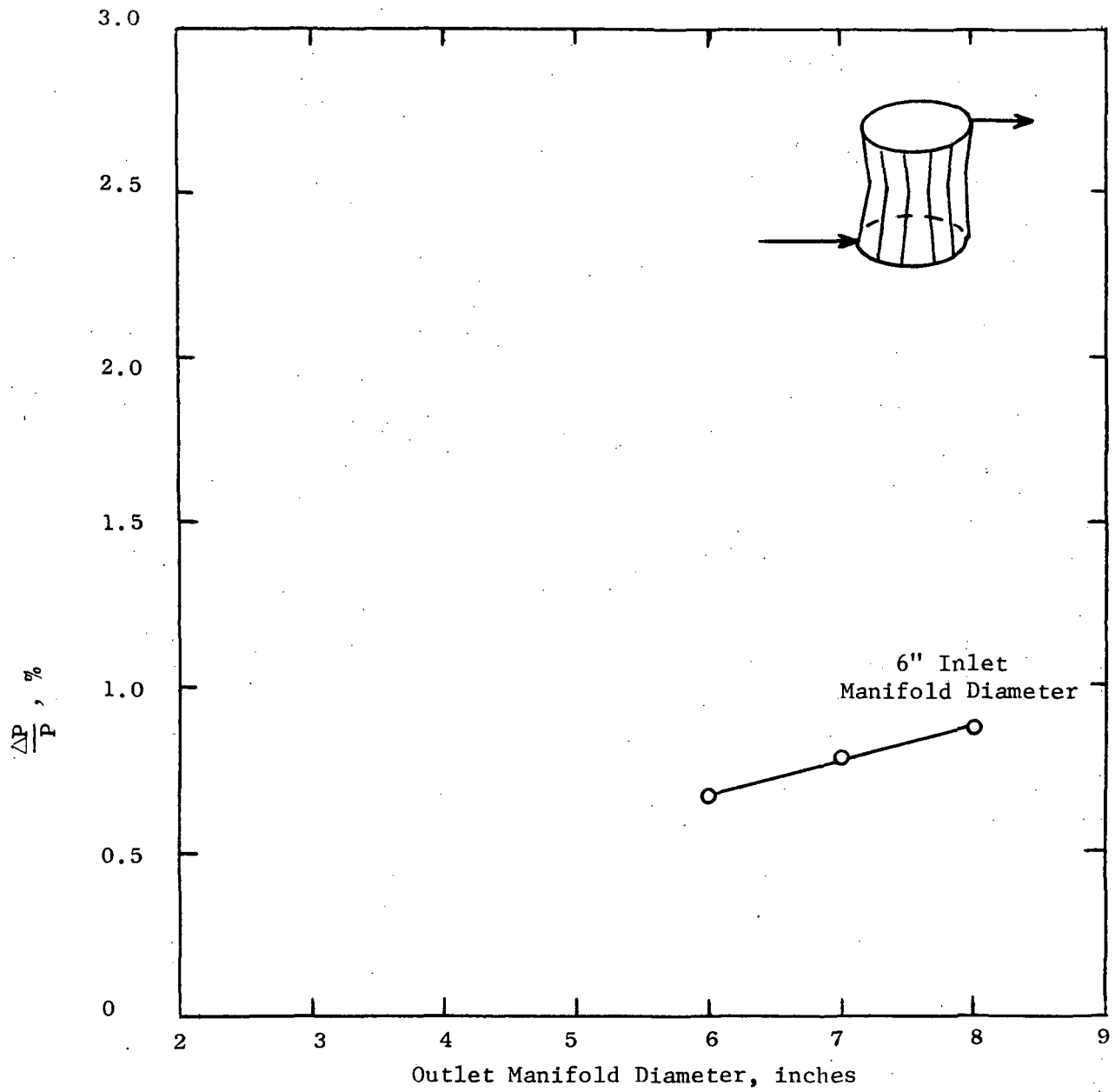


Figure 14. $\frac{\Delta P}{P}$ Versus Outlet Manifold Diameter for Opposed-Ducts With 2% Flow Maldistribution.

Inlet and Exit Losses - The gas entering the receiver undergoes losses due to a 90° bend and an abrupt expansion as it enters the inlet manifold. Similarly, the gas suffers an abrupt contraction loss and another 90° bend loss as it leaves the outlet manifold. These losses were calculated from

$$\Delta P = K \frac{\rho V^2}{2g_c} \quad (2)$$

The loss coefficient, K, was taken to be 1.0 for the expansion loss and 0.5 for the contraction loss. Figure 15 is a plot of these losses as a function of the diameter of the pipe at the manifold. The pressure drops are expressed as a percentage of the inlet pressure of 53.92 psia. As will be discussed later (Section 3.3.2) 3-inch diameter bimetallic joints were selected based primarily on anticipated reliability improvement as compared with larger sizes. If the inlet and outlet pipes at the manifolds were 3-inches, the corresponding losses would be 0.8% and 0.5%, respectively, for a total of 1.3% out of the 2% allowed. In order to reduce the pressure drop, the decision was made to provide a 3-inch to 4-inch diffuser section at the inlet, thus reducing the inlet expansion loss from 0.8% to 0.25%.

For the 90° Bends, a loss coefficient of 0.3 (Reference 7) was used. The resulting inlet and outlet bend losses are 0.237% and 0.298%, respectively. Table III is a summary of the gas pressure losses in the receiver. Each of the gas tubes was provided with an orifice to further assure uniform flow distribution. The total loss for 100% flow and orifices in all the tubes is calculated to be 1.938% which is less than the 2% specification maximum.

3.3.2 Mechanical Design

Bimetallic Joints - Since the bimetallic joints were long lead-time items, they had to be sized and ordered early in the program. The specifications called for coextruded Cb-1%Zr-to-300 series stainless steel transition elements (bimetallic joints). Figure 16 shows the design of the coextruded joints. The selection of a 3-inch inside diameter was a compromise between joint reliability and gas pressure drop. Joint sizes ranging from 2-inches to 4.5-inches were considered.

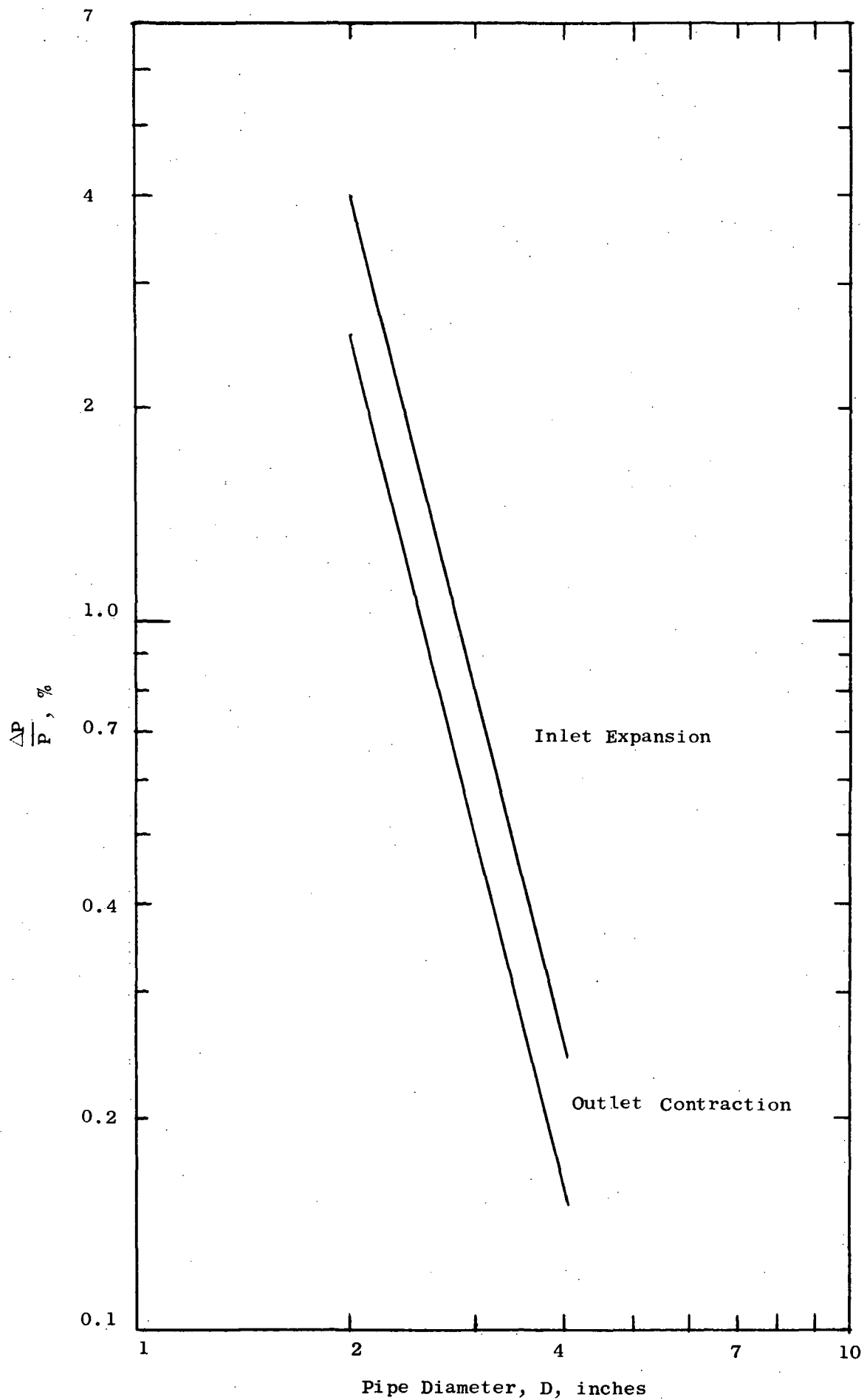


Figure 15. Inlet Expansion and Outlet Contraction Losses.

TABLE III

TABULATION OF GAS PRESSURE LOSSES

TOTAL ALLOWABLE LOSS = (53.92) x (.02) = 1.078 PSI

	<u>100% Flow</u>		<u>50% Flow</u>
	<u>No Orifices</u>	<u>With Orifices</u>	<u>With Orifices</u>
90° Bend Loss at Inlet	0.237%	0.237%	0.059%
Inlet Diffuser Loss	0.022%	0.022%	0.0056%
Expansion Loss from 4" Inlet to 6" Inlet Manifold	0.252%	0.252%	0.063%
Loss Across Tubes	0.430%	0.645%	0.171%
Contraction Loss from 6" Manifold to 3" Outlet Pipe	0.482%	0.482%	0.121%
90° Bend Loss at Outlet	<u>0.299%</u>	<u>0.299%</u>	<u>0.074%</u>
Total Loss	1.723%	1.938%	0.493%
Maximum Flow Maldistribution	0.64%	0.41%	0.44%
Maximum Pressure Variation Within a Manifold	0.023%	0.023%	0.0056%
Orifice Size	None	0.72 in.	0.72 in.

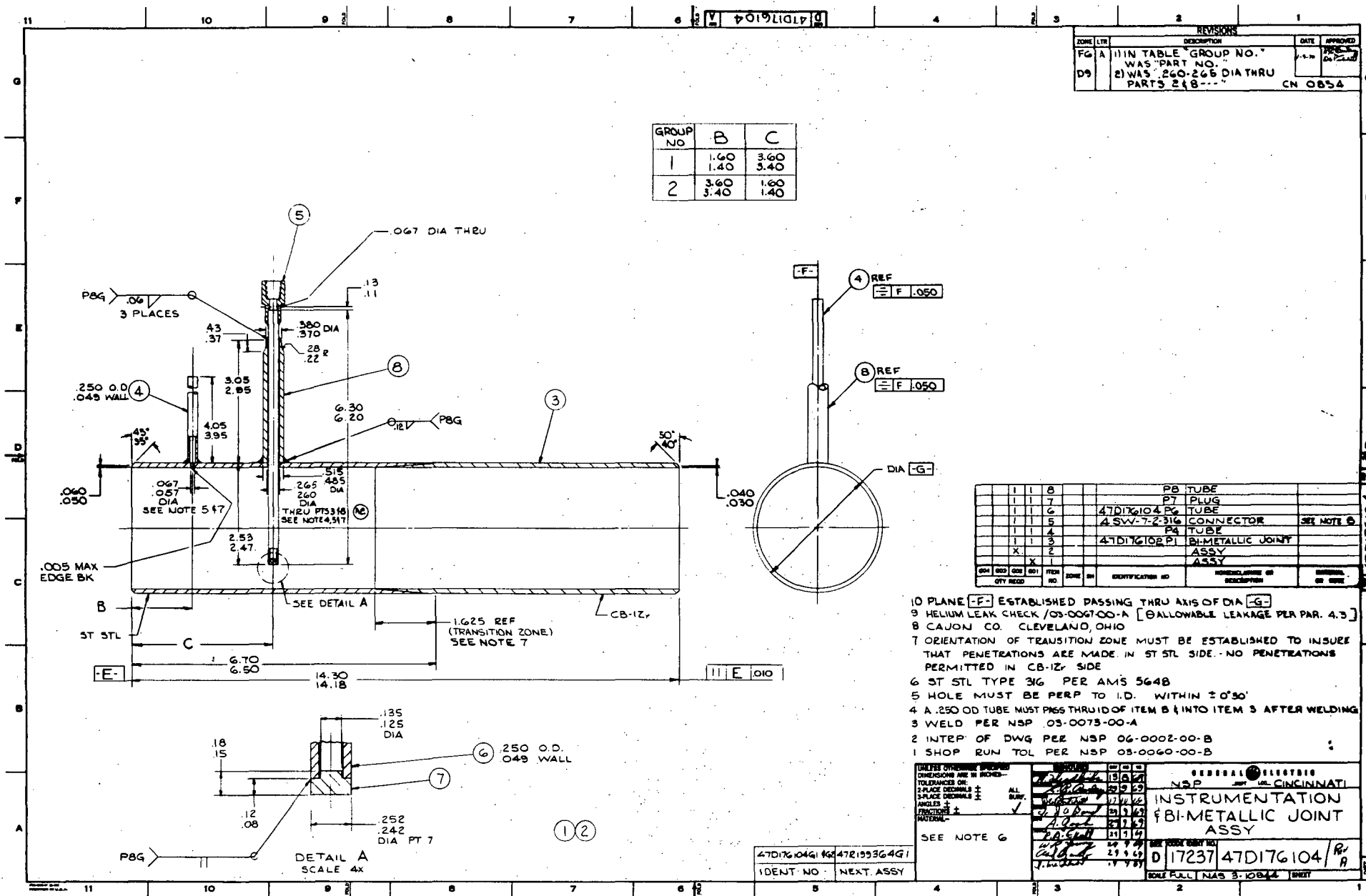


Figure 16. Bimetallic Joint Assembly. (Dwg. No. 47D176104)

Although very little reliability data was available, it was felt that the smaller diameters would be more reliable. Further discussion relative to the basis for specifying Type 316 for the 300 series stainless portion is presented in Section 4.2.1.

The wall thickness for the joints was selected on the basis of creep for sustained high temperature operation. The primary stress on the joints is hoop stress due to the internal gas pressure. The maximum gas temperature is 1500°F at the outlet. The allowable hoop stress was taken to be 80% of the stress for 1% creep in 5 years at a temperature of 1500°F. This allowable stress was taken to be 900 psi. For an allowable stress of 900 psi and a gas pressure of 54 psia, the minimum wall thickness required is 0.090-inches. Based on the above stress criterion, the inlet joint could have been thinner, since it runs at a temperature of 1100°F. Practical considerations, however, indicated that both joints should be the same size.

Manifolds - The gas manifold sizes for the heat receiver were established at the preliminary design review as follows:

	<u>Inlet Manifold</u>	<u>Outlet Manifold</u>
Inside Diameter, Inches	6	6
Torus Diameter, Inches	66	58

The inside diameters were chosen on the basis of the gas flow analysis as discussed above. The torus diameters were specified by NASA. The manifold wall thickness was determined according to the ASME code for unfired pressure vessels (Reference 8). Openings in pressure vessels weaken the basic vessel. In order to provide adequate strength, the opening may be reinforced or, alternatively, the pressure vessel may be made thicker than that required for the same vessel without openings. Comparison of manufacturing costs for the two methods led to the selection of the latter method particularly since quantity production was not required. The following values were used:

1. Welded joint efficiency = 0.8
2. Allowable stress = 3000 psi
3. Internal pressure = 54 psia

Using these values, the calculated minimum wall thickness for a cylinder

with no openings is 0.068-inches (the effect of the torus configuration adds about 6% for the dimensions of the receiver). The procedure for determining the wall thickness with openings is given in Reference 8. The resulting minimum wall thickness was calculated to be 0.120-inches.

Gas Tube Extensions - Without some sort of support structure, the gas system would collapse during a launch environment. During operation, however, the gas tubes and support structure will, in general, operate at different temperatures. This could lead to excessive stresses due to differential thermal expansion. During the preliminary design, several schemes for accommodating the differential expansion were considered. The final solution was to make the gas tubes flexible enough to accommodate the differential thermal expansion by incorporating reduced-diameter tube extensions at the tube outlets.

The mathematical model used in the preliminary design analysis considered the support structure as a rigid member. A deflection, δ , equal to the differential thermal expansion was then imposed on the gas tube as shown in Figure 17. The tube ends were assumed fixed. The maximum stress occurs at the upper end. Figure 17 is a plot of calculated maximum bending stress per unit temperature difference ($\sigma_b/\Delta T$) as a function of tube extension length with extension tube diameter as the parameter. Examination of the calculated temperature distributions indicated that a typical value of temperature difference was about 100°F. A 9-inch long tube extension with a 0.75 OD x .025 wall was selected. This results in a bending stress of about 4000 psi for a ΔT of 100°F. Figure 18 is a plot of calculated maximum bending stress in the selected tube extension as a function of temperature difference.

Effect of Shell on Gas Tubes - The design and analysis of the shell is discussed in the following section. The final shell design is rigid relative to the tubes such that any thermal expansion of the shell will be transmitted to the tubes. Since the temperatures vary periodically during a sun-shade cycle, an analysis was made to determine the cyclic stress imposed on the tubes due to differential thermal expansion between the shell and tubes. The thermal expansion of the shell was first calculated as a function of time during a typical sun-shade cycle. These thermal deflections, along with tube temperature distributions, were used

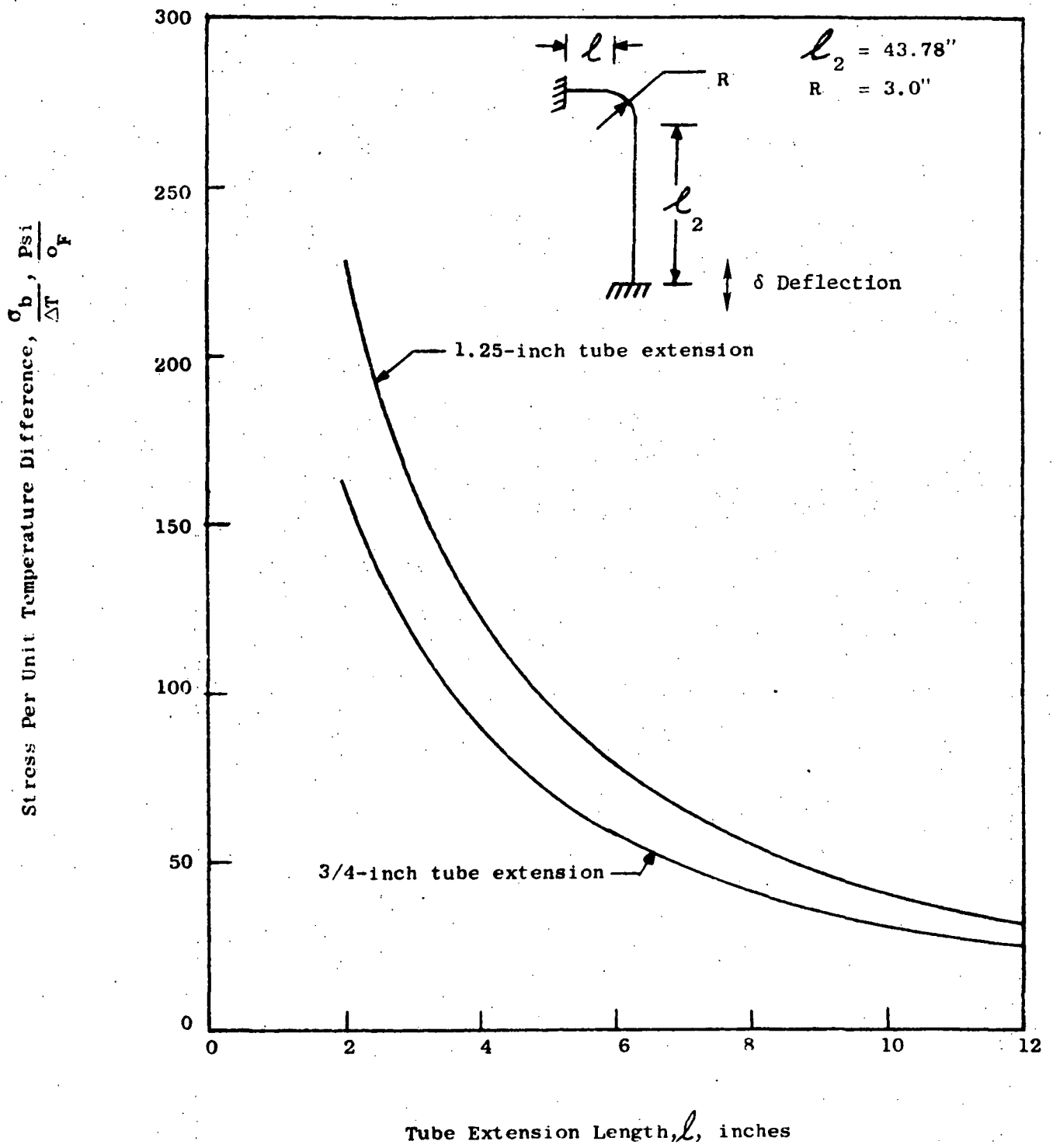


Figure 17. Gas Tube Stress Versus Tube Extension Length.

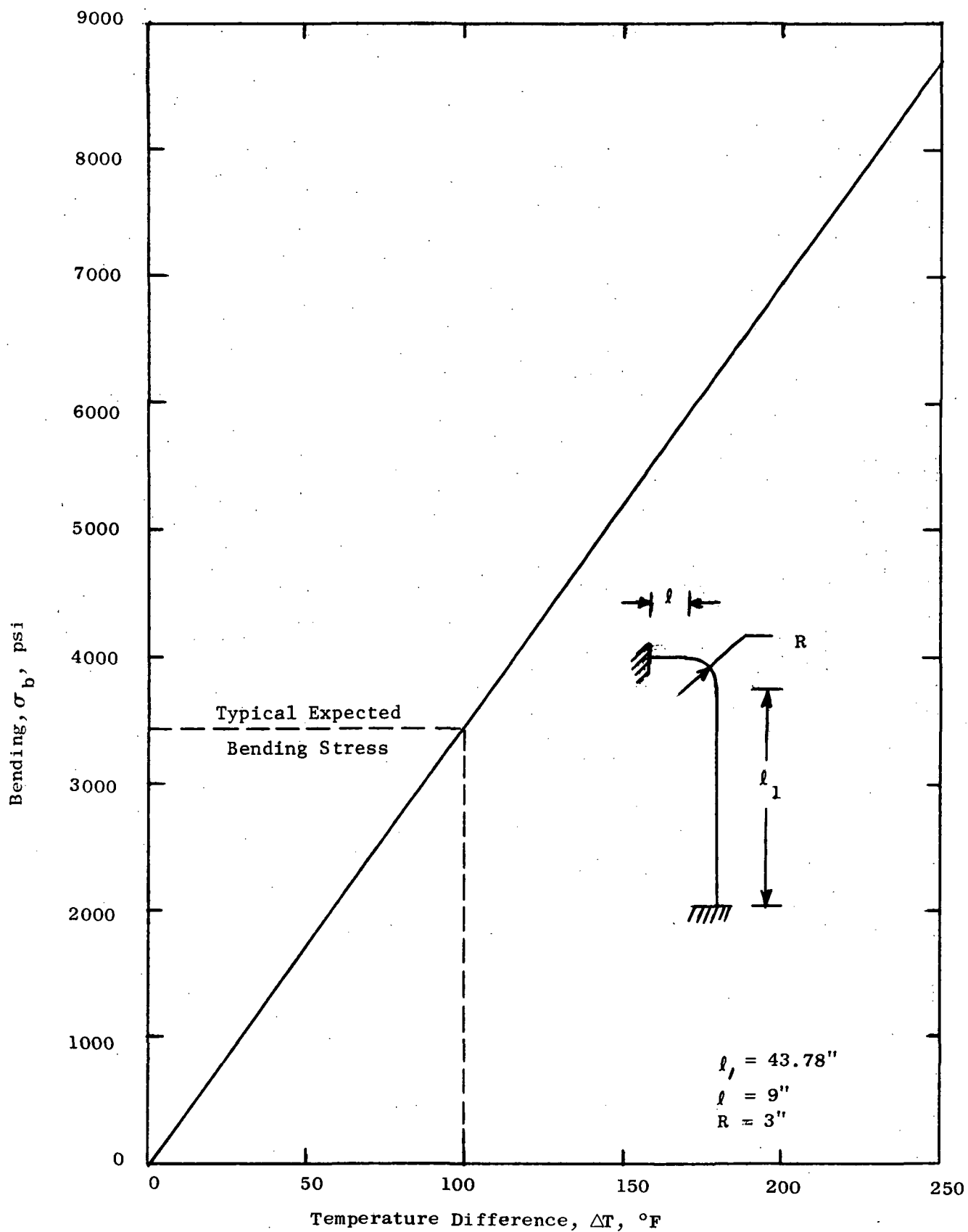


Figure 18. Gas Tube Stress vs. Shell-Tube Temperature Difference.

as input to the MASS computer program (Reference 9) which calculated the corresponding gas tube stresses. Figure 19 is a plot of temperature and corresponding stresses for the two most highly-stressed points in the gas tubes near the outlet. The average stress is on the order of 1400 psi and the alternating stress is less than 400 psi.

3.4 SHELL DESIGN

Figure 10 shows the shell design features and Figure 3 illustrates how it attaches to the gas system assembly. The functions of the shell are: (1) to provide structural support for the gas system assembly and (2) to form the envelope of the receiver cavity. Basically, the shell is assembled from six sheet metal panels (.04-inch thick) which are bolted together along longitudinal flanges to form a shell-of-revolution. Reflectors (or gutters), attached to the inner surface of the shell, direct the radiation passing between the tubes to the back of the tubes. The shell assembly is attached to the gas system assembly by bolting to the inlet and outlet manifolds. The longitudinal and circumferential flanges of each panel section are riveted to the 0.040 thick sheet metal. The lower portion of the shell is a truncated cone which encloses the contour formed by the outer extremities of the gas tube convolutions. The upper portion of the shell is another truncated cone which makes an angle of 45° with the receiver centerline. These two cones are connected by a toroidal transition section. The following discussion outlines the design analyses which were performed.

3.4.1 Launch Conditions

The most significant inertial load requirement is the 20 g "half-sine" acceleration pulse with a 100 millisecond duration. The shock spectrum approach was used to evaluate the inertial response. The shock spectrum corresponding to the 100 millisecond pulse is shown in Figure 20 where the spectrum corresponding to 10% of critical damping was used for purposes of design. From this it was estimated that about 30 g's is representative and this value was used in evaluating the inertial loading upon the design.

Buckling Strength - For this analysis, the shell was approximated as being made up of two truncated cones whose generators make angles of 21° and 45° with the receiver centerline. The buckling strength of each

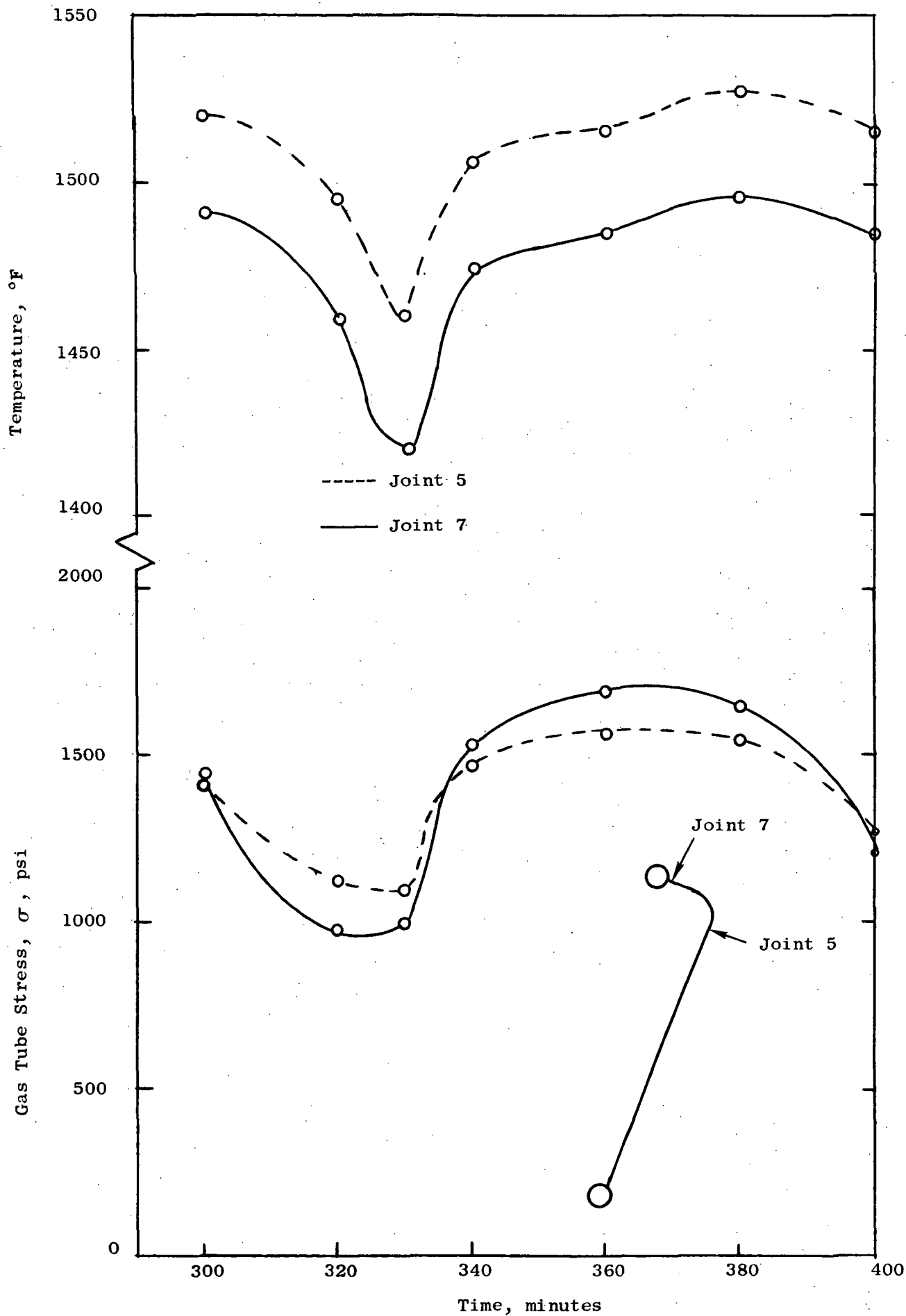


Figure 19. Gas Tube Stress as a Function of Time.

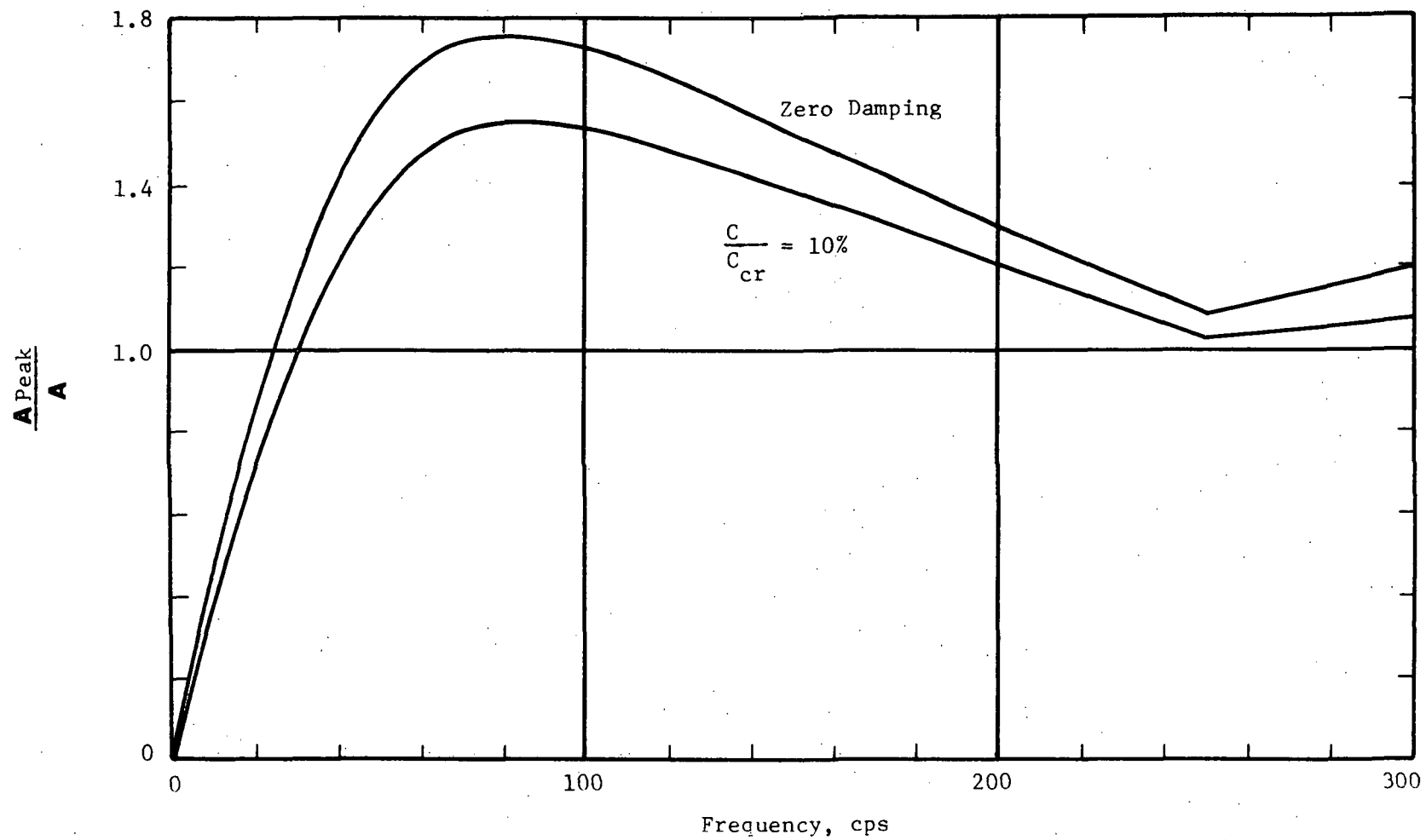


Figure 20. Shock Spectrum for 100 Millisecond Half Sine Acceleration Pulse.

of these cones was calculated and the smaller value was assumed to be the shell buckling strength.

The buckling load of a truncated cone was estimated from (Reference 10)

$$P = (P_{cyl\infty}) \cos^2 \alpha \quad (3)$$

where $P_{cyl\infty}$ is the buckling load of an infinite cylinder with the same thickness. From Reference 11,

$$P_{cyl\infty} = 2\pi [0.3E] t^2 \quad (4)$$

Figure 21 is a plot of calculated buckling loads of the two cones as a function of shell thickness. The weight of the outlet manifold and top closure is about 300 pounds, which results in a 30 g shock load of 9000 pounds. For a thickness of 0.04-inches, the buckling load of the 45° cone is about 24,000 psi, which is a factor of safety of about 2.7 with respect to an applied load of 9000 pounds.

Launch Stresses - The stresses induced in the shell by a 30 g shock load were studied as a function of shell thickness. The calculations were performed with a computer program (Reference 12) which determines elastic stresses and displacements in assemblies of axi-symmetrically loaded shells of revolution. Figures 22 through 25 show the calculated shock-induced stresses in the shell as a function of position and shell thickness. Shell thicknesses of .02, .03 and .04 inches were considered. The largest stresses occur in the toroidal transition section which connects the two conical sections. On the basis of these calculations and on the buckling analysis, a shell thickness of 0.04 inches was selected. The final weight of the outlet manifold and the top closure was about 40% higher than that for which these calculations were made, resulting in a maximum hoop stress of about 15,000 psi. This is within the allowable stress of 19,500 psi established for the launch condition. The stiffening effect of the longitudinal flanges was neglected in the buckling and launch stress calculations, thereby indicating additional conservatism in the analyses.

3.4.2 Thermal Stresses in Shell

The thermal stresses in the shell were calculated with the shell-of-revolution computer program. The temperature distribution supplied by

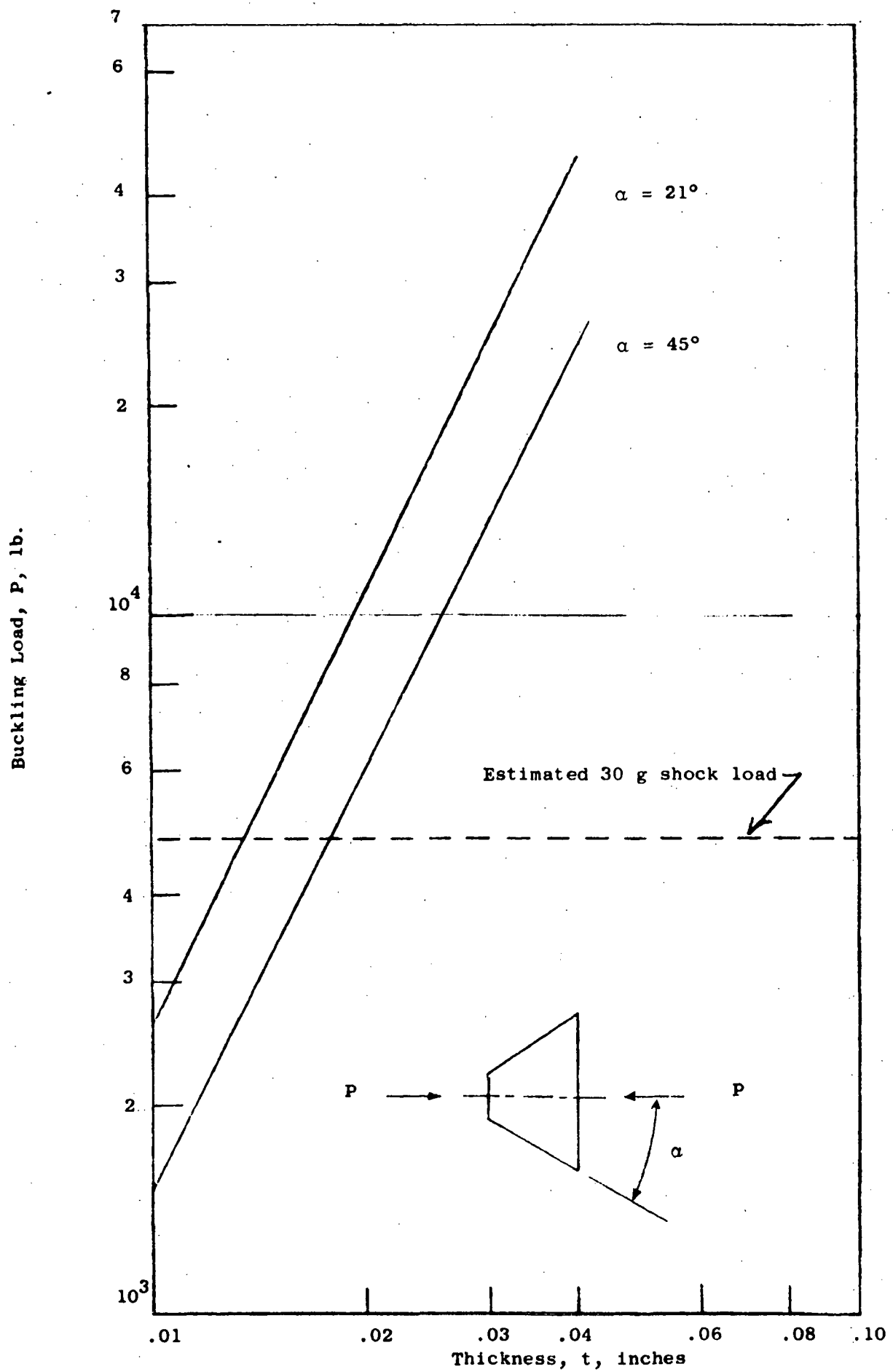


Figure 21. Buckling Loads of Truncated Cones Due to Axial Compression.

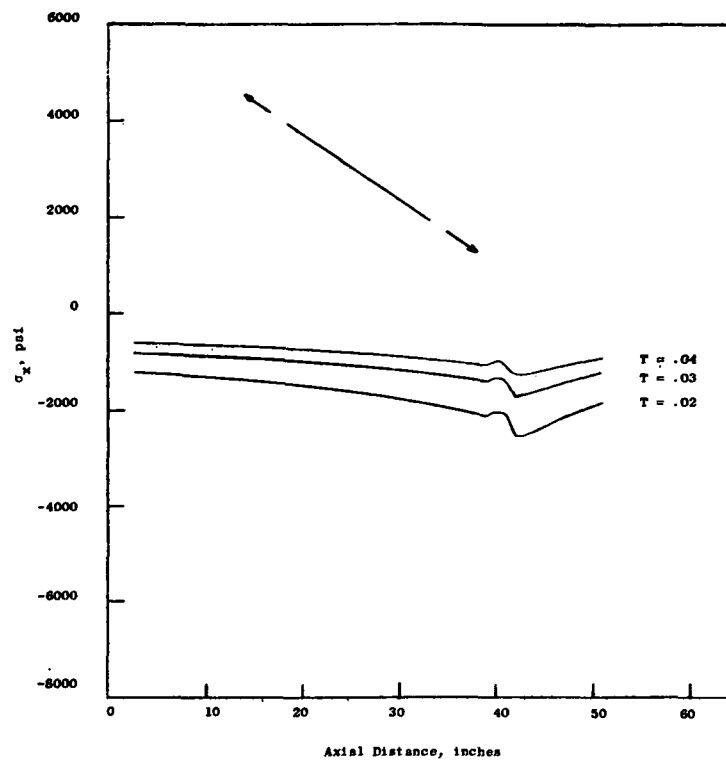


Figure 22. Membrane Stress Along the Meridian for 30 g Shock Load.

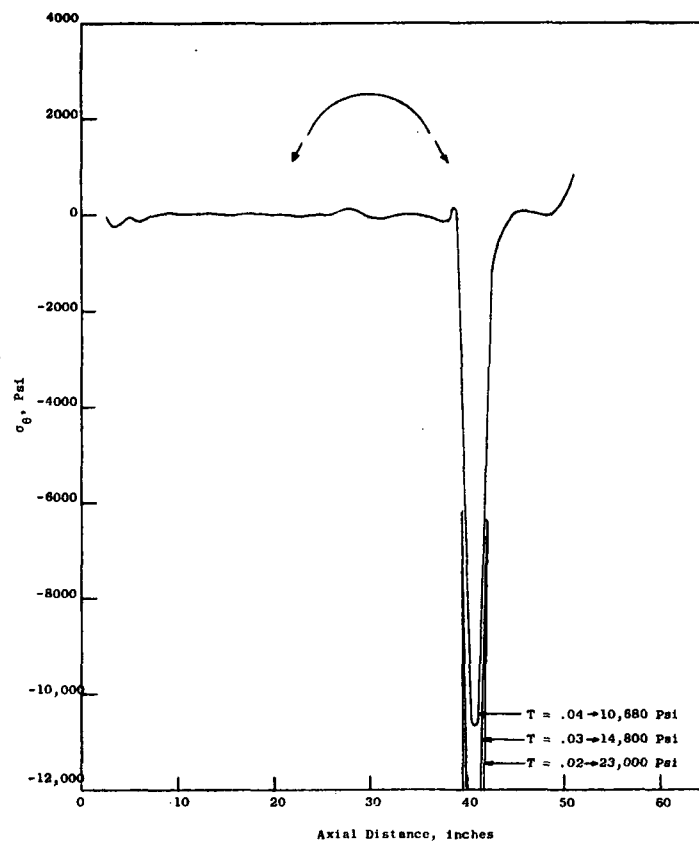


Figure 23. Hoop Stress for 30 g Shock Load.

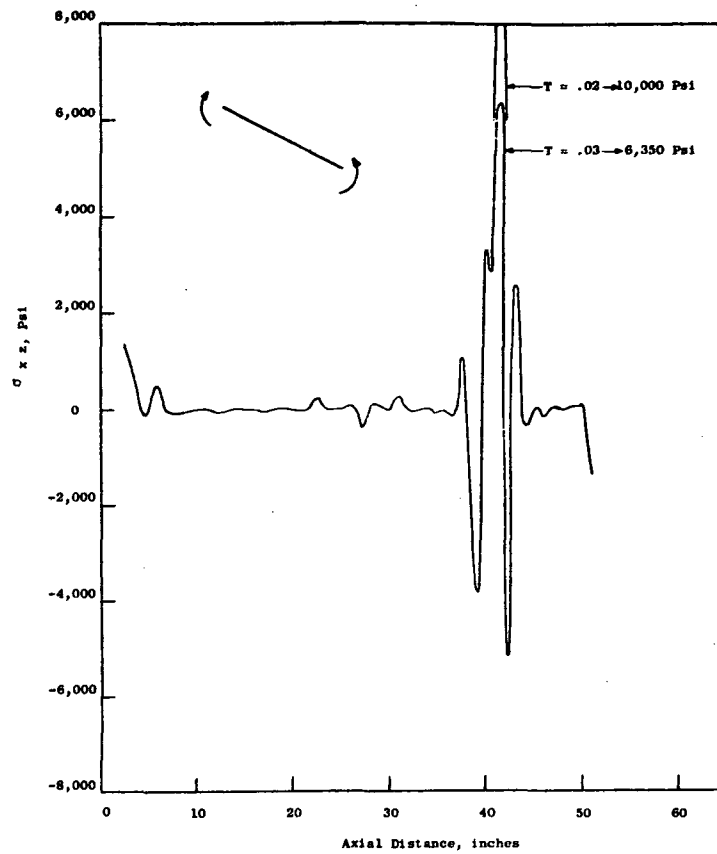


Figure 24. Bending Stress Along the Meridian for 30 g Shock Load.

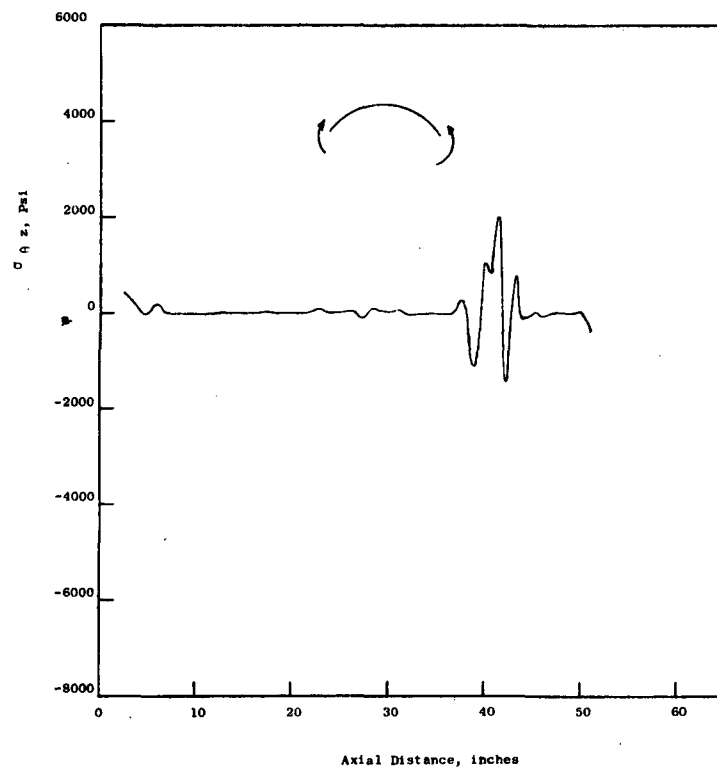


Figure 25. Bending Stress in the Hoop Direction for 30 g Shock Load.

NASA was used as input for the thermal stress calculations. Figure 26 shows typical steady-state and transient temperature distributions in the shell. The corresponding stress distributions are shown in Figures 27 through 34. The highest stress occurs near the inlet manifold during the start-up transient. This stress is well within the allowable thermal stress of 12,000 psi.

3.5 TOP CLOSURE

Design of the top closure assembly can be seen in Figure 10. This assembly completes the cavity enclosure and is fabricated entirely from Cb-1Zr. Initially, the design incorporated six local pads on the outer periphery. These pads were to have been the mounting points for the assembly. As described later in Section 6.4, fabrication problems required a design revision which incorporated a reinforcing plate around the entire periphery.

An analysis was performed to determine an optimum contour of the top closure such that heat losses from the aperture are minimized. The analysis consisted of graphical ray tracing techniques and yielded a contour with two cone angles. While the top closure contour has only a small effect on total heat loss, its effect on temperature distribution is significant. Since all temperature distribution studies were made assuming the preliminary design contour, NASA directed that it be retained in the final design.

The top closure is attached to the outlet manifold through flexure plates similar to the aperture assembly attachment. The design procedure for the top closure flex plates and the aperture assembly flex plates was the same and will be outlined in Section 3.6.4. Examination of the calculated structure temperature distributions revealed that a maximum temperature difference between the top closure and the outlet manifold was about 1000°F during a start-up transient. This Δt was used in the flex plate design. Although the flex plates are in tension during a ground test, the direction of loading during launch is unknown and, hence, the plates were designed for compression. Based on the selection of Cb-1Zr material, results of the flex plate analysis are shown in Figure 35. The final design incorporates six groups of two plates per group. Each of the plates has a flex length of 4 inches, a thickness of 0.036 inches and corresponding width of 5 inches.

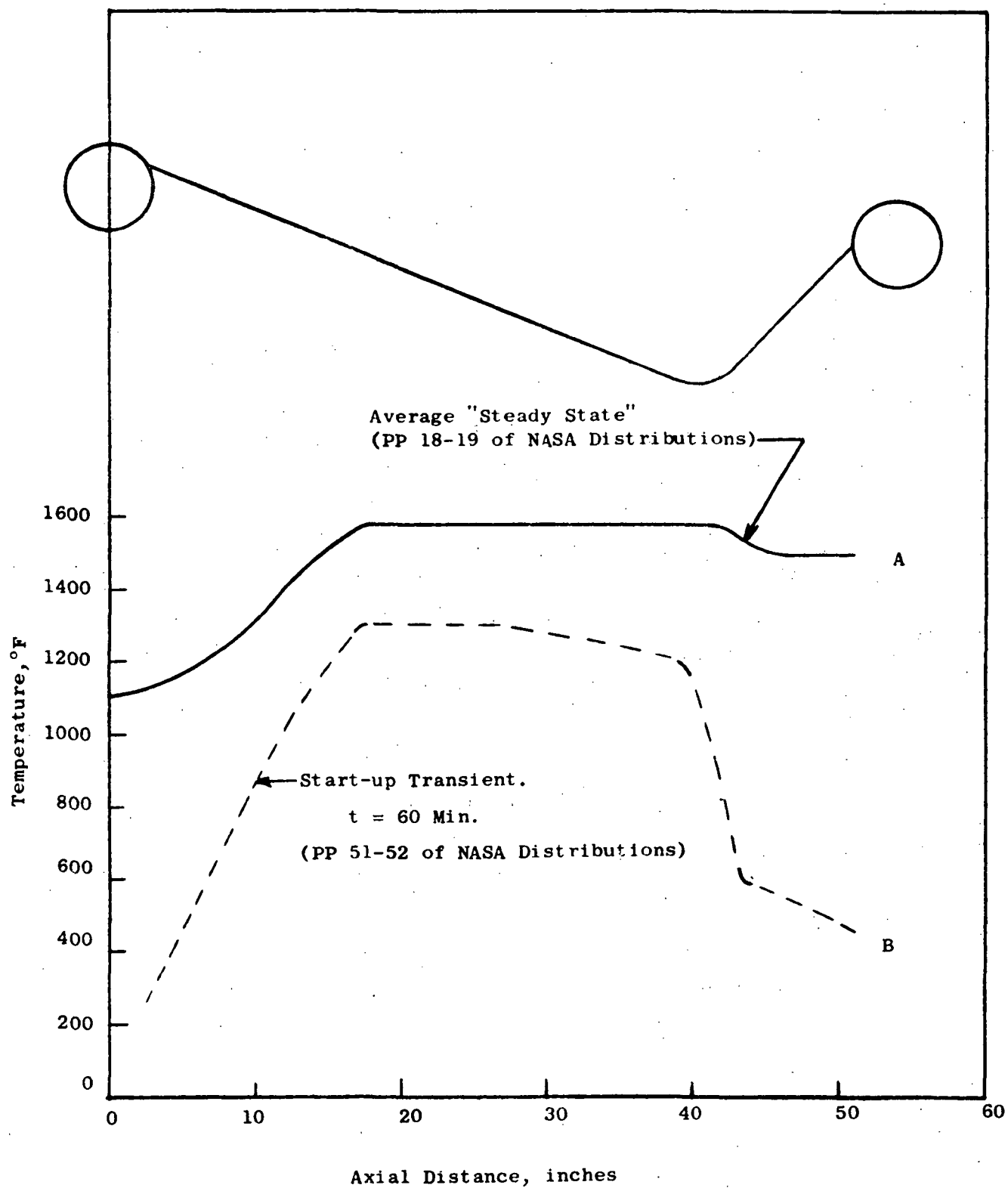


Figure 26. Temperature Distributions for Typical Thermal Cases.

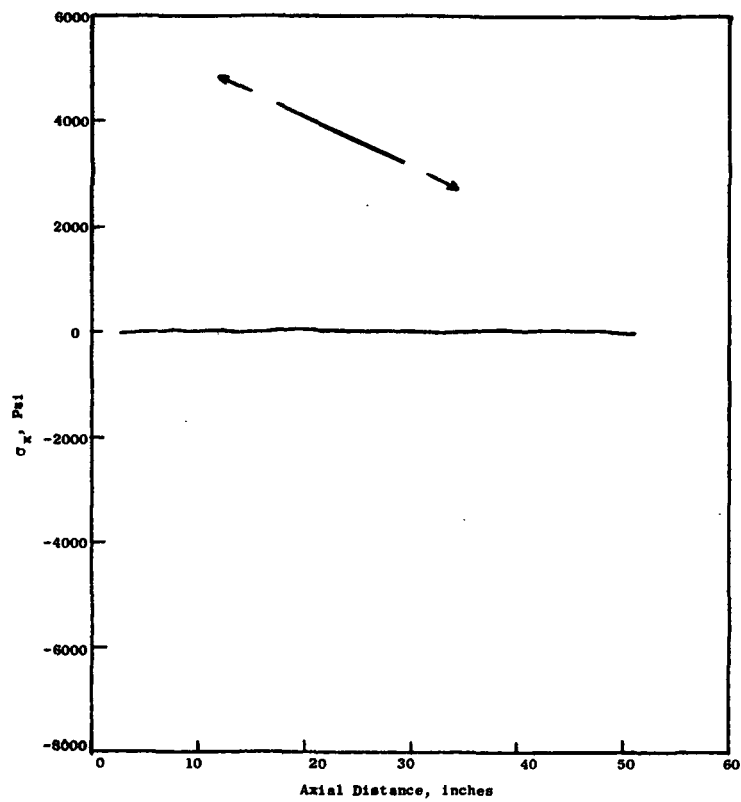


Figure 27. Membrane Stress Along the Meridian for Temperature Distribution A.

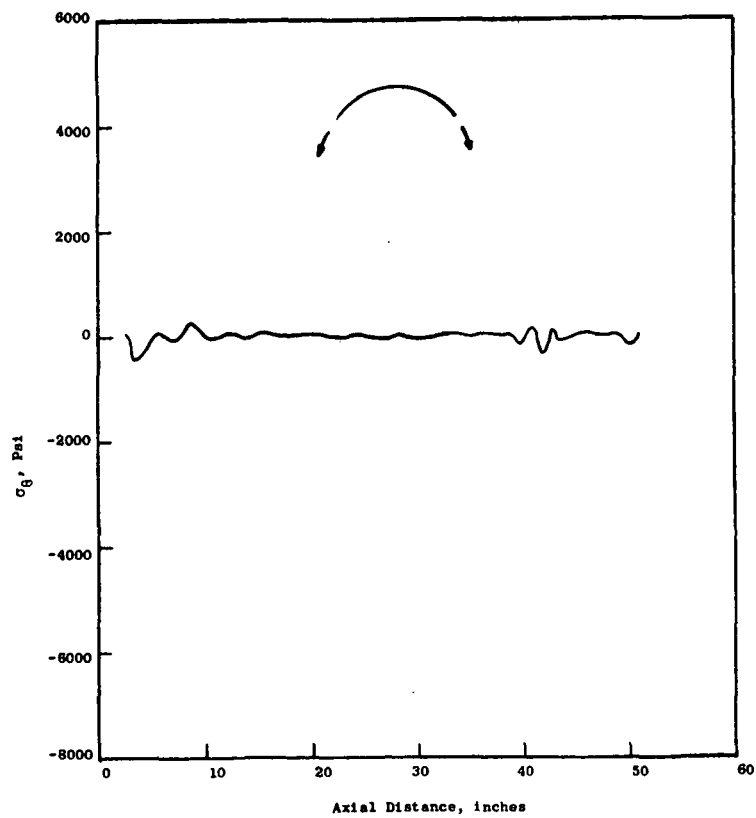


Figure 28. Hoop Stress for Temperature Distribution A.

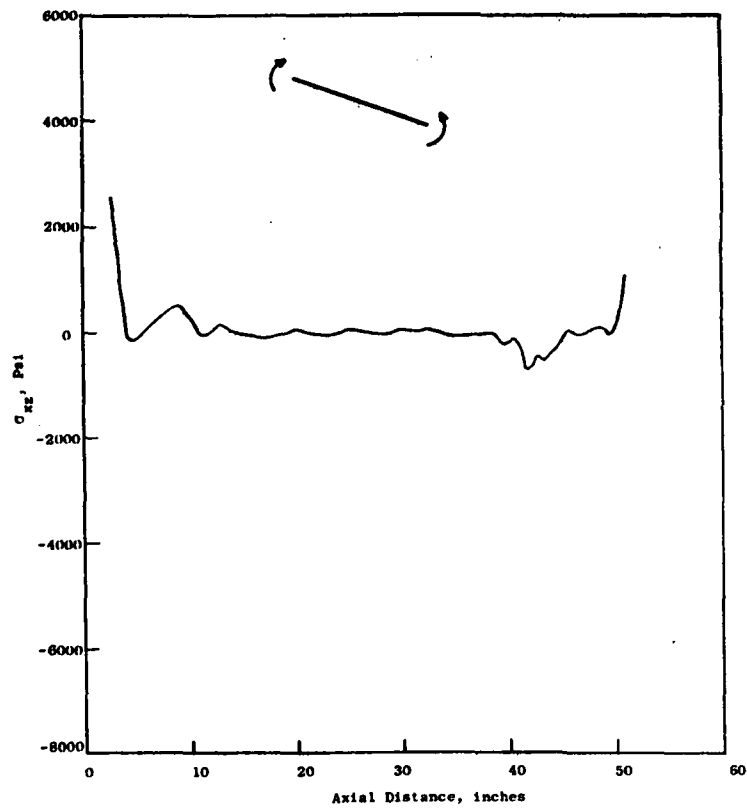


Figure 29. Bending Stress Along the Meridian for Temperature Distribution A.

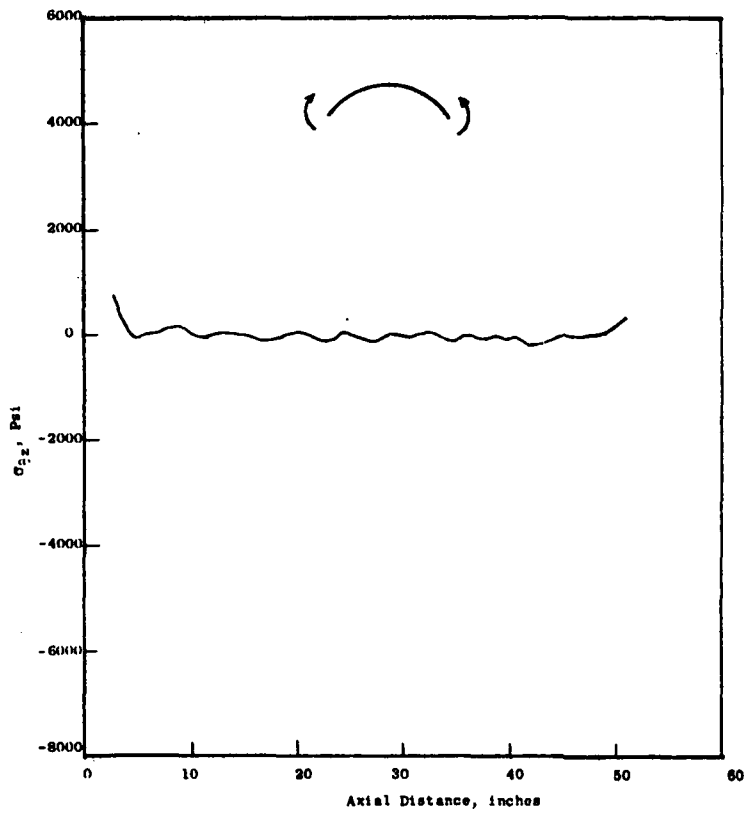


Figure 30. Bending Stress in the Hoop Direction for Temperature Distribution A.

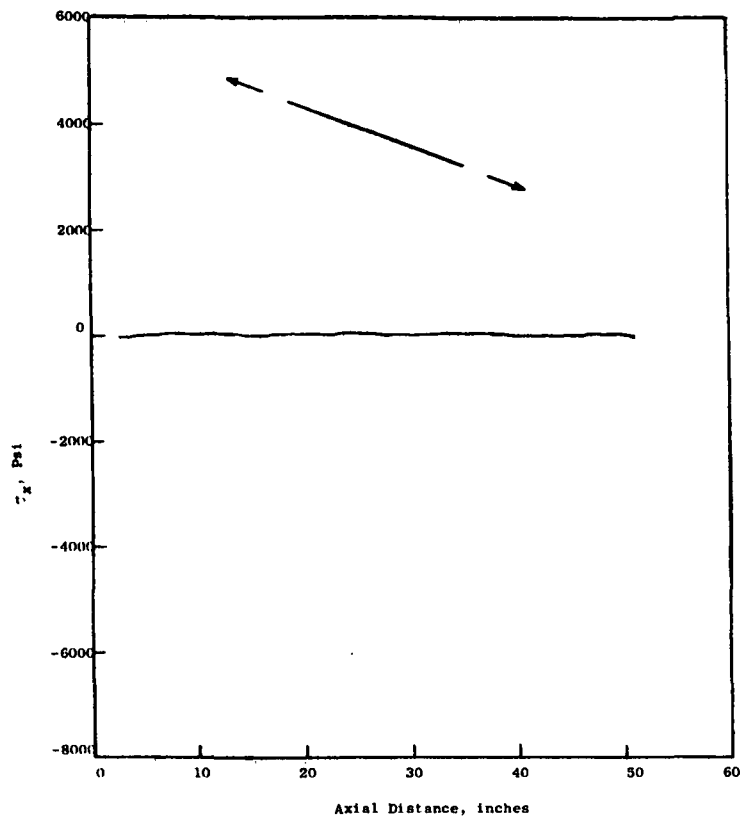


Figure 31. Membrane Stress Along the Meridian for Temperature Distribution B.

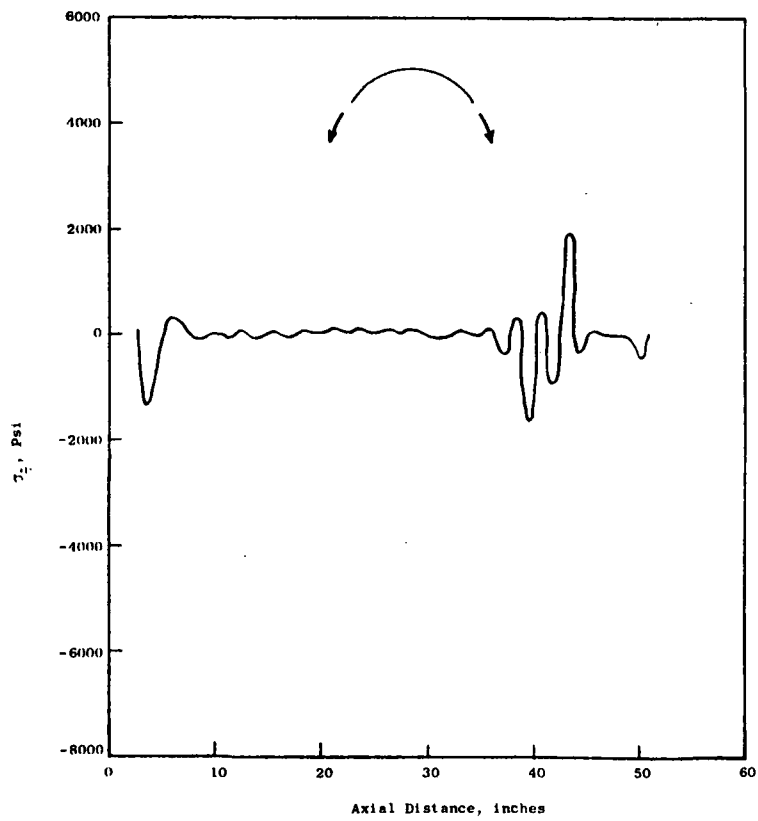


Figure 32. Hoop Stress for Temperature Distribution B.

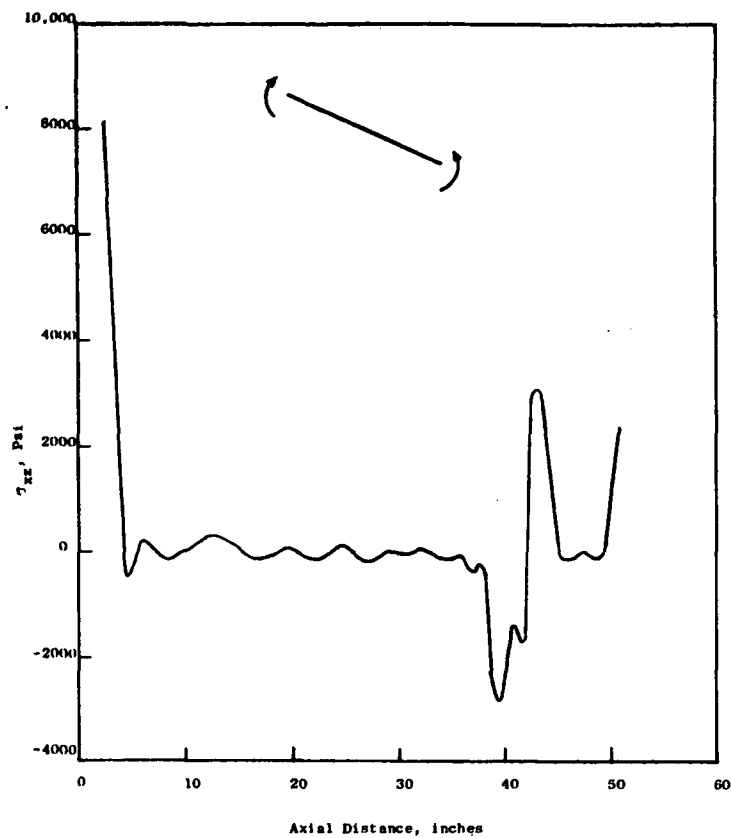


Figure 33. Bending Stress Along the Meridian for Temperature Distribution B.

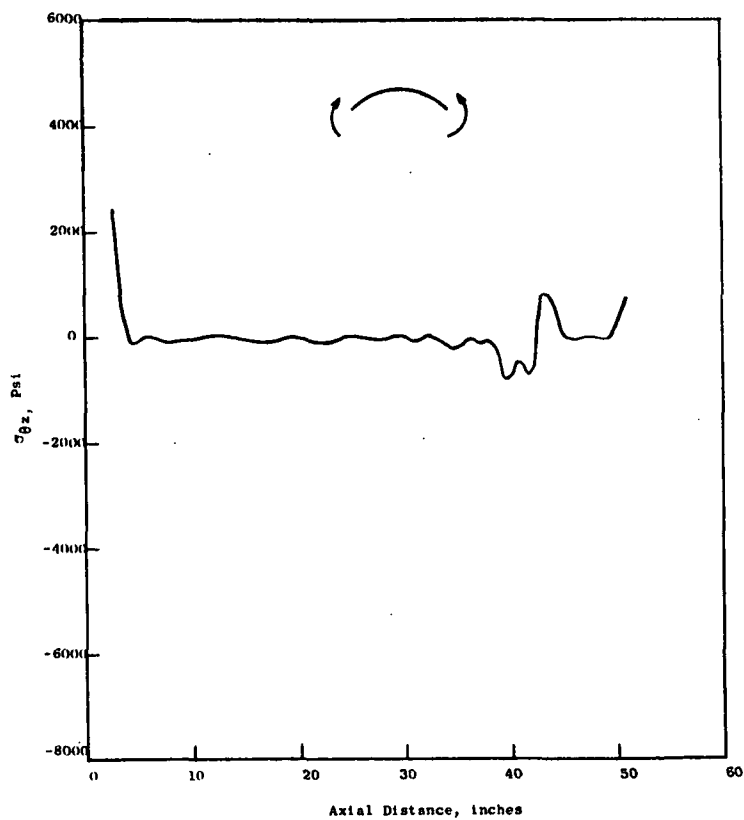


Figure 34. Bending Stress in the Hoop Direction for Temperature Distribution B.

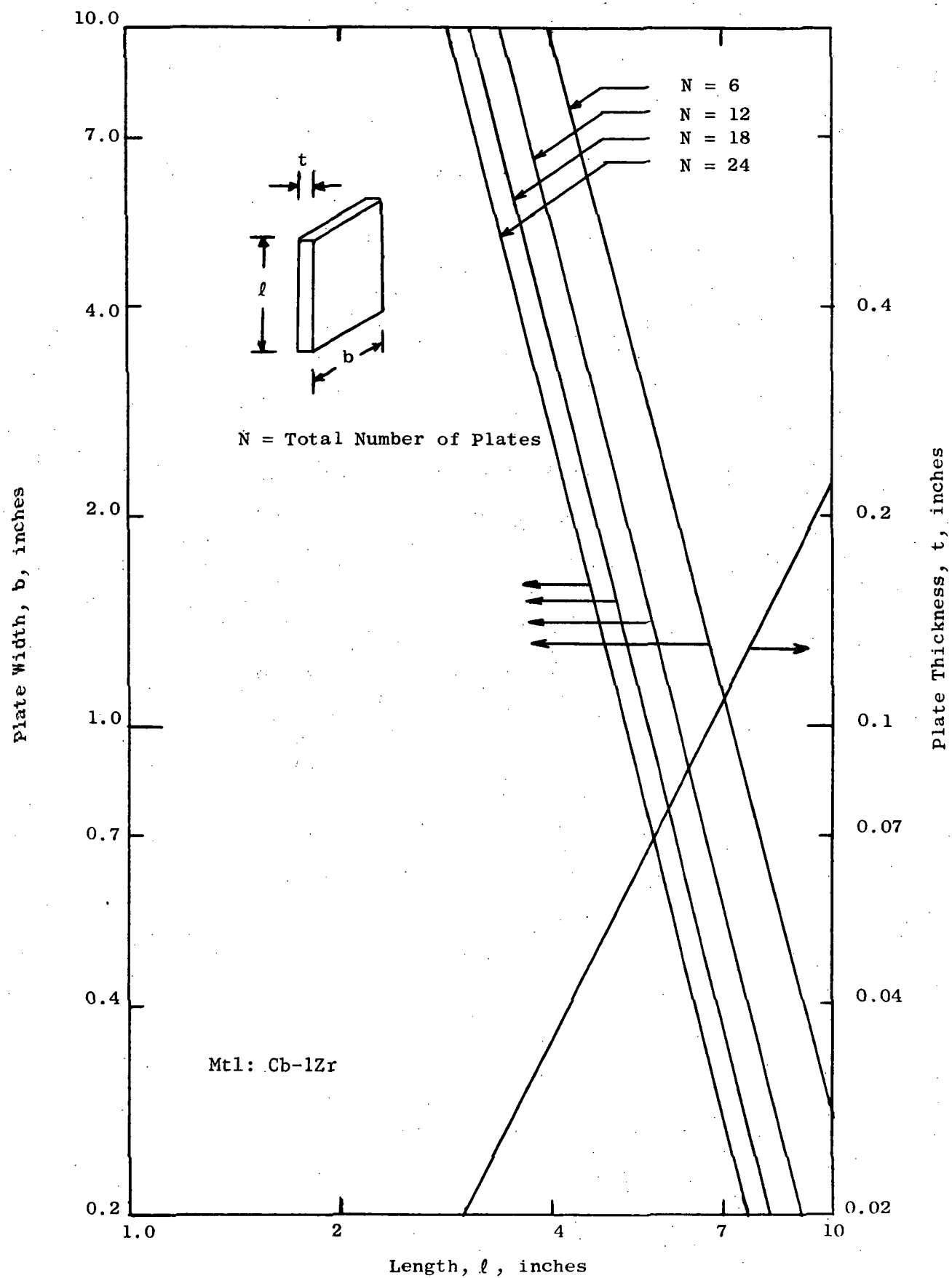


Figure 35. Top Closure Flex Plate Parameters.

3.6 APERTURE ASSEMBLY

The aperture assembly is attached to the inlet manifold and consists of the door and frame assembly, the aperture plate and the door actuators. The aperture plate contains a 14-inch diameter hole through which incident radiation from the mirror passes. The door and frame assembly makes up the lower envelope of the receiver cavity. The temperature within the cavity is controlled by opening and closing six doors whose motion is controlled by six electric actuators.

The aperture assembly of the NASA preliminary design had the form of a cone. Based on manufacturing considerations, the decision was made early in the program to make the aperture assembly in the form of a six-sided pyramid. The flat sides would thereby permit the door fit-up to be accomplished more easily. Figure 10 shows the final design of the assembly.

3.6.1 Thermal Considerations

The NASA preliminary design specified a thermal insulation system contained between the Cb-1Zr inner and outer surfaces of the heat rejection cone. The same configuration was also shown for the heat rejection doors. In effect the insulation was contained within shallow box-like structures. The insulation system itself was indicated as reflective foil separated by what would appear to be conduction type insulation material. The inner and outer surfaces overlapped each other but were separated by layers of Refrasil tape in an attempt to provide thermal isolation between the hot inner and cold outer surfaces. Refrasil tape was also indicated between mating surfaces of the brackets mounting the heat rejection cone to the lower manifold.

Some of the early concerns for the NASA preliminary design concept were related to the possibility of outgassing and material compatibility problems associated with the Refrasil type insulation material particularly as it would affect the Cb-1Zr alloy used extensively throughout the receiver. The shallow box-like structures were also a concern for several reasons as noted below:

1. Large potential heat losses caused by conduction around the edges.
2. Possibility for structure warpage due to the large temperature gradient across the box.

3. Entrapment of outgassing products.

In an effort to eliminate the problems itemized above a different design approach was considered. The insulation would be attached to the outer surfaces of the aperture assembly structure thereby substantially reducing the potential for heat loss. Since the entire structure would be located within the hot side envelope of the insulation, much more uniform temperatures could be expected throughout the structure. This would also minimize the possibility of door warpage or other distortions which could compromise the intended functions. Installing the insulation on the outside surfaces of the aperture structure appeared to be consistent with the approach NASA intended for the remainder of the heat receiver: the top closure and shell assembly.

A plot of aperture assembly heat loss as a function of average surface temperature is shown in Figure 36. In order to stay within a reasonably low heat loss limit of about 2 KW, the surface temperature must be less than about 500°F. Considering the need for mounting actuators, door hinges and other attachment members from the structure, significant local heat leaks would result. Recognition of this potential penalty led to the concept of attaching high temperature insulation to the inside surfaces of the aperture assembly such that the structure and its many attachments would operate at low temperature.

Operating the aperture structure at low temperature eliminated the need for Cb-1Zr refractory metal. Conventional stainless steel could now be used for the aperture assembly and most of its structural attachments since even local hot spots due to edge and insulation attachments are expected to be only 200°F higher than the average temperature of about 500°F. While there are many advantages with this approach, the problem of differential thermal expansion between the inlet manifold and the aperture assembly was made more severe. This problem was solved however, with the use of flex plate mountings as described subsequently.

The use of refractory metal in the aperture assembly was eliminated with the exception of the aperture plate. Figure 37 is a plot of the incident heat flux distribution in the plane of the aperture. The aperture diameter was determined by minimizing the net heat losses.

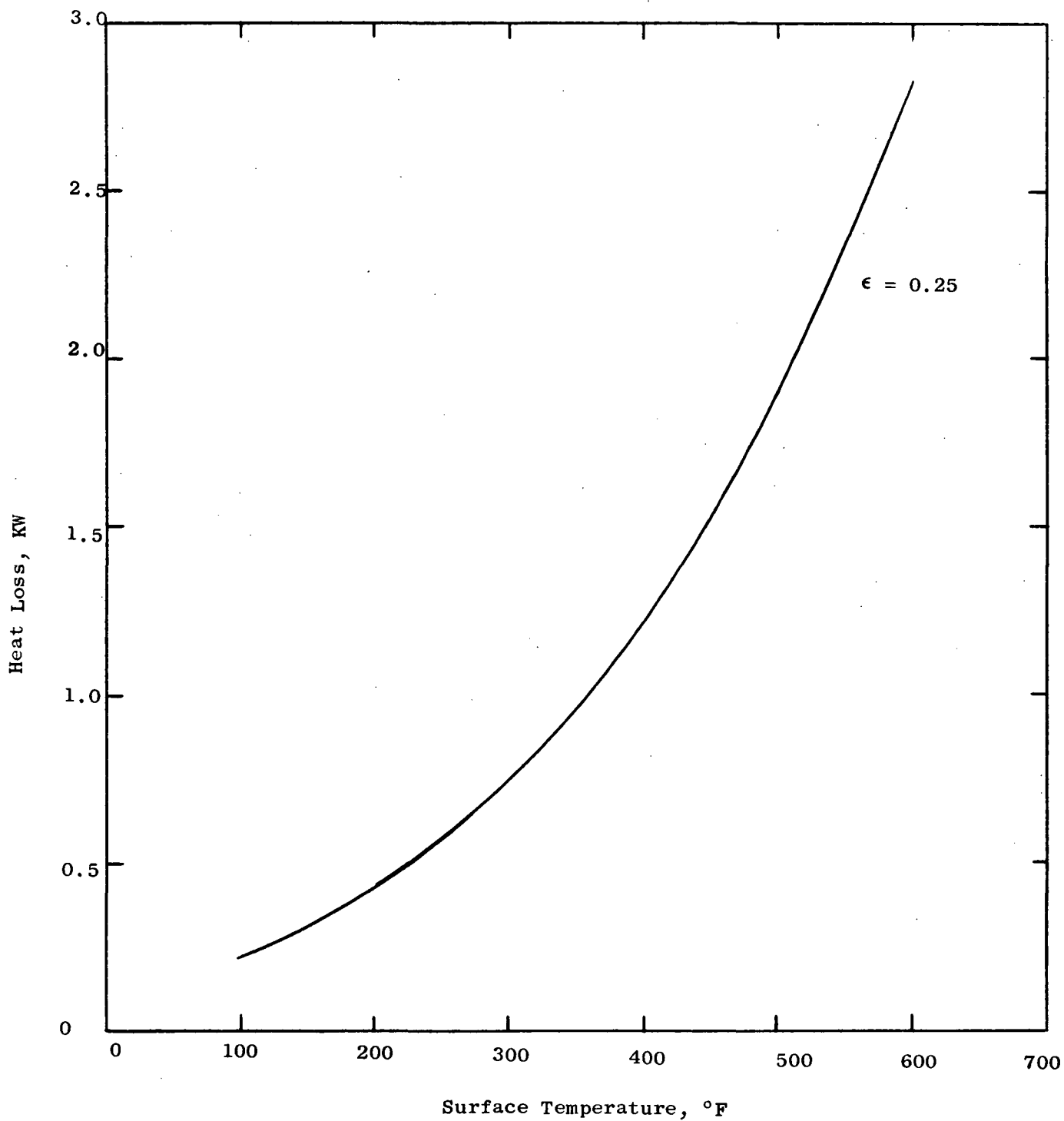


Figure 36. Aperture Assembly Heat Loss.

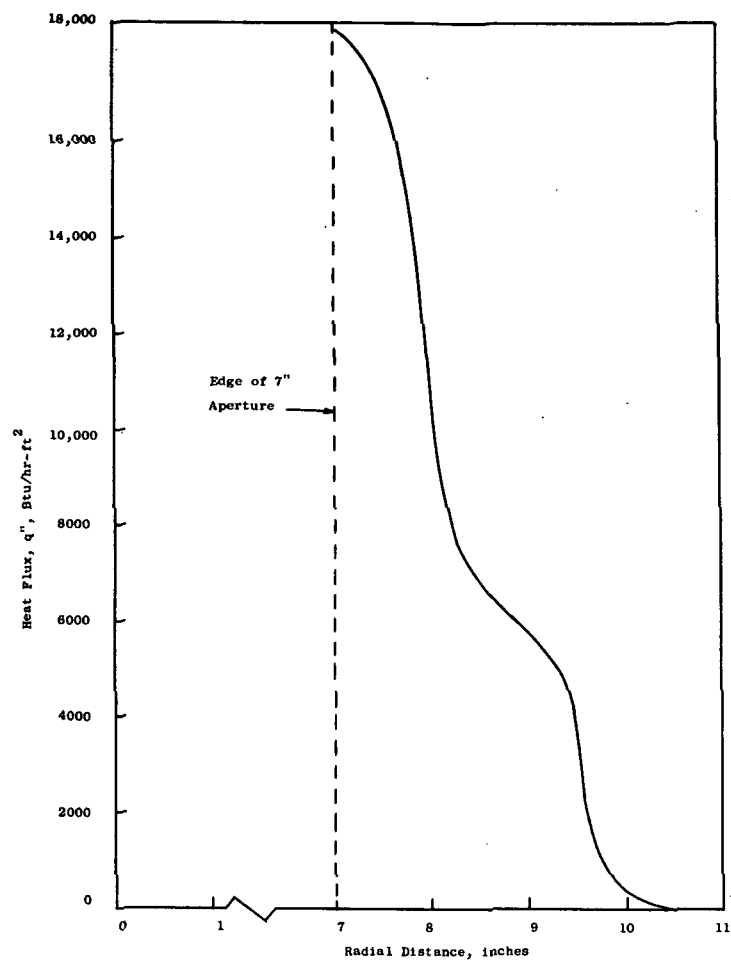


Figure 37. Heat Flux Distribution in the Plane of the Aperture.

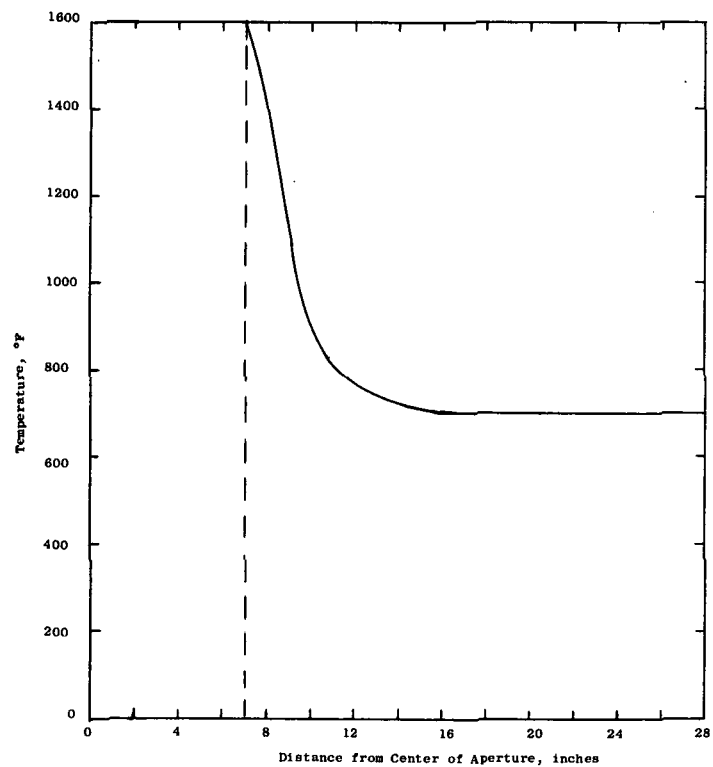


Figure 38. Aperture Plate Temperature Distribution.

As the diameter is increased, more of the incident radiation enters the cavity, but also more energy is reradiated out of the aperture. The result of the optimization is that some of the incident radiation impinges upon the aperture plate. Figure 38 is a plot of the calculated temperature distribution in the aperture plate. The maximum temperature is about 1600°F. Consequently, Cb-1%Zr was selected as the material for the aperture plate. Stresses and possible distortions due to the radial temperature gradient in the plate are reduced by providing a conical element in the plate.

3.6.2 Structural Design

The preliminary design of the aperture assembly utilized sheet metal panels rigidized with hat sections. Following the decision to fabricate the assembly from stainless steel, honeycomb sandwich panels came under consideration. An all-welded honeycomb panel design manufactured by Stresskin Products Company of Santa Ana, California was selected for the basic structure. The six flat door frames are assembled using flanges attached to the honeycomb by pin welding and bolting.

The actuator supports are A-frames made up of channel sections welded to a base plate, which in turn is pin-welded to the honeycomb panel. The A-frame design transmits the actuator loads to the aperture assembly near the six support points, such that the deflections are minimized.

The door actuators as will be discussed later in Section 3.8 are intended to be ground test type equipment rather than flight type. Consequently the actuator structural mounting details would most likely need to be redesigned for the flight application. Lighter and more compact flight actuators would result in a lighter mounting structure.

3.6.3 Door Hinge and Bearings

The door hinges were originally specified as a pin-bushing design fabricated of cobalt-moly alloy material. With the change in aperture insulation concept, all outside structural surfaces would operate at much lower temperatures, thus permitting consideration of alternate approaches for the hinges. To improve the reliability against seizure, rolling element bearings were suggested to replace the sliding contact

inherent in the pin-bushing design. Approval was provided to replace the co-moly pin bushing design with an all carbide rolling element bearing in the hinge and door-to-actuator linkage pivots. The particular rolling element bearing selected is an all carbide self-aligning ball bearing which had been developed on a previous NASA program. Additional discussion of materials considerations is presented in Section 4.2.6. The same carbide ball bearing is used in the door-to-actuator linkage and its design is discussed in Section 3.8.3. An alumina coated stainless steel door stop is bolted to each heat rejection door. The alumina coating is intended to prevent bonding of the mating door stop surfaces in the vacuum environment. Additional discussion is presented in Section 4.2.6.

3.6.4 Flex Plate Support

The aperture assembly is attached to the inlet manifold which operates at about 1100°F. Consequently, some means had to be provided to accommodate differential thermal expansion between the manifold and the aperture assembly. One scheme which received consideration involved a sliding bearing arrangement. Due to the uncertainties of self-welding of parts at high temperature in a vacuum, the concept was rejected. The final design uses flex plates at six locations around the assembly to accommodate the differential expansion while maintaining stiff support in the axial and all lateral directions. Figure 39 illustrates the model used in the analysis. Since the plates are in compression, they must also be designed to withstand buckling under launch load conditions. The flexure requirements would indicate a plate with a large ℓ/t making it flexible. Resistance to buckling requires a plate with a short ℓ/t . Figure 40 is a plot of plate parameters which satisfy both of these requirements. The final design incorporates six groups of two plates per group. Each of the plates is 0.036 inches thick, 5.3 inches long, 7 inches wide and is fabricated of Type 321 stainless steel.

3.7 INSULATION

The only insulation installed on the as-shipped receiver assembly consisted of layers of dimpled, .002-inch thick Cb-1%Zr foil. The advantage of this insulation is that it is compatible with the Cb-1%Zr structural material and does not present an outgassing problem. The

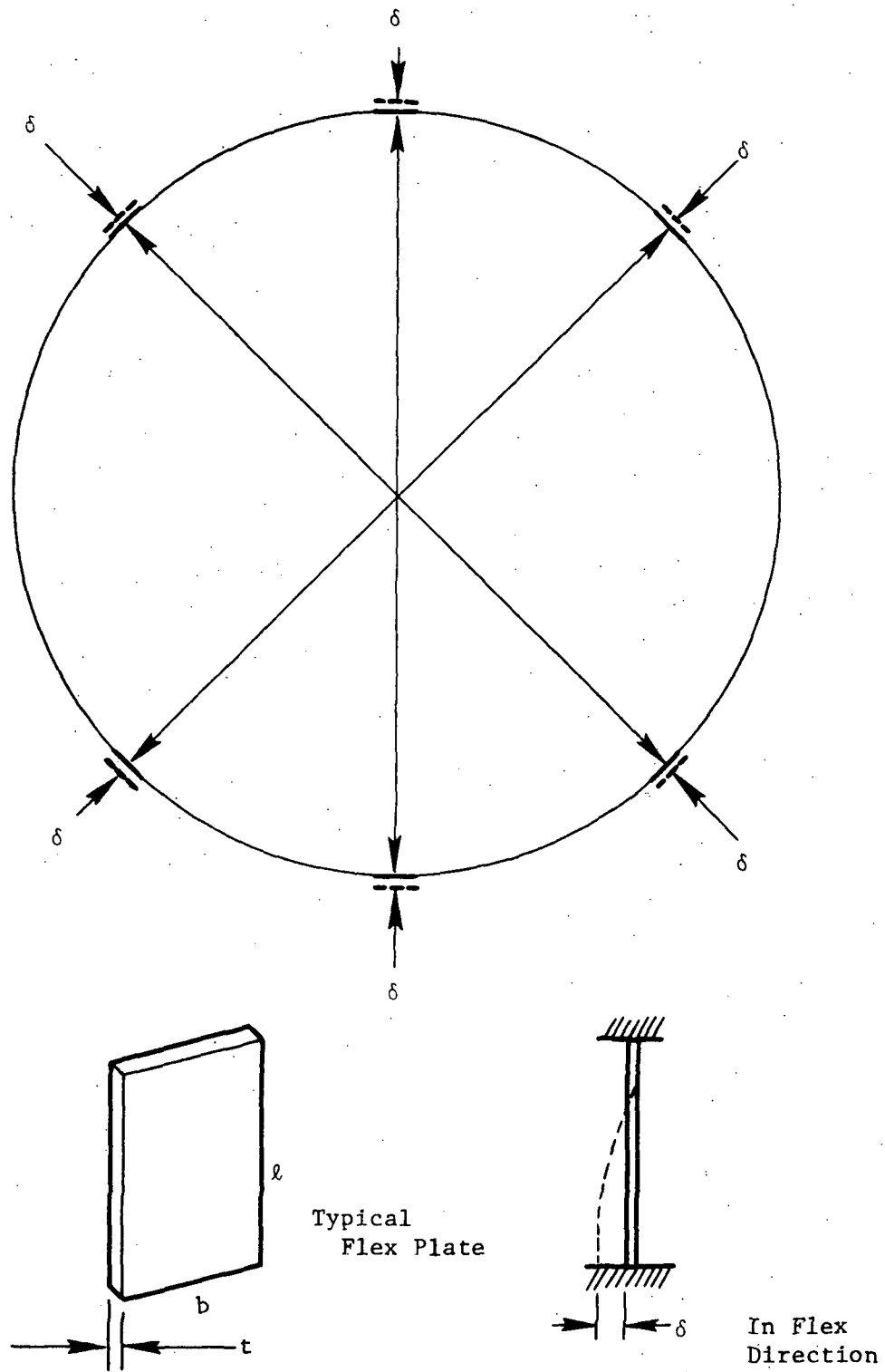


Figure 39. Flex Plate Support Concept and Model.

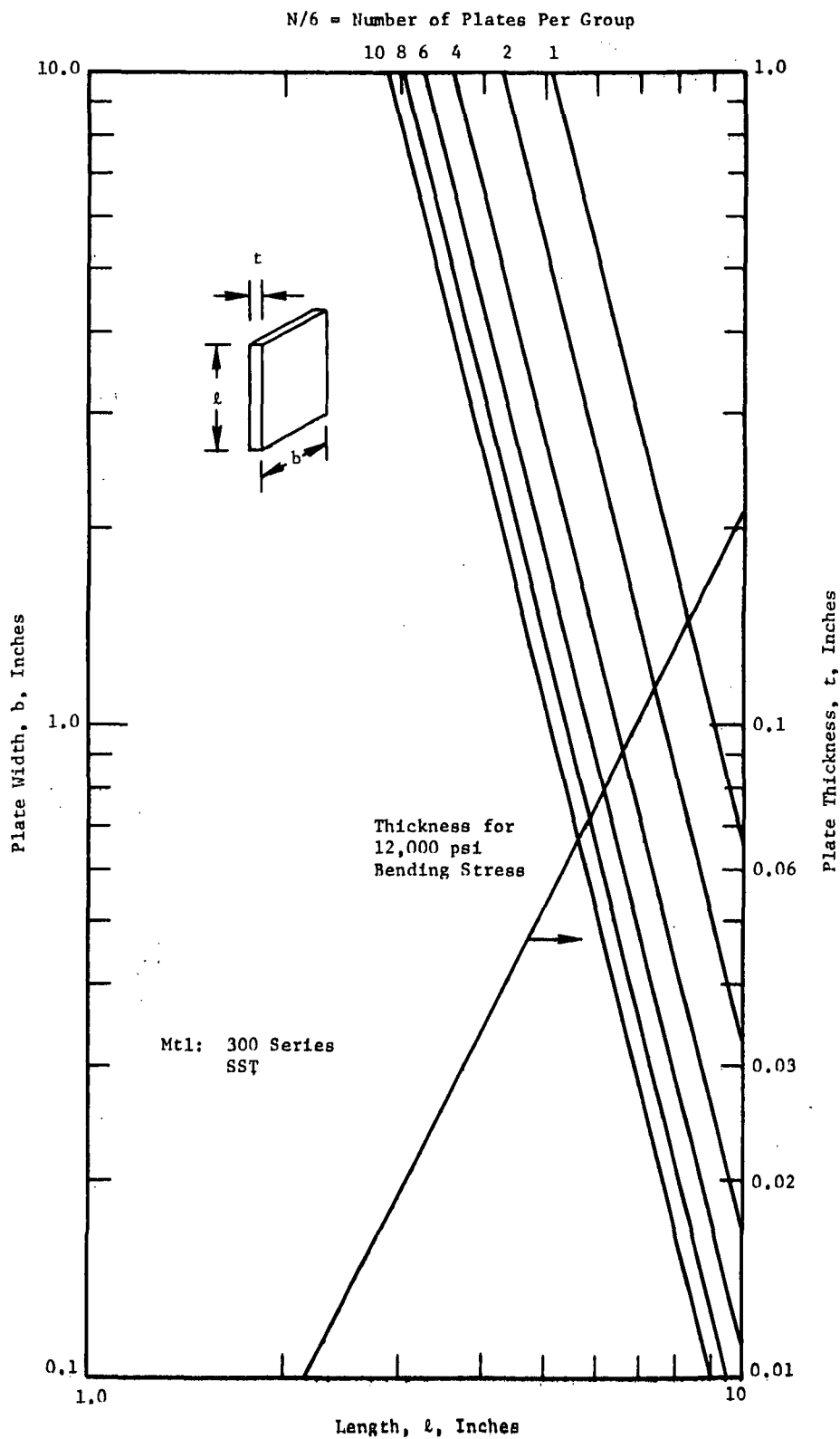


Figure 40. Aperture Assembly Flexure Plate Parameters.

disadvantage is that it has a relatively high effective thermal conductivity for the very stringent heat loss requirements of the receiver. Figure 41 is a plot of effective thermal conductivity of dimpled Cb-1Zr foil based on a limited amount of testing. Extrapolation of this data beyond the range of the tests is not recommended. Possibly a better way of presenting the data is that shown in Figure 42. Various predictions for parallel planes are shown for comparison.

During the course of the design, thermal calculations were performed at NASA to determine the effect of heat input (due to direct incident energy and reradiation) to the gas through the sections of tube between the inlet manifold and the first convolution, and between the last convolution and the exit manifold. The results showed that the heat input would cause an unstable gas outlet temperature. During the sun portion of the cycle, excess energy would heat the gas to temperatures above those of the turbine inlet requirement, depriving heat storage requirements. Consequently, in the shade, the gas outlet temperature would drop below that required because of insufficient energy storage. To avoid this variation of gas outlet temperature, the gas tube sections above and below the convolutions were insulated with dimpled Cb-1Zr foil. Ten layers of foil 1/2-inch wide x 0.002-inch thick were applied by wrapping the foil ribbon around the gas tubes with about 50% overlap.

The terminal junctions for the receiver thermocouples are located in four aluminum blocks encased in stainless steel enclosures. These enclosures are supported by brackets attached to the aperture assembly mounting pads located on the inlet manifold. The temperature of the terminal junctions is limited to 400°F. Since the inlet manifold operates at 1100°F, spacers and five layers of dimpled Cb-1Zr foil were placed between the brackets and hot mounting pads. Similarly, in order to reduce heat losses from the mounting pads to the aperture assembly, spacers and five layers of foil were placed between the mounting pads and the flex plate brackets.

Insulation of the aperture assembly presents a formidable problem. Refrasil insulation type material was eliminated due to its outgassing behavior (Reference: Section 4.2.6). Multilayers of dimpled Cb-1Zr foil, although an ideal candidate from a metallurgical standpoint has much

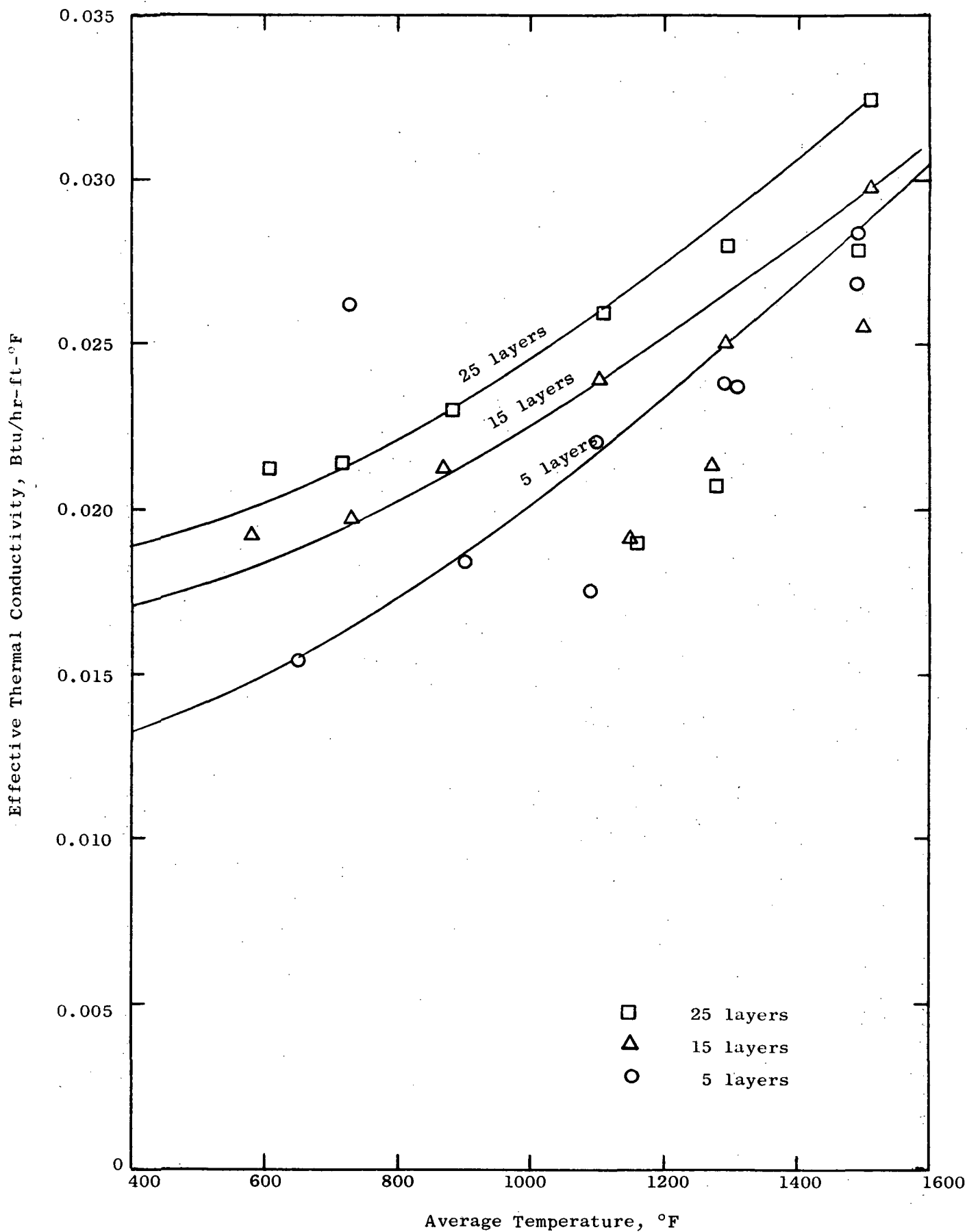


Figure 41. Effective Thermal Conductivity of Cb-1%Zr Knurled Foil.

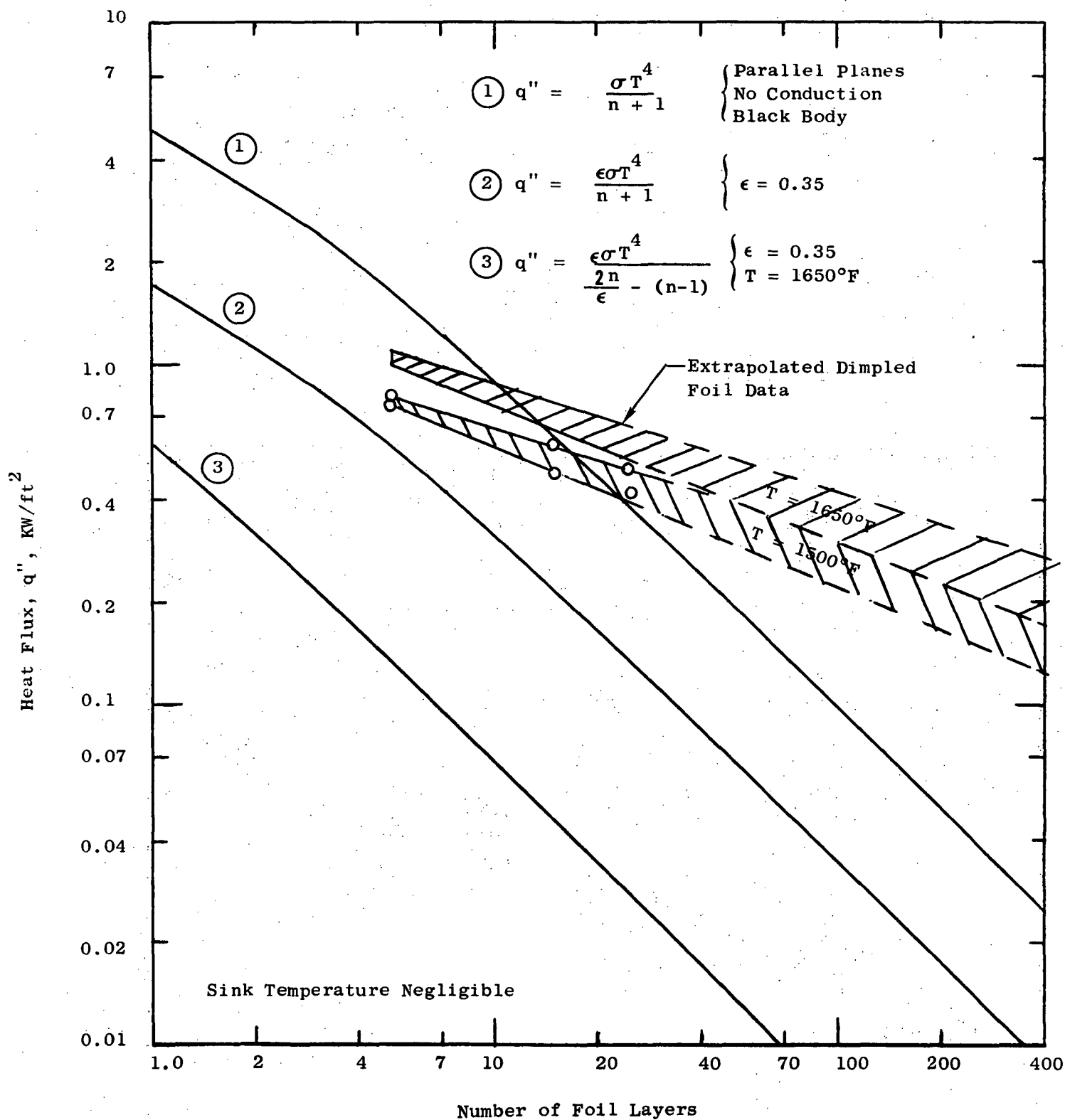


Figure 42. Heat Flux Versus Number of Foil Layers.

poorer thermal performance than Refrasil. In order to keep the heat losses below the 2 KW level which is itemized for reference in the NASA Specification, it is necessary for the heat flux to be less than about 0.1 KW/ft². This is based on the aperture assembly surface area of about 17.5 ft² and allowing only 0.25 KW for the total of all losses through edges, joints and attachments. Based on the extrapolation of dimpled foil data shown in Figure 42, it might require something on the order of 1000 layers if the 0.1 KW/ft² heat flux level is not to be exceeded. This is probably more than would actually be required, but test data would be needed for confirmation. Consequently NASA directed that the dimpled Cb-1Zr foil not be used for aperture assembly insulation.

Various alternate insulation systems offered by specialty vendors were under consideration throughout the program. Evaluation of two of the candidate insulation systems, namely Multi-Foil developed by Thermo-Electron Company (TECO) and Super Insulation as developed by Linde Division of Union Carbide Corporation involved certain test efforts as discussed in Section 4.2.6.

While the TECO Multi-Foil is clearly superior to the Linde Super Insulation for material compatibility and outgassing, the feasibility of applying it to large flat plate type structures such as those on the aperture assembly has not been established. The Linde Super Insulation as originally proposed was entirely unsatisfactory due to excessive outgassing. Subsequent developments and improvement by Linde almost at the completion of the program prompted NASA to direct that additional test evaluations be performed. Results of the additional evaluations indicated that the improvements developed by Linde made it appear worthy of serious consideration for the intended application (Reference: Section 4.2.6).

Design development of the aperture assembly was carried on simultaneous with the evaluation of the various candidate insulation systems. The intent was to have the final aperture assembly design configuration be such that any of the insulation systems could be installed without requiring changes to the aperture structure. As part of the test evaluation effort on improved Super Insulation systems, criteria for specifying tolerable outgassing levels were also developed.

These considerations and others as discussed above would enable suitable insulation systems to be specified and procured in fulfillment of NASA's advised intent to install insulation on the aperture assembly along with the remainder of the receiver after delivery of the completed solar heat receiver.

3.8 DOOR ACTUATORS

3.8.1 Specification Development

Specifications for the door actuators which are delineated in the contract work statement are very broad and outline only the fundamental requirements as summarized below:

- A.1 All doors must start to open when cavity sensor temperature reaches 2130°R.
- A.2 All doors must be fully open when cavity sensor temperature reaches 2200°R.
- A.3 "Manual" override is required for remote actuation from outside the vacuum test facility.
- A.4 Controller output required to operate heat rejection doors to be specified by contractor.

More detailed specifications were evolved as response requirements to satisfy thermal characteristics were determined by NASA simultaneous with design development of the heat receiver. Layout studies investigating several actuator design concepts were also accomplished. Evaluation of concept trade-offs and program developments resulted in the following more specific door actuator requirements and/or clarifications:

- B.1 Actuators are required to operate at the vacuum test facility and not intended to be flight-type.
- B.2 Provision for "manual" override is intended to be by means of backup push button type of control in the event the automatic control system loop fails.
- B.3 Proportional operation with all doors operating together is required for proper temperature control.
- B.4 Maximum response time allowed is 30 seconds from fully closed to fully open.
- B.5 A commercial electromechanical actuator packaged within an environmental enclosure is the specific configuration selected

for implementation. Special attention is directed to the bellows rod seal to insure high reliability. Cooling gas will be provided to the actuator enclosures to maintain the commercial unit within its environmental capabilities. Infinite resolution feedback potentiometers are required to indicate door position and are to be incorporated within environmental enclosures.

In reviewing the detail design implementation for the selected actuator concept the following detail design features were essentially added to the specifications:

- C.1 Bellows for rod seal to be hydroform type.
- C.2 Double bellows configuration to be incorporated at rod seal for redundancy.
- C.3 Actuator assembled length to be adjustable externally.
- C.4 Spring loaded overtravel to maintain doors in closed position relatively independent of small dimensional changes in door and related structures.

The summation of requirements A.1-4, B.1-5 and C.1-4 above constitute the total specification developed for the door actuators.

3.8.2 Actuator Design

While the actuators are not required to be designed for flight application, the need for high operational reliability and leak tight integrity is essentially not diminished. Inherently reliable design features such as the double bellows seal and conservative design practices were followed throughout. The assembly and operational schematic are shown in Figures 43 and 44 respectively.

Performance parameters and design data for the door actuators are shown in Table IV. Results of a thermal analysis are shown in Figure 45 providing additional information on cooling gas flow requirements.

To achieve maximum reliability against the possibility of contaminating the test facility chamber with cooling gas, a pressure sensing line should be connected to the Swagelok fitting at the bellows header. By monitoring pressure between bellows, a leak in either of the two bellows can be detected. The initial cavity pressure should be maintained at some value between external facility vacuum level and internal actuator pressure.



Figure 43. Door Actuator Assembly. (Dwg. No. 47E193580 Sheet 1)



09 059

TABLE IV

DOOR ACTUATOR PERFORMANCE

AND DESIGN DATA

Output shaft speed	4.6 in/min
Linear stroke	1.49 to 1.56 inches
Door operating angle	70 to 75 degrees
Time to open or close the door	20 seconds
External environment	
Pressure	Vacuum or atmospheric
Temperature	700°F max.
Internal environment	
Pressure	24 psia Nom (30 psia max.)
Temperature	* 200°F max. at motor hsg.
Coolant gas requirements	Nitrogen: 8.2 #/hr max. or Argon: 16.4 #/hr max. for 90°F max. gas inlet and continuous duty.
* To limit linear actuator temp. to 200°F as indicated by T/C on motor hsg.	
Assy and wiring schematic	GE Dwg. 47E193580
Installation	GE Dwg. 47R199396

(from coolant gas). By assuming steady-state conditions in the cavity, that is, constant temperature and volume, an increase in cavity pressure would indicate a leak in the outer bellows while a decrease in cavity pressure would indicate a leak in the internal bellows.

Additional information relative to major actuator components including their temperature limitations is presented in Appendix B.

3.8.3 Linkage and Ball Bearings

Linkage

The linkage between the actuator and the door consists of a turnbuckle, bearing housing, bearings and fasteners. Adjustment of the turnbuckle enables attainment of the required clearances between door stops and the frame when the actuator is fully extended.

Ball Bearings

Each actuator linkage has two self-aligning, double row, spherical-type ball bearings. As used in the linkage, each bearing angular misalignment capability is three degrees from center. The ball bearing design is per AFBMA No. 08BS10J with the race material being General Electric Company Carboloy 883 and the ball material General Electric Company Carboloy 44A. These carbide materials were selected to prevent cold welding when the bearing is used in a hard vacuum. (S.K.F. Bearing No. 108-13303 is a commercially available version of this design with conventional materials which was used as a slave bearing.) Additional basis for selection of the bearing which is identical to the bearings used in the door hinge pivots are presented in Section 4.2.6.

4.0 M A T E R I A L S

Page intentionally left blank

4.0 M A T E R I A L S

4.1 REFRACTORY RAW MATERIAL

All structural material of the heat receiver was originally specified to be Cb-1Zr except for 300 series stainless steel which was to be part of the bimetallic joints. The corrosion resistance, weldability, strength, fabricability, and availability of Cb-1Zr alloy made it a sound selection as the primary structural material. The minimum design data obtained from thin-walled tubes, sheet and rod of Cb-1Zr, showed that the selected alloy had adequate strength for the containment of LiF and for use as structural components of the heat receiver within the allowable design stresses and operational temperature for a period of five years.

GE-NSP procured all the required raw materials for the heat receiver except for the following items which were supplied by NASA-LeRC:

- a. All Cb-1Zr alloy storage tubes filled with LiF;
- b. Cb-1Zr 0.75-inch-OD tubing for the gas tube extension;
- c. Cb-1Zr, in various forms, obtained from Oak Ridge National Laboratory. However, the lack of processing history and available property data on the material generally restricted the use to only noncritical components or welding fixtures.

Later in the program, with the approval of NASA, a design change resulted in the insulation for the aperture assembly being moved from the outside to the inside surface. This greatly reduced the anticipated service temperature of the aperture assembly structure and permitted the use of PH15-7Mo stainless steel for the honeycomb stiffening panels, 304 SS for attachments and brackets, and 321 SS for the lower flexplates. In addition to materials changes for the aperture assembly, some of the fasteners, other than rivets, were ultimately made from unalloyed tantalum.

4.1.1 Specifications

All Cb-1Zr material was ordered to GE-NSP specifications which had been developed by GE-NSP for utilization in NASA programs. A list of the materials and nondestructive specifications applicable to this program are shown in Table V. The major supplier of Cb-1Zr for this program, Wah Chang Corporation, took exception to the required minimum values for tensile properties as stated in the NSP specification and would guarantee only a 20 Ksi 0.2% yield strength (vs. 30 Ksi per specification) and a 36 Ksi ultimate yield strength (vs. 40 Ksi per specification). The exceptions were considered acceptable for the Heat Receiver application and permission to order with these stipulations was given by NASA.

4.1.2 Procurement Control

Control over the procurement and documentation of the materials purchased for this program was governed by SPPS Instruction 09.102, "Control of Reactive Metals/Alloys, Refractory Metals/Alloys and Super-alloys." This instruction establishes procurement policy and assigns specific personnel responsibilities and outlines detailed procedures for the materials procurement, handling and documentation of incoming products and inventory control.

The majority of the Cb-1Zr alloy material was procured from Wah Chang Corporation with small quantities of Cb-1Zr alloy (primarily wire and foil) and tantalum (rod and sheet for post weld annealing furnace and threaded fasteners) being procured from four other refractory alloy vendors.

During the procurement, raw materials vendor's facilities (particularly test facilities and vacuum annealing furnaces) were reviewed and qualified. Details are given in the quality assurance section. Visits, phone and written contacts were made by metallurgical personnel to provide technical assistance to vendors, to monitor vendor processing and its program, and to assist in evaluating field discrepancies. Considerable effort was also expended in monitoring the production of bimetallic joints and the spinning of the top closure cone which are discussed later.

4.1.3 Quality Assurance

Because of the critical application to which the Cb-1Zr was applied, quality assurance testing was performed on each lot of material. The extent of quality assurance testing depended on the particular application; however, all Cb-1Zr products were 100% inspected visually and ultrasonically either at NSP or in the presence of NSP personnel. In addition, where appropriate, selected samples of each type of material were evaluated for one or more of the following properties: stress-rupture strength, chemistry, grain size, and metallurgical structure.

A list of the quality assurance data performed and documented for each lot of Cb-1Zr thru a combination of vendor and NSP testing is given in Table VI. In general, the materials met the applicable specification, and where deviations from specifications occurred, Material Review Board action was taken to assure proper use of the material.

During the procurement, vendor's test facilities were reviewed to assure that tests were performed in accordance with specification requirements. A major effort was made to assure ultrasonic and penetrant inspections were performed as required. Also, to minimize the possibility of contamination during annealing, the vacuum heat treating facilities of vendors processing Cb-1Zr mill forms for this Program were qualified according to NSP Instruction #2 for Qualification of Vacuum Annealing Forms. In addition, all post-weld annealing facilities were qualified in accordance with the GE-NSP Specification 03-0037-00-A.

4.1.4 Material Control

The control and documentation of the refractory alloy materials was performed in accordance with the SPPS Instruction 09.102. Documented control of materials was handled with a basic assignment of a Material Control Number for each item received. The Material Control Number designated the program for which the material was intended, the task of that program, a sequential file number, and the number of the pieces within a lot. For each Material Control Number a corresponding numbered metallurgical processing and test history and inventory file was established.

TABLE V

NSP MATERIAL AND NONDESTRUCTIVE TESTING SPECIFICATIONS

<u>TITLE</u>	<u>SPECIFICATION NUMBER</u>
Sheet, Strip, and Plate: Cb-1Zr Alloy	01-0053-00-C
Bar and Rod: Cb-1Zr Alloy	01-0052-00-C
Seamless Tubing and Pipe: Cb-1Zr Alloy	01-0004-00-D
Foil: Cb-1Zr Alloy	01-0054-00-A
Wire: Cb-1Zr Alloy	01-0055-00-A
Method for Ultrasonic Inspection	03-0001-00-C
Fluorescent Penetrant Inspection	03-0027-00-B

TABLE VI

DOCUMENTATION OF QUALITY ASSURANCE DATA FOR Cb-1Zr ALLOY

1. Item, Nominal Size
2. Heat Number
3. Lot Number
4. Ingot Vendor
5. Processing Vendor
6. Material Control Number
7. Weight (100%)
8. Dimensions (100%)
9. Surface Condition, Visual (100%)
10. Penetrant Inspection (100%)
11. Ultrasonic Inspection (100%)
12. Grain Size/Microstructure (2/Lot)
13. Microhardness Traverse (2/Lot)
14. Room Temperature Tensile Properties (2/Lot)
15. Bend Ductility (For sheet only)
16. Stress-Rupture Properties (2/Lot)
17. COHN Analysis, Final Product (2/Lot)

4.2 SPECIAL PROCESSES AND EVALUATIONS

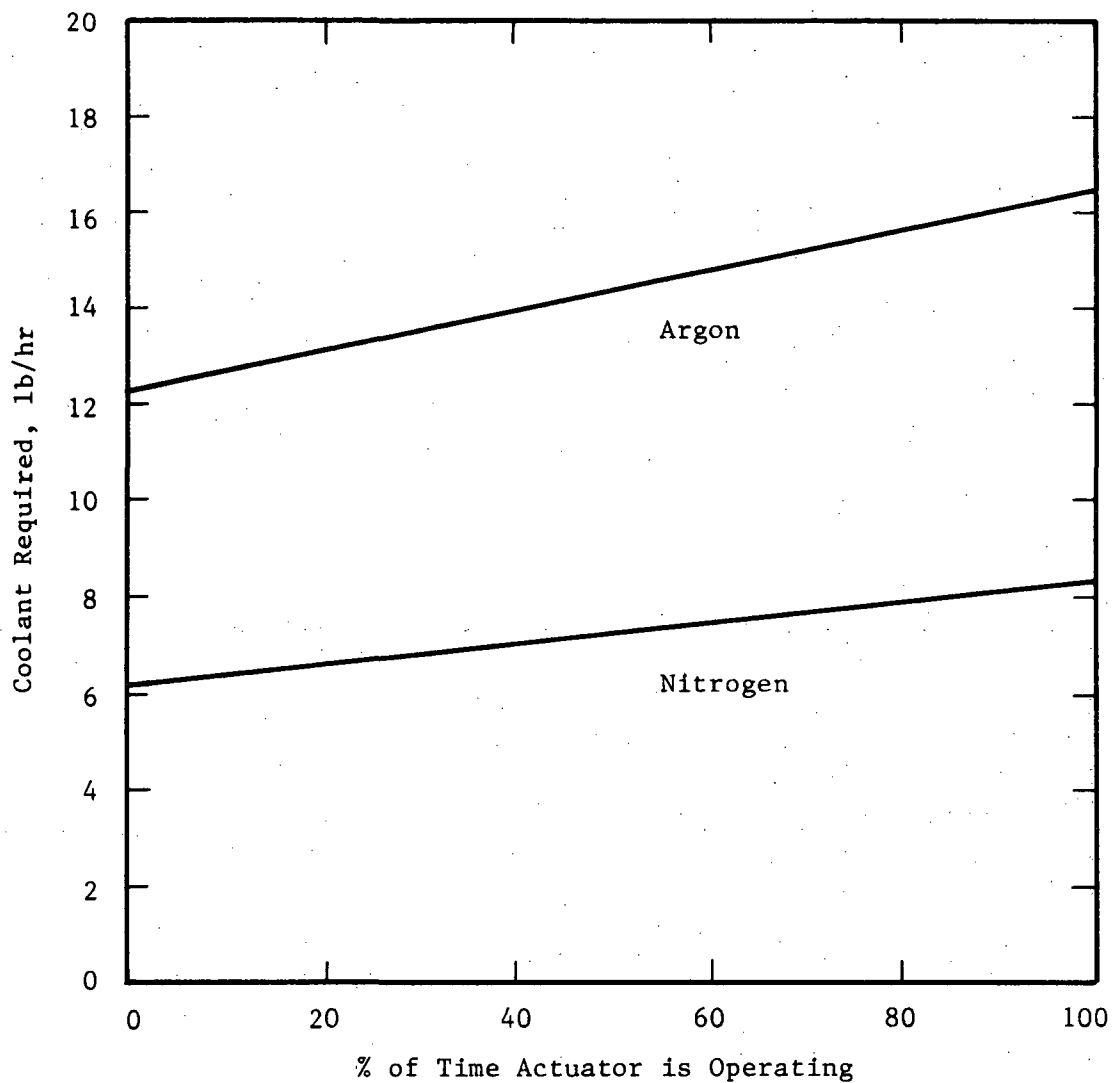
4.2.1 Bimetallic Joint

Transition joints were required between the Cb-1Zr manifolds of the heat receiver and the Type 304 stainless steel inlet duct (from the recuperator) and Hastelloy X exit duct (to the turbine). Because of the large differences in melting point between the Cb-1Zr and the duct materials, transitions fabricated by some process other than welding were required. Coextrusion seemed to be a promising route for fabricating the inlet transition because Cb-1Zr/SS joints as large as 3.5-inch OD had been satisfactorily produced by Nuclear Metals Division of Whittaker Corporation prior to this program. A sketch of a longitudinal full section view of a coextruded joint is shown in Figure 46. However, Cb-1Zr/Hastelloy X coextruded joints had never been developed. A review of the risk, cost and time involved in developing such a coextruded joint made its selection unattractive. To circumvent the need for the costly and lengthy development of a coextruded Cb-1Zr/Hastelloy X bimetallic joint, a Cb-1Zr/stainless steel-to-Hastelloy X transition joint such as shown in Figure 47 was used on the outlet header. This transition employed a coextruded Cb-1Zr/stainless steel joint to which a Hastelloy X extension could be gas-tungsten-arc welded. By designing the stainless steel portion heavier than the Hastelloy, the reduced strength of the stainless steel at the operating temperature of the system was compensated for.

Coextrusion Process

The coextrusion process utilizes only the two metals to be joined, forming a metallurgical bond by working (extrusion) of the two metals at elevated temperatures. The resulting joint is a tapered section as shown in Figure 46. This tapered section provides a large joint area to accommodate the shear stress imposed by differential thermal expansions of two dissimilar metals.

Type 316 stainless steel was selected for the steel joint component because of Nuclear Metals past successful experience with this combination and because of its adequate elevated temperature strength. The metallurgical interactions which occur at elevated temperatures between Cb-1Zr



Temperature Conditions:

Actuator Housing 700°F
 Coolant Inlet 90°F
 Coolant Outlet 160°F

Figure 45. Cooling Gas Flow Requirements.

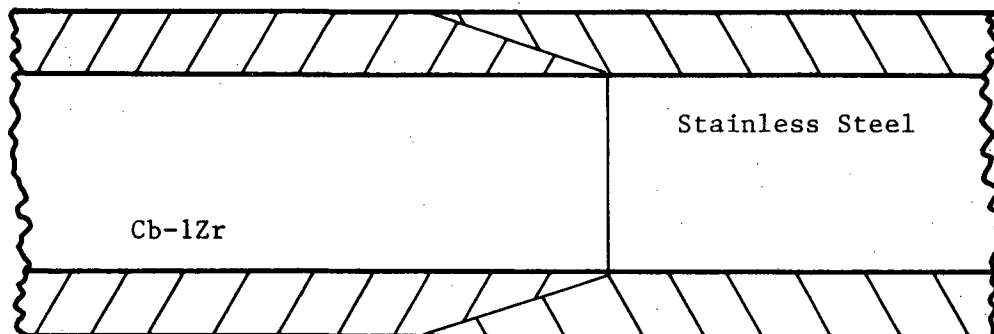


Figure 46. Sketch of a Longitudinal Full Section View of a Coextruded Joint.

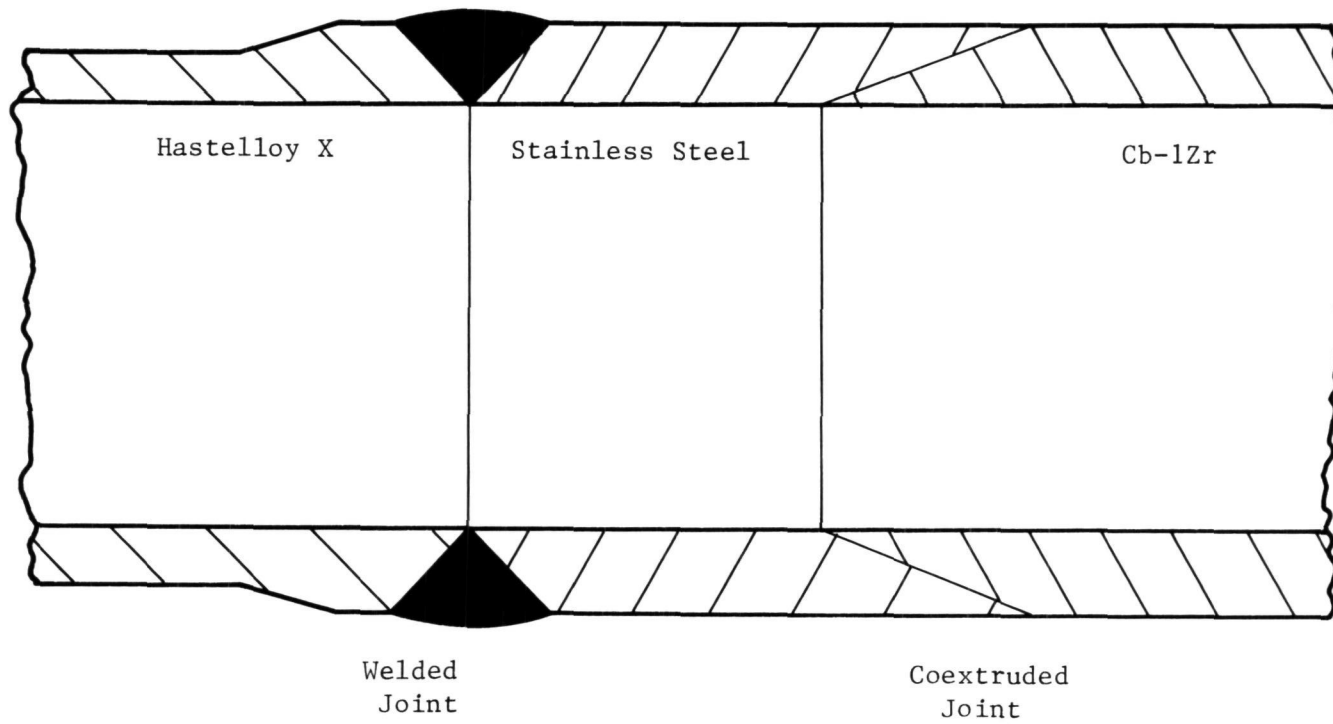


Figure 47. Schematic Cb-1Zr/Stainless Steel/Hastelloy X Transition Joint for Receiver Exit Header.

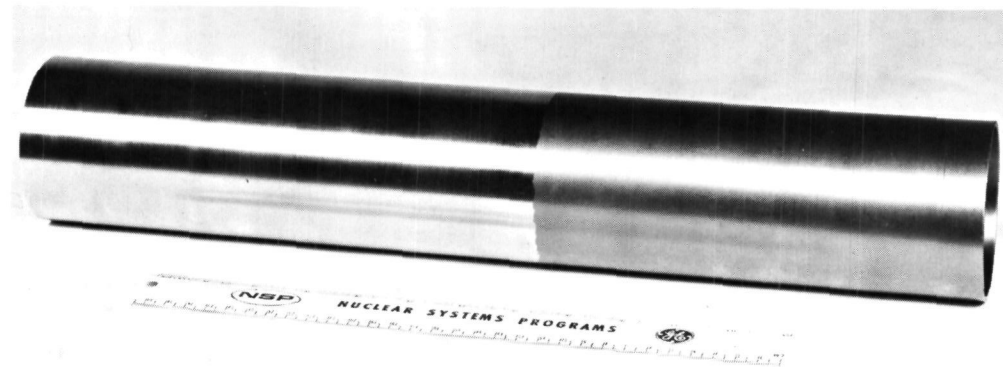


Figure 48. Typical Coextruded Joint.

and Type 316 stainless steel have been well documented in the classified literature. Similar work by Ferry and Page (Reference 13) on duplex columbium/Type 316 stainless steel tubing reports the expected diffusion zone thickness between Cb and Type 316 stainless steel as a function of thermal exposure. At 1500°F, diffusion zone thicknesses were .0003 inch after 1000 hours and increased to approximately .001 inch after 10,000 hours.

The diffusion zone is primarily iron-columbium intermetallic compounds, containing varying amounts of nickel and chromium. The intermetallic compound is extremely brittle and should be considered in any bimetallic transition element intended for long-time service. The effect of intermetallic compounds on joint integrity could be determined only by experimental evaluation under simulated operating conditions. It is apparent that with increasing service temperature and time, the thermal shock behavior of joints can be impaired by formation of a brittle diffusion zone. Whether such an interaction would cause joint failure in the particular application was highly speculative. As described later, tests were performed by NASA-LeRC on the first coextruded joint produced on this program to assess joint performance.

Joint Materials and Fabrication

Relatively large tube hollows, approximately 5-inch OD x 2.76-inch ID, were required for extrusion in order to produce the 3.0-inch ID by 0.090-inch-wall joints. The required raw materials were procured by GE-NSP and supplied to Nuclear Metals Inc. after passing quality assurance testing. Type 316 SS hot rolled 5.125-inch-diameter rod was purchased to ASTM Specification A-276 in the annealed condition. Cb-1Zr rod, 4.91-inch-diameter, was procured to NSP Specification 01-0052-00-C in the annealed condition. The 316 SS rod was machined to $5.0 \pm \begin{smallmatrix} 0.063 \\ 0.000 \end{smallmatrix}$ -inch OD x $2.75 \pm \begin{smallmatrix} 0.000 \\ 0.063 \end{smallmatrix}$ -inch ID and supplied to the coextrusion vendor as extrusion blank material. The Cb-1Zr rod was supplied to the coextrusion vendor in the as-received condition. The coextrusion vendor processed the solid rod into an extrusion blank by back-extruding the rod into a cup shape and removing the closed end of the cup. Sufficient Cb-1Zr and 316 SS material was supplied to the coextrusion vendor to allow production of transition pieces having a tapered joint interface 2.5 inches long plus a minimum of six inches of 316 SS on one side of the

tapered joint and six inches of Cb-1Zr on the other side. These lengths were required to allow welding of the extremities of the transition pieces without overheating the tapered joint.

Tapered sections as short as 1.5 inches were produced because of the large grain size (ASTM No. 0 to 6) in sections of the Cb-1Zr rod. The coarse grain size necessitated a smaller extrusion reduction ratio over that originally anticipated. This lowering of the reduction ratio was necessary to allow for more metal removal during final machining to insure complete removal of surface irregularities usually associated with the extrusion of coarse grained materials. A tapered joint section 1.5 inches long was equivalent to an overlap of the two materials of approximately 16 times the wall thickness. Joints between Cb-1Zr and stainless steel, as well as other material combinations, had been made by Nuclear Metals with overlaps as low as five times the wall thickness without any degradation of joint integrity.

Nuclear Metals was to produce one joint for GE-NSP approval prior to completion of the order for three more coextruded joints. The first joint passed GE-NSP quality assurance testing (i.e., ultrasonic, fluorescent penetrant and dimensional inspection, metallography and chemical analyses). The fabrication procedure used in making the first joint was followed in processing the three remaining joints. The procedure is summarized in Table VII. A photograph of a typical finished coextruded transition piece is shown in Figure 48. Photomicrographs of typical sections of the stainless steel and Cb-1Zr portions of the finished transition pieces are shown in Figures 49 and 50. No photomicrographs of the tapered section are available because such evaluation would cause destruction of a joint.

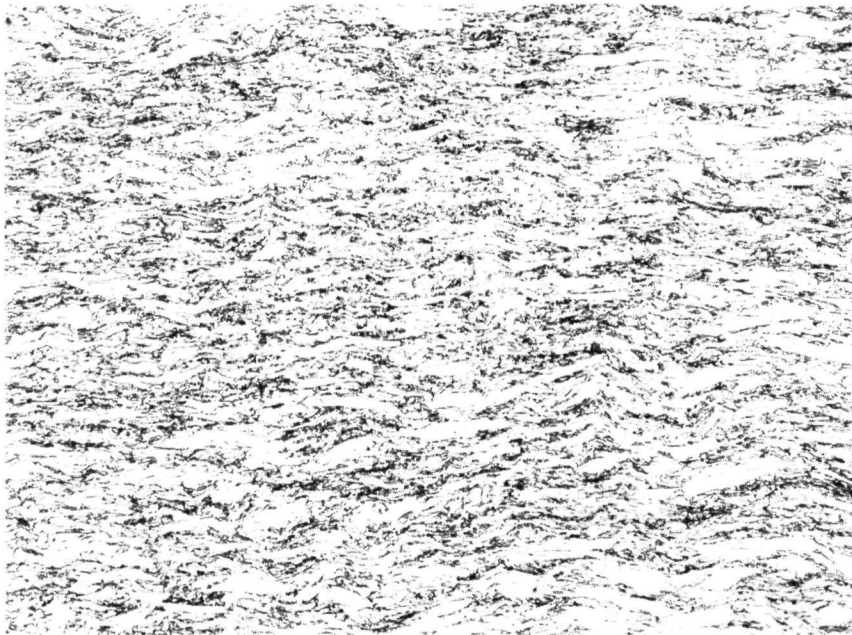


Transverse 100 X (Neg. No. 11640)

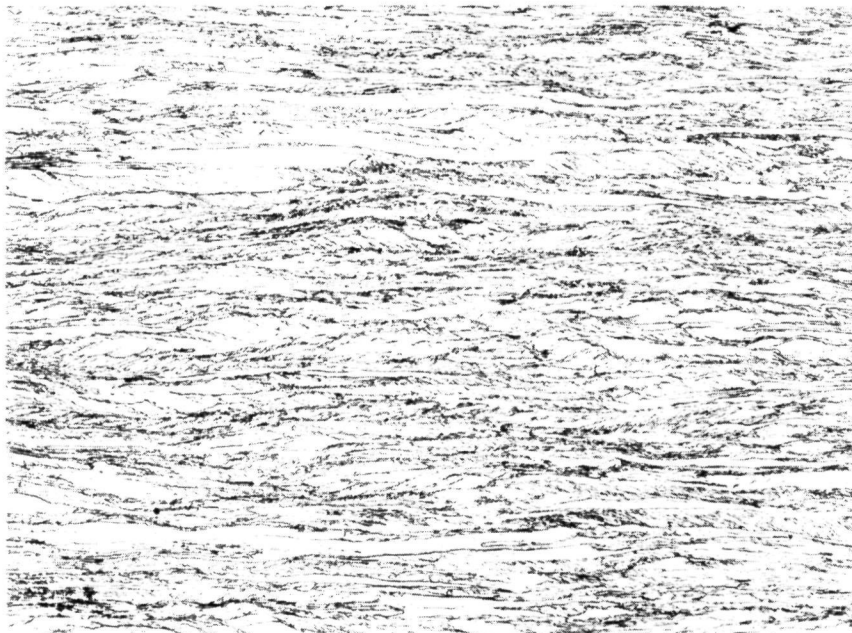


Longitudinal 100 X (Neg. No. 11642)

Figure 49. Typical Microstructure of Stainless Steel Portion of Coextruded Joints.



Transverse 100 X (Neg. No. 11629)



Longitudinal 100 X (Neg. No. 11631)

Figure 50. Typical Microstructure of Cb-1Zr Portion of Coextruded Joints.

TABLE VII

SEQUENCE OF OPERATIONS IN FABRICATING COEXTRUDED JOINTS

1. Enclose Cb-1Zr blank in a mild steel vacuum jacket.
2. Heat and cup blanks.
3. Remove mild steel jacket and machine Cb-1Zr blank.
4. Machine SS blank.
5. Enclose both machined blanks in mild steel vacuum jacket.
6. Heat Cb-1Zr and stainless parts, assemble on tooling, extrude joint.
7. Pickle to remove jacket.
8. Rough machine joint area and inspect.
9. Finish machine and inspect.
10. Non destructive testing.

Evaluation of Coextruded Joints

Because of uncertainty of the coextruded joint performance capabilities, the first joint was supplied to NASA-LeRC for testing (Reference 20). Three tests were conducted in a Brew vacuum furnace. Except for the first heat-up, vacuum was at 2×10^{-7} torr range, and at no time greater than 1×10^{-5} .

The following tests were conducted:

Test No. 1

Twenty thermal cycles - 450° - 1500° F

Average rate of temperature rise - 25° /min

Maximum rate of temperature rise - 50° /min

The test included several periods at 1500° F totaling 164.9 hours.

Test No. 2

500 thermal cycles - 1450° F to 1600° F

A typical cycle was of one-hour duration with about 45 minutes at 1550° F, five minutes at 1600° F, and five minutes at 1450° F. The remaining five minutes was transition time.

Total test time: 502 hours

Test No. 3

58 cycles - 400°F - 1540°F

Each cycle was three hours in duration with one-hour heatup, two-hour cooldown.

Maximum rate of temperature rise - 30°/min

Total test time - 191 hours, including 17 hours at 1550°F

Summary: 79 "deep" cycles

500 close cycles

Approximately 600 hours at 1500°F or above

The coextruded joint showed no leaks but dimensionally deformed in the tapered joint area. An evaluation of these changes and their significance was made at NASA-LeRC. On the basis of no leaks and no visible delamination, the joint was judged by NASA-LeRC to be acceptable for use on the receiver.

4.2.2 Iron Titanate Coating

Based on the test results with iron titanate (Fe_2TiO_5) described below (primarily those obtained at NSP), which indicated coating degradation and oxygen contamination as high as 2300 ppm which might lead to embrittlement of the Cb-1Zr bellows, NSP recommended that grit blasting instead of iron titanate coating be used to improve the emissivity of heat storage tube convolutions. NASA concurred with this recommendation, which was then implemented.

To improve emissivity an iron titanate (Fe_2TiO_5) coating was originally specified for application to the surface of the heat receiver tubes and other selected heat receiver components. The maximum operating temperature of the iron titanate coating on the heat storage tubes is expected to be between 1700° and 1800°F. NSP has had the opportunity to evaluate this coating on Cb-1Zr in two long-term, high-temperature, high-vacuum tests. The first experiment involved the evaluation of 2-inch x 2.5-inch thick Cb-1Zr specimens coated with four mils of iron titanate. The purpose of the test (Reference 14), which consisted of thermally cycling the specimen between 1500° and 150°F during a 1000 hour test, was to determine the stability of the coating on Cb-1Zr prior to using it to coat the condenser fin of the Prototype Corrosion Loop which will be discussed later. A steady-state temperature gradient (1495° to 1075°F) was maintained across the coated region of the specimen. The visual and

metallographic appearance of the specimen following test is illustrated in Figure 51. A slight increase in porosity occurred in the region of the coating which operated at the highest temperature, 1495°F, although no significant change in the heat rejection performance of the specimen could be detected.

The iron titanate coating was subsequently applied to the condenser-subcooler fin of the Prototype Corrosion Loop shown in Figure 52. During the course of the 5000 hour test on this loop, which was completed on March 9, 1966, no degradation in the performance of the coating was detected. The temperature of the coating varied from 1400°F in the hottest regions to 800°F in the coolest regions. The visual appearance of the coating following the 5000 hour test is illustrated in Figure 53. No evidence of degradation or change in general appearance was observed.

The iron titanate coatings described above were applied by an outside supplier who for several years has been evaluating high emittance coatings under NASA sponsorship (Contract NAS 3-4174). A 10,000 hour - 1700°F thermal cycling test of the iron titanate coating on a Cb-1Zr tube was recently completed as part of the referenced NASA program (Reference 15). During this test the specimen was thermal cycled between 1700°F and room temperature 51 times. No visual degradation of the coating was noted, although the emittance of the specimen at 1700°F did decrease from 0.88 to 0.84 during the test period. Post-test evaluation of the iron titanate coated Cb-1Zr specimen revealed a considerable oxygen concentration in the substrate as well as evidence of diffusion of titanium and iron.

A recently completed 5000 hour test (Reference 16) of the iron titanate coating was conducted using time-temperature conditions closely simulating the conditions proposed for the lithium fluoride heat receiver. The coated Cb-1Zr tube was cycled between 1500°F and 1800°F. The emittance of the iron titanate coating was quite stable at a value of 0.85 throughout the experiment. Preliminary X-ray diffraction evaluation of the coating indicated the formation of a small amount of TiO₂ in the coating and oxygen contamination of the Cb-1Zr tube wall.

Even more pertinent to the Heat Receiver Program were the results of the GENSP post-test evaluation of the Fe₂TiO₅ coating on lithium

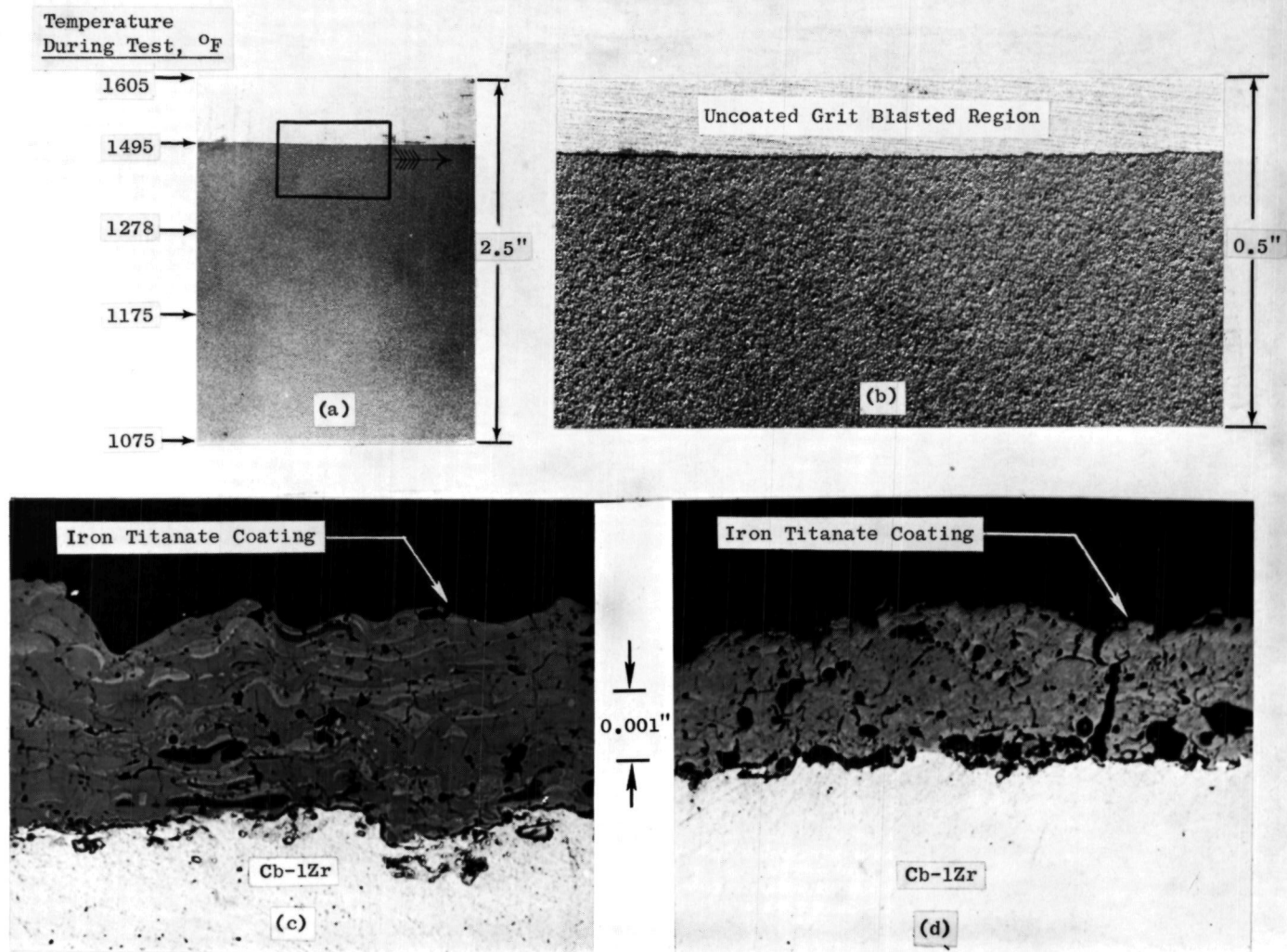


Figure 51. Cb-1Zr Alloy Fin Specimen Coated with Iron Titanate. The Appearance of the Surface of the Coating at Low Magnification After the 1000-Hour Evaluation Test is Shown in (a) and (b). Metallographic Cross Sections of the Coating Before Test (c) and After Test (d) are also Included.

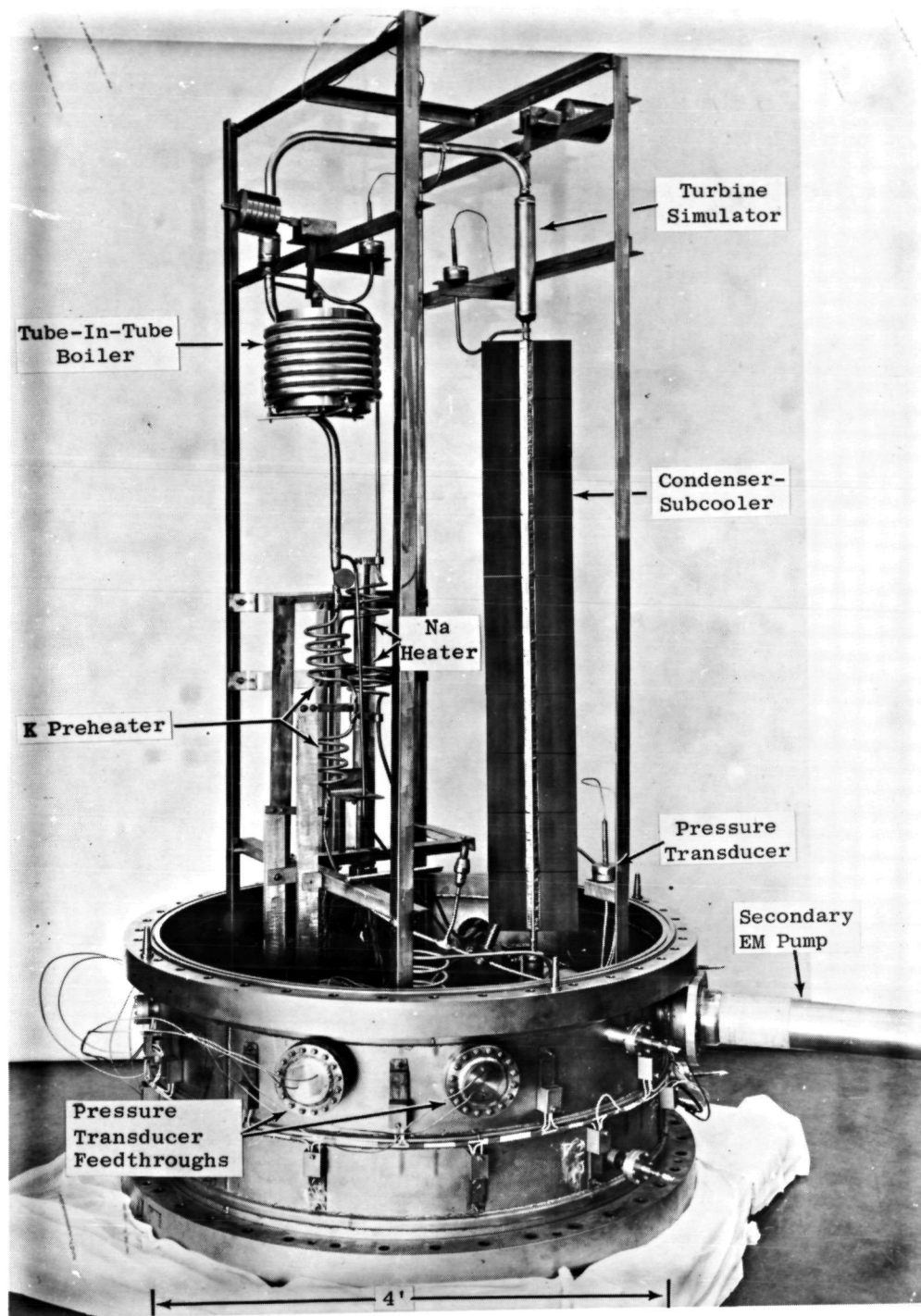


Figure 52. Prototype Corrosion Loop Following Installation in the Test Chamber Spool Piece. The Iron Titanate Coating was Applied to Both Sides of the 8-Inch Wide x 60-Inch Long Condenser Fin.

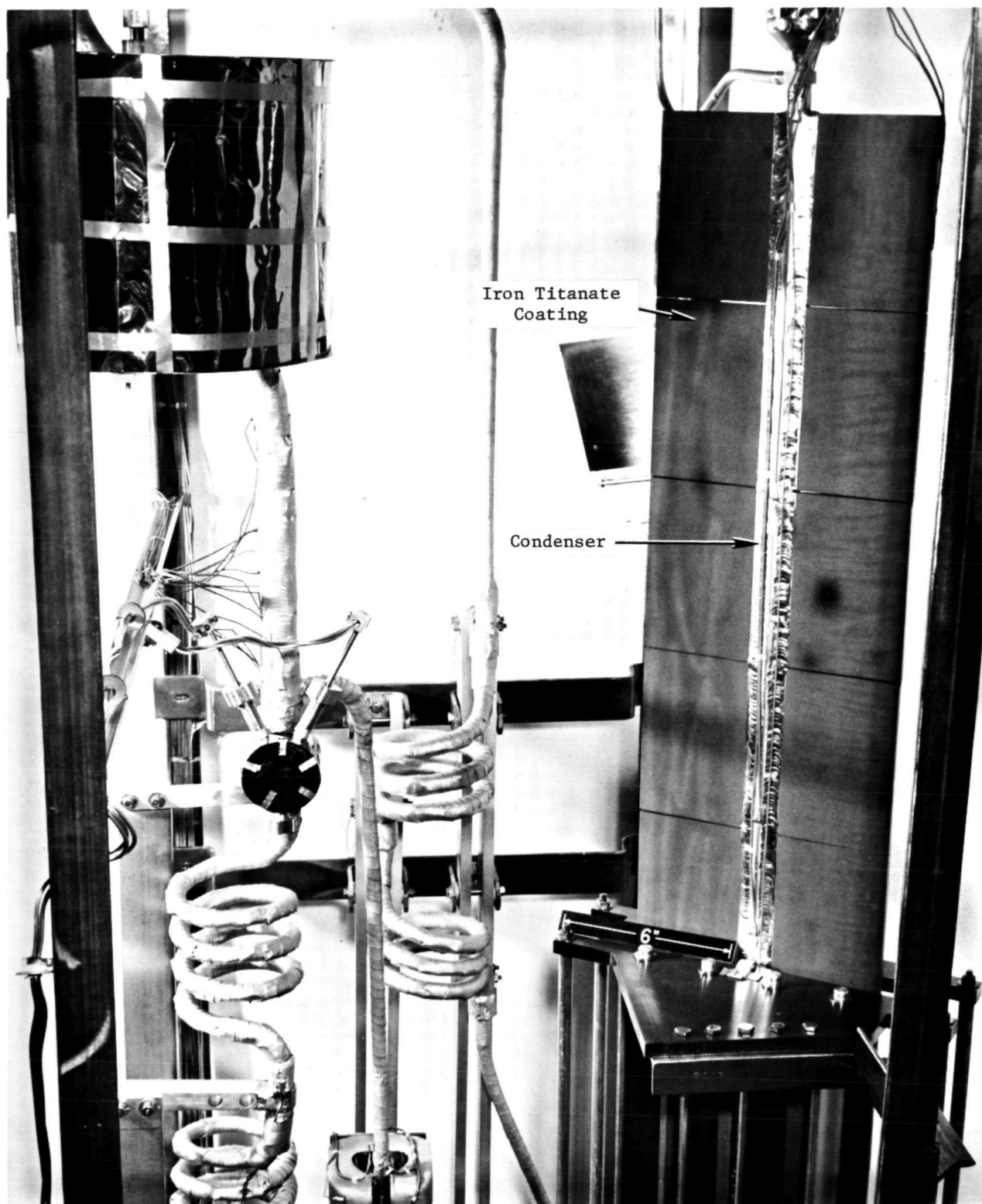


Figure 53. Close Up View of Corrosion Loop After Test. (C66031426)

fluoride bellows capsule II (NASA-LeRC Contract NAS 3-8523). In this test a Cb-1Zr bellows tube (similar in design to heat storage tubes) coated with Fe_2TiO_5 was thermally cycled 1500° to 1700°F in contact with LiF to simulate the sun-shade cycle of a heat receiver in a 300-nautical-mile orbit. The results indicated extreme oxygen contamination in the Cb-1Zr resulting from the decomposition of the Fe_2TiO_5 coating during a 3000 hour test period. Oxygen concentration as high as 2300 ppm were formed in the Cb-1Zr after the iron titanate coating was removed. Micro-probe analysis indicated additional reactions within the coating and between the substrates and coating. This test and evaluation effort is described in Reference 17.

4.2.3 Cb-1Zr Reducers

In the initial design of the Heat Receiver, 1.250-inch OD Cb-1Zr alloy tubes with 90° formed bends were designated for the gas tube extensions to connect each of the heat storage tubes to the outlet manifold. To provide flexibility for differential thermal expansions (as discussed previously in Section 3.3.2) the tube extensions were reduced to 0.75-inch OD. This required transitions at the exit end of each heat storage tube which has a 1.250-inch OD. The transitions, or reducers, were to be supplied by NASA. NASA's approach was to room temperature spin-form the required reducers from excess 1.250-inch OD Cb-1Zr alloy tubing used to fabricate the heat storage tubes.

The high ductility of the Cb-1Zr alloy readily lent itself to this type of forming technique. However, a highly stressed surface condition resulted from the localized work hardening incurred during spinning, which produced narrow crack defects. The defects were in the axial direction on the OD and ID. Mechanical removal of the defects would have resulted in a wall thickness below acceptable tolerance.

NASA and GE-NSP concurred that schedule commitments dictated another approach to the fabrication of the reducers, i.e. by machining reducers from solid bar stock. To obtain qualified Cb-1Zr bar stock in minimum time the following steps were taken:

- a) Reviewed two lots of in-house round bar sufficient for 17 reducers and initiated additional Q.A. tests. Based on avail-

able Q.A. data, conditionally released material. Results of the Q.A. tests confirmed the material was suitable for the intended application.

- b) Attempted, unsuccessfully, to obtain remaining material from suppliers in shorter than normal delivery.
- c) Internally processed several short length, but large rectangular cross section bars cut off from the manifold shell support rings. Six such bars were press forged to improve grain size. The bars were then machined to 1.5" diameter, vacuum annealed and ultrasonically inspected. All necessary QA was initiated and after evaluation of initial results (final results were acceptable) this bar stock was conditionally released to be machined into additional reducers. The remaining 2-4 reducers needed for the program were made from a small excess quantity of available ferrule stock.

4.2.4 Rivets

A length of 0.125-inch diameter Cb-1Zr alloy weld wire was supplied to a speciality vendor for cold heading on a trial basis. 360 trial rivets were produced and returned to GE-NSP. All of these rivets were radiographed, approximately 10 percent were fluorescent penetrant inspected and one was metallographically examined. The test results indicated the rivets were of acceptable quality and an order was placed for a supply of the various sizes required for fabrication assembly of the shell and top closure.

4.2.5 Top Closure

Fabrication of the top closure required a large diameter cone shaped part which distorted during several spinning attempts. Evaluations involving material integrity aspects were made in consultation with the manufacturing effort. This is described in greater detail in Section 6.4.

One of the materials areas which required specific attention concerned the vacuum stress relief anneal which was performed prior to final spinning operations. After an extensive survey of vacuum furnace facilities large enough to accept the top closure a Wall Colmonoy furnace in Dayton, Ohio (100-inch diameter x 86-inch high cold wall furnace with

carbon elements and shielding) was qualified for the thermal treatment provided the part would be doubly wrapped in sacrificial foil. The stress relief temperature was set at 1900⁰F to avoid grain growth which could lower the reliability of the part during subsequent spinning.

To minimize contamination during vacuum annealing of columbium and tantalum alloys, standard GE-NSP practice is to characterize the vacuum furnace environment as part of the qualification before committing these alloys to heat treatment. Controlled Cb-1Zr coupons are used in the bare and wrapped conditions, to determine the amount of interstitial element (O,N,H,C) pickup during an assimilated annealing run. If the pickup is less than 85 ppm, the furnace is considered qualified.

4.2.6 Aperture Assembly

Honeycomb Panel

The criteria for material selection for the aperture assembly door and frame structure were chemical compatibility, thermal expansion, dimensional stability, surface stability, and mechanical strength. As discussed previously (Section 3.6.1), a design change resulting in locating the insulation of the aperture assembly on the internal surfaces and the NASA specification for heat loss requirements resulted in an estimated uniform structure temperature of 400⁰ - 600⁰F. This range of anticipated service temperature and the fact that a temperature differential across the panels is essentially nonexistent, permitted the consideration of more conventional materials for the aperture structure.

A honeycomb sandwich structure was considered for this application because of its excellent strength-to-weight ratio and excellent stiffness-to-weight ratio. An all-welded (resistance) honeycomb sandwich was chosen because of its high reliability and because it minimizes the chemical compatibility and temperature limitations that are inherent in other honeycomb sandwich fabrications. At the present "state-of-the-science" PH15-7Mo and Inconel 718* have been used more than other materials in welded honeycomb sandwiches for aerospace applications.

* Nominal Compositions

Ph15-7Mo: 0.09C + 15Cr + 7Ni + 1Al - 2Mo + Bal Fe.

Inconel 718: 0.10C max + 19Cr + 5 (Cb+Ta) + 3Mo + 1 Ti + 0.50Al + 20Fe + Bal. Ni.

PH15-7Mo is a precipitation hardenable stainless steel. The chemistry of the alloy is balanced so that the alloy is austenitic in the annealed condition, martensitic in the hardened condition, and precipitates nickel-aluminum compounds during aging. The high alloy content provides excellent corrosion resistance. This is especially true in the annealed condition where the material displays chemical, physical, formability, fabricability, and mechanical properties similar to austenitic stainless steel. The material also has 2 percent molybdenum to provide better elevated temperature strength.

Inconel 718 is a nickel-base age hardenable superalloy. This alloy relies on the precipitation of $\text{Ni}_3(\text{Al},\text{Ti})$ and solid solution strengthening with refractory metal elements for its excellent elevated strength up to 1200°F .

The properties of Inconel 718 in the solution treated condition are not significantly different from its properties in the aged condition. Hence, the solution treated condition was considered. The material is formable and weldable when the proper techniques (methods and material condition) are used. Also, the high percentage of chromium and aluminum provides excellent oxidation resistance.

The chemical compatibility of either PH15-7Mo or Inconel 718 is adequate for the aperture structure application. Both of these materials are extremely resistant to oxidation and other corrosive media and would not pose a compatibility problem with any likely insulation system to be used on the aperture assembly.

The linear expansion match between the material selected for the door and frame application and the 304 SS used for brackets and attachments was extremely important if interface problems were to be avoided. Figure 54 shows a plot of the total thermal expansion of 304 SS, 15PH-7Mo, and Inconel 718 as a function of temperature. It can be seen from this curve that 15PH-7Mo in the annealed condition closely matches the expansion characteristics of the 304 SS. In the hardened and aged condition, the expansion of PH15-7Mo is similar to the lower expansion martensitic stainless steels.

Dimensional stability of the PH15-7Mo in the annealed condition was considered because of the possibility of this material experiencing micro-

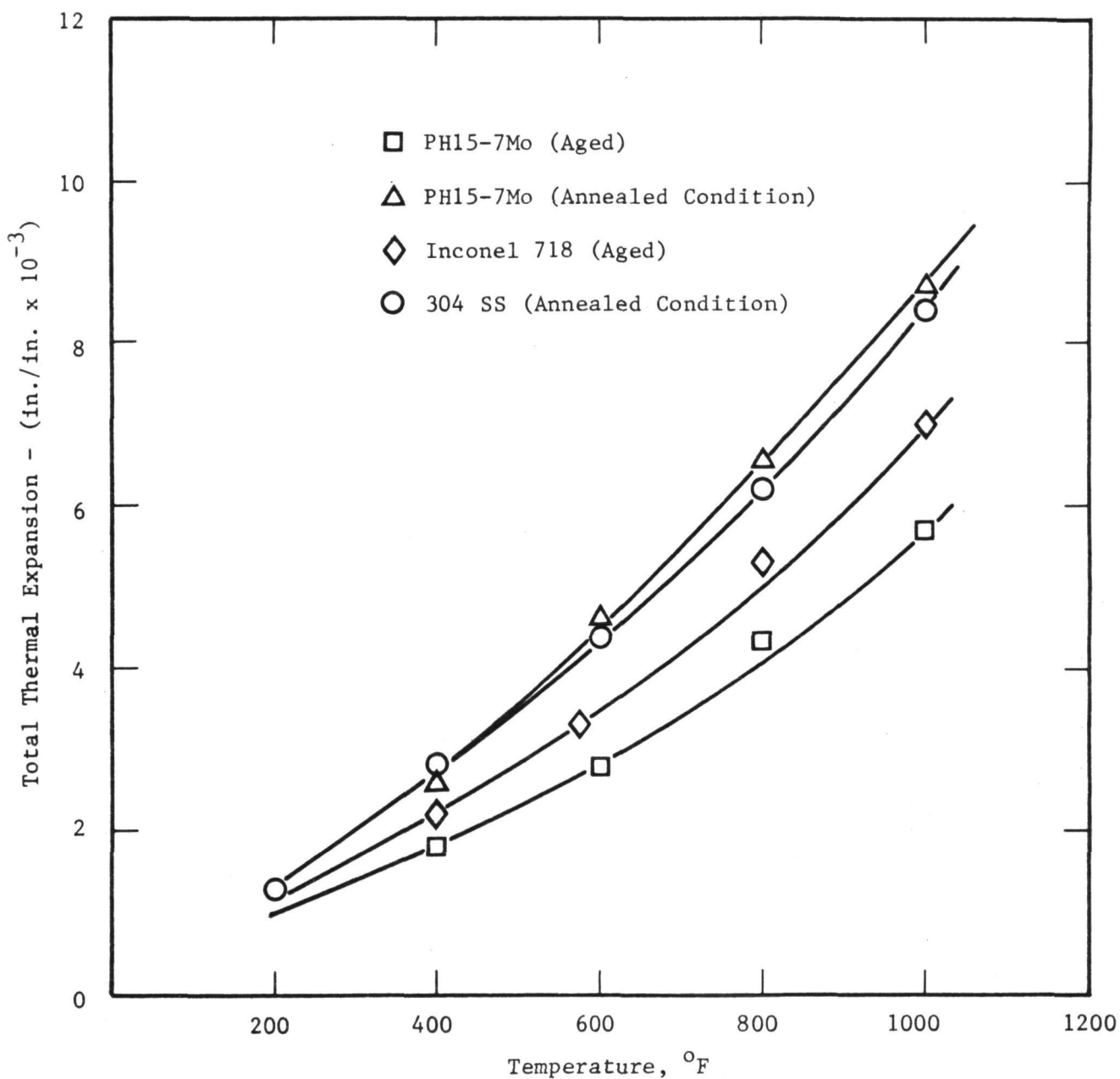


Figure 54. Thermal Expansion of Aperture Cone Candidate Materials.

structural instabilities during service in which carbon precipitation could result in the conversion of the austenite phase to martensite or ferrite. This conversion is accompanied by an expansion of 0.0045 in/in which could cause considerable distortion. Republic Steel research metallurgists were contacted regarding this possibility. Assurance was provided that at the low operating temperatures of the aperture assembly, this phenomenon is virtually impossible.

The surface stability of both of these high-chromium content alloys, PH15-7Mo and Inconel 718, is poor at high temperatures in hard vacuums; however, at the low operating temperatures (400° - 600° F) the evaporation rate is relatively low and loss of material due to evaporation was not considered a problem. The mechanical strength of either alloy was considered adequate for this application.

The PH15-7Mo in the annealed condition was selected for the honeycomb sandwich because of the similar expansion characteristics of this material with 304 SS, the interfacing material, and because of more reliable welding characteristics of this material in the annealed condition with the mating austenitic stainless steel members. Almost any of the austenitic stainless steels would have been suitable for this application; however, as mentioned previously, PH15-7Mo has been used extensively for all welded honeycomb sandwich for aerospace applications and was more readily available.

Hinge and Linkage Bearings

The selection of a bearing geometry and material for the heat rejection door hinges changed markedly as the design progressed. The original hinge concept was a pin and sleeve type bearing in which all the hinge assembly components were either Co-25Mo or Co-25Mo-10Cr alloy. These alloys developed at NASA (Reference 18) possess adequate high temperature strength and have a very desirable coefficient of sliding friction ($\mu = 0.4$ at 1300° F). Two significant developments led to important changes in the hinge design and material. First, the design temperature of the hinge dropped to a maximum temperature of about 700° F, when approval was obtained to move the aperture cone insulation inside the heat receiver. This change permitted the consideration of better developed bearing materials. The Co-base alloys mentioned earlier,

had never been fabricated into bearing shapes of interest and, of course, there was no performance data on similar parts made from these alloys. On the other hand, hard materials, such as refractory carbides and Vasco Hypercut, were well developed and had been made into bearing shapes.

The second development was the acceptance by NASA of GE-NSP's recommendation to select a ball bearing concept instead of a pin and bushing on the NASA-sponsored High-Temperature Valve Program (NAS 3-8514). Past experience at GE-NSP had indicated that the pin-bushing design was a higher-risk design compared to a ball bearing.

Two ball bearings having Vasco Hypercut* (high-speed steel) races and carbide balls had operated successfully as part of a valve actuation system on the High-Temperature Valve Program conducted at NSP. The bearings operated in a vacuum of 10^{-8} to 10^{-9} torr at estimated temperatures up to 800°F for 1500 hours and were still on test when the time for a decision was needed on the bearing for the Brayton Cycle Heat Receiver Program. Based on this experience, the only remaining problem concerned the selection of the specific materials of the ball bearing. An all carbide bearing, Carboloy 883 (WC-6Co), was recommended and ultimately selected. The all carbide bearing was selected over a carbide ball - Vasco Hypercut race bearing or an all Vasco Hypercut ball bearing because of its greater elevated temperature hardness stability and its superior oxidation resistance as compared to Vasco Hypercut. The carbide maintains a high hardness at elevated temperatures (~ 85 Rockwell A at 1200°F) well beyond the temperatures expected for the heat receiver application. The superior oxidation resistance of the carbide was important during nonvacuum exposure times such as assembly, installation, and checkout of the solar heat receiver.

The size and geometry of the ball bearings selected were the same as those used on the High-Temperature Valve Program.

The balls and races were obtained from General Electric Company Metallurgical Products Division in Detroit, Michigan.

* Vasco Hypercut Nominal Composition (wt %):
Fe, 8.0Co, 9.5Mo, 1.15V, 3.75Cr, 1.5N, .22Mn, .22Si, 1.07C.

The reduction in design temperature of the aperture assembly not only modified bearing material requirements but also eliminated the need for refractory metal hinge and linkage components; common commercially available materials were used for these applications.

Door Stops

The original estimated temperature of the contact surfaces between the doors and the aperture panels was expected to be in the range of 1600° to 1800° F. In this temperature range diffusion bonding of mating surfaces was a potential problem. Refractory metal carbides were being recommended as the material for this application because of their resistance to bonding and the fact that fabrication techniques are more well known for the carbides than for the cobalt-moly alloy specified in the original NASA design. Mechanical joining of carbide pads to the Cb-1Zr door/cone mating surface was also recommended.

As a result of a subsequent design change which moved the location of the insulation from the outside to the inside of the aperture cone, the maximum anticipated operating temperature of the pad region decreased to approximately 700° F. This change permitted the use of 300 series stainless steel for the aperture structure and the consideration of detonation sprayed Al_2O_3 (on a 304SS substrate) as the agent to resist bonding. There was concern that spalling or cracking of the Al_2O_3 coating might occur because of the difference in thermal expansion between it and 304SS. To evaluate the mechanical stability of the coating, 0.040-inch thick rectangular sheet coupons were prepared for thermal shock testing. Al_2O_3 coatings of 0.001 and 0.002-inch thickness were detonation sprayed on one side of each coupon by the Coating Service Department of Union Carbide Corporation. The Al_2O_3 , designated LA-2 (AMS2436), was 99+% Al_2O_3 and typically has a density of 0.1246 lb/in^3 and an average coefficient of expansion ($20\text{--}1800^{\circ}\text{F}$) $3.8 \times 10^{-6} \text{ in/in/}^{\circ}\text{F}$.

The thermal shock test which was planned was far more severe than any thermal transient anticipated during the operation of the heat receiver. The coupons were heated in an air furnace to 1200° F at a rate of 40°F/min. , held at temperature for 30 minutes and quenched into room temperature water. Minor edge cracking of the coating was observed.

Also, a minor flaking, which did not expose bare metal, was noted where the coating was abnormally thick.

The test results indicated that pads having either 0.001 or 0.002-inch thick coatings would perform well under expected service conditions. Based on these results, one coated stop (0.065 x 1.44 x 11.0) or flange bolted to each door was incorporated as the door stop configuration. To further alleviate the concern for differential thermal expansion, the design of the aperture door stop or flange was altered to permit slotting of each flange resulting in a discontinuous coated area. This "comb" configuration also permitted a degree of mechanical flexibility to insure positive closure of the doors thereby reducing thermal losses.

Insulation

Refrasil (Composition given in Table VIII) tape or cloth was initially specified by NASA as an insulation material for the aperture assembly. Refrasil has low thermal conductivity over the temperature range of interest. It has good flexibility, is readily available, and the tape or cloth can be used continuously at temperatures as high as 2100°F without losing its structural integrity. However, preliminary tests at NSP indicated that the excessive out-gassing behavior of Refrasil would probably lead to contamination of Cb-1Zr components.

TABLE VIII

TYPICAL COMPOSITION OF REFRASIL*

<u>Component</u>	<u>Concentration, W/O</u>
SiO ₂	99.30
TiO ₂	0.38
Al ₂ O ₃	0.18
B ₂ O ₃	0.07
ZrO ₂	0.02
CaO	0.01
MgO	0.01
Na ₂ O	0.01

* Personal Communication, Barrage, C.H.I,
Thompson Company, Gardina, California
September 11, 1967

Three alternate insulation concepts were considered: dimpled multi-layered foil, and two proprietary insulation systems. Dimpled or knurled, multilayered, 0.002-inch thick Cb-1Zr foil has the advantage that no filler insulation is required and there is no problem of chemical compatibility between the Cb-1Zr alloy structure and the insulating material. The large numbers of layers needed to maintain the very small heat loss was discussed in Section 3.7. Since the heat loss was very small a decision was made not to utilize it for the aperture assembly.

Both proprietary concepts, (one developed by Thermo-Electron Company (TECO) and the other by the Linde Division of Union Carbide Corporation) involved insulation packets consisting of alternating layers of metal foil and insulating material. For both concepts, the foil material was either Mo or Ni depending on the anticipated temperature.

In TECO's composite layered structure, called Multi-Foil, the metal foil layers were separated by a discontinuous film of oxide, such as ZrO_2 . The film was applied by spraying oxide particles dispersed in a binder on the foil. Subsequent heating removed the binder and promoted some diffusion bonding of the oxide to the metal. Vibration tests conducted by NSP of samples of TECO's Multi-Foil confirmed that there was adequate bonding.

Linde submitted a composite called Super-Insulation which was composed of alternate layers of metal foil and Astroquartz cloth or Refrasil fiber with a proprietary ceramic type reinforcing agent applied as a slurry. The composite was baked to remove the binding agents.

To evaluate the outgassing behavior of the candidate Linde materials, tests were conducted at the General Electric Tube Department, Owensboro, Kentucky. The tests were conducted on Astroquartz cloth, Refrasil quartz fiber and a composite of molybdenum foil/Astroquartz containing two types of proprietary reinforcing agents. The details relating to these tests, test results, conclusion and recommendations are contained in Reference 19.

Only the Astroquartz cloth was found to be suitable for the heat receiver application. Both the refrasil and rigidized composite exhibited excessive out-gassing characteristics.

Subsequent discussions with Linde concerning the excessive out-gassing of the composite revealed that the type and quantity of the ceramic binders could be altered to greatly reduce the out-gassing. Because of NASA's advised intent to apply insulation to the entire Heat Receiver upon its delivery to LeRC and the potential use of the Linde Super-Insulation for this application, NASA assumed the predominant role in following further development efforts at Linde. Ultimately, tests conducted by Linde on another generation of compositers, confirmed that an insulating package having an acceptable out-gassing level could be produced.

5.0 WELDING DEVELOPMENT AND QUALIFICATION

Page intentionally left blank

5.0 WELDING DEVELOPMENT AND QUALIFICATION

5.1 QUALIFICATION PLAN

Weld qualification for the Brayton Cycle Solar Heat Receiver consisted of personnel qualification for the manual welding requirements and weld process qualification for each unique joint type used in the fabrication of the heat receiver. Weld process qualification also included welding equipment, fixtures and tooling required for each weld. All welding by the inert gas tungsten-arc process was in accordance with NSP Specification 03-0025-00-A.

Welders were qualified for the manual welding requirements by making full fusion butt joints in sheet and plate. The test piece illustrated in Figure 55 was fabricated to qualify the Cb-1Zr alloy weldments required for gas system assembly. As the design progressed, additional joint types such as the support brackets-to-manifold and shell support ring-to-manifold were added. Three joints of each type were made and evaluated after preliminary welding trials had established welding parameters. Each type weld was made using the welding equipment, process and weld position intended for application to the heat receiver welding. Weld evaluation consisted of radiographic inspection as applicable, followed by sectioning and metallographic examination. The sheet and plate welds were also bend tested per NSP Specification 03-0025-00-A. This not only provided qualification of each weld type but furnished additional verification of the personnel qualification.

The automatic weld required for the manifold circumferential joints was qualified by making two weld specimens from 0.125-inch Cb-1Zr sheet using the welding equipment and process intended for application to this weld. The evaluation of these specimens was the same as for the sheet and plate manual weld samples. A full sized manifold mock-up, made from Type 304 stainless steel, was fabricated to qualify the tooling and fixtures required

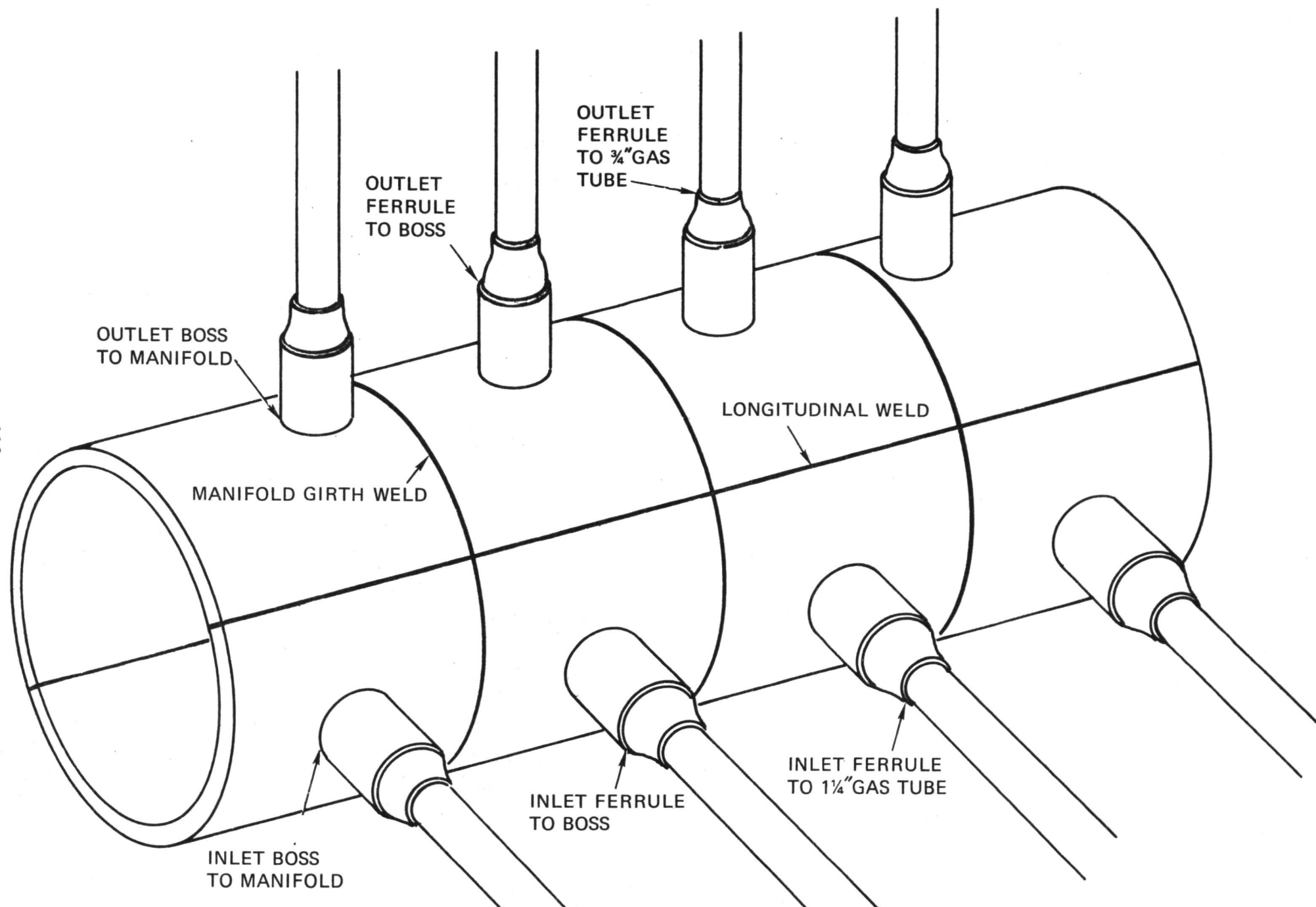


Figure 55. Brayton Cycle Heat Receiver Weld Qualification Tests.

for this weld as well as an additional qualification of the welding equipment and process.

5.2 PROCEDURES

Two men were qualified for the manual welding requirements by each welder making full fusion butt joints in 0.040-inch-thick sheet and 0.025-inch-thick plate. These weld specimens were evaluated by radiographing for soundness and bend testing in accordance with NSP Specification 03-0025-00-A.

A weld qualification test piece was fabricated per Drawing 47D173046 to qualify each type of weld joint and procedure used in the construction of the heat receiver. These welds are listed in Table IX, Items 4 through 19. This test piece was a 6-inch diameter cylinder made from eight pieces of 0.125-inch-thick Cb-1Zr alloy sheet using the weld procedures for the manifold girth welds and the longitudinal welds required for the nozzle diffuser and elbow sections. After holes were drilled, four inlet bosses and four outlet bosses were welded to the test piece. The bosses were then machined in accordance with established procedures.

The automatic tube-to-tube weld samples consisting of the (1) inlet ferrule to 1.25-inch diameter tube; (2) 1.25-inch diameter tube to reducer; (3) outlet ferrule to 0.75-inch diameter tube; and (4) 0.75-inch diameter tube to reducer welds were fabricated using the welding equipment, fixtures and procedures intended for application to the heat receiver welding. These weld samples were then used for the boss-to-ferrule weld qualification.

Additional parts were welded to the test piece to qualify the remainder of the welds. These were the (1) elbow-to-manifold weld; (2) support tube-to-manifold weld; (3) support pad-to-tube weld and; (4) shell support ring-to-manifold weld.

Another test piece was fabricated to make additional boss-to-manifold and elbow-to-manifold welds after preliminary welding trials showed that a change in the weld joint design or process was required. This is discussed in the Weld Development section (5.3).

All weld joints of the test pieces were evaluated by radiographing for soundness and then sectioning three of each type of weld joint for metallographic examination. Results of this evaluation are listed under Qualification Results and Documentation (Appendix C).

TABLE IX

BRAYTON CYCLE HEAT RECEIVER WELD QUALIFICATION TESTS

Item No.	Weld	Type	Material Requirement	Weld Position	Drawing No.
1	Personnel Qualification	Manual TIG	.040 thick x 4 x 10	Weld Horizontal	Weld prep per Spec. 03-0015-00
2	Personnel Qualification	Manual TIG	.250 thick x 4 x 10	Weld Horizontal	Weld prep per Spec. 03-0015-00
3	Manifold-Circumferential	Automatic TIG with filler wire .045 dia.	2 pcs. - .125 thick x 4.5 x 36 lg	Weld Horizontal	47D173030
4	3" dia. Bimetallic Joint to Elbow	Manual TIG	.125 thick x 11 x 34 lg	Pipe Axis Horizontal Fixed Position	47D173046 Girth Weld
5	6" dia. Manifold - Girth				
6	3" dia. Diffuser to Elbow				
7	Diffuser - Longitudinal	Manual TIG	.125 thick x 11 x 34 lg	Weld Horizontal	47D173046 Seam Welds
8	Elbow - Longitudinal	Manual TIG	.125 thick x 11 x 34 lg	Weld Horizontal	47D173046 Seam Welds
9	Manifold - Inlet Boss	Manual TIG	1.5 dia. x 8 lg	Bosses to be welded in two positions equivalent to plane of manifold in horizontal and vertical positions	47D173046
10	Manifold - Outlet Boss	Manual TIG	1.125 dia. x 8 lg		47D173046
11	Inlet Ferrule to 1.25 dia. x .025 wall Tube	Automatic TIG No Filler Wire	1.25 OD x .025 wall tube x 9 lg 1.5 dia. x 6 lg	Tube rotation on horizontal axis	Ferrule Dwg. 47B116899
12	Outlet Ferrule to .75 dia. x .025 wall Tube	Automatic TIG No Filler Wire	.75 OD x .025 wall tube x 9 lg 1.0 dia. x 6 lg	Tube rotation on horizontal axis	Ferrule Dwg. 47B116900
13	1.25 OD Tube to Reducer	Automatic TIG No Filler Wire	1.25 OD x .025 wall tube x 9 lg 3 - 1 1/4 to 3/4 tube reducer	Tube rotation on horizontal axis	Reducer Dwg. 47C146031
14	.75 OD Tube to Reducer	Automatic TIG No Filler Wire	.75 OD x .025 wall tube x 9 lg - reducer same as item 13	Tube rotation on horizontal axis	Reducer Dwg. 47C146031
15	Boss to Inlet Ferrule	Manual TIG No Filler Wire	Items 9, 10, 11 and 12 will be used	Tube in two positions equivalent to plane of manifold in horizontal and vertical positions.	Welds per Dwg. 47D173031
16	Boss to Outlet Ferrule	Manual TIG No Filler Wire	Items 9, 10, 11 and 12 will be used	Same as Item 15.	Welds per Dwg. 47D173031
17	3" dia. Elbow to Manifold	Manual TIG	.125 thick x 11 x 34 lg	Weld Horizontal	47D173046
18	A. Support Tube to Manifold B. Support Pad to Tube	Manual TIG	3 pcs. - .250 thick x 4" x 4"	Weld Horizontal	47D173046
19	Shell Support Ring to Manifold	Manual TIG	Section of P2 Ring	Weld Horizontal	47D174871

5.3 WELD DEVELOPMENT

One of the primary purposes of the weld qualification task was to identify problems with weld joint designs, welding procedures or fixtures prior to commitment of hardware. Five of the weld joints used in the heat receiver required a change in either the joint design or welding procedure which resulted from the welding qualification trials.

1. Boss-to-Manifold Welds

The original boss-to-manifold weld joint design is illustrated schematically in Figure 56. It was anticipated that full penetration would be achieved during the fusion pass applied to the OD. A second weld pass with filler metal addition would complete the weld. Initial welding trials indicated that full penetration could be achieved, however the weld heat input caused erratic melting of the ID edge of the manifold. Although the joint was structurally sound, the uneven and rough appearance and possible adverse effects due to potentially excessive geometric distortions were causes for rejection of the original welding procedure.

The new welding procedure devised for this joint incorporated both automatic and manual welding techniques. Initially bosses were GTA tack welded to the manifold as shown in Figure 57. The root pass was then made using the internal rotary welding torch illustrated in Figure 58. This procedure resulted in very uniform fusion between the boss and manifold. Weld inspection was simplified because the extent of penetration could be determined visually at the joint OD. A manual filler pass was then applied to the OD of the joint.

2. Inlet and Exit Tube-to-Manifold Weld

A problem similar to the boss-to-manifold weld was encountered, that is, uneven and rough melting at the manifold ID. In this case, however, the automatic internal welding technique could not be applied because a 3.0-inch diameter elbow was welded directly to the outlet manifold. This problem was resolved by enlargement of the manifold hole as illustrated in Figure 59. By maintaining the joint overlap at a maximum of 0.020-inch, it was possible to fully penetrate

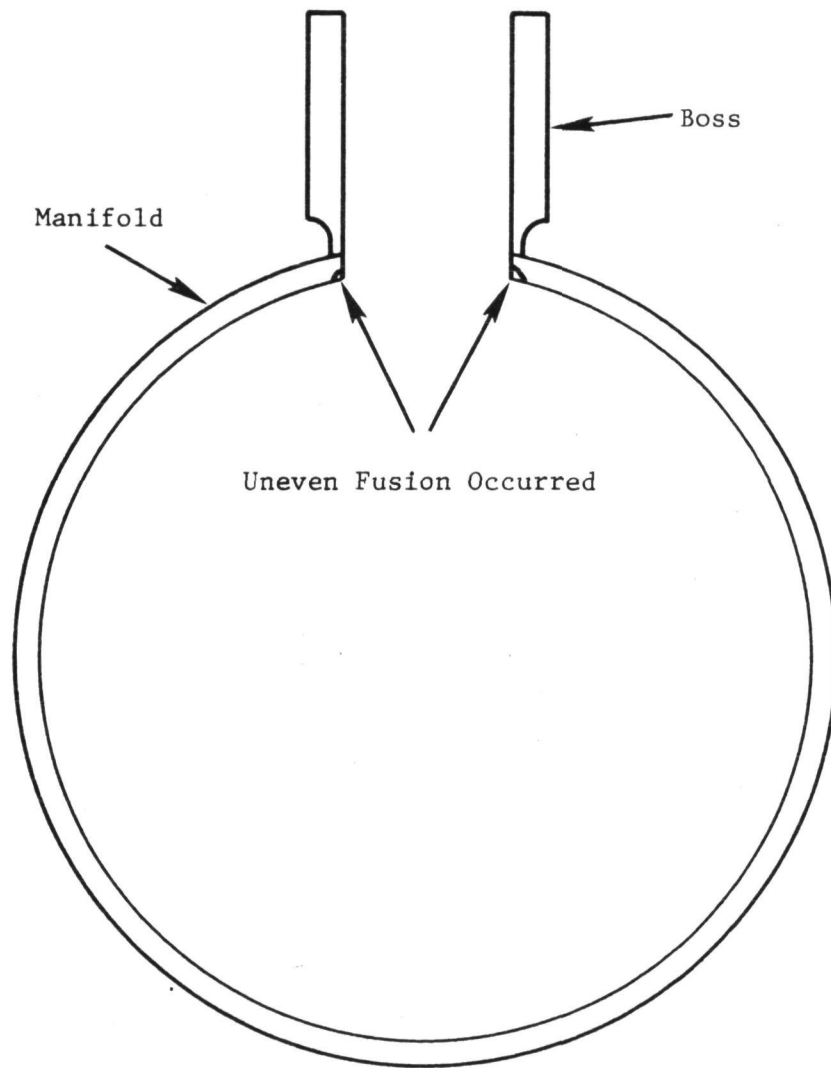


Figure 56. Original Design Typical Boss-to-Manifold Joint.

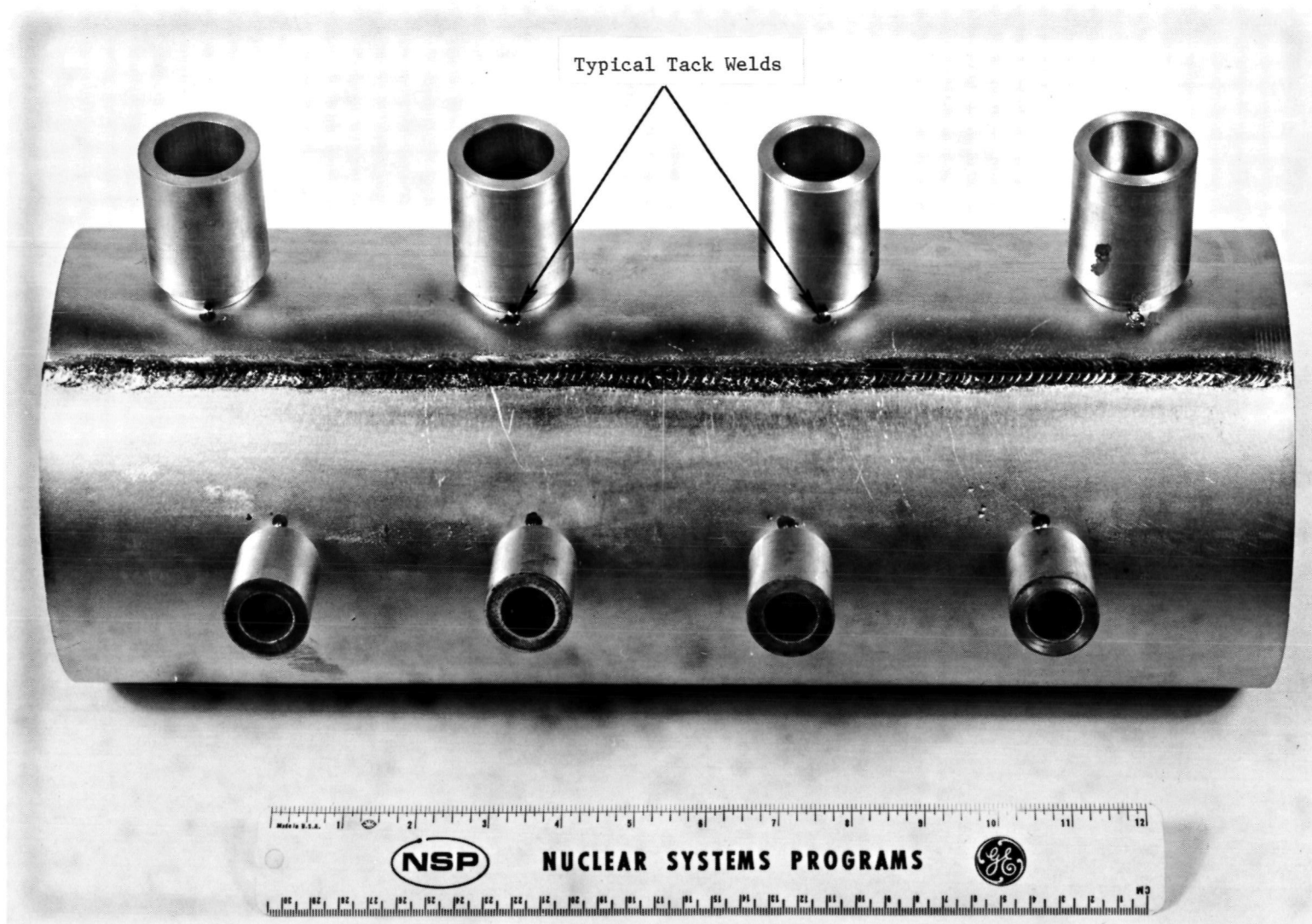


Figure 57. Weld Qualification Test Specimen Illustrating GTA Tack Welds Used for Boss Positioning. (P69-2-42A)

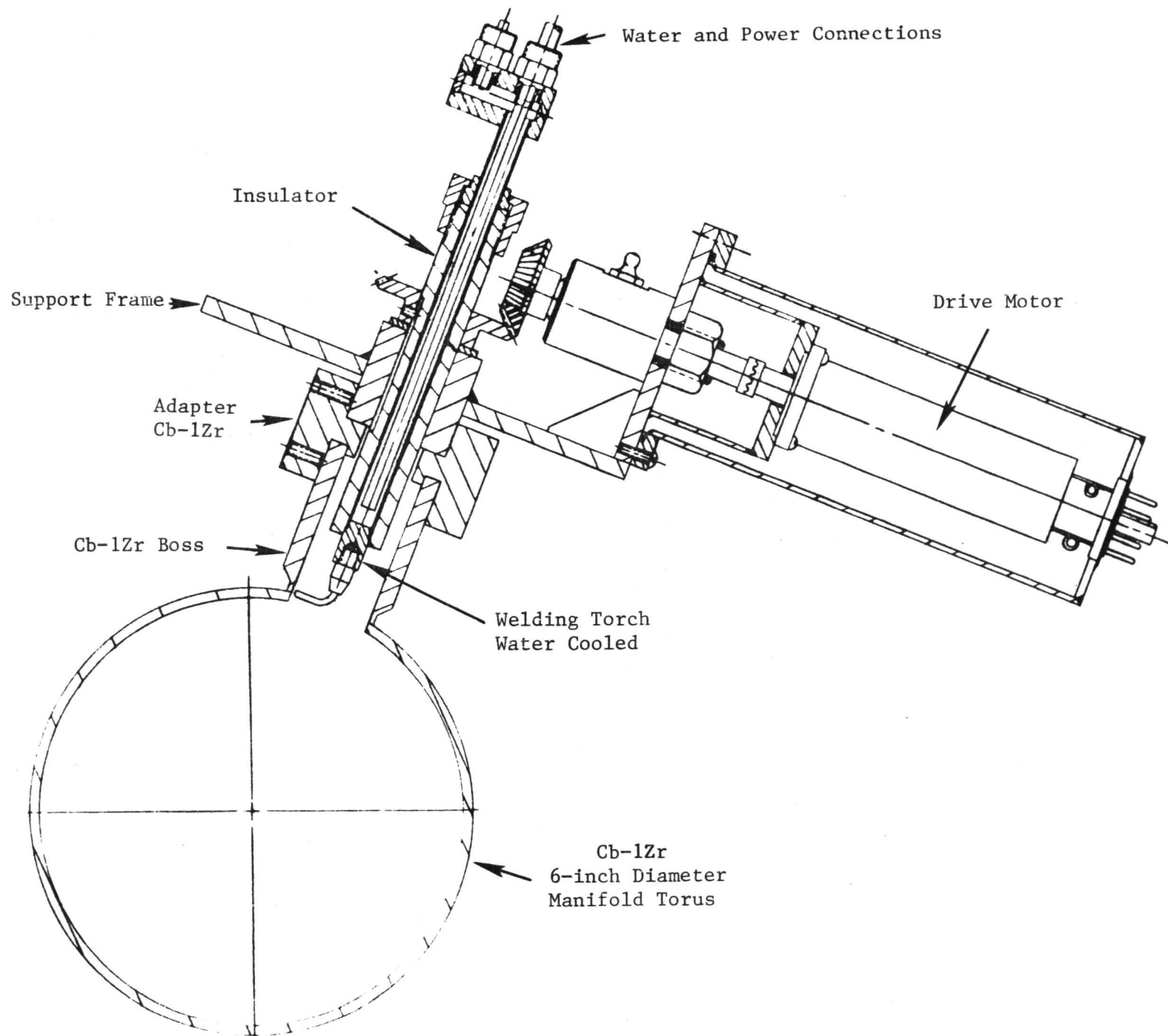


Figure 58. Internal Rotary GTA Welding Torch.

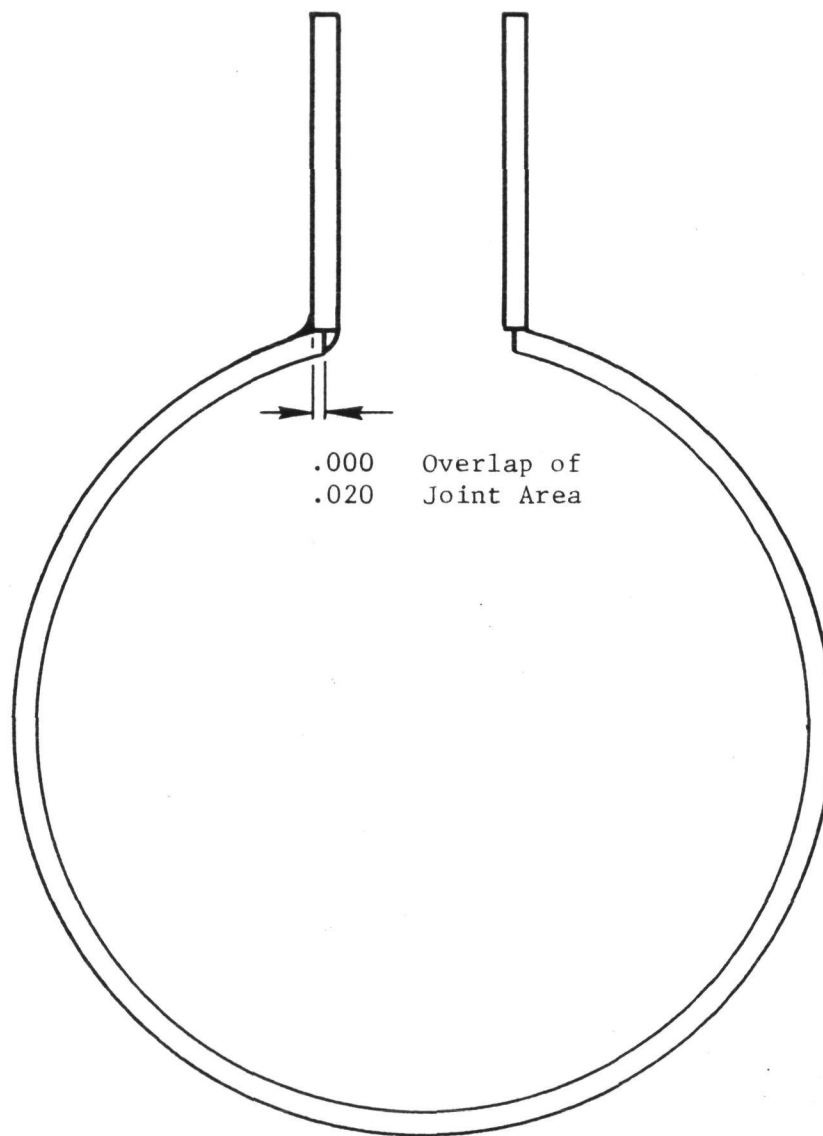


Figure 59. Design of Tube-to-Manifold Weld Joints.

the joint. This resulted in complete fusion at the joint ID. A manual filler pass was then applied to form a reinforcing fillet.

3. Boss-to-Ferrule Weld

This joint was originally planned to be made using the Orbit arc welding equipment. This equipment, illustrated in Figure 60, consisted of a portable welding head with a motor driven split-ring electrode holder. Thus, tube-to-tube joints can be welded automatically without rotation of the tubular members. This process was abandoned for the heat receiver application when, after repeated attempts and redesigns, the equipment failed due to breakdown of internal insulation.

During the weld fixture planning stages, design provisions were made to allow for positioning the heat receiver for manual welding of boss-to-ferrule joints. This approach was adopted and qualification joints were prepared. During welding, the joint position was equivalent to that required during final assembly of the heat receiver. That is, each joint was welded in 180° increments to simulate the two positions required on the assembly.

4. Tube-to-Ferrule Weld

These joints were produced by rotation of the tubular joint under a stationary GTA torch. Preliminary trials indicated lack of weld penetration. Variation in weld parameters to obtain full penetration, such as increased welding current or decreased welding speed, resulted in severe undercutting of the tube wall.

The ferrule was redesigned to reduce the wall thickness at the socket joint by 0.010-inch. Full penetration welds without undercutting were then made without difficulty.

5. Support Pad-to-Tube Weld

Metallographic examination of initial joints of this type indicated that weld fusion area was less in cross section than the base metal. This condition was corrected by adding a filler pass to the weld procedure for this joint.

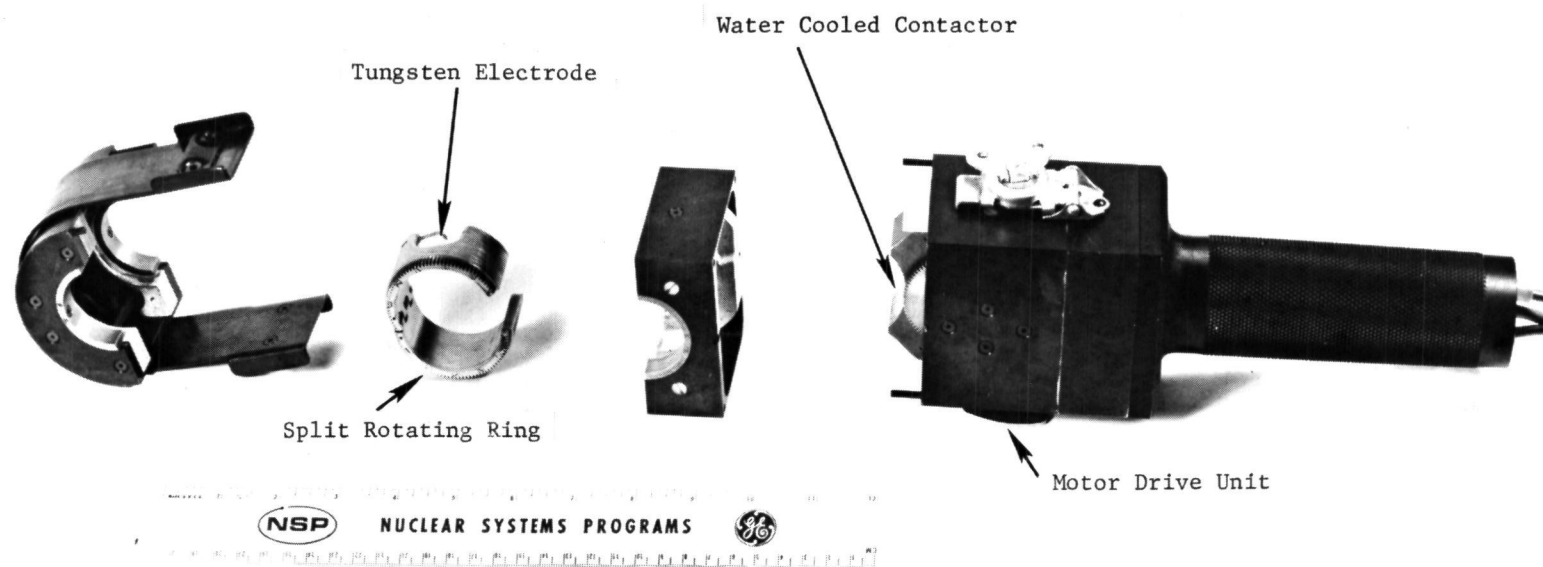


Figure 60. Special Water-Cooled Tube Welding Head. (P69-2-38B)

5.4 QUALIFICATION RESULTS AND DOCUMENTATION

The qualification results are given in Appendix C for each weld item number listed in Table IX. Each unique joint configuration, welding parameters and test results are listed on the qualification form. In addition, weld process control records and applicable photomicrographs are presented.

6.0 F A B R I C A T I O N A N D A S S E M B L Y

6.0 F A B R I C A T I O N A N D A S S E M B L Y

6.1 OVERALL SEQUENCE

The complete fabrication sequence for the Brayton Cycle Heat Receiver is depicted in Figure 61. For the gas system assembly, close integration was required of the four basic fabrication processes: machining or forming, cleaning, welding, and postweld annealing. Each component fabrication and assembly was controlled by manufacturing instructions which defined the detailed sequences and inspection points.

6.2 GAS SYSTEM

The major fabrication effort involved the gas system assembly sequences as shown schematically in Figures 62 to 67 and Table X. Consideration of refractory alloy welding and related sequences were of particular significance and are therefore discussed in detail prior to discussing the gas system fabrication effort itself.

6.2.1 Welding

Welding Specifications

All gas tungsten arc (GTA) welding of the gas system was done using the weld chamber shown in Figure 68. This welding system consisted of the basic 3.0-foot diameter by 6-foot long chamber shown on the left to which two 8-foot diameter x 4-foot long chamber extensions were attached. Not shown is the universal welding positioner incorporated in the two 8-foot diameter chamber extensions which was especially developed for welding the refractory metal gas system. Welding per Specification NSP 03-0025-00-A was conducted after purging the system by evacuation to a pressure in the 10^{-5} torr range and backfilling with high purity helium gas. During the welding cycle helium purity was monitored using a gas chromatograph for oxygen and nitrogen content and an electrolytic hygrometer for moisture content. All welding was conducted within the specification limits of 5 ppm oxygen, 15 ppm nitrogen and 20 ppm moisture content.

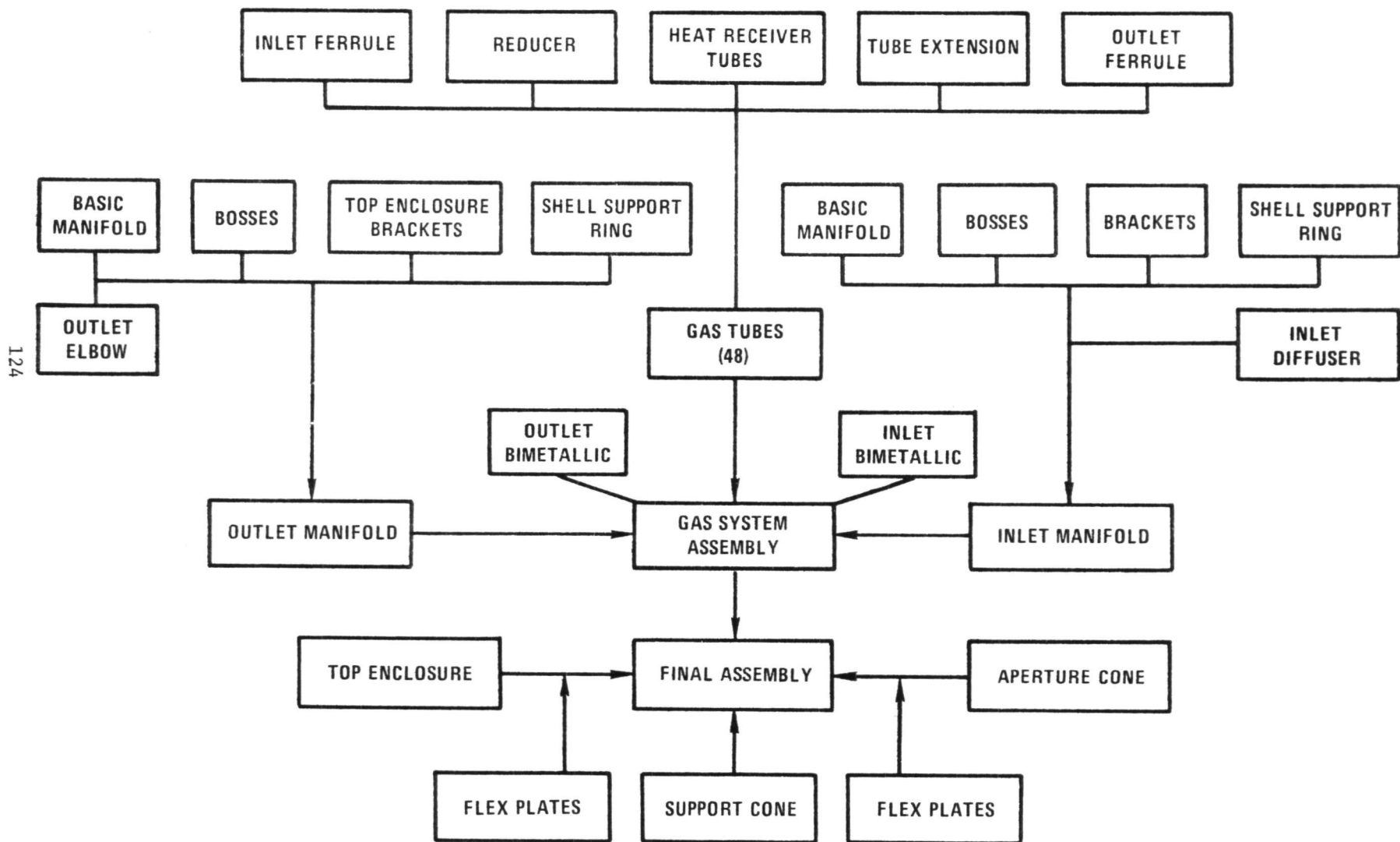
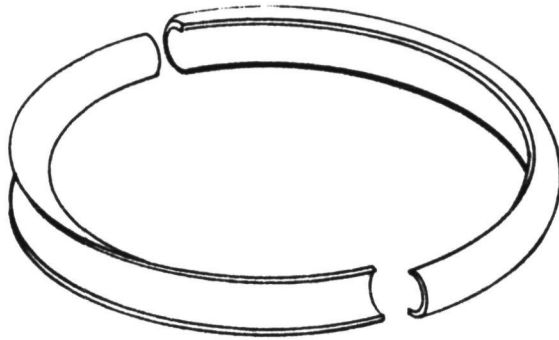
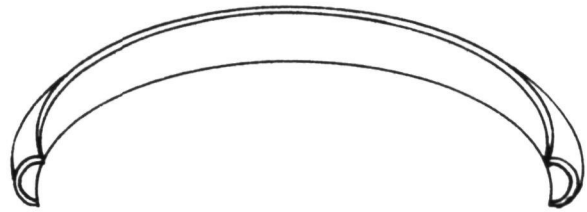


Figure 61. Brayton Cycle Heat Receiver Fabrication Sequence.

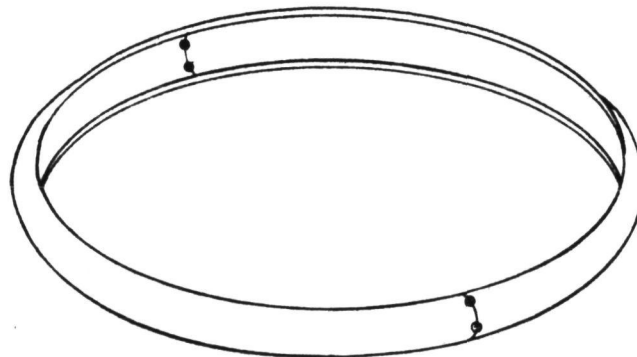
**STEP 1 FORM INNER AND
OUTER SEGMENTS**



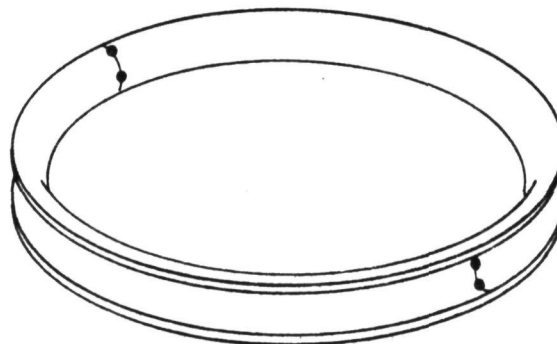
STEP 2 TRIM ENDS TO SIZE



**STEP 3 TACK WELD ENDS TO
FORM HALF-TORUS AND
MACHINE CIRCUMFERENTIAL
WELD JOINT**



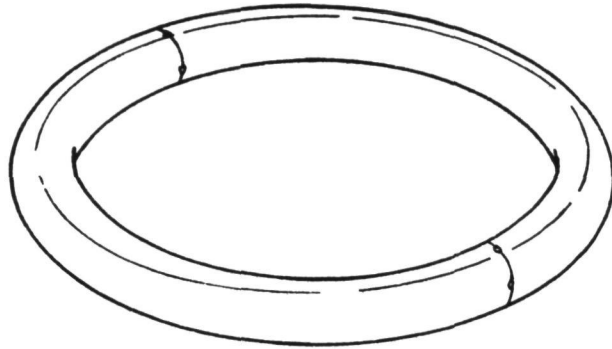
OUTER



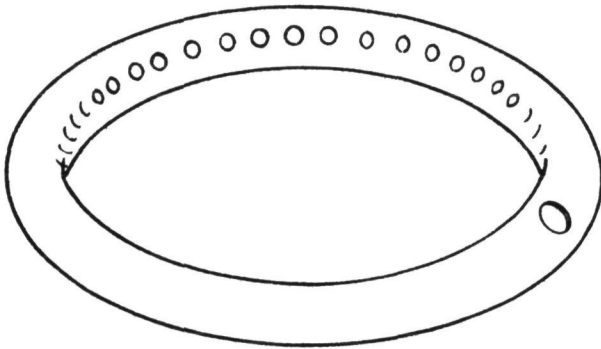
INNER

Figure 62. Manifold Forming and Machining.

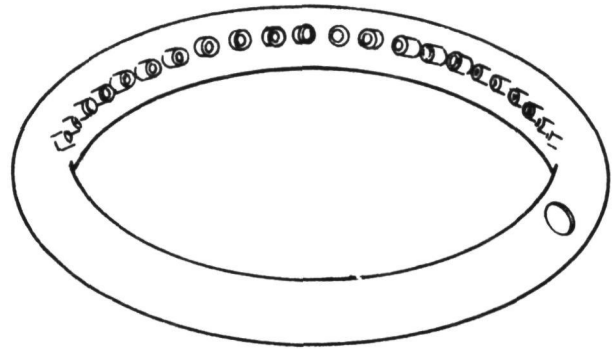
**STEP 1 WELD INNER AND OUTER
HALVES TOGETHER**



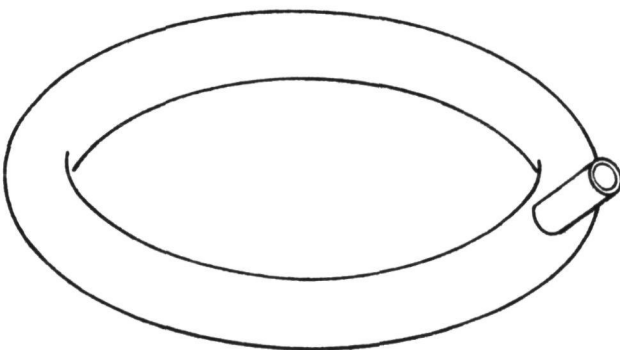
**STEP 2 MACHINE HOLES FOR
BOSSES AND NOZZLE**



STEP 3 WELD BOSSES TO TORUS



**STEP 4 WELD INLET OR OUTLET
TO MANIFOLD**



**STEP 5 WELD BRACKETS AND
SHELL SUPPORT RINGS**

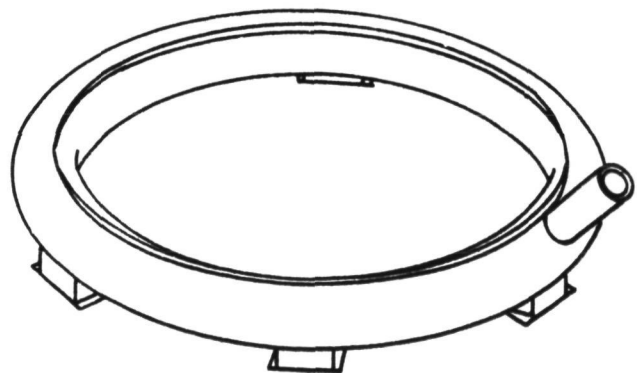
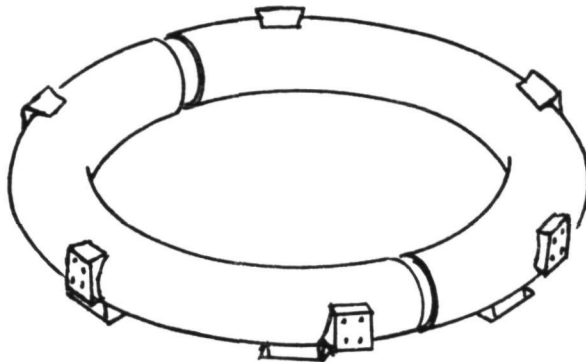
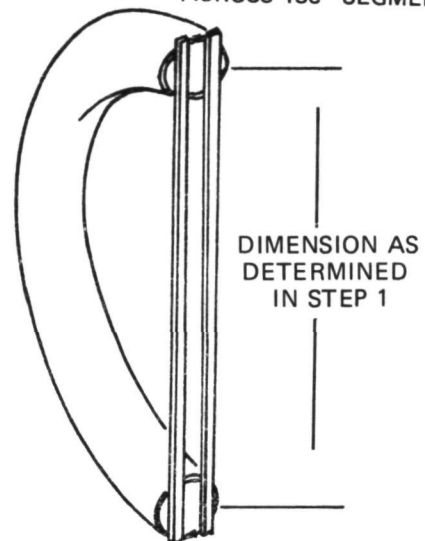


Figure 63. Manifold Welding.

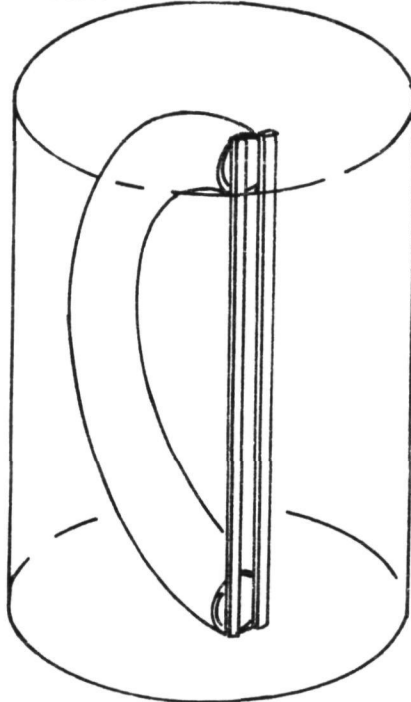
STEP 1 SPLIT MANIFOLD AT TACK WELDS
AFTER ESTABLISHING UNSPRUNG
TORUS DIMENSION



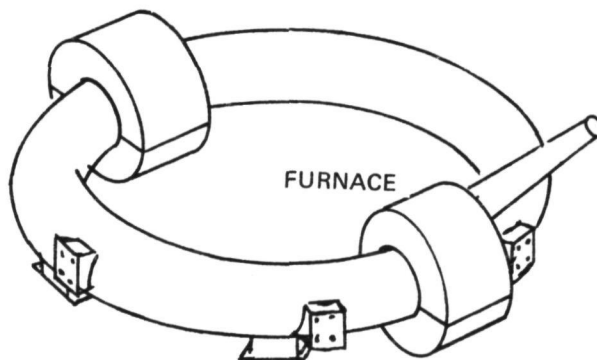
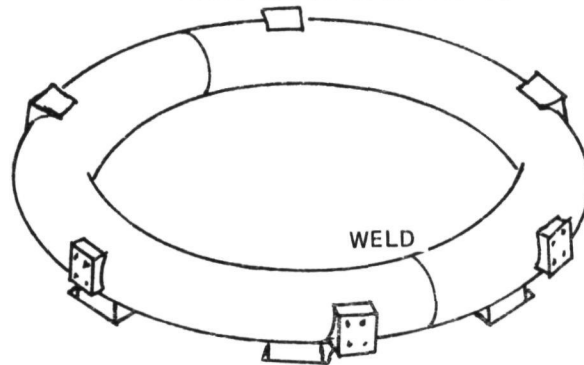
STEP 2 WELD TIE BARS
ACROSS 180° SEGMENT



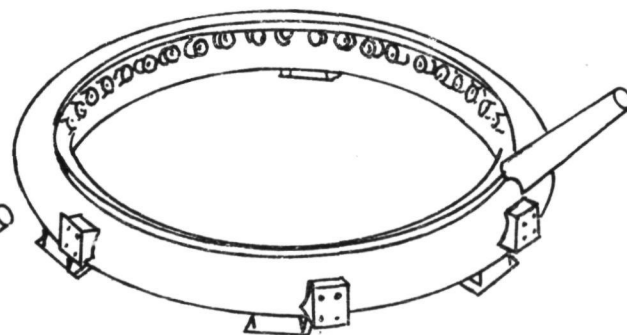
STEP 3 POST-WELD ANNEAL AT 2200°F



STEP 4 REMOVE TIE BARS, WELD PREP
FIXTURE FOR GIRTH WELDS



STEP 5 LOCAL ANNEAL GIRTH WELD



STEP 6 FINAL MACHINING OF BOSSES,
BRACKETS, AND SHELL SUPPORT
RING

Figure 64. Manifold Annealing, Final Welding and Machining.

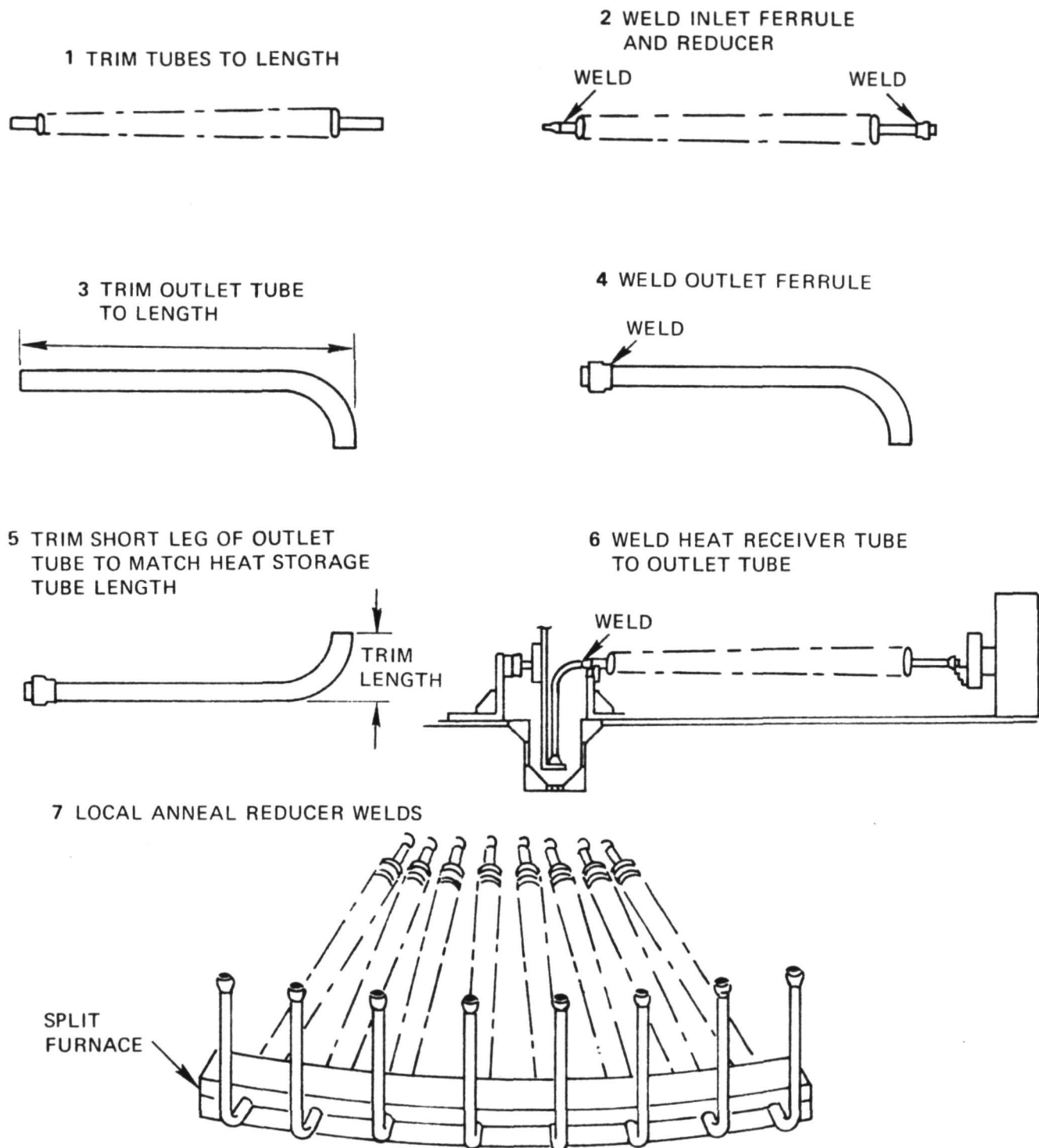


Figure 65. Heat Storage Tube Weld Sequence.

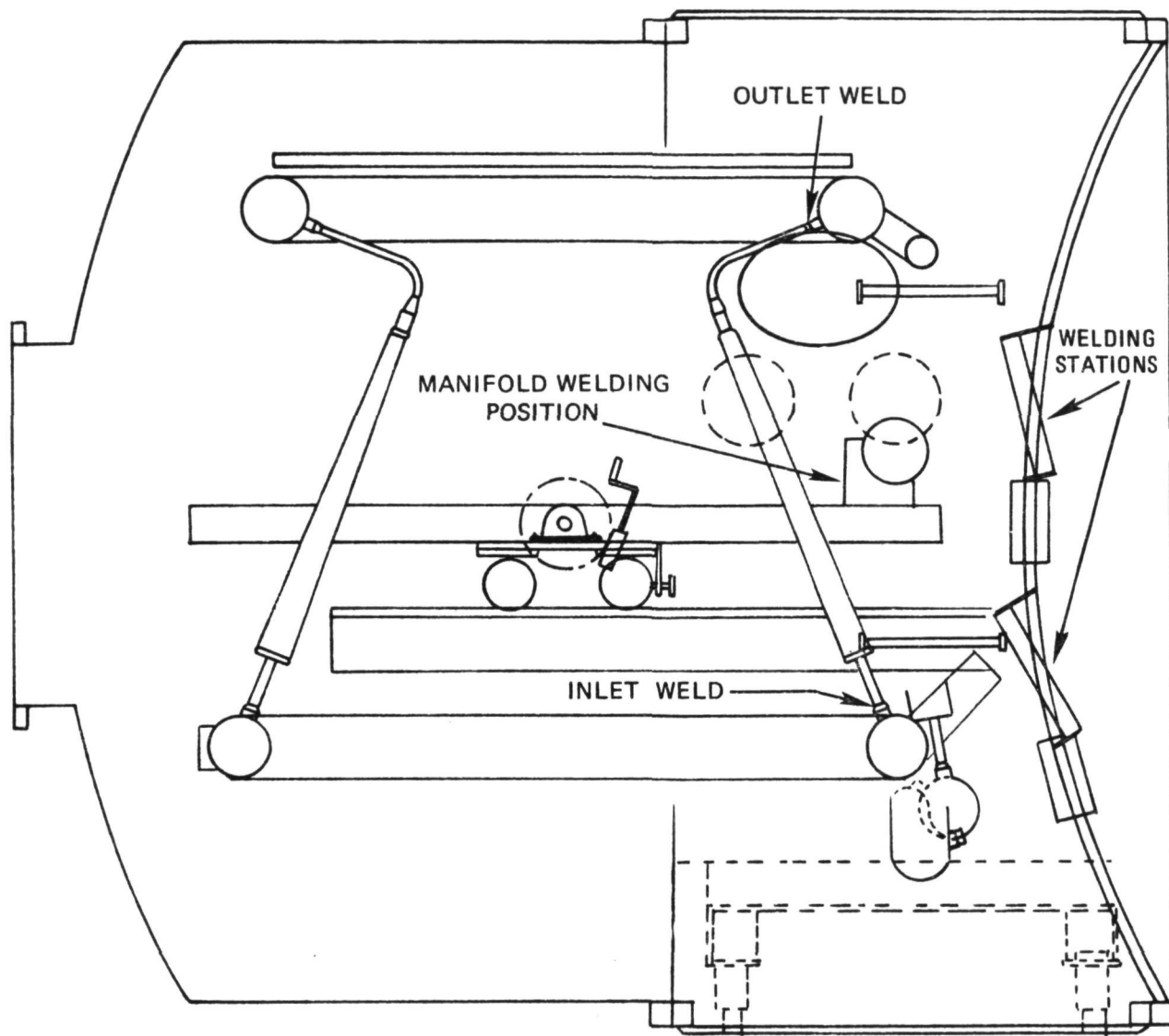


Figure 66. Welding Chamber Installation, Side View.

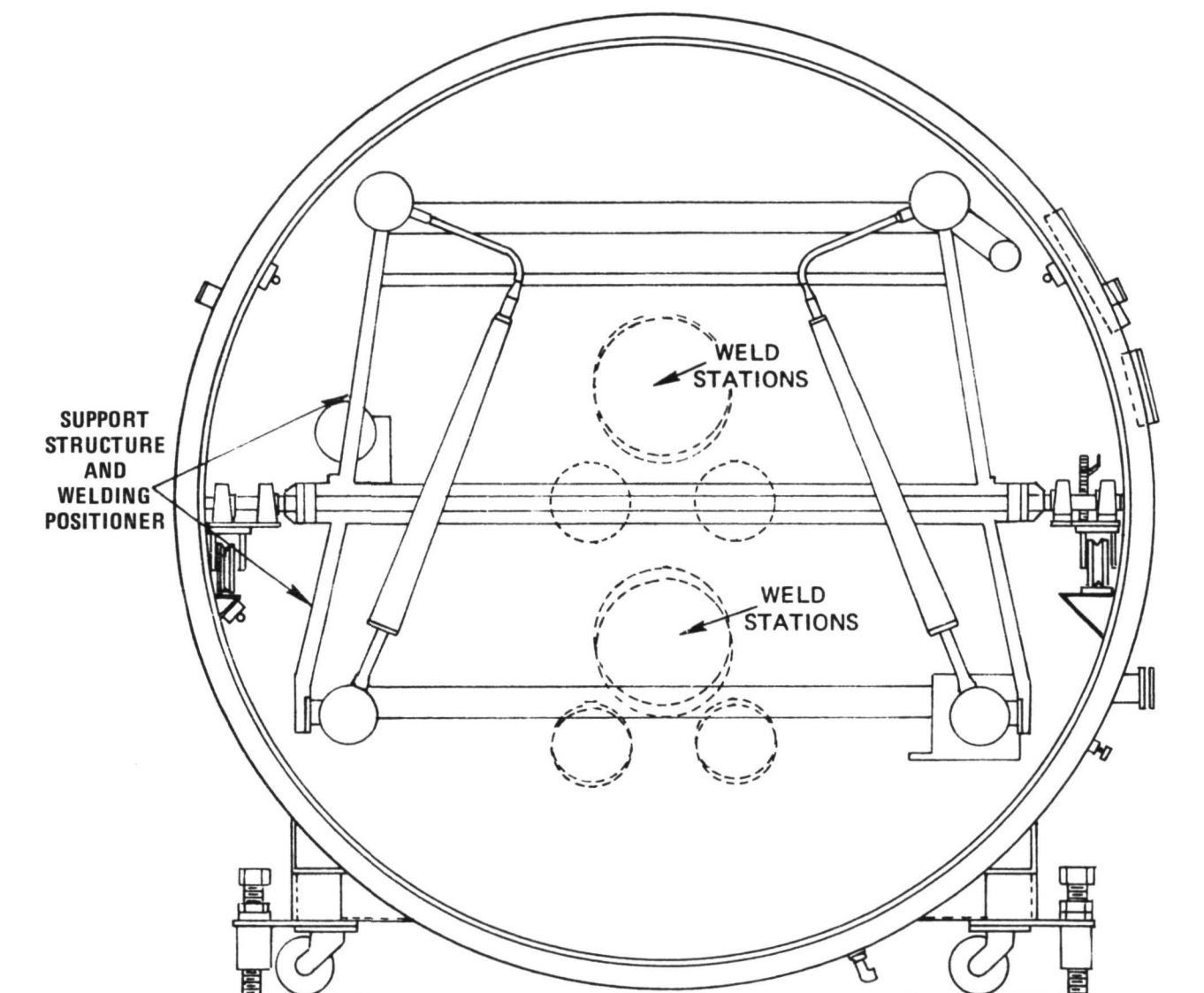


Figure 67. Welding Chamber Installation, End View.

TABLE X

FABRICATION SEQUENCE
BRAYTON CYCLE HEAT RECEIVER

Manifolds (Inlet and Outlet)

Upper Items 1 and 2	<u>Operation</u>	<u>Sequence</u>
10		Radial Draw Form Two (2) each item
Lower Items 3 and 4	10	Radial Draw Form Two (2) each item
	20	Trim ends of segments
	30	Clean segments
		Handle with clean white gloves and cover with polyethylene during shipment and storage.
	40	Tack weld two (2) each items 1, 2, 3, and 4 at ends.
	50	Machine diameters A per drawing and weld prep.
		All machining to be done without coolant or cutting oil.
	60	Clean manifold halves with freon wipe
	70	Position in weld fixture and tack weld
	80	Automatic TIG weld of circumferential weld joints
	90	Drill 48 holes for bosses
	100	Machine openings for inlets
	110	Clean manifolds to remove chips and degrease with freon
	120	Manually weld 48 bosses to torus (plug through bosses and holes in manifold for alignment)
	130	A Tube B Pad Weld top closure brackets to outlet manifold

NOTE: Each ten series represents one chamber weld set-up - Ex. 140, 145, and 148

TABLE X (cont'd)

135	A Tube	Aperture cone brackets to inlet manifold
	B Pad	
140		Shell support ring to outlet manifold
145		Shell support ring to inlet manifold
148	A Tube	Main support brackets to inlet manifold
	B Pad	
150		Weld nozzle to inlet manifold
153		Weld elbow to outlet manifold
155		Wire brush weld areas
160		Split into 180 ⁰ halves
165		Freon clean and inspect inside of manifolds
170		Weld tie bar across 180 ⁰ segments
180		Heat treat anneal
190		Remove tie bars
200		Weld prep ends of manifold segment
210		Clean ends - freon wipe
220		Manually weld two halves together
230		Local anneal two girth welds each manifold
240		Finish machine bosses, brackets and shell support ring - plug all openings during machining
250		Clean-degrease with freon

Gas Tube Assembly

10	Trim heat storage tube to length
20	Clean ends
30	Weld inlet ferrule to heat storage tube inlet
40	Weld reducer to heat storage tube outlet
50	Trim tube extension to length on outlet end and clean
60	Weld outlet ferrule to tube extension

TABLE X (cont'd)

70	Measure length of heat storage tube and trim short leg of extension tube to length-clean
80	Install in fixture and weld tube to reducer on heat storage tube
90	Local anneal two reducer welds
<u>Gas System - Final Assembly</u>	
10	Align and secure manifolds in welding fixture - install gas tubes (48), secure and rotate set-up to check alignment
20	Tack weld 48 inlet manifold/gas tube joints
30	Weld OD side, 48 outlet manifold/gas tube joints
32	Weld ID side, 48 outlet manifold/gas tube joints
34	Weld ID side, 48 inlet manifold/gas tube joints
36	Weld OD side, 48 outlet manifold/gas tube joints
40	Reposition and weld bimetallic joint on inlet manifold
50	Reposition and weld bimetallic joint on outlet manifold
60	Post weld anneal locally-all welds per 03-0037-00

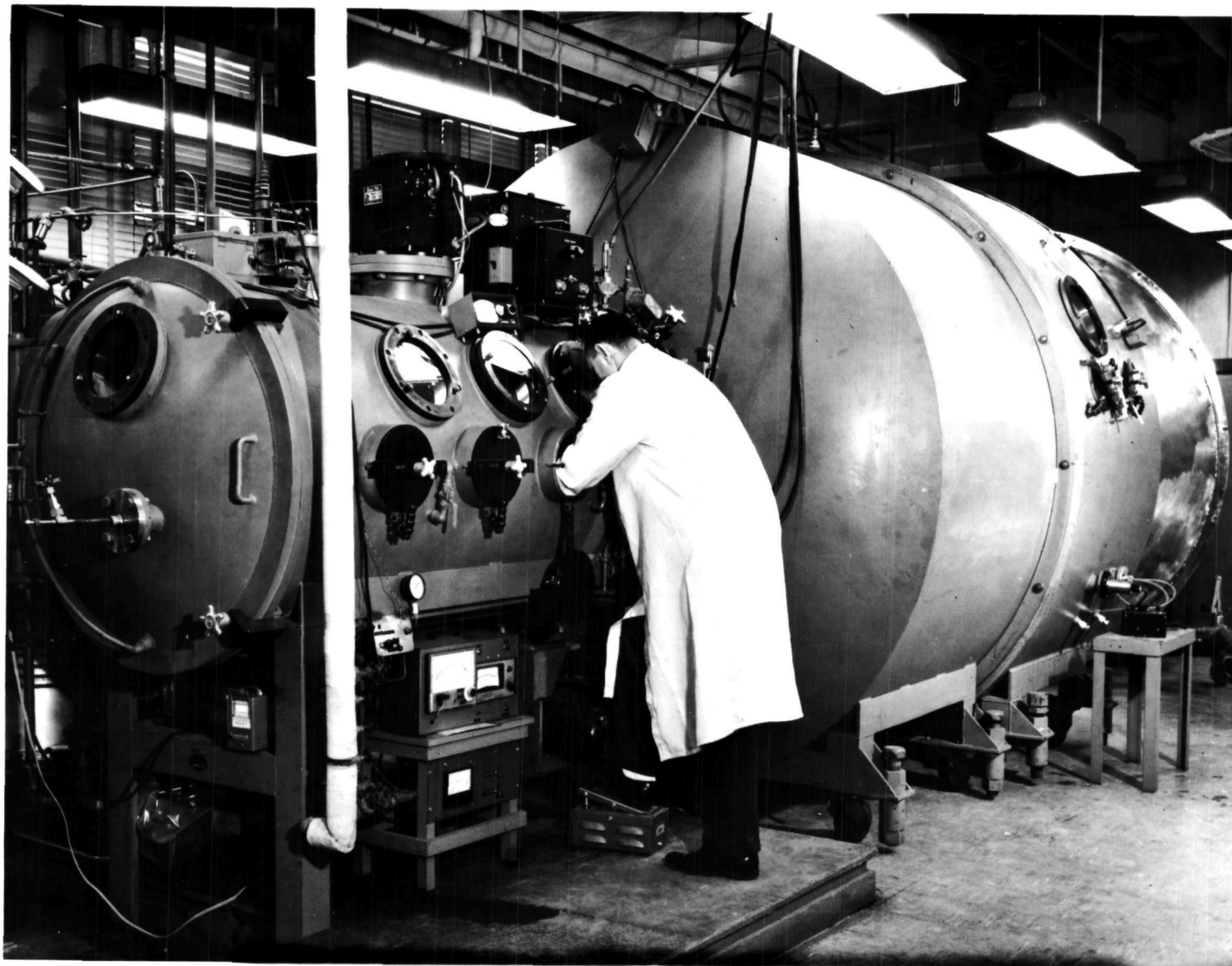


Figure 68. Weld Chamber. (P69-2-3E)

Welding Sequences

The welding sequences employed were dictated somewhat by the requirement for postweld anneal of all weldments at 2200⁰F for 1 hour in vacuum. Thus, during manifold welding sequences as shown in Figures 62 to 64, the girth joints were only tacked to provide for later splitting of the manifolds for annealing. This operation was necessary because the complete manifolds could not be accommodated in vacuum furnaces which could be qualified per Specification NSP 03-0037-00. The remainder of the manifold welding followed the natural fabrication sequence. Two circumferential welds produced the basic manifold sections. After machining of boss and nozzle holes, bosses were welded in place by a combination of internal GTA welding of the root pass and a second manual filler pass on the boss OD. The support brackets, shell support ring, and inlet or outlet were then welded to the manifolds. After splitting of the manifold and postweld annealing, the halves were rejoined by a manual girth weld. These two welds were annealed locally using a portable furnace specially constructed for this purpose. The vacuum environment during annealing was provided by the welding chamber.

The heat storage tubes were supplied by NASA with the lithium fluoride fill of the convolutions complete. As shown in Figure 65, each tube was trimmed to the proper length prior to automatic GTA welding of the inlet ferrule and reducer to the 1.25-inch OD gas tube. The 0.75-inch OD outlet tube was then trimmed to length (long leg) and the outlet ferrule welded. At this point, the short leg of the outlet tube was trimmed to compensate for length variations in the as received gas tubes. This operation produced a matched pair which was maintained by serial number until the final weld between the extension tube and reducer on the gas tube. The two welds at the reducer were then vacuum postweld annealed in the welding chamber with the use of a specially designed furnace. Tube-to-ferrule welds were annealed later in conjunction with the final assembly boss-to-ferrule welds.

The welding of 48 gas tubes to the two manifolds was accomplished with the assembly positioned in the large rotatable welding fixture. As mentioned in Section 5, these 96 welds were originally planned to be made by the orbit arc technique. As shown in Figures 66 and 67, the rotating fixture would be used to position each weld in front of the welding stations.

Because it was necessary to use manual welding techniques, access to the ID and OD of each weld was required. This was accomplished by rotating the entire fixture 90 degrees on its trunnions, such that the planes of the manifolds were in the vertical position. One half of each weld joint was made in each of the four welding positions. To equalize weld distortions as much as possible, welds to each manifold were made in six groups of eight, alternating back and forth across the manifold diameter. These welds were postweld vacuum annealed using two specially designed furnaces, each capable of accepting eight weld joints.

The gas system assembly was completed with the welding of the bimetallic joint assemblies to the manifolds. These welds were last in the fabrication sequence because with the bimetallics in position the gas system assembly could not be rotated within the welding chamber. To change welding position, it was necessary to move the assembly onto the transfer dolly, rotate, then reposition in the welding chamber. Postweld anneals were done with the same furnace previously used for the manifold girth weld anneals.

6.2.2 Fabrication

As illustrated in Figure 61, the inlet and outlet manifolds and the 48 gas tubes were the major components of the gas system. The fabrication sequence is outlined in Table X. These hardware fabrications will be discussed in this section.

Manifolds

The basic manifold sections were formed by radial draw forming. Because of the high cost of tooling this method is generally considered only for parts which cannot be formed by more conventional methods or for production quantities. However, since draw forming required significantly less raw material than would have been required for other methods being considered, the savings in material costs more than offset the higher cost of tooling.

As depicted in Figures 62 and 63, four 180° segments were required for each manifold. Tool try-outs were done with stainless steel and these parts were later used to fabricate an inlet manifold for tooling, welding and other checkouts.

Forming the Cb-1Zr segments was highly successful in that only nine close trimmed pieces of material were required to produce the eight manifold

segments. A chip, edge burr or other contaminant caught by the die was the apparent cause of the one scrap piece. Radial draw forming was done at the Cyril Bath Co., Solon, Ohio. The various operations involved are shown in Figure 69.

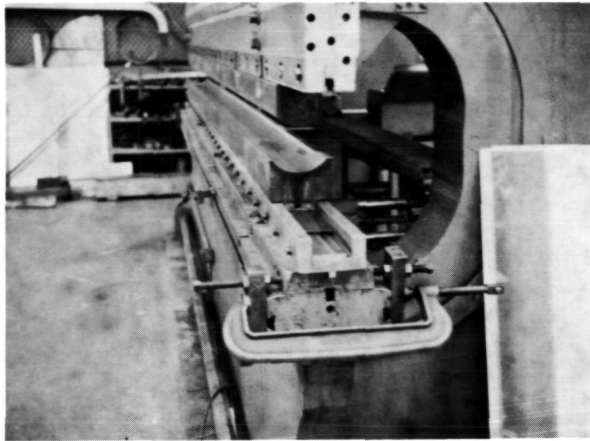
After being accurately machine-trimmed at the 180° center plane, the basic manifold sections shown in Figure 70 were GTA tack welded at the girth joints to form 360° half shells. The weld fixturing for a typical inner manifold section is shown in Figure 71. The inside-the-chamber view of the tack welding operation for a typical outer section is shown in Figures 72 and 73.

Each of the four 360° half sections was machined and weld prepped for the circumferential weld joint. An inner section is shown being machined in Figure 74.

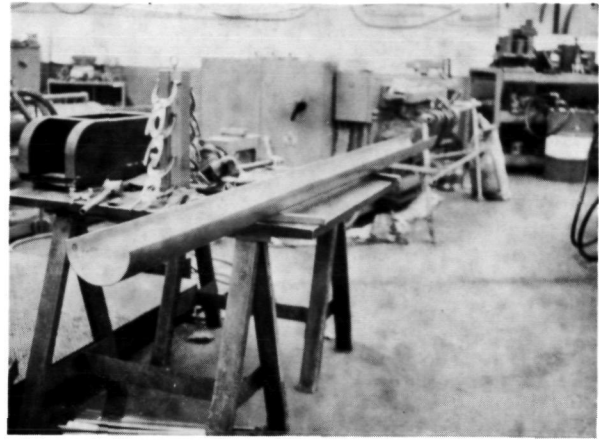
The inner and outer manifold sections were cleaned and both manifolds were set up for welding of the circumferential joints as shown in Figure 75. The joints were aligned and GTA tack welded during the first welding operation. The manifolds were then removed from the welding fixture, reversed, and tack welded on the opposite side. The automatic GTA weld of one joint in each manifold was then made, and the manifolds again reversed to provide access to the first tack welded side. The automatic GTA welding of these joints was done in a single pass with filler wire addition.

After completion of the circumferential welds, the boss location holes were drilled and reamed on a horizontal boring mill equipped with a P&W rotary table. A large Bridgeport head was mounted to the machine which enabled the machining of the holes at the proper angle with the manifolds in the horizontal position. The inlet nozzle and outlet elbow openings were also machined at this time. Figure 76 shows the inlet manifold set up on the HBM for machining of the boss holes. The inlet manifold after completion of all hole drilling is shown in Figure 77.

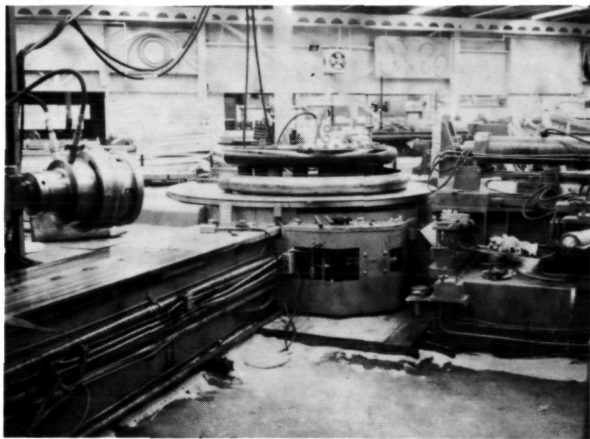
The boss-to-manifold welds required three operations; tack weld, automatic internal root weld, and manual filler pass. Alignment of the bosses for tack welding was accomplished by a molybdenum plug which extended through each boss and the machined hole in the manifold. The alignment fixture is shown in Figure 78. The manifold mounting arrangement during tack welding and subsequent operations is shown in Figure 79.



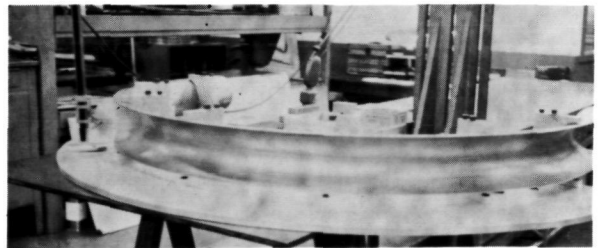
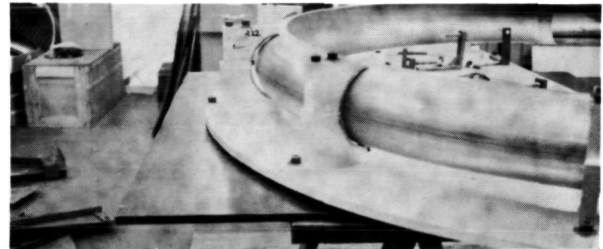
Preform Brake Die



Preformed Manifold Section



Radial Draw Forming Die
and 180° Outer Manifold
Section



180° Manifold Sections - Partially
Mounted in Inspection Fixture
Upper View: Outer Section
Lower View: Inner Section

Figure 69. Manifold Sections - Forming and Inspection.

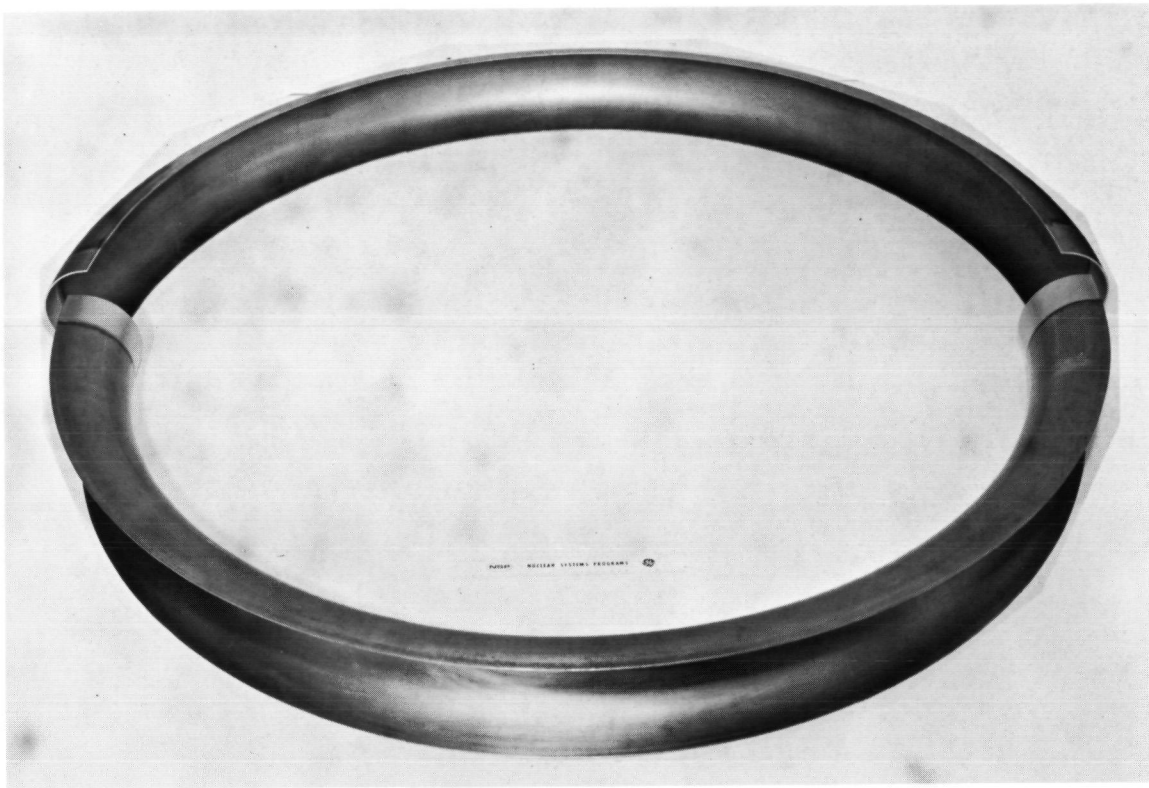


Figure 70. Inner and Outer Manifold Sections - Cleaned in Preparation for Girth Tacking. (P69-1-42G)



Figure 71. Inner Manifold Section - Being Loaded into Weld Chamber for Girth Tacking. (P69-2-3F)



Figure 72. Outer Manifold Section Set-up in Weld Chamber for Tack Welding of Girth Joints. (P69-2-3B)



Figure 73. Tack Welding Girth Joint of Outer Manifold Section. (P69-2-3A)

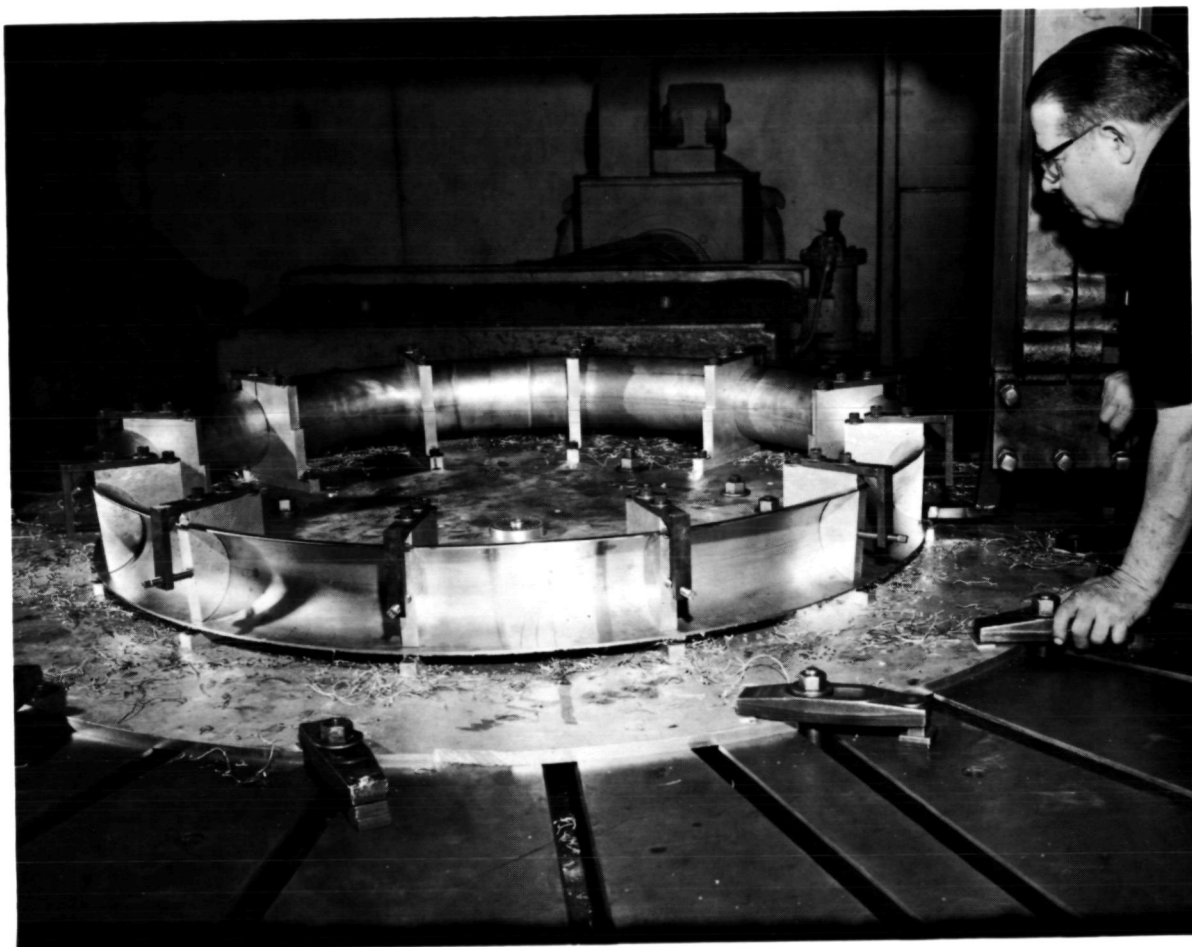


Figure 74. Machining for Circumferential Weld Joint on Inner Manifold Section. (P69-2-36D)



Figure 75. Inlet and Outlet Manifold Being Set-Up for Automatic TIG Welding. (P69-3-23B)



Figure 76. Inlet Manifold Set-up on Horizontal Boring Mill for Machining Boss Holes.
(69-3-49)

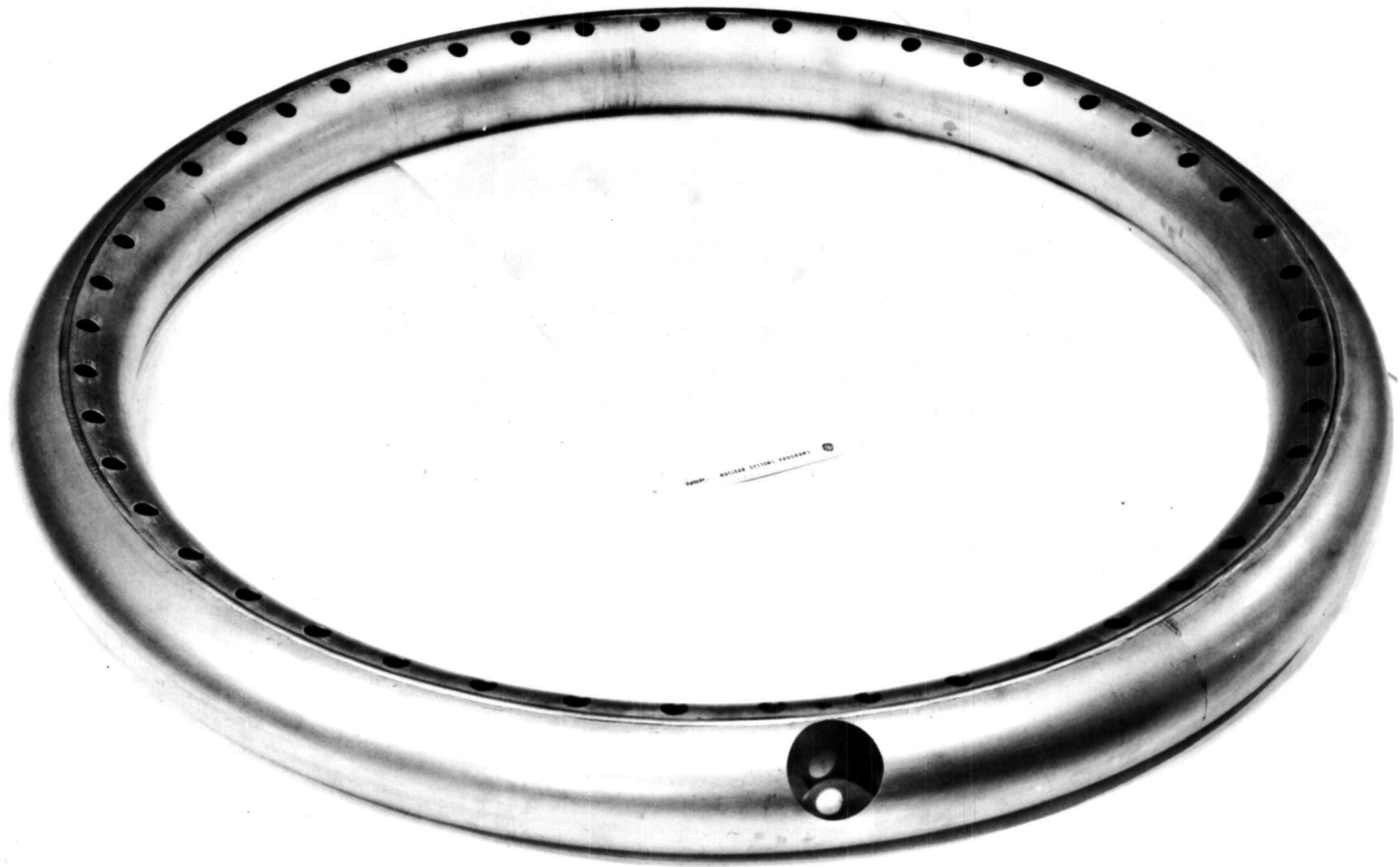


Figure 77. **Inlet Manifold After Machining of 48 Boss Holes and Nozzle Opening.**
(69-4-1)

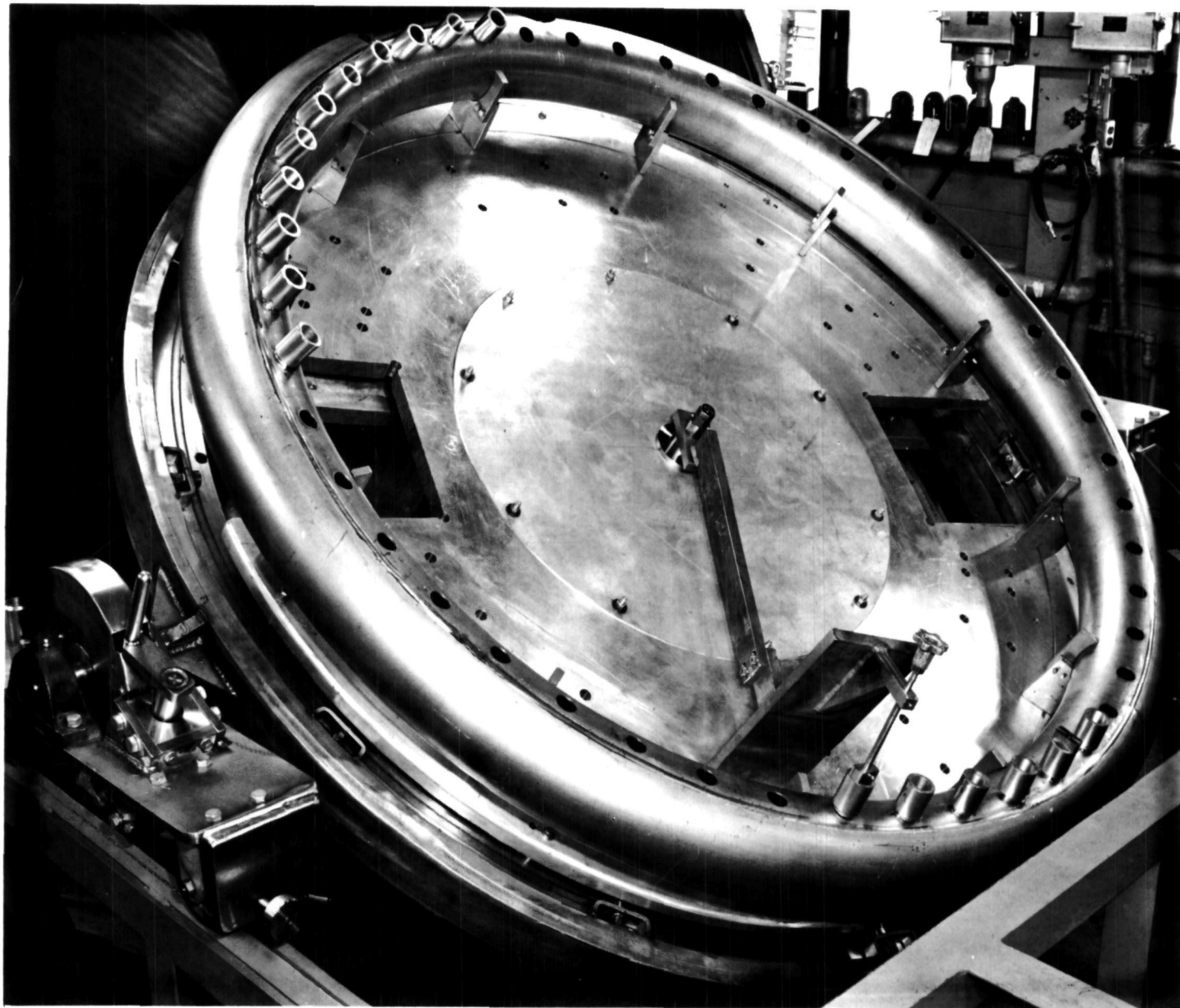


Figure 78. Boss Alignment Fixture Locating a Boss on Inlet Manifold. Other Bosses Shown Have Been Tack Welded.

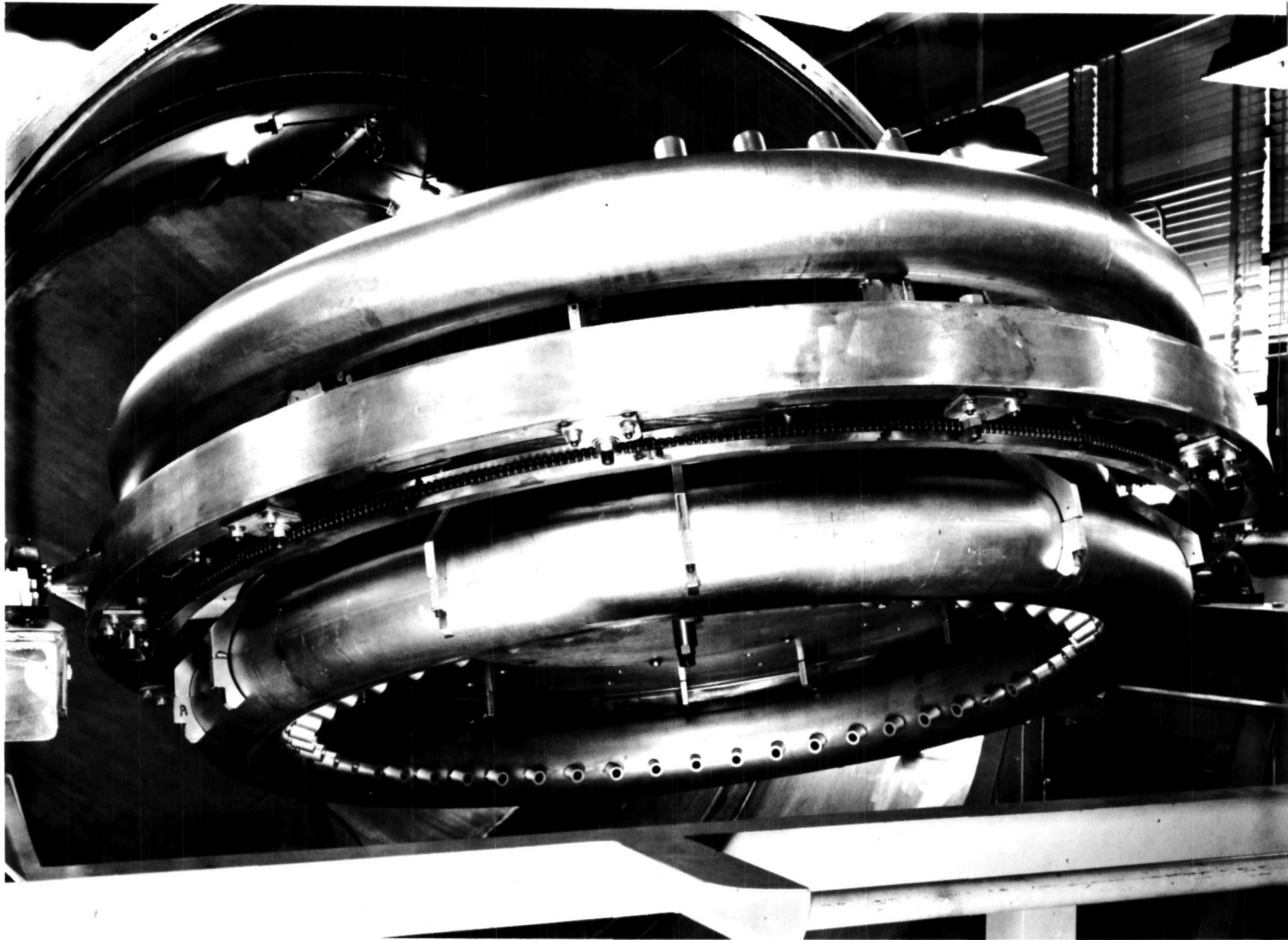


Figure 79. Inlet and Outlet Manifolds Mounted on Rotating Weld Fixture. Fixture Shown With Outlet Manifold Rotated to Lower Position After Tacking All 48 Bosses.

While performing the root pass internal boss-to-manifold welds on the outlet manifold, a failure of the internal welding head occurred. Welding of 27 bosses had been completed before the failure. The cause of failure was traced to the automatic welding equipment. Although set for 160 amps, a current in excess of 400 amps was recorded, which resulted in failure of the torch end of the internal welding head. Primarily copper, some stainless steel, and Teflon melted off the end of the head, and the torch cooling water was released by the failure.

The boss-to-manifold joint which was being welded was severely embrittled due to contamination, as shown in Figure 80. Coating-type deposits of copper and other materials probably carried by the steam were more widespread. Larger spatter or dropping-type deposits were located at the bottom of the manifold directly below the boss which was being welded.

The rework procedure outlined in Table XI was implemented. In addition, it was determined that loss of the feedback signal had driven the output of the welding machine above the 400 amp rating and caused the welding head failure. To prevent a recurrence, a meter relay circuit was incorporated to provide failsafe shutdown in the event that output current exceeded a preset value for any reason. A new internal welding head was also fabricated and checked on trial welds prior to resuming manifold welding. Automatic internal welding of the remaining bosses on the outlet manifold and the 48 inlet manifold bosses was then completed without difficulty. Addition of the manual filler pass on each boss OD completed the boss-to-manifold welding.

The attachment of support brackets, shell support rings, inlet nozzle and outlet elbow (operations 130 through 153, Table X) was accomplished with both manifolds in the welding chamber, such that at least two welding operations could be performed during each chamber cycle. Typical attachment components: the shell support rings and bracket support tubes are shown in Figures 81 and 82. Alignment fixtures were used to position each component as illustrated in Figures 83 and 84 for the outlet manifold support tube welds and for the outlet manifold-shell support ring. Typical weldments for the inlet manifold are shown in Figure 85.

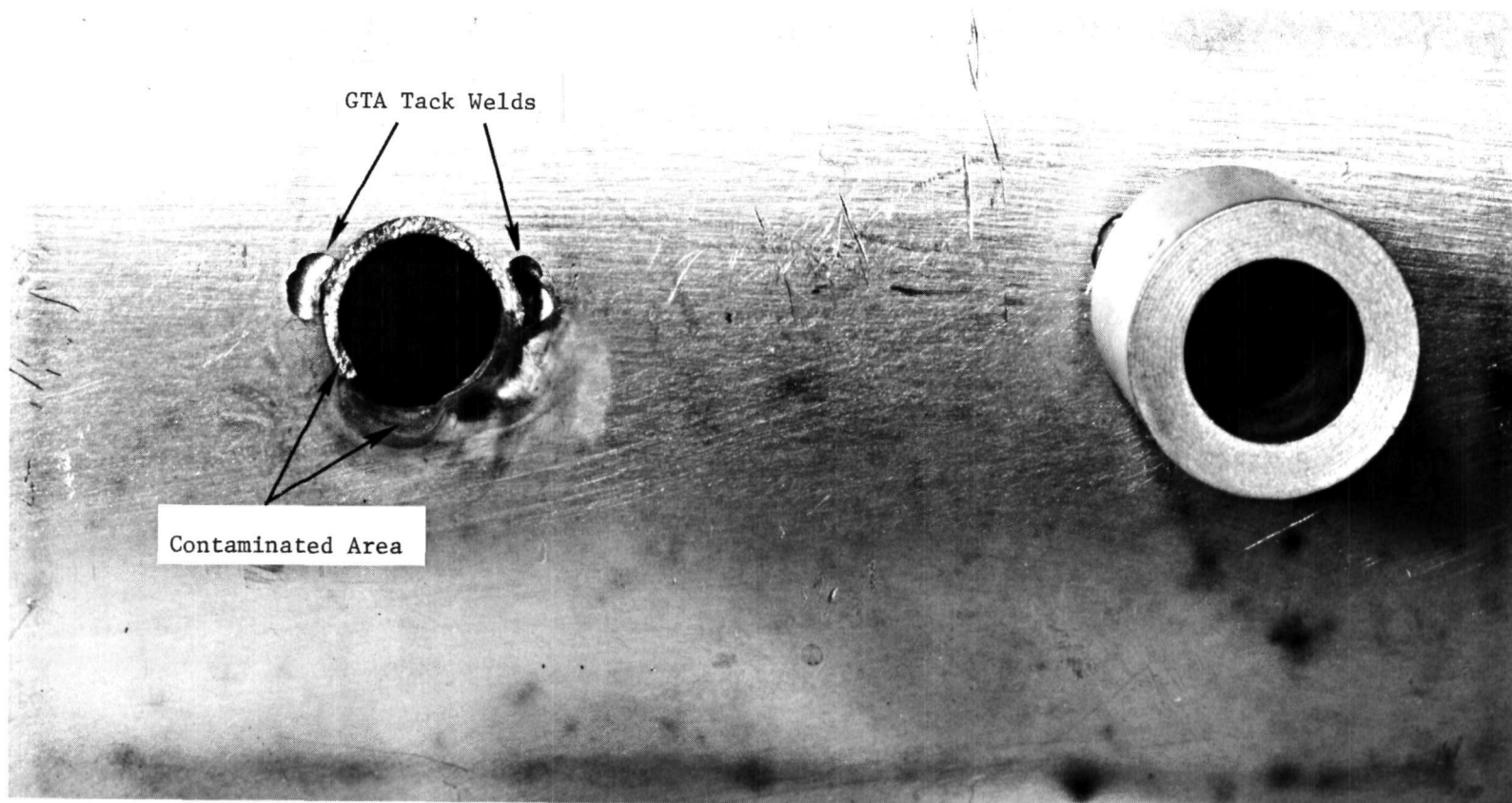


Figure 80. Outlet Manifold Illustrating Boss Location Where Welding Torch Failure Occurred. (P69-4-53G)

TABLE XI

REWORK PROCEDURE FOR OUTLET MANIFOLD - BOSS WELD FAILURE

-
-
1. Remove all tack welded bosses (not the 27 welded bosses).
 2. Trepan machine 3" dia. hole at contaminated boss on existing \mathbb{E} .
 3. Perform interstitial analysis on disk removed to verify that all contaminated Cb-1Zr material has been removed.
 4. Perform cleaning trials on internal surface of slug to verify adequacy of cleaning techniques. Also check out pickling method using foil to insure hydrogen embrittlement will not occur in manifold.
 5. Mechanically remove local deposits from manifold.
 6. Nitric acid pickle and rinse (primarily to remove copper).
 7. Nitric HF pickle and rinse.
 8. Machine and weld prep insert piece to fit 3" dia. hole with predrilled boss hole. Use piece removed from manifold section girth trim so as to match contour.
 9. Clean, weld and x-ray.
 10. Reclean bosses and retack in preparation for internal root pass welding.
-
-

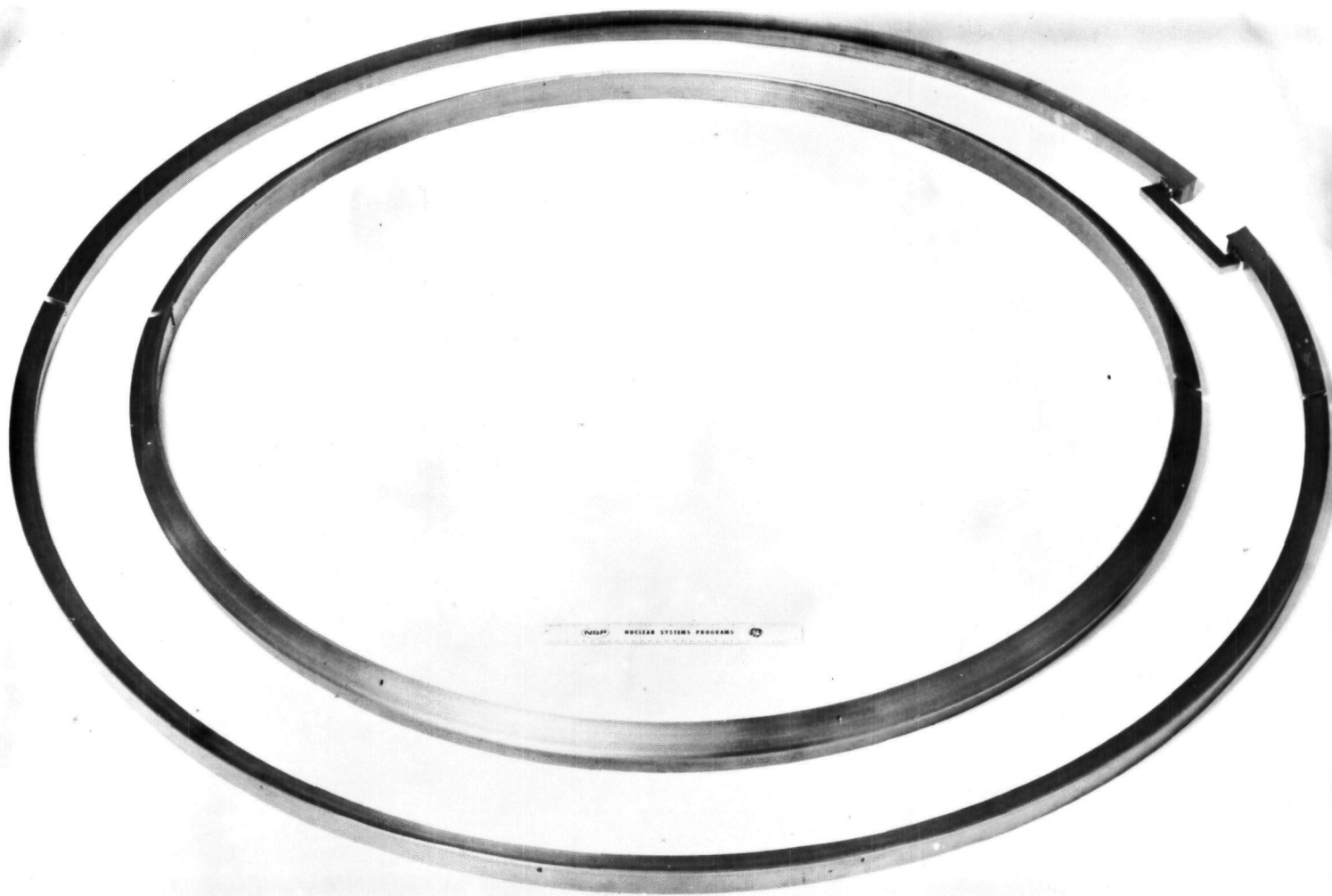


Figure 81. Shell Support Rings for Inlet and Outlet Manifolds. Temporary Bridge Shown Tack Welded at Nozzle Cutout Location on Inlet Ring. (P69-4-30)

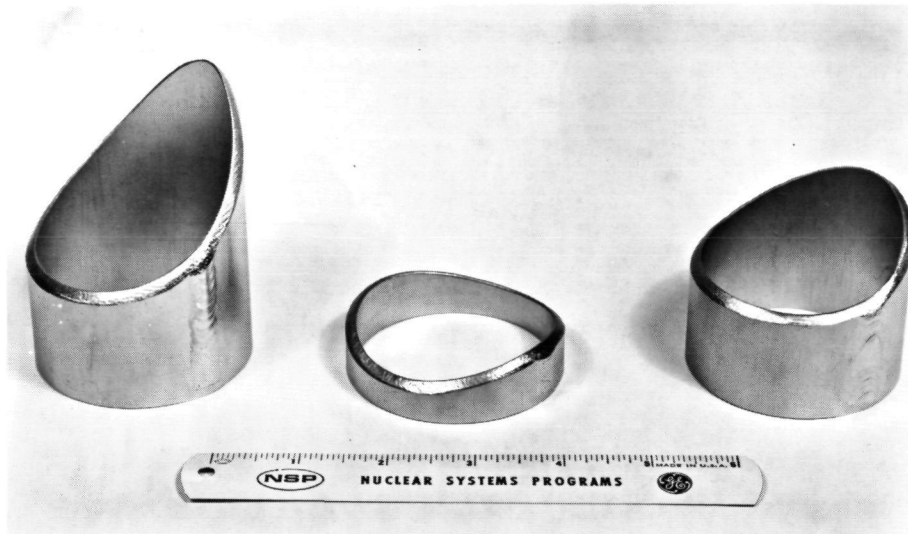


Figure 82. Typical Manifold Support Tubes. (P69-5-17)

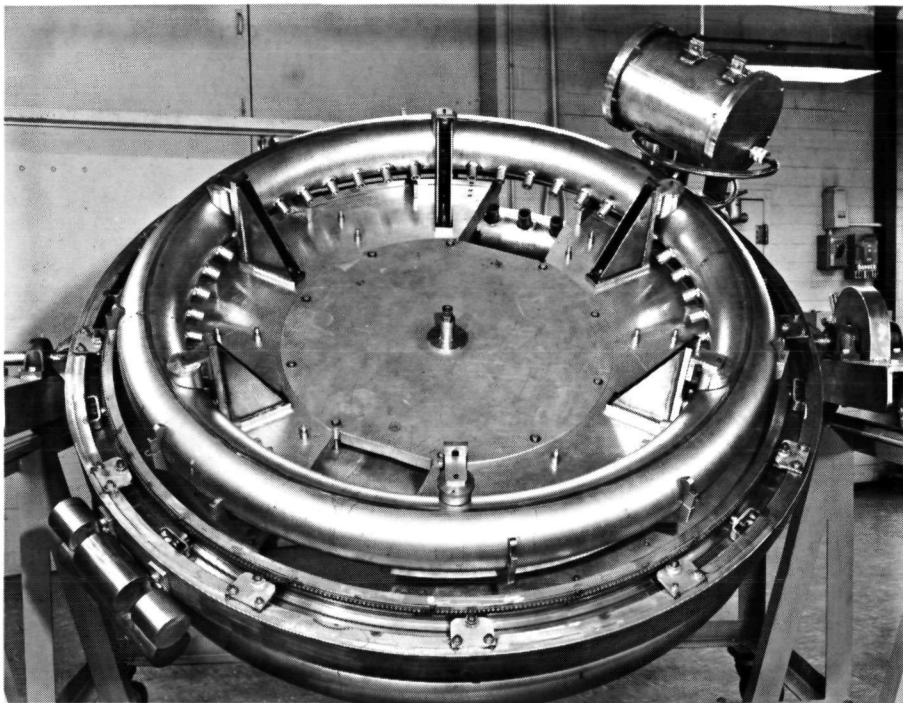


Figure 83. Welding Alignment Fixture for Outlet Manifold Support Tube. (P69-5-29A)

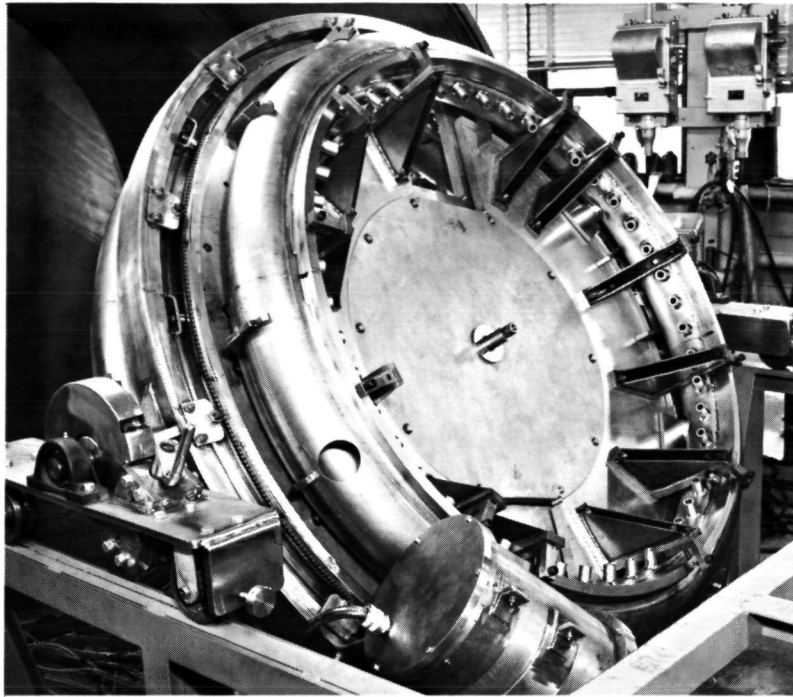


Figure 84. Weld Alignment Fixture for Outlet Manifold Shell Ring. (P69-6-10B)

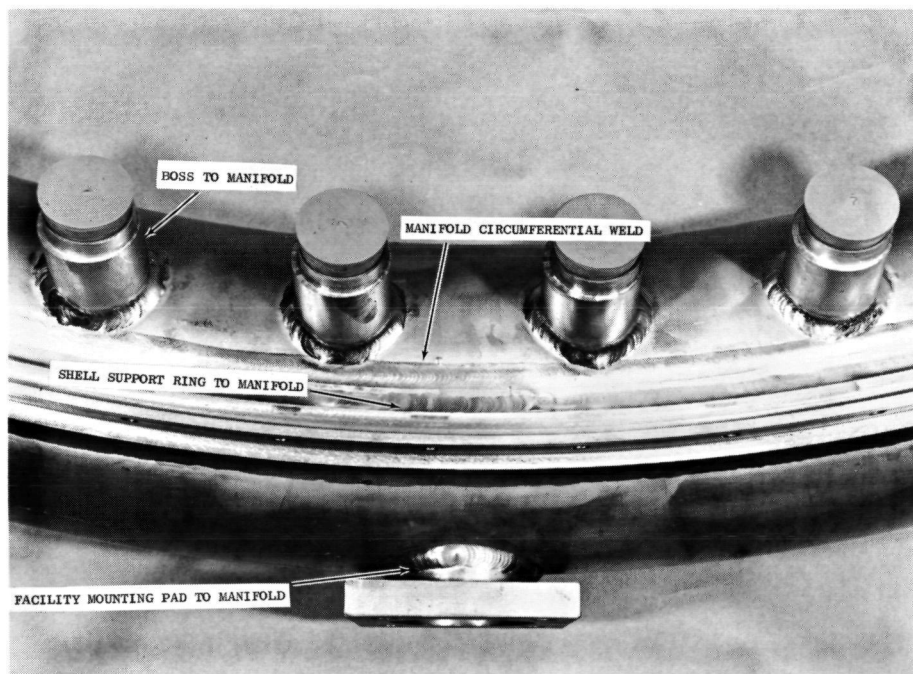


Figure 85. Inlet Manifold - Typical Weldments Required During Fabrication. (P69-9-10D)

Upon completion of welding, each manifold diameter was measured at the girth tack weld area prior to splitting the manifolds. The restraining tie bars required for postweld anneal were then machined to dimensions which maintained the actual manifold diameters. The tie bars, fabricated from Cb-1Zr alloy tube and discs, were then welded to each half manifold as shown in Figure 86. Postweld annealing per Specification NSP 03-0074-00-A was performed in two 2200[°]F/1-hour cycles of the Brew Model 922 vacuum furnace, located at Stellite Division, Cabot Corporation, Kokomo, Indiana. The stress relieving achieved during the postweld anneal was evident by the complete lack of manifold spring-back when the tie bars were removed.

The manifolds were then set up in the welding fixture for the manual welds of the girth joints. Upon completion of this operation, the girth joints were vacuum annealed using the local furnace setup in the welding chamber shown in Figure 87. During the anneal of the outlet manifold, girth weld No. 1, a pressure surge aborted the run after 55 minutes of the 60-minute anneal cycle. An air leak occurred in plastic tubing used to connect the sealed motor housing on the weld fixture to a vacuum feed-through. The results of various tests and analyses performed to determine the condition of the manifold indicated that contamination was superficial (Appendix D). Polishing with abrasive paper was used to remove surface contamination. The outside of the manifold was then acid cleaned and rinsed.

The final machining of manifolds required extensive set up and dimensional checks to insure machining features and dimensions would result. As anticipated during the design phase, distortions were present in features and feature locations due to general welding distortions and the need to fabricate the manifolds in 180[°] half-sections (because of annealing furnace limitations). Planning, tooling and stock allowances proved to be both necessary and sufficient.

All openings were plugged or otherwise sealed to maintain internal cleanliness. Exterior surfaces were protected when not involved in the specific work area. The bosses were rough and finish "turned" with special hollow mills again using the Bridgeport head mounted on the Lucas HBM.

The horizontal pads on the manifolds were milled with a right angle attachment and drilled with the Bridgeport head. The facility mounting pads (for attachment of the receiver to the Brayton System) were milled and drilled with the spindle of the machine. The shell support rings

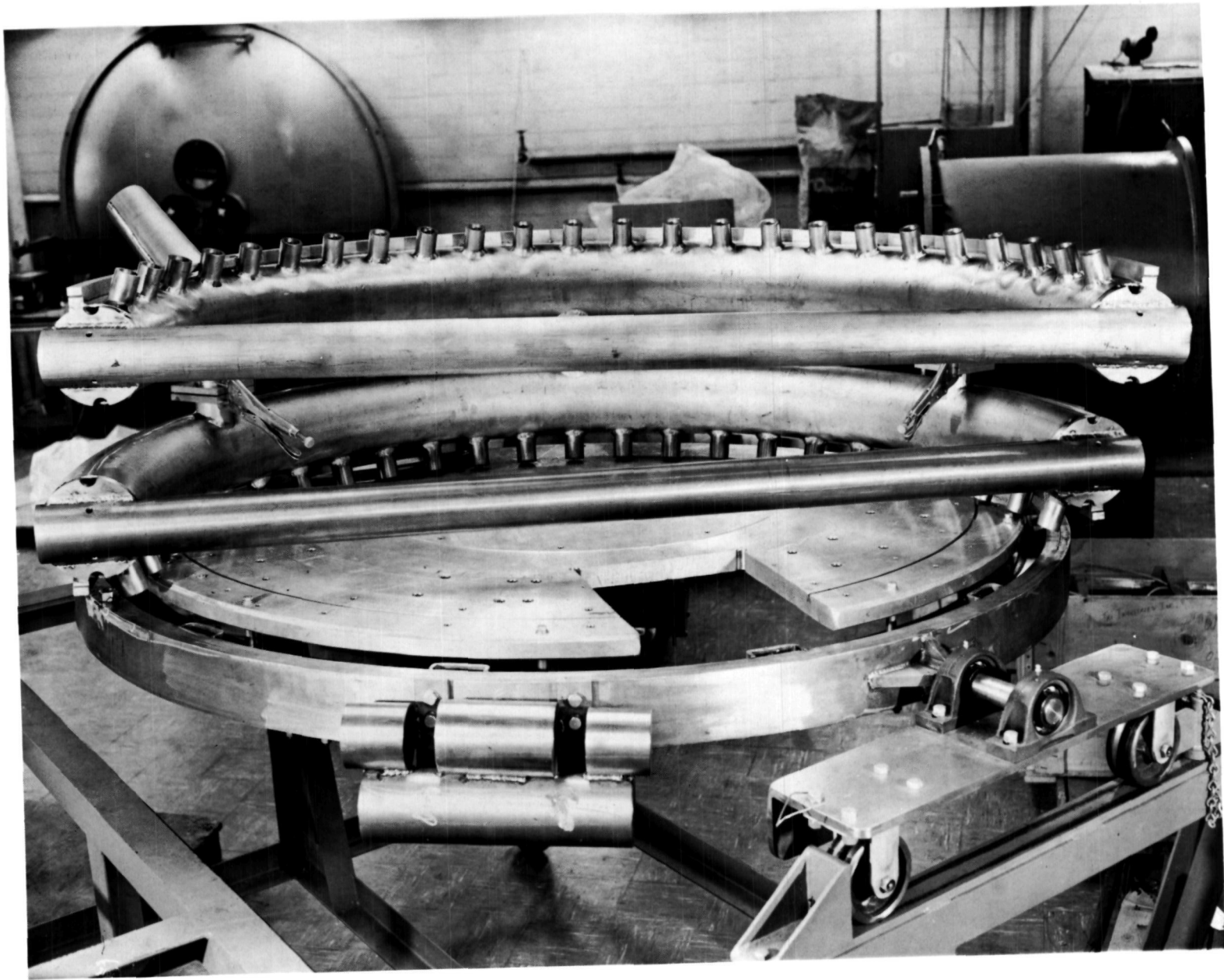


Figure 86. Inlet Manifold - Restraining Tie Bars Tack Welded to Halves for Post Weld Anneal.
(P69-7-1B)

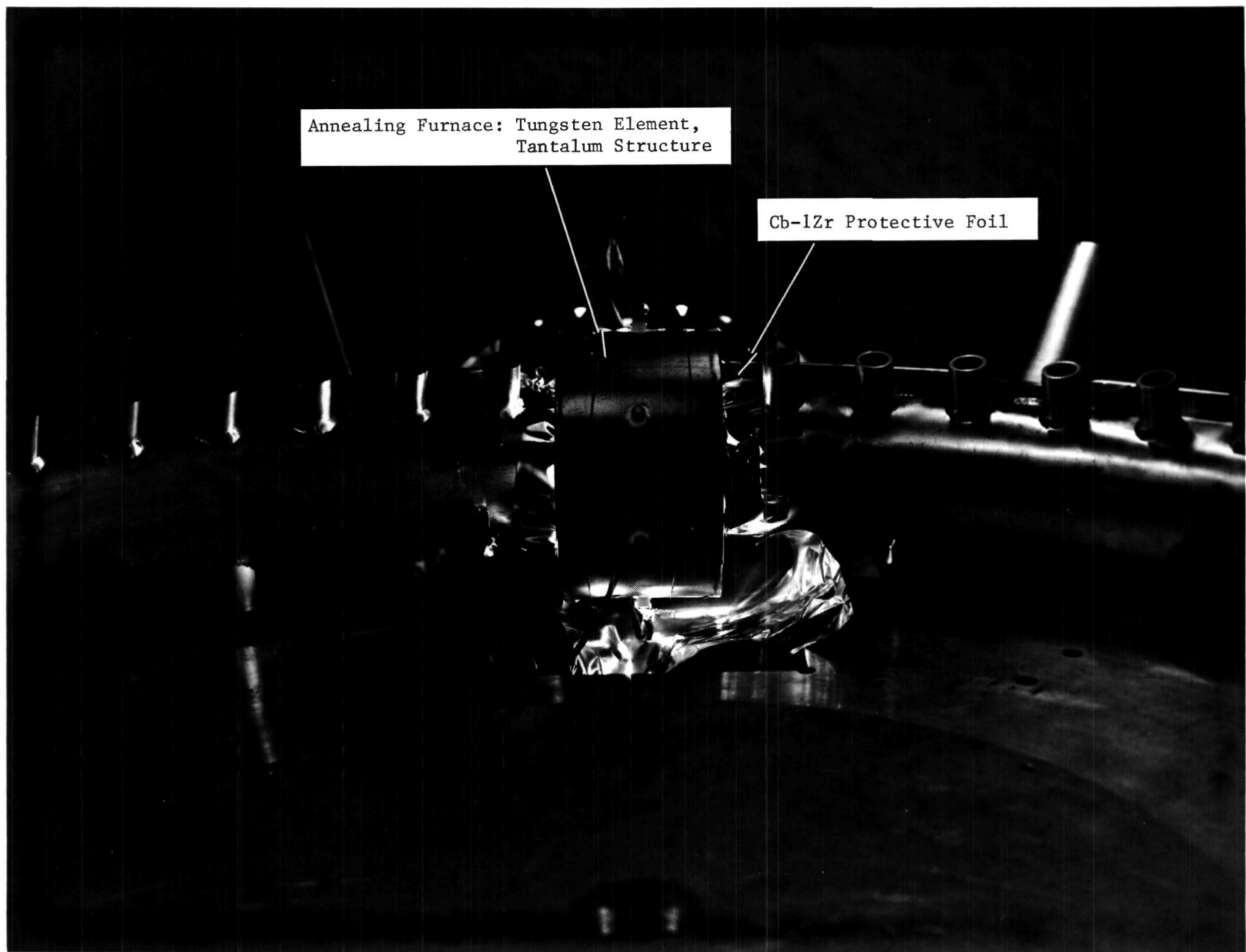


Figure 87. Typical Manifold Girth Joint Postweld Anneal Using Local Furnace. (P69-7-45)

were rotary milled with a right angle attachment and drilled with the machine spindle.

After final machining, cleaning, and inspection the inlet and outlet manifolds, shown in Figures 88 and 89 were ready for gas system assembly.

Gas Tube Assembly

The fabrication sequence depicted in Figure 65 was followed exactly during gas tube assembly welding. The heat storage tubes were fabricated at LeRC and shipped to ORNL to be filled with lithium fluoride and sealed (Reference 1). Upon return to LeRC the heat storage tubes underwent straightening, zygo inspection and grit blast surface treatment. Inspection of tubes at NSP for contour conformance is shown in Figure 90. A typical welding operation on the heat storage tubes is shown in Figure 91. Typical weld joints for outlet ferrule-to-tube and inlet ferrule-to-tube are shown in Figures 91 and 92. A plastic covered wire rack was constructed to provide handling of eight tube assemblies during each welding chamber cycle. The typical gas tube assemblies are shown in Figure 93.

Gas System Assembly

The assembly fixture consisted basically of stainless steel angle brackets which bolted to the manifolds and rotating ring of the welding fixture. The manifolds were mounted as shown in Figure 94, aligned, and secured to correct dimensions. The welding fixture was then rotated with the manifolds in the horizontal and vertical planes and dimensions rechecked to insure that no significant shifting would occur during final assembly welding.

The 48 gas tubes were then installed as shown in Figure 95. Originally, it was planned to install the support spider after all gas tubes were in position. However, in an attempt to slowly raise this support, five gas tube extensions were dented. Although leak tight, these damaged areas were reworked by the addition of a small amount of filler metal followed by postweld anneals. X-ray and helium leak check inspections were also performed successfully.

The spider and its support brackets were then modified to eliminate the potential for damaging other tube assemblies. A heavy center disc was removed and the heavy spider support brackets were replaced with the smaller

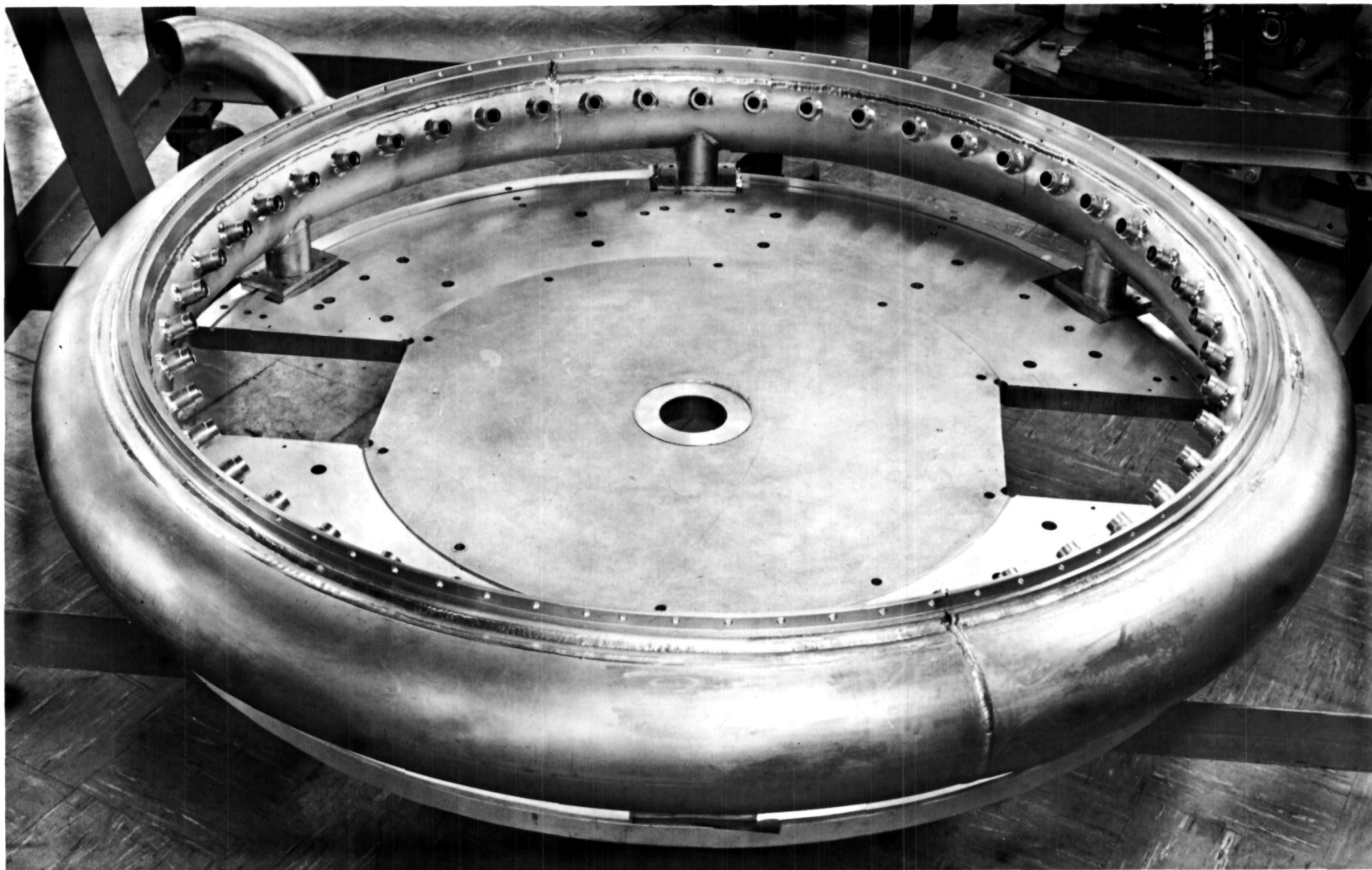


Figure 88. Outlet Manifold Prepared for Gas System Assembly. (P69-9-10B)

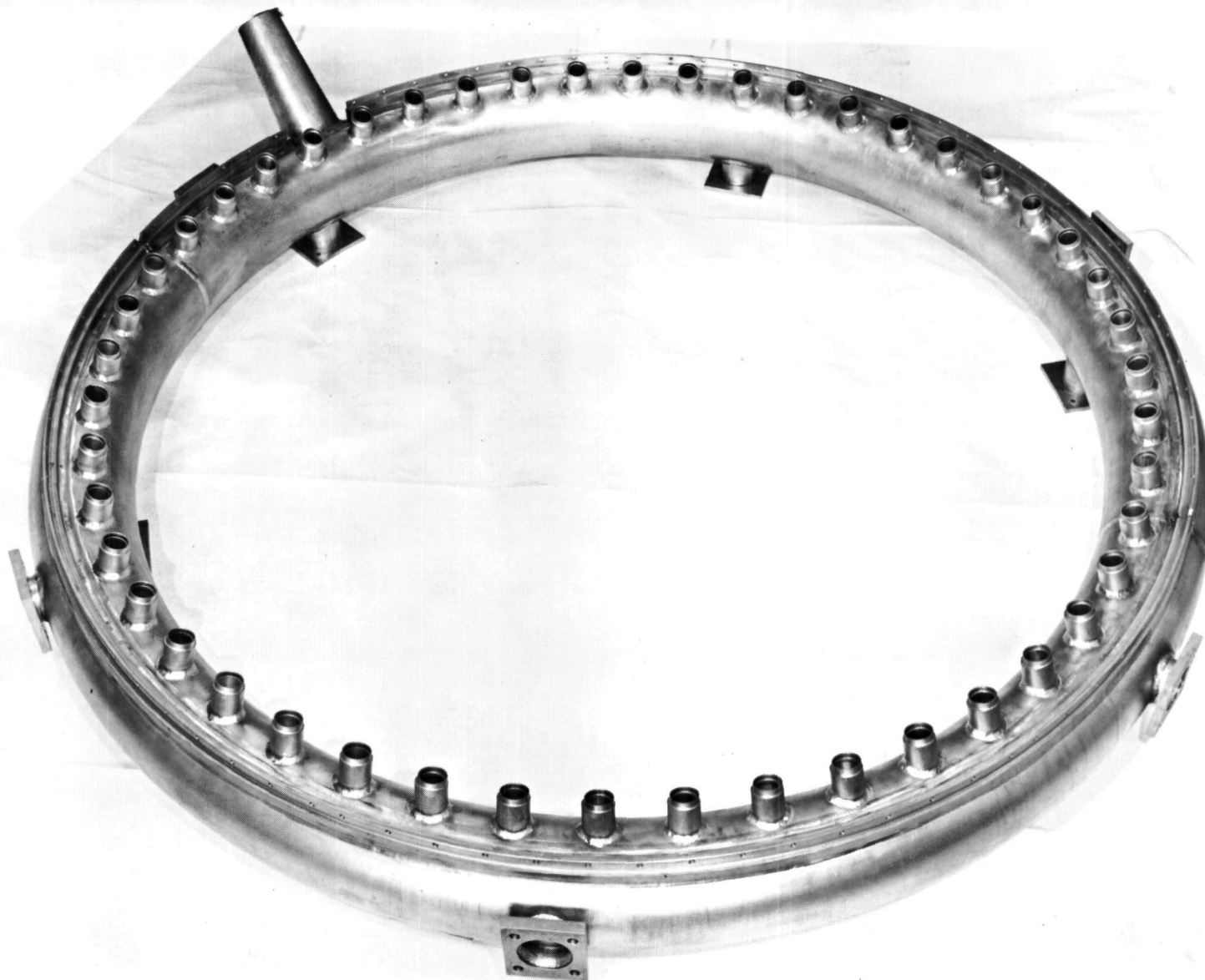


Figure 89. Inlet Manifold Ready for Gas System Assembly. (P69-9-17B)



Figure 90. LiF Heat Storage Tube From Third Batch Being Inspected for Envelope Conformance Using Contour Template Fixture. (P69-3-19B) (P69-3-19A)

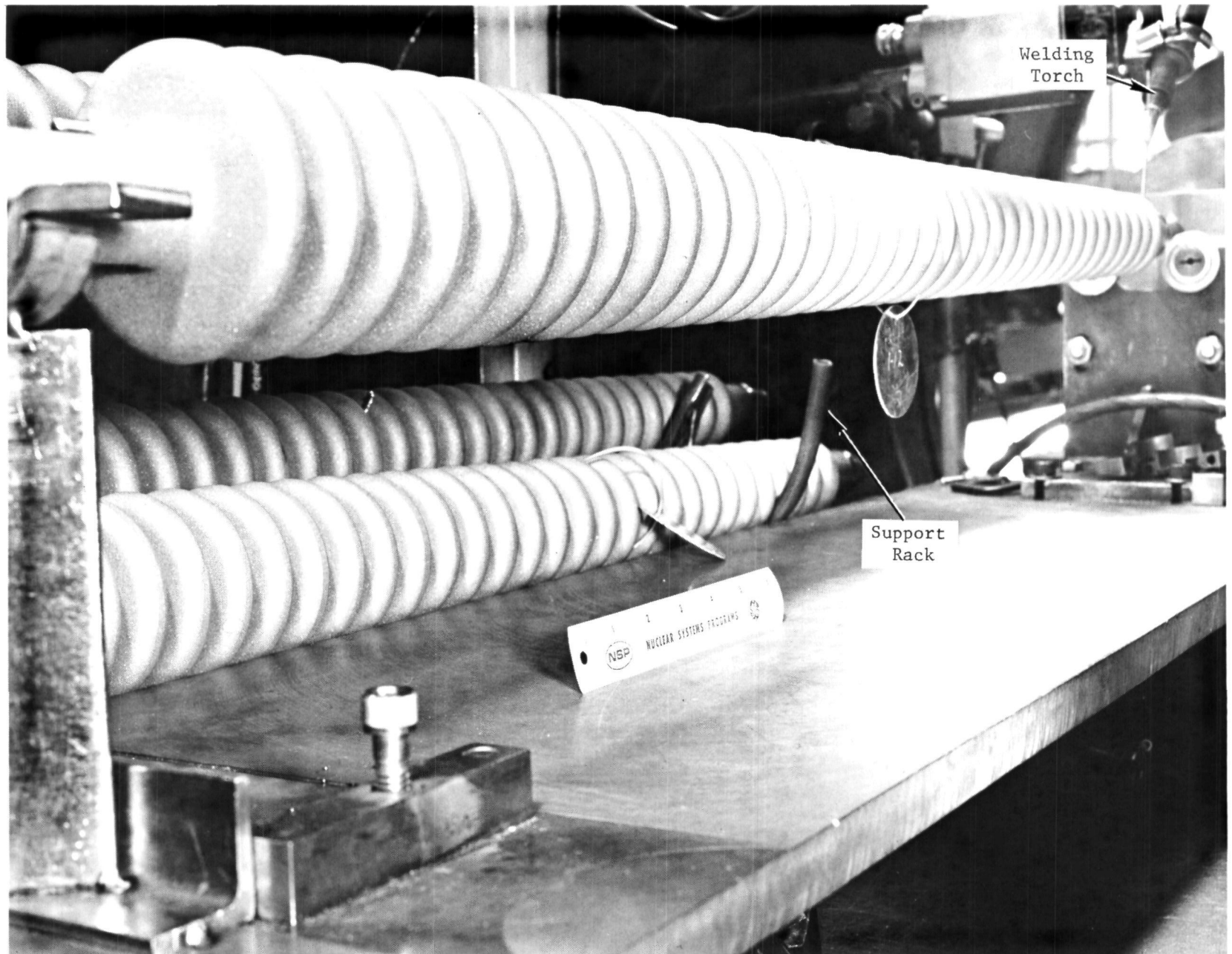


Figure 91. Heat Storage Tubes Loaded for Assembly Welding of Inlet Ferrules and Reducers.
(As Seen Through Vacuum Chamber Viewport) (P69-5-36C)

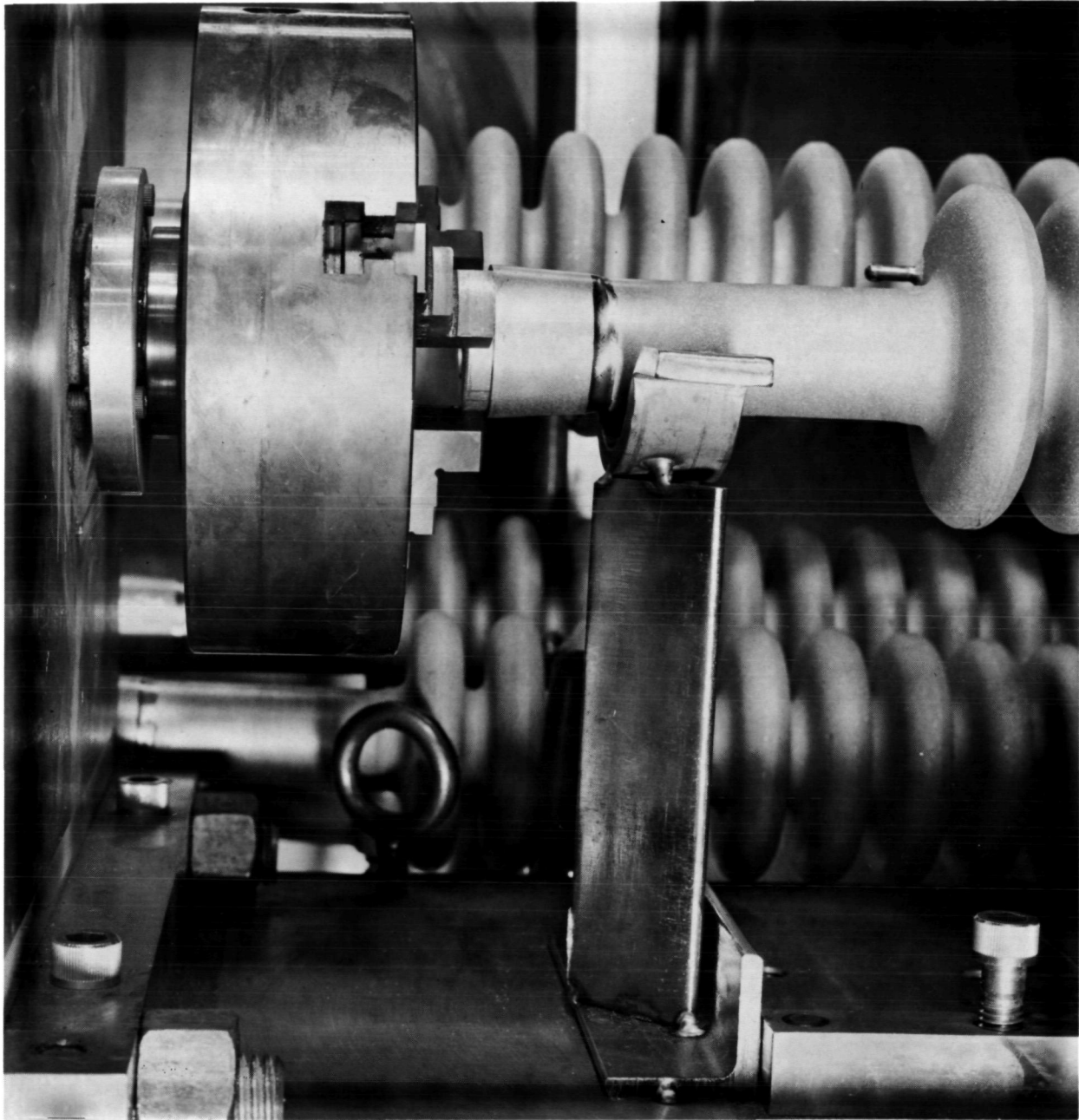


Figure 92. Close-Up of Typical Automatic Weld Inlet Ferrule-to-Tube.
(As Seen Through Vacuum Chamber Viewport) (P69-7-21B)

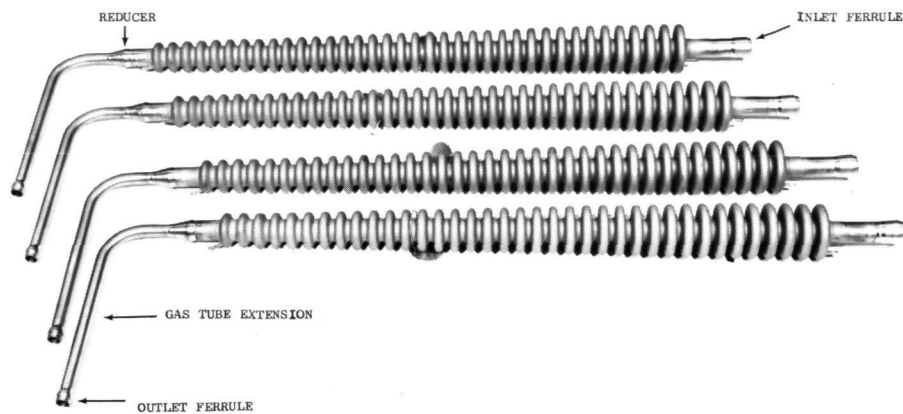


Figure 93. Typical Heat Storage Tube Assemblies. (P69-9-17F)

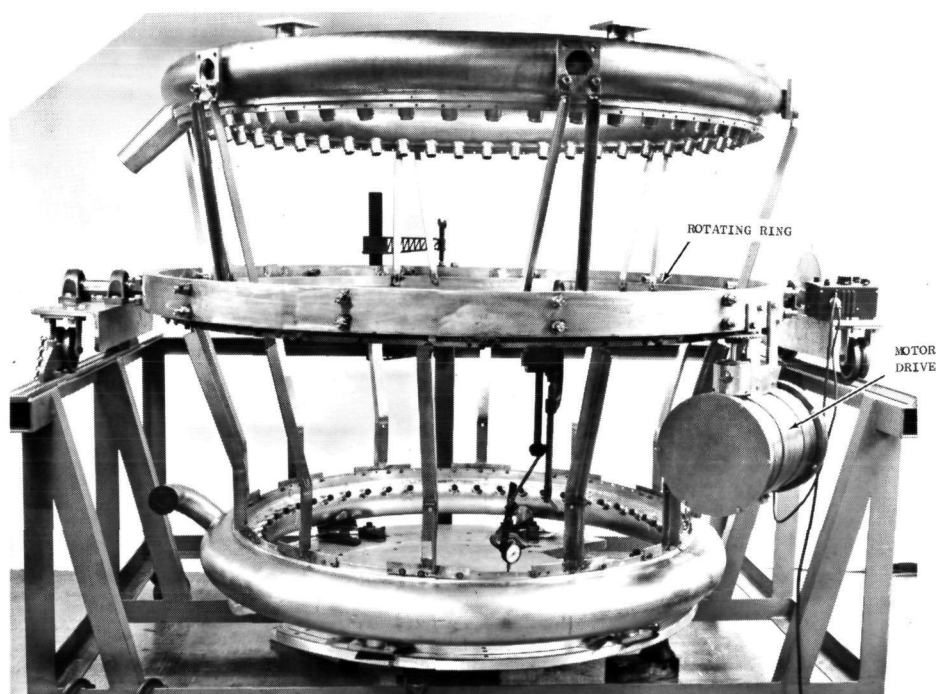


Figure 94. Manifold Mounted on Rotating Weld Fixture. (P69-9-35C)

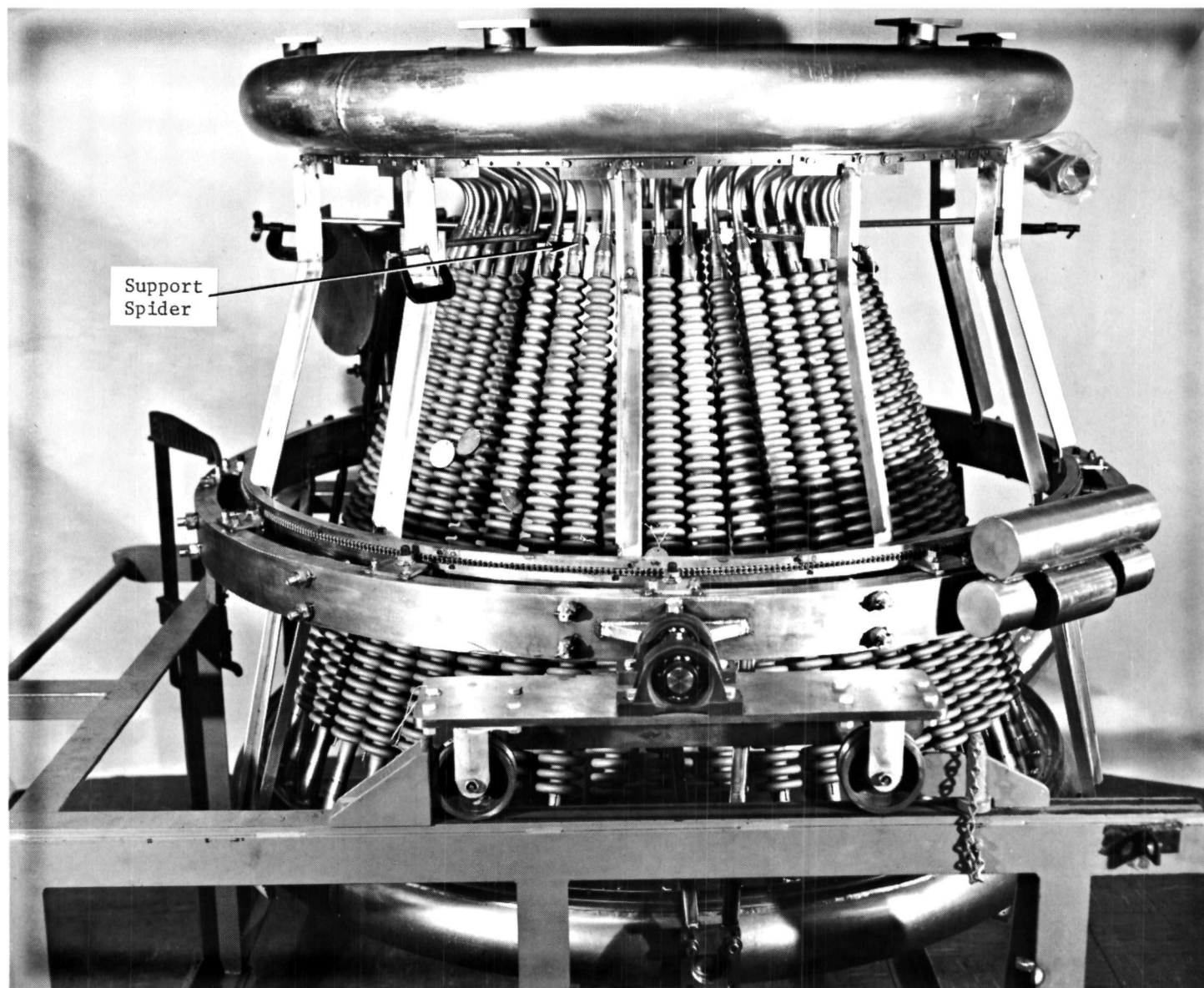


Figure 95. Gas System Set-Up for Assembly Welding. (P69-10-2B)

and lighter spoke-like support shown in Figure 95. It was now possible to install all the tubes after the spider was positioned. All the tubes were then reinstalled and shimmed with foil at the spider cutouts.

The 96 tube ferrule-to-manifold boss welds were initiated by first tack welding the 48 inlet manifold welds. The welding proceeded as each joint weld was made in two half-circumference passes. The welding fixture was rotated in four positions to obtain access for the following welding sequence: (1) outlet manifold, OD side; (2) outlet manifold, ID side, (3) inlet manifold, ID side, (4) inlet manifold, OD side. At each position welds were made in groups of eight, alternating back and forth across the manifold diameter. After careful visual examination a few joints were rewelded to insure that a sufficient overlap was in evidence at adjacent weld passes. A helium leak test indicated that all joints were leak tight.

Postweld annealing of these tube welds was accomplished using the same local furnaces that had been used previously for gas tube anneals. At each joint location, there were two welds actually annealed: tube-to-ferrule and ferrule-to-boss. Each of the two furnaces covered eight tube joints such that 16 anneals were accomplished during each vacuum cycle of the welding chamber. Furnace locations were alternated back and forth across the manifold diameters for each annealing cycle.

The final gas system assembly welds were those which attached the coextruded joints to the inlet and outlet manifolds. These were manual welds in the 3-inch diameter duct tubing as shown in Figure 96. The furnace which had been used for manifold girth weld anneals also accomplished the postweld anneals of these joints.

Intermediate leak checks had been performed on each component of the gas system assembly as well as all individual assembly welds. The acceptance mass spectrometer leak test of the entire gas system was performed by independent evacuation of the gas system while it was positioned inside the welding chamber. Helium was then introduced into the welding chamber and thus completely surrounded the gas system.

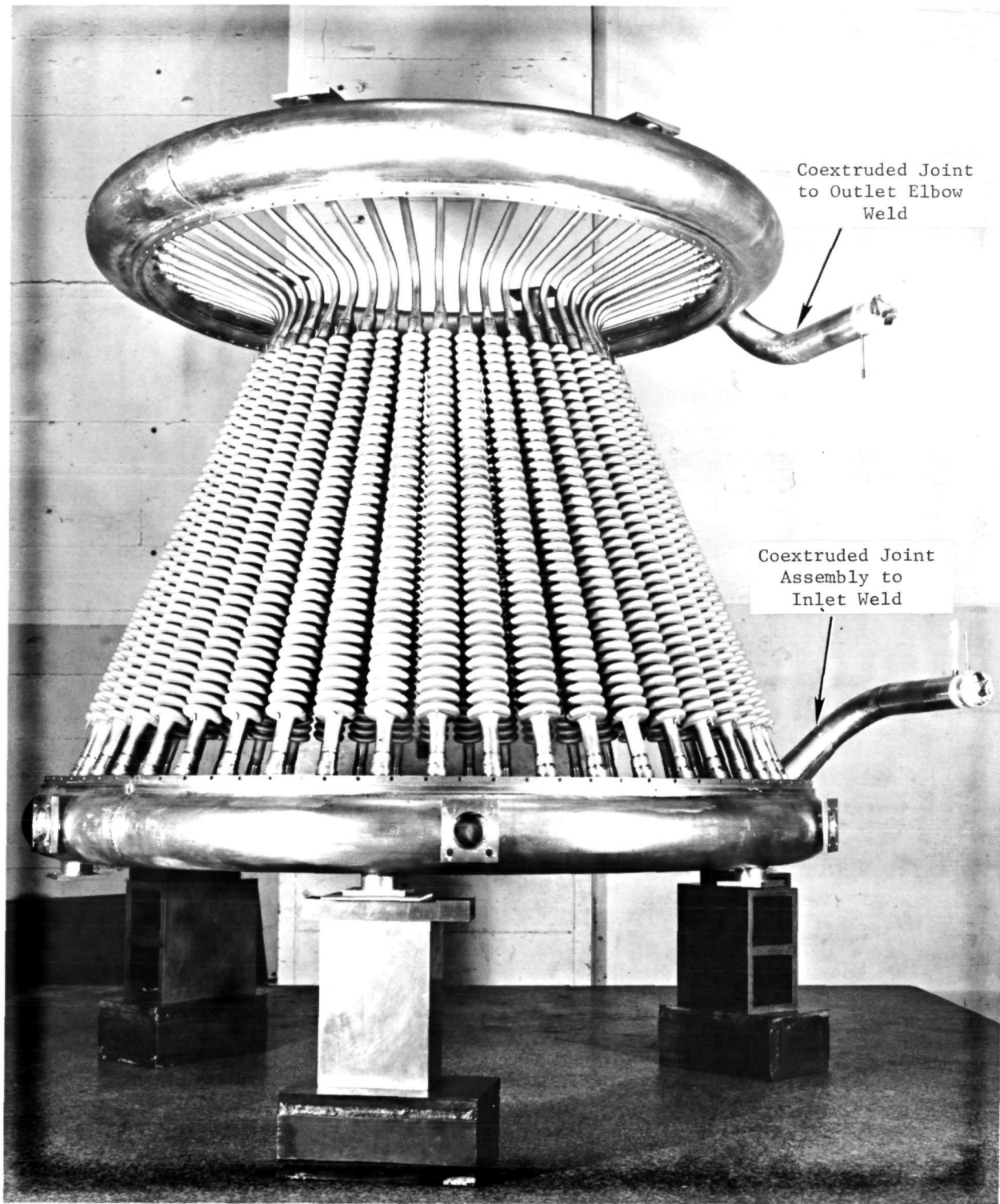


Figure 96. Completed Gas System.

6.3 SHELL ASSEMBLY

The shell support assembly was designed as a riveted and bolted structure. For final assembly reasons the structure was made in six segments so that it could be bolted together at its longitudinal flanges. The shell circumferential flanges would be attached to the inlet and outlet manifolds by bolting at the machined support ring flanges.

Cost considerations dictated that the sheet metal segment panels be fabricated in three sections: an upper cone section, a transition section and a lower cone section. The three sections were riveted together to complete the panel before riveting the flanges to it. The two cone sections were cone rolled with conventional methods and the transition section was die formed on kirkstone dies with a lead punch using a standard drop hammer. During this forming operation it was necessary to anneal the parts before final setting because the material "twisted" during the forming operation, probably as a result of the material "stretching".

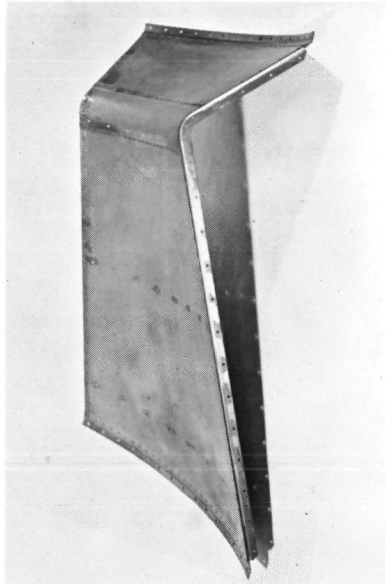
The reflectors were made with simple press-break operations. Three mounting clips were riveted to each reflector. To facilitate blind assembly each clip had a tapped hole to hold the fastener firmly while being inserted in the mounting holes of the panels.

Typical panel segments of the all-refractory shell assembly are shown in Figure 97. Reflectors were assembled to each individual segment before the shell support would be assembled to the manifold flanges.

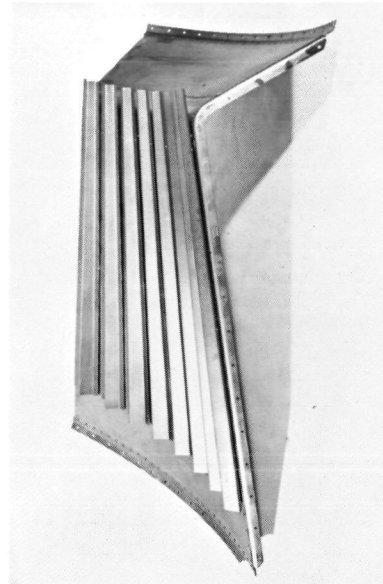
6.4 TOP CLOSURE

The top closure design calls for a 52-inch diameter spinning of .040-inch Cb-1Zr as shown in Figure 10 which includes a conical section for heat reflection purposes, a flat flange for joining the top enclosure to the flex plates, and a short outer skirt (later eliminated) for stiffening purposes. To incorporate the three features within dimensional tolerances, made this a most difficult spinning effort.

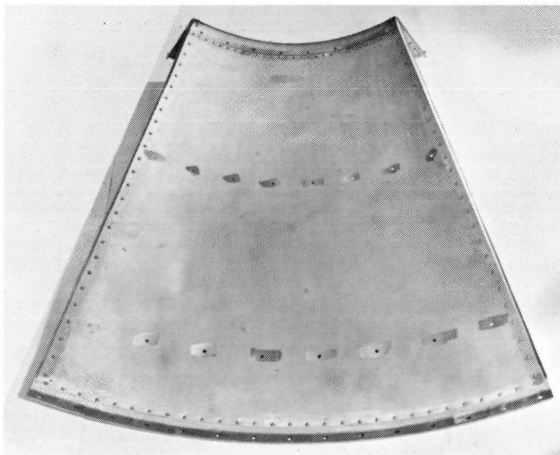
To check out the mandrel and process before committing the Cb-1Zr 0.040-inch sheet, a mild steel trial spinning was made first. The spinning was dimensionally acceptable and did not indicate any problems that were later encountered in the Cb-1Zr spinning.



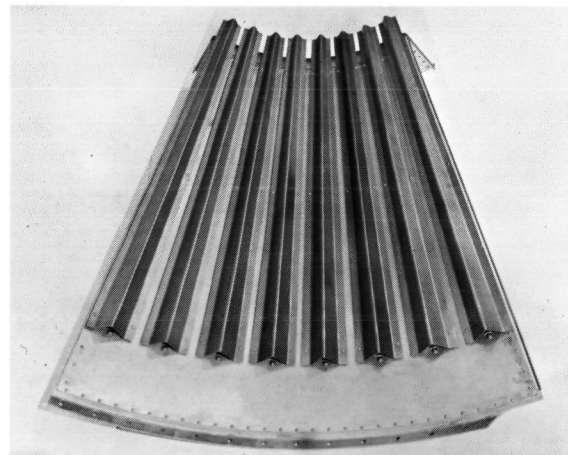
69-12-11M



69-12-11G



69-12-11L



69-12-11H

Figure 97. Shell Assembly Panels - Before and After Installation of Reflectors.

The initial spinning attempts by the vendor of the Cb-1Zr were quite discouraging, the flat flange area had distorted, similar to a sinusoidal wave and was about $1\frac{1}{2}$ -inch out of flat. At this time, a field evaluation was made to determine the reliability of the sheet for additional spinning passes. Visual examination, bend test, and hardness tests indicated that the component could undergo additional spinning passes without adverse effects. The results of the second spinning pass were encouraging, however, it caused an increase of 1-inch in the skirt length. When this excess material was cut off, the top closure again distorted in the flange area. The thickness of the material removed from the skirt was checked and no thinning was indicated. It was apparent that material movement was limited to the work surface layers (surface in contact with forming wheel) and the difference between the worked surface and bottom surface appeared to be causing the distortion. An additional spinning pass was made with a pre-formed mild steel overlay to avoid additional working of the surface. However, when excess material was removed from the skirt area the part distorted again. It was at this point that spinning efforts were suspended pending additional evaluation. It was decided that the part would require a vacuum stress relief anneal, after which either respinning could be attempted or a design change made to incorporate a heavier flange which would mechanically hold the part to the desired shape. The part was successfully vacuum stress relief annealed (as discussed previously in Section 4.2.5) and it was decided to respin. A rework sequence was established which called for respinning with a mild steel preformed overlay and modifying the wood mandrel to provide a sharper corner at the cone-to-flat transition.

Respinning improved the part; however, it was still not to print. A new wood mandrel was made which would allow the top closure to be formed on the reverse surface in an attempt to cancel out the differences in the top and bottom surface stresses. Although this technique improved the part, a design change was incorporated which added a flange to mechanically restrain the part. The 0.250-inch thick restraining flange was riveted to the flat section. The flange was made up of six segments and bridged at each joint by a 0.140-inch thick doubler.

It is thought that the top closure spinning suffered from the low tensile modulus of Cb-1Zr (16×10^6 psi at room temperature) which resulted in excessive springback. In some ways the Cb-1Zr did display desirable spinning

qualities. Its excellent room temperature elongation and low work hardening characteristics allowed several spinning passes before stress relieving without any detrimental surface effects.

The addition of a flange ring to the flat section of the spinning resulted in achieving the desired top closure part as is shown in Figure 98.

6.5 APERTURE ASSEMBLY

With the exception of the aperture plate itself, the aperture structure was fabricated entirely of stainless steel, including the honeycomb panels. The panels were easily sawed, machined and drilled. All attachments were finish machined as details and assembled to the panels.

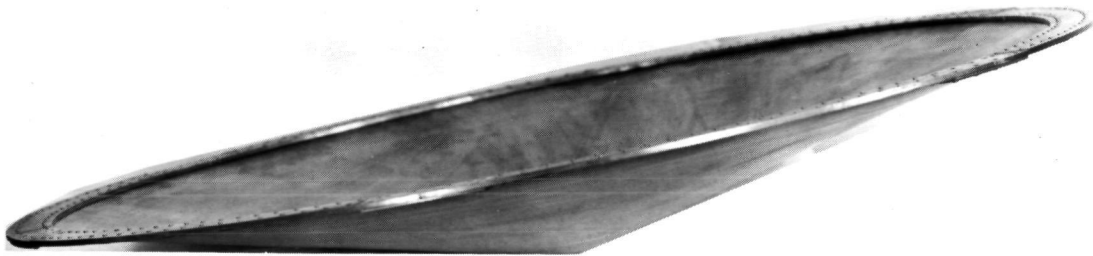
The doors were cut out of the frame panels and maintained as matched sets. This not only minimized material requirements but also provided good mating of door to frame. All machining, line reaming and line boring was performed prior to assembly. Match drilling was done to assure proper fit up for pin-weld attachments.

The 0.060-inch thick Cb-1Zr aperture plate was a shallow spinning and was accomplished without incident.

A dummy door and frame assembly (one-sixth segment) with a mating panel was also required to provide NASA with a mockup for subsequent installation of insulation (Reference: Section 3.7). This mockup provided an excellent opportunity to check out almost every operation prior to performing it on the product hardware.

The aperture door and frame sectors were assembled and checked for proper door operation as well as dimensional requirements. The aperture plate, flex plate and mounting brackets were then assembled in preparation for final heat receiver assembly operations. Instrumentation (described subsequently in Section 7.0) was also added while the unit was more accessible as is shown in Figure 99.

Assembly of the door actuators started with the welding of each double bellows to its clevis and housing (Reference: Figure 43). Radiographic examination showed good bellows alignment as is shown in Figure 100 for a typical unit. Upon completion of all assembly and operational checks, housing

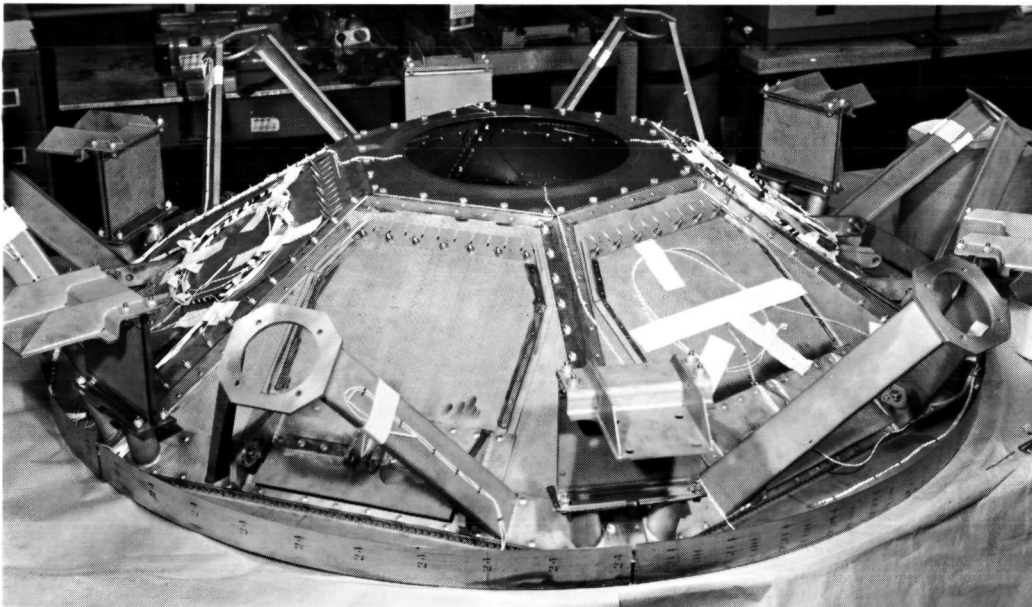


69-12-11AL

Figure 98. Cb-1Zr Top Closure Fabrication. (P69-12-11AL)



Instrumenting the Door and Frame Subassembly 69-12-11P



Aperture Assembly and Flexure Support Ready for Mounting 69-12-11AK

Figure 99. Aperture Assembly and Instrumentation. (69-12-11P)(69-12-11AK)



Bellows at Free Height
(Actuator Retracted)



Bellows Compressed
(Actuator Extended)

Figure 100. X-Ray Examination of Actuator Bellows Alignment.

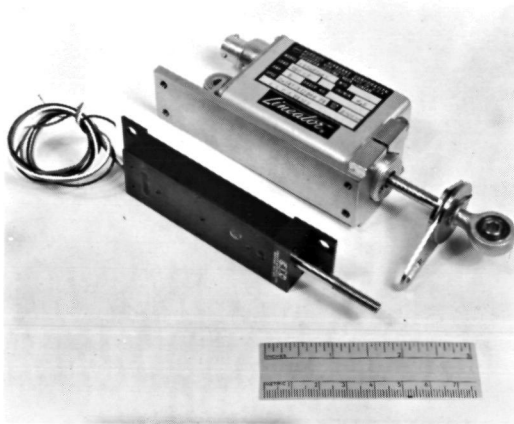
covers were installed and pressure integrity of all door actuators was verified by a final helium leak check. Typical parts and assemblies are shown in Figure 101. Installation of the actuators and linkage was accomplished subsequently as part of the final assembly.

6.6 FINAL ASSEMBLY

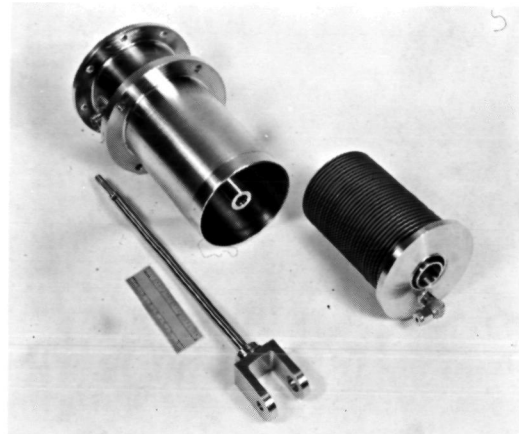
To facilitate the instrumentation and assembly of the Heat Receiver, a large frame was designed to support the gas system assembly and in such a manner that it would accommodate the subsequent assembly of all appendages and brackets. It also served as a shipping and handling fixture.

The frame was made in two halves such that one half could be removed to allow for installation of the aperture assembly without lifting the gas system assembly. Because of the limited widths of available transportation equipment, the frame could not be made large enough to surround the inlet manifold bimetallic joint which therefore extended beyond the structure. A heavy formed plate was bolted to the frame to protect the joint against damage during handling and shipment.

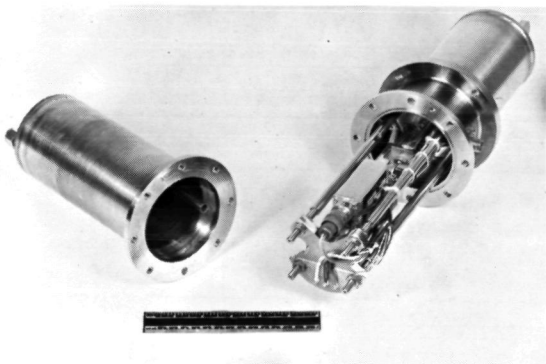
The gas system assembly was transferred from the weld laboratory to the machine shop high bay area for removal of the assembly from the dolly and dismantling of the center spider and special weld fixtures. Arrangements for disassembly were planned so that the "free state" gas system was left on a large inspection type surface plate after removal of all weld fixture restraints. Equal height blocks had been set under the lower manifold pads so that the special handling and shipping fixture could be installed around the gas system and attached to the lower manifold receiver pads. In this way, the "free state" gas system assembly would be lifted and handled only one time. This one time was from the surface plate to the precision assembly area and by means of the special handling and shipping fixture. The frame was bolted to the inlet manifold facility pads after checking bolt hole and pad alignments to insure against the possibility of introducing distortions. Protective Cb-lZr foil was also installed at all contacting surfaces. The completed gas system is shown in Figure 1 in position for assembly with the special handling and shipping fixture.



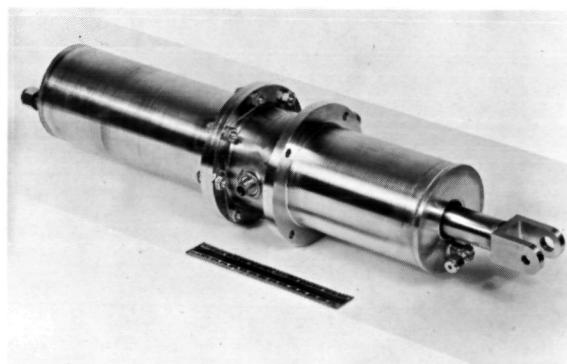
69-12-4B



69-12-4A

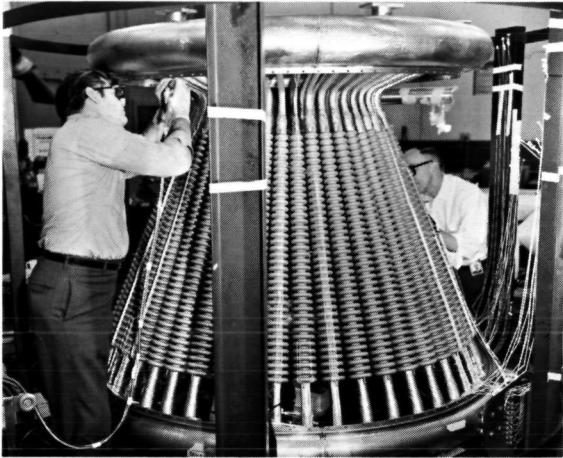


69-12-6A

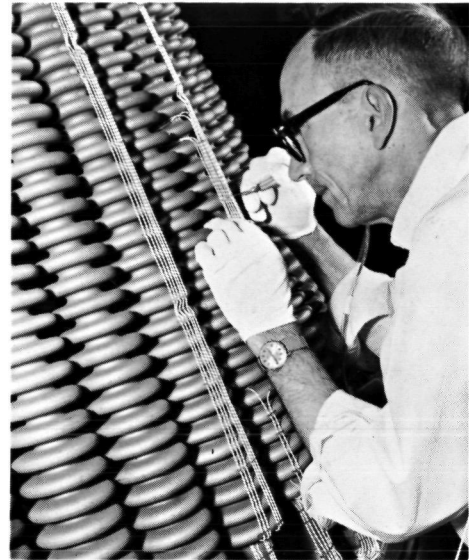


69-12-11Z

Figure 101. Door Actuator and Typical Subassemblies.



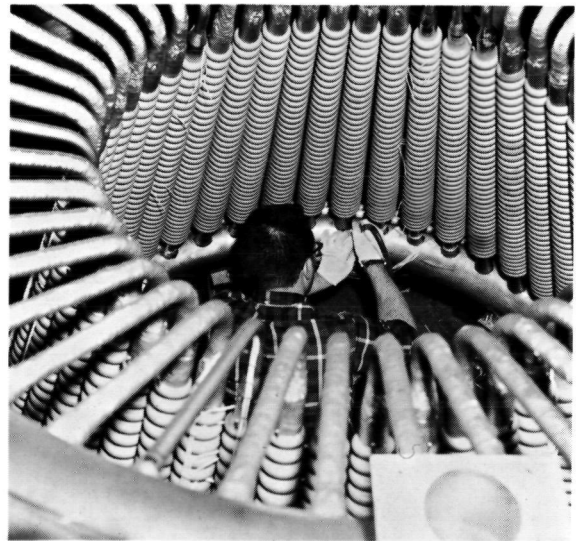
69-11-12P



69-11-12N



69-11-12Q



69-11-12M

Figure 102. Gas System Instrumentation Typical Application Sequences.

All instrumentation of the gas system assembly was accomplished (after installation in the special handling fixture) as described in Section 7.0 before starting further mechanical assembly. The application of Cb-1Zr foil insulation on the gas tubes and other local areas as required by the drawings was also accomplished before proceeding with mechanical assemblies. The process of instrumenting the gas system is shown in Figure 102.

Application of Cb-1Zr foil insulation on all gas tubes and other local pad areas as required by the drawings was also completed as shown in Figure 103.

The first component to be assembled to the gas system was the shell support. The reflectors had been pre-assembled to the panel segments and each panel was then installed after carefully aligning mating bolt holes as well as the reflector-to-tube spacing. Indicators were mounted on the outlet manifold to monitor any movements during assembly to assure proper fit-up relationship between the relatively flexible gas system members and the more rigid shell support. Monitoring of the indicators was continued until all bolts were properly torqued. Careful visual examination indicated that the resulting geometric relationships between all heat storage tubes and reflectors was excellent. Clearances between the closely spaced top convolutions are uniform and symmetrical all over, as can be seen in Figure 104.

The aperture assembly as previously discussed was pre-assembled including the flex plates and mounting brackets. The assembly was placed on a special plywood pallet fitted with a center lifting eyebolt. In contact with the pallet were the A-frame actuator mounting brackets which are the lowest surfaces (prior to installing actuators). With a portion of the handling and shipping fixture removed, the aperture assembly was properly located beneath the inlet manifold and carefully lifted into position for bolting the aperture support brackets to the manifold pads. Cb-1Zr shims had been preplaced on the manifold ID to prevent the aperture assembly from hitting the inlet manifold and damaging the instrumentation leads.

To complete installation of the aperture assembly, all actuators and linkage were installed. After each turnbuckle was properly adjusted, the doors were operated through several cycles for checkout. Some of the

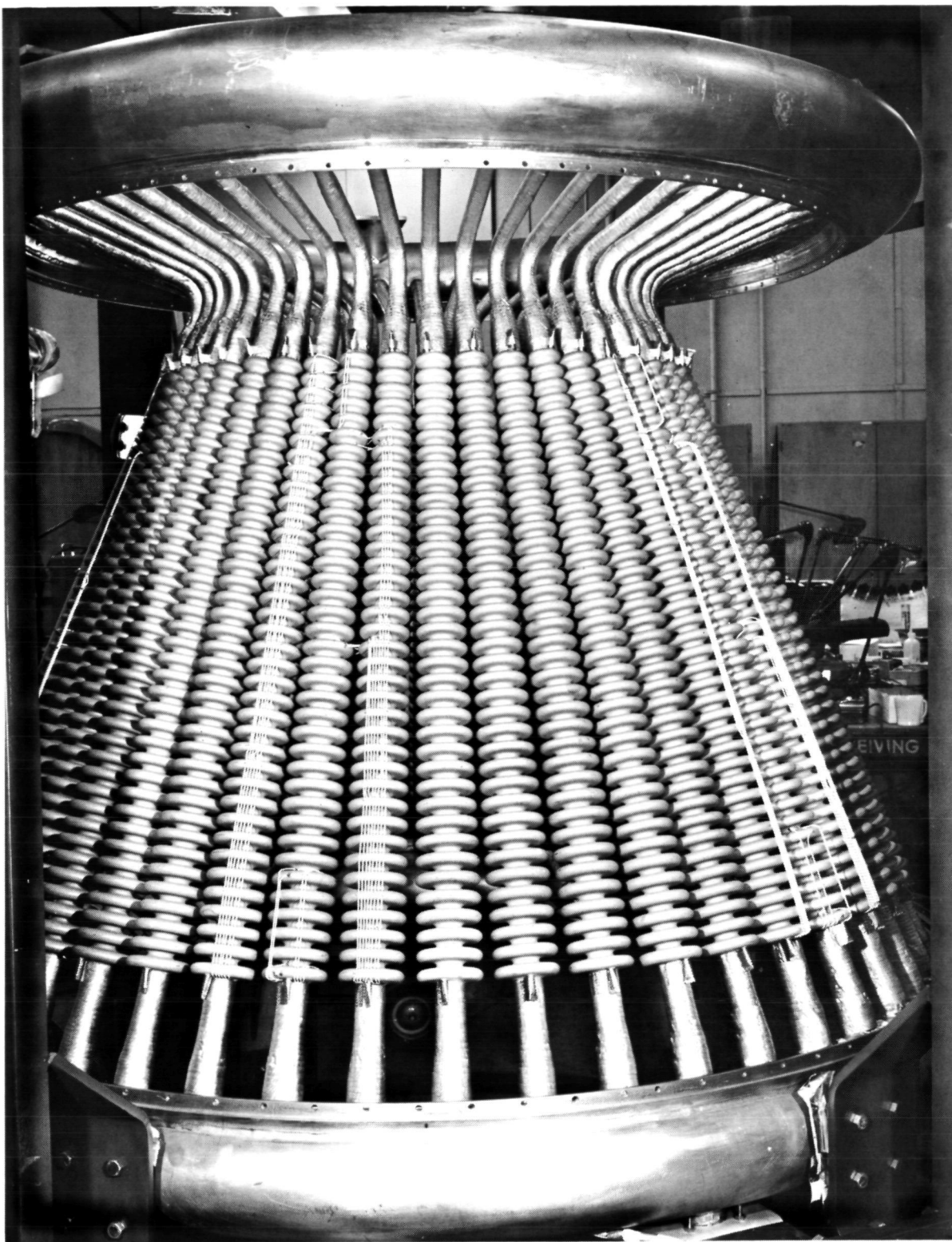
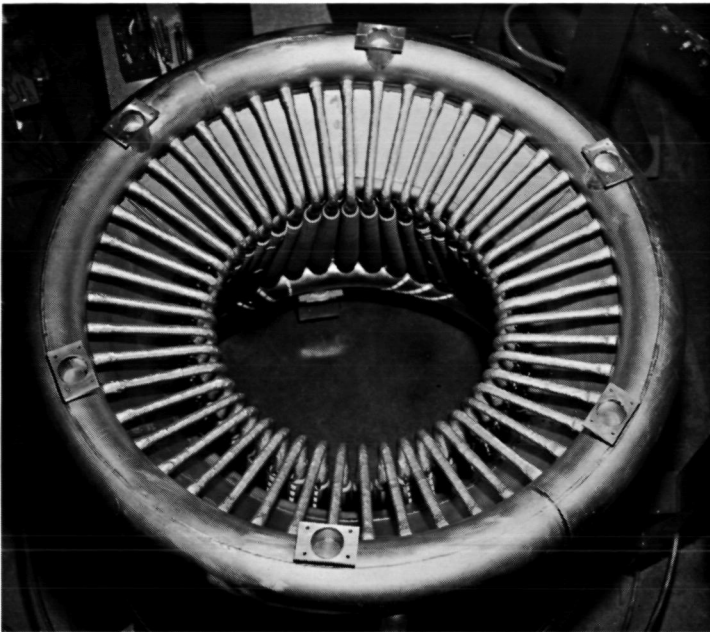


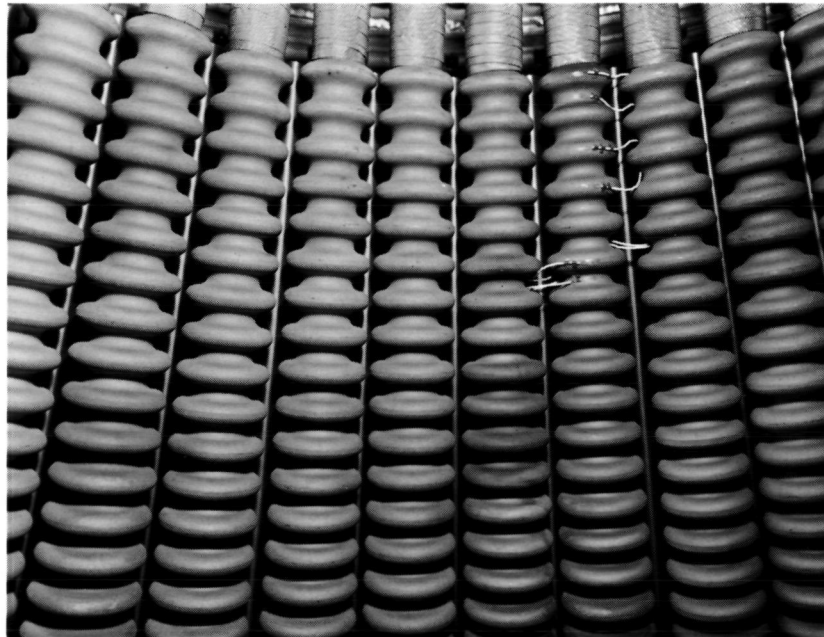
Figure 103. Gas Tube Instrumentation and Insulation Solar Heat Receiver.
(P69-12-11Y)



Overhead View

69-12-11AH

Close up of Outlet
End from Inside
Receiver Cavity



69-12-11AC

Figure 104. **A**sssembly of Shell, Reflectors and Gas System.

aperture assembly installation and checkout sequences are shown in Figure 105.

As the final component for assembly, the top closure preassembled with flex plates and support brackets was hoisted over the outlet manifold, properly oriented and carefully lowered into final position. All brackets were bolted to manifold pads after insuring that the flex plates would not be distorted. Both external and internal views of the top closure as installed are shown in Figure 106. The instrumentation leads for the top closure surface can also be seen in the overhead view.

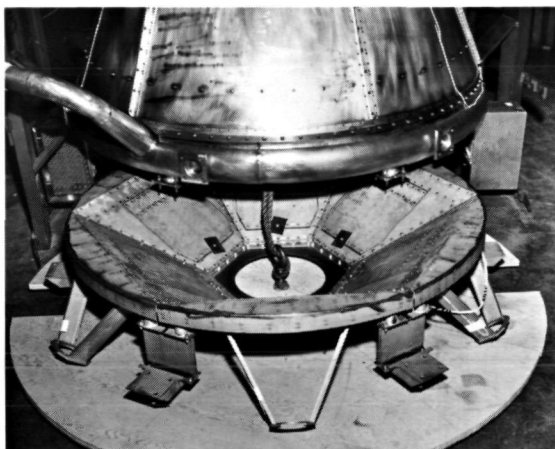
Thermocouple installation, routing of leads to junction boxes for termination, and checkout was completed for all required instrumentation locations as further described in Section 7.0. The completed solar heat receiver, ready shipping preparations is shown in Figure 107.

Components were weighed at appropriate times during the fabrication and assembly sequences. Total weight of the as-shipped receiver assembly was recorded at 1874 pounds which includes 100 pounds for the instrumentation junction boxes and mounting brackets. A breakdown by significant elements is provided in Table XII.

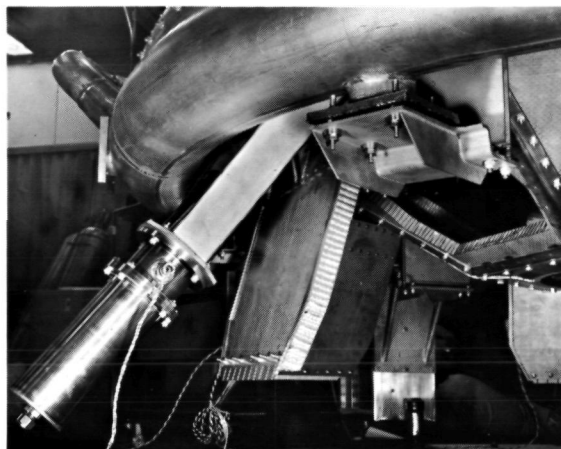
In preparation for shipment, the gas system was purged and sealed off with argon gas thereby inerting it internally. The receiver and handling fixture assembly was placed on a special shipping skid. Heat sealed plastic sheeting was installed to permit inerting the entire receiver assembly internally with argon gas.

Prior to preparing for shipment, the NASA Project Manager released the heat receiver by signing the DD250 form as the authorized NASA representative. During his visit on 12/22/69 H. Cameron witnessed the operation of all doors, spot checked several thermocouples and performed a detailed visual examination.

Special shipping arrangements were made and coordinated with the NASA Project Manager. An NSP representative rode with the exclusive use air ride van. Both the NSP representative and the NASA Project Manager witnessed the unloading at LeRC on December 24, 1969.



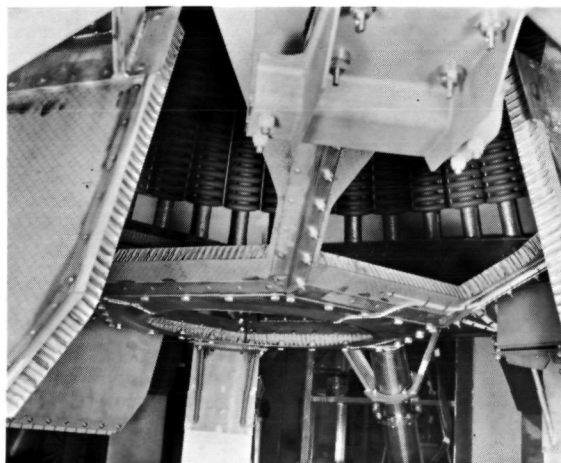
69-12-11AP



69-12-11BB

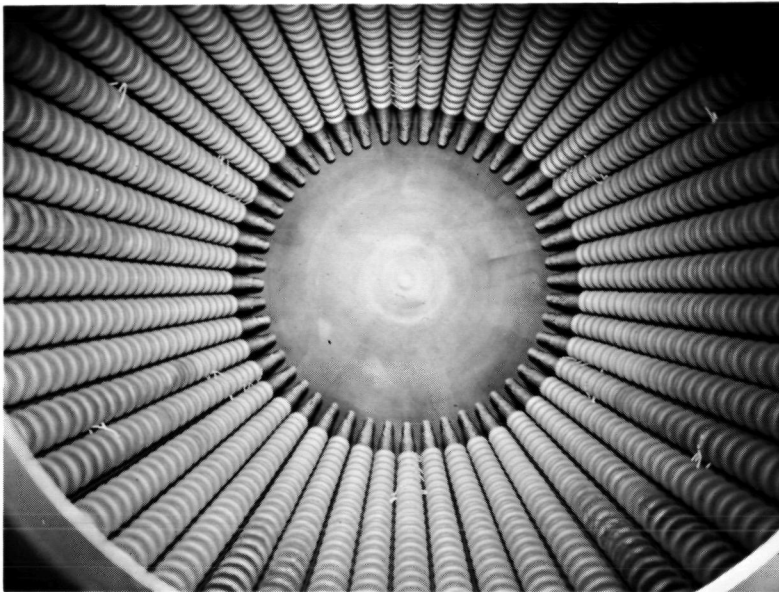


69-12-11AX



69-12-11AV

Figure 105. Aperture Structure, Doors and Linkage - Installation and Checkout.



View of Top Closure
and Tubes from
Aperture Opening

69-12-11AR

Overhead View of Top
Closure as Installed
on Gas System



Figure 106. Top Closure.



69-12-11AQ

Figure 107. Brayton Cycle Solar Heat Receiver - Installed in Shipping Fixture. (P69-12-11AQ)

TABLE XII

WEIGHT BREAKDOWN - SOLAR HEAT RECEIVER

Gas System Assembly		1131
Gas Tubes (includes 266 pounds LiF)	576	
Inlet Manifold	260	
Outlet Manifold	230	
Ducts (elbows and bimetallics)	35	
Foil Insulation and Thermocouples	30	
Shell Assembly (with reflectors)		230
Top Closure (with flex plates and bkts)		70
Aperture Assembly (less actuators)		175
Actuators (total of six)		133
Miscellaneous Hardware		35
Refractory Alloy	25	
Stainless Steel	10	
<u>Total Heat Receiver Weight</u>		<u>1774 Pounds</u>
Instrumentation Junction Boxes and Mounting Brackets		100
Shipping Frame and Plate		976
<u>Total Shipping Weight</u>		<u>2850 Pounds</u>

7.0 I N S T R U M E N T A T I O N

Page intentionally left blank

7.0 I N S T R U M E N T A T I O N

Instrumentation required to be installed by General Electric consisted primarily of thermocouples located on the surfaces of the heat storage tube assemblies and at various locations such as doors, actuators, and the top closure. The number and location of all thermocouples was originally specified and subsequently modified as shown in Table XIII to provide a better basis for correlation with temperature distribution predictions throughout the heat receiver as part of the intended system test evaluations by NASA. The basic requirements for thermocouples to be (1) compatible with the surface to which they are attached and (2) capable of continuous operation in a high vacuum environment dominated the selection of the thermocouple configuration discussed hereafter. Related instrumentation requirements included termination reference junctions for connection of leads from thermocouples to facility readout instrumentation and installation of pressure taps in the inlet and outlet manifolds.

7.1 THERMOCOUPLE ALLOY SELECTION

The NASA specifications delineated platinum-rhodium--platinum or tungsten 3% rhenium/tungsten 25% rhenium for all thermocouples attached to refractory surfaces. Chromel-alumel could be used on stainless steel components.

Considerations for the choice between platinum-rhodium--platinum and a tungsten-rhenium combination were based on several interrelated factors. Platinum-rhodium--platinum has an advantage relative to accuracy because it is used to define a portion of the International Practical Temperature Scale and the manufacturing process has been refined to the point where precise thermoelectric tolerances can be predicted for specific grades of wire. Verification of accuracy is

TABLE XIII

THERMOCOUPLE LOCATIONS

<u>Type & Location</u>	<u>Quantity Installed As Shown On Drawing 47R199377 Sh 2</u>		<u>Quantity Specified On Original Contract</u>	
	<u>Unit</u>	<u>Total</u>	<u>Unit</u>	<u>Total</u>
Surface Temp. on Each of 6 Equally Spaced Gas Tubes	22	132	12	72
Tube to Exit Manifold Surface on Each of Same 6 Equally Spaced Gas Tubes	2	12		0
Outer Shell Surface Directly Opposite Gas Tube Thermocouples on Convolutions 6, 19 & 32 of Tubes 12, 28, 44		9		0
Outside Surface of Top Closure		3		0
Outside Surface of Aperture Assembly		5		0
Surface Temp. on Each of 6 (Other) Equally Spaced Gas Tubes		0	8	48
Total W3%Re -- W25%Re		<u>161</u>		<u>120</u>
Well Temp. in Inlet & Outlet Manifold Ducts	3	6	3	6
Actuator Temp. (2 Per Actuator)	2	12		0
Door Temp.	1	3		0
Aperture Frame & Surface		6		0
Door Hinge		1		0
Pad		1		0
Total Chromel-Alumel		<u>29</u>		<u>6</u>

easily accomplished by calibrating at fixed freezing points in air. However, the use of platinum-rhodium--platinum in a vacuum environment can lead to contamination of the platinum by impurities particularly from the insulators, thereby changing the thermoelectric characteristics of the wire and causing temperature measurement errors. Also, a reaction between platinum and Cb-1Zr has been reported at temperature levels above 2000°F. Although temperatures of the heat receiver elements should be considerably less, there is no precise knowledge of the level at which the reaction becomes significant or of the rate at which it proceeds. Another disadvantage of the platinum is its relatively low strength which makes the use of wire smaller than 0.010 inch diameter impractical. Since it is practical to use some of the tungsten-rhenium combinations in 0.005 inch diameter and since only one leg of this type is expensive (the high rhenium leg) the overall cost for the bare wire is approximately three times more for the platinum-rhodium--platinum.

The alloy selected for attachment to refractory surfaces was tungsten 3% rhenium--tungsten 25% rhenium. It is compatible with Cb-1Zr and can be resistance welded directly to the surface of the heat storage tubes without fear of reaction. It is reasonably stable over long periods of time. It has an output of approximately 10 microvolts per degree F at 1700°F (which is significantly greater than the 6 microvolts per degree F of platinum 10% rhodium--platinum). The only disadvantages are (1) the embrittlement in the W3%Re leg after welding of the junction and (2) the fact that this alloy is not recognized as a standard by NBS. As a result, there is no standard calibration curve. The embrittlement (at the junction) problem can be minimized by installation procedures and techniques which have been established and used within GE-NSP. The calibration problem was solved by obtaining matched wire specified to be accurate within $\pm 1\%$ of a calibration curve furnished with the wire. Verification within NSP of the accuracy of such calibrations has been established on previously purchased quantities of matched wire from Englehard Industries.

For reasons of reliability, material compatibility as well as in order to maintain material compatibility and economy, chromel-alumel thermocouples were used on stainless steel components. The welded

junction of the chromel-alumel combination is considerably more ductile than that of the W3%Re--W25% rhenium.

7.2 REFERENCE JUNCTIONS

Selection of the reference cold junction configuration was based on (1) the fact that the heat receiver would be tested near the center of a large vacuum chamber and (2) that it was necessary to make provision for connecting the thermocouple leads to facility instrumentation transmission lines. The technique which was selected permits use of copper leads and provides for connection of these leads at the heat receiver, thereby avoiding the necessity of using W3%Re--W25%Re leads (and connector components) all the way to the readout instruments or of accepting the error associated with using a matching lead wire of inexpensive alloy. The reference junctions are located in one of four isothermal junction blocks mounted on the heat receiver. This is the point at which the W3%Re and W25%Re wires are terminated. Each of the blocks has provision for connecting 52 thermocouple alloy pairs to copper leads. Each of the blocks are made from an aluminum plate through which 104 holes of 0.50 inch diameter have been drilled. An anodized aluminum cylinder (slightly less than 0.50 inch diameter) with a tapered hole in one end and an 8-32 tapped hole in the other is cemented into each hole in the plate with materials and techniques certified for 400°F and 10^{-6} torr environment. The cylinder is thereby thermally connected to but electrically isolated from the aluminum plate. The thermocouple alloy wires are held into the tapered hole by means of a tapered filled-teflon plug so that electrical contact is made between the wire and the inside of the tapered hole. Copper lead wire is connected by means of an 8-32 screw at the other end of the plug. The fact that the thermoelectric circuit includes part of the aluminum cylinder (between the alloy wire and copper lead) does not cause an error if the aluminum cylinder is isothermal. The entire assembly is designed to achieve this condition. Specifications on the commercially available reference junction system for which this unit was designed indicate a temperature uniformity across all 104 holes of within 0.25°F.

It is necessary to measure the absolute temperature of each of the 4 reference junction blocks by forming a thermocouple (preferably under one of the spare plugs) and running the leads (of the same material) to a controlled temperature reference junction (ice bath for example) at any convenient location. Care should be taken to insure that these thermocouples are installed and used correctly since they determine the absolute level of the reference junction blocks and therefore affect the reading of each thermocouple associated with that block.

The plugs used to hold the thermocouple alloy wires into the tapered holes in the aluminum cylinders presented a problem. Sample plugs were machined from teflon and found to lose most of their retention capability when cycled between room temperature and 400°F. The thermal expansion coefficient of pure teflon is about four times that of aluminum. Therefore, as the temperature increased, the teflon expanded faster than the aluminum and as the stresses built up the teflon took a set in diameter. As temperature decreased, the teflon shrank more than the aluminum, thereby, not returning completely to its original interference condition. To overcome this potential problem the plugs were actually made of a filled teflon material (FLOUROSINT^R by POLYPENCO) which has a thermal expansion coefficient which is considerably less than teflon and much closer to that of aluminum. As compared with pure teflon the filled teflon also has significantly better physical properties, particularly in its resistance to creep.

Each reference junction block was located in an enclosure as shown in Figure 108 to enhance its capability for maintaining isothermal conditions. Each assembly was then mounted around the perimeter of the heat receiver at locations specified by NASA so that the thermocouples could be routed by the shortest path and permanently connected to a reference channel. Field connections can be made at the rear face of the reference block without disturbing the thermocouple connections.

7.3 THERMOCOUPLE CONFIGURATION AND INSTALLATION

The specific configuration of the 161 W3%Re--W25%Re thermocouples

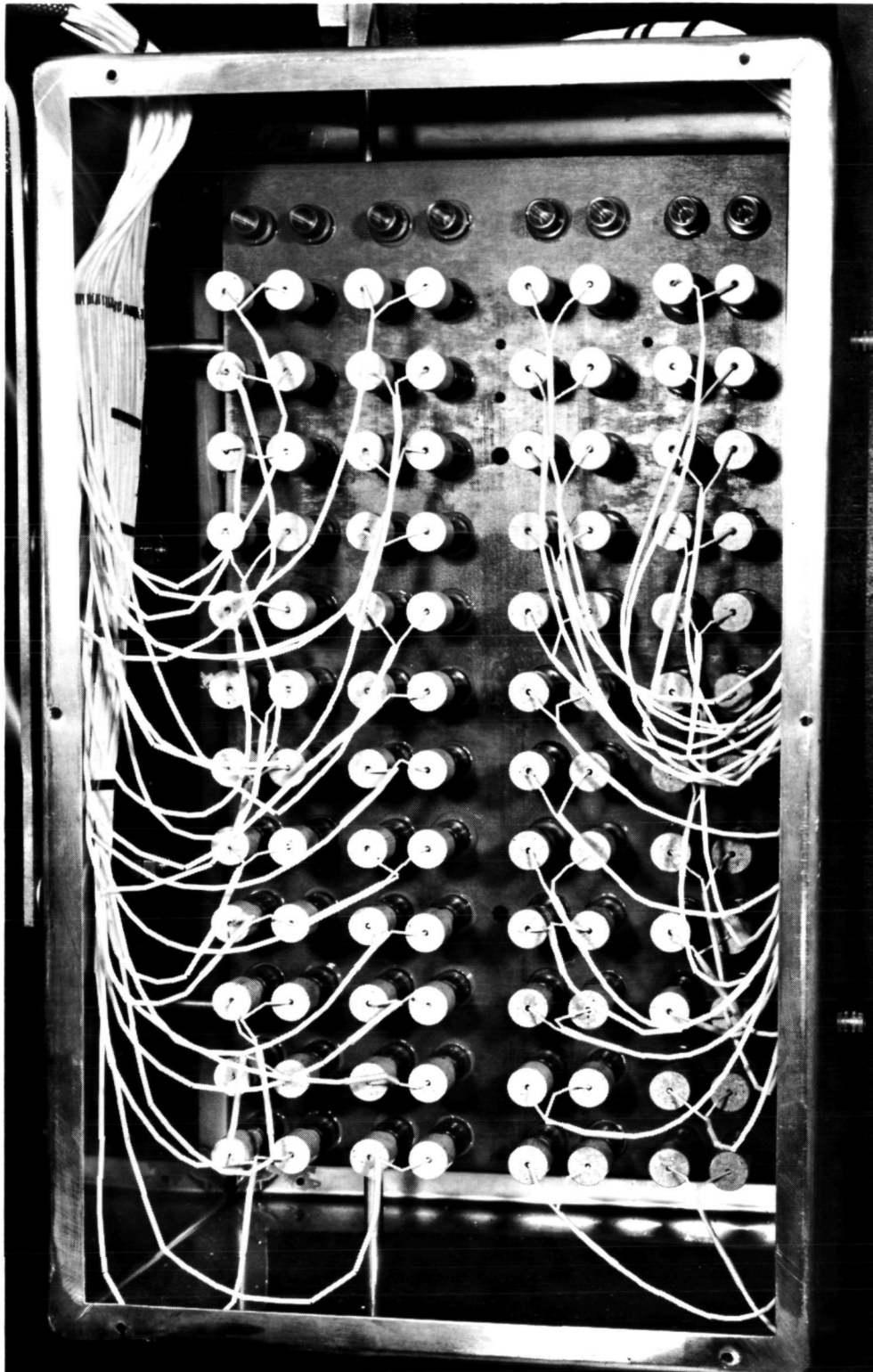


Figure 108. Thermocouple Junction Box Solar Heat Receiver. (P69-12-11D)

used on refractory surfaces consisted of 0.005 inch diameter alloy wires strung through double bore alumina insulators nominally 0.062 inch O.D. At termination or connection points, single hole insulators were used. The insulators were a high purity (99.% min.) impervious type. Routing around corners was accomplished by breaking the insulators into a series of short lengths at the vicinity of the bend so that the angular deflection between two adjacent insulator lengths was relatively small. This type of thermocouple has been successfully used within GE-NSP for systems located in ion-pumped vacuum chambers operating at pressure levels down to 10^{-11} torr. Details and installation procedures are covered in Specifications 03-0019-00-A and 03-0075-00-A. Junctions for surface temperature thermocouples were formed by resistance welding the individual alloy wires to the surface at the point to be measured after firmly supporting the thermocouple insulator assembly to minimize the stresses induced at the junction by the leads. The surface thus becomes a part of the junction. It can be shown that there is no error introduced by the use of the surface material in series with the thermocouple circuit if the surface area between the alloy wires is isothermal.

The 29 chromel-alumel thermocouples for surface temperatures on stainless steel components were made, installed, routed, and terminated using the same techniques described previously for tungsten-rhenium except that the bare alloy wire diameter was 0.010 inch (instead of 0.005 inch). The junction box configuration permitted use of any type of thermocouple alloy in a wide range of wire sizes.

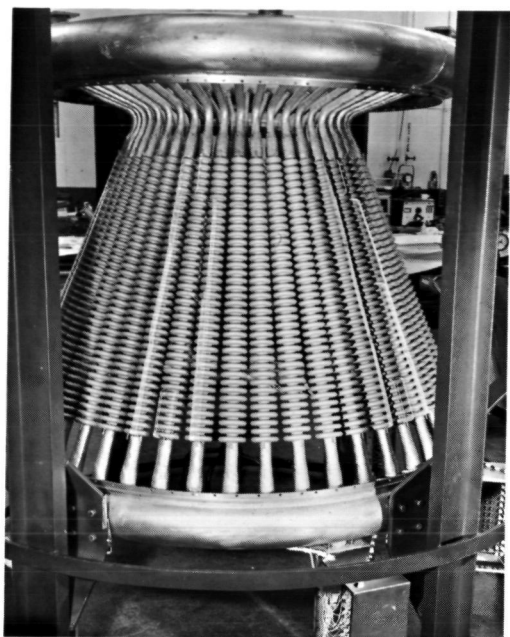
The instrumentation application, routing and related requirements for the heat receiver were accomplished as delineated in Figure 10. It should be noted that the bulk of the thermocouples were located on six equally spaced gas tubes. Since it was necessary to bring all thermocouple leads out along the inlet manifold (where the terminal junction boxes were mounted) a significant amount of tube surface blockage could have been present at the inlet end of the tube. In order to avoid this and the possible change in the performance of the instrumented tube resulting from it, only eight of the total thermocouples located on a given tube were routed along the outward facing section of that

particular tube. Other thermocouples (from areas farther removed from the inlet end) were routed along the outward facing sections of adjacent tubes. Figures 102 and 109 show details of gas system thermocouple routing and terminations. The upper right view in Figure 102 shows the typical expansion loops provided in the longer leads to minimize the effects of differential thermal expansion between the thermocouple assemblies, the gas tubes and other members. Typical routing of leads at the inlet manifold can be seen in the lower left view of Figure 105.

Well thermocouples for the inlet and outlet ducts were made from bare chromel and alumel wires strung through a single six hole alumina insulator. All six wires were welded together to form a common hot junction for three thermocouples. This assembly was installed in a spring loaded adapter and fixed at the cold end of the insulator tube by means of a compression fitting (similar to flareless type tube fitting). This enables the fitting to spring load the common hot junction against the bottom of the well. This assembly was designed to provide relatively simple replacement with little or no compromise in accuracy in comparison with a welded-in configuration.

7.4 PRESSURE TAPS

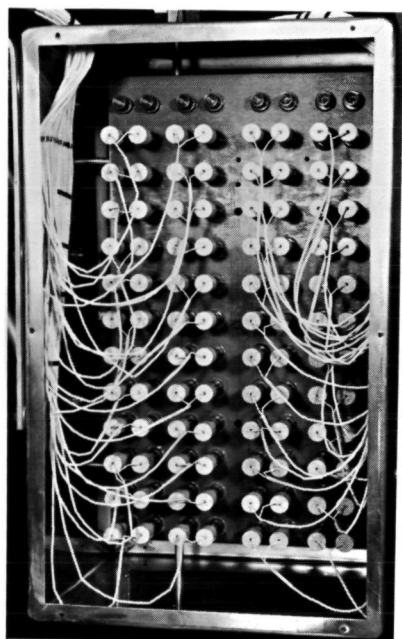
A static pressure tap was provided in each manifold duct to permit instrumentation of heat receiver inlet and exit pressures. Specifically the taps are located in the stainless steel portion of each bimetallic joint. In each case the pressure tap is located upstream of the thermocouple well. Both wells and taps can be seen in Figure 110. A similar view of this detail can be seen in Figure 107 after installation of the thermocouple.



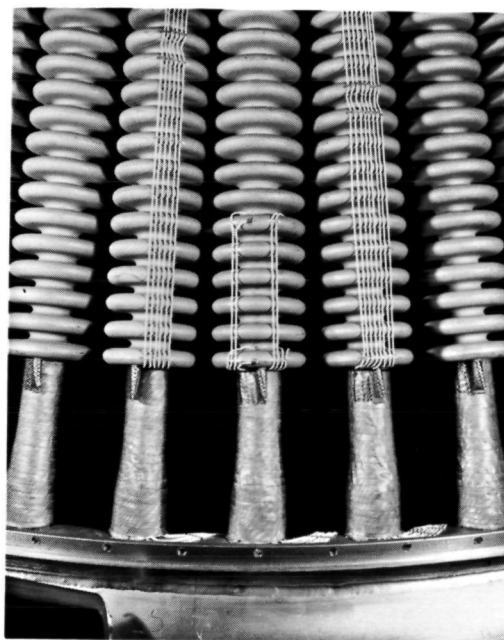
69-12-11V



69-12-11E



69-12-11D



69-12-11X

Figure 109. Gas System Instrumentation and Insulation.

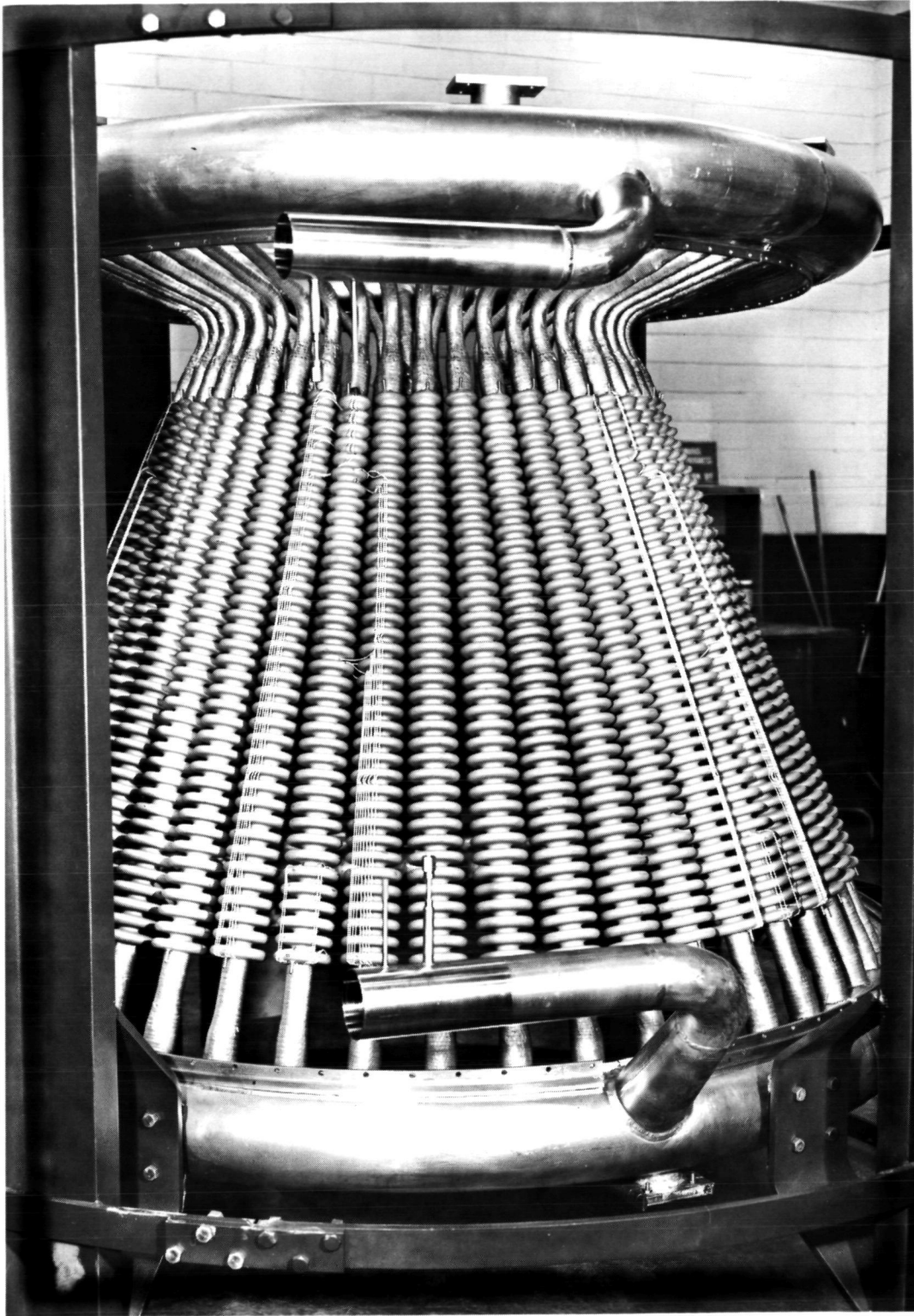


Figure 110. Gas System Showing Duct Instrumentation Features Solar Heat Receiver. (P69-12-11W)

8.0 Q U A L I T Y C O N T R O L

Page intentionally left blank

8.0 Q U A L I T Y C O N T R O L

The Quality Control activities on the Brayton Cycle Solar Heat Receiver began with preliminary design and continued in all phases of procurement, manufacturing and assembly. At the outset of the program a Quality Control Manual, GESP-23, was prepared by NSP and approved by NASA. The manual described the manner in which NSP would operate to assure quality and reliability throughout the program. Its contents provided detailed procedures in the following areas:

1. Design Review

A design review team was established consisting of representatives from:

- NSP - Program Manager
- NSP - Quality & Reliability Engineering
- NSP - Systems Material Technology
- NSP - Manufacturing Engineering
- NSP - Design Engineering
- NSP - Drafting
- NASA - (Two formal design reviews for end product drawings of the receiver)

2. Drawing and Specification Control

After approval by the design review team, drawings and specifications were issued and controlled through existing NSP procedures. Drawings were prepared in accordance with MIL-D-1000, Category E, Form 3; all characteristics were classified in one of three categories (1) critical, (2) major, or (3) minor. Parts lists were provided on the drawings.

3. Planning

Fabrication, assembly, special processing and inspection plans were written in advance of performing various operations. Planning sheets were detailed commensurate with the complexity of the parts being manufactured and inspected.

4. Purchasing and NSP Manufacturing

All items were reviewed for "Make or Buy" decision in accordance with NSP procedures prior to placement of orders in the NSP shop or outside vendors. All orders were processed through Quality Control for quality requirements and reviewed and approved by the Program Manager.

5. Vendor and Process Control

Vendors were required by Purchase Order to report dimensional and material characteristics. Special processes, such as zyglo and heat treating, were approved by NSP prior to their use. Field inspection was performed to assure compliance.

6. Inspection

All components manufactured by outside vendors were processed through receiving inspection or inspected by GE at the source. Components manufactured by NSP underwent in-process and final inspection and records were maintained throughout the program.

7. Material Traceability and Control

Chemical and physical properties and/or certifications were required on all materials. Material control numbers were assigned to all refractory alloys to permit traceability of material processed.

8. Discrepancy Review Board (D.R.B.)

A Discrepancy Review Board was established consisting of representatives from:

NSP - Quality and Reliability

NSP - Engineering

NASA - (critical and major characteristics)

Copies of D.R.B. actions forwarded to NASA following disposition. NASA's approval was obtained for discrepancies on critical or major characteristics and for discrepancies requiring repairs beyond the drawing limits.

9. Calibration

Outside vendors as well as the NSP shop were required to maintain a suitable system for calibrating measuring instruments used for determining product acceptability.

10. Failure Reporting and Analysis

Discrepancies and process and equipment malfunctions were documented and analyzed to determine disposition and possibility of failure recurrence. Significant defects and non-conformities were summarized and corrective actions were submitted to NASA on a monthly basis.

11. Functional Inspection Testing

Electrical Components and moving parts were functionally tested to assure operational design features were achieved.

12. Equipment Log

At the conclusion of the program, an Equipment Log was compiled from records maintained throughout the program and submitted to NASA. The Log contents included:

1. Drawing List
2. Flow Chart
3. Serial Number Identification
4. Certification
5. Manufacturing Instructions
6. Quality Control Instructions, Inspection Results and Material Review Reports

Page intentionally left blank

Page intentionally left blank

R E F E R E N C E S

Page intentionally left blank

REFERENCES

1. Gnadt, P.A., "Filling Heat Storage Tubes for Solar Brayton Cycle Heat Receiver with Lithium Fluoride," ORNL-TM-2732, July 1970.
2. Harrison, R.W. and Hendrixson, W.H., "Lithium Fluoride Bellows Capsule Tests," Topical Report No. 2, NASA Contract NAS 3-8523, GESP-436, January 1970.
3. Harrison, R.W. and Hendrixson, W.H., "The Compatibility of Columbium Base Alloys with Lithium Fluoride," Topical Report No. 1, NASA Contract NAS 3-8523, GESP-261, September 1969.
4. ASME Boiler and Pressure Vessel Code, Section III, The American Society of Mechanical Engineers, 1959.
5. Keller, J.D., "The Manifold Problem," Journal of Applied Mechanics, Vol. 16, No. 1 p. 77-85, March 1949.
6. Fraas, A.P. and Ozisik, M.N., Heat Exchanger Design, John Wiley & Sons, New York, 1965.
7. Vennard, J.K., Elementary Fluid Mechanics, John Wiley & Sons, New York, 1954.
8. ASME Boiler and Pressure Vessel Code, Section VIII, The American Society of Mechanical Engineers, 1959.
9. Beitch, L., "MASS System - The Computer Program for General Redundant Structures with Vibratory and General Static Loading," General Electric AT & DPD, Report No. R66FPD172, September 12, 1966.
10. Nash, W.A., "Current Shell Buckling Theory and Experiment. A Survey," General Electric Report R59FPD315, 1959.
11. Roark, R.J., Formulas for Stress and Strain, McGraw-Hill Book Company, New York, 1965.
12. Beitch, L., "SNAP - Improved Computer Program for the Analysis of Shell of Revolution with Axisymmetric Loading," General Electric Co., Report No. R66FPD171, November 15, 1966.
13. Ferry, P.B. and Page, S.P., "Niobium/Type 316 Stainless Steel Duplex Tubing," Atomics International Report NAA-SR-11191, January 1966.
14. "Potassium Corrosion Test Loop Development," Quarterly Progress Report No. 6 for Period Ending January 15, 1966, NASA Contract NAS 3-2547, NASA CR-54344, p. 36.
15. Walek, W.J., et al., Semiannual Progress Report "Determination of the Emissivity of Materials," NASA CR-72058, June 30, 1966.
16. Walek, W.J., et al., Semiannual Progress Report, Report Period: November 15, 1966 through May 14, 1967, "Determination of the Emissivity of Materials," NASA CR-72294.

17. Harrison, R.W. and Hendrixson, W.H., "Topical Report II Corrosion Tests of Lithium Fluoride in Contact with Columbium Alloys," NASA Contract NAS 3-8523, General Electric Company, January 29, 1970.
18. Buckley, D.H. and Johnson, R.L., "Marked Influence of Crystal Structure on the Friction and Wear Characteristics of Cobalt and Cobalt-Base Alloys in Vacuum to 10^{-9} mmHg II - Cobalt Alloys," TN D-2524, December 1964.
19. Lyon, T.F. and McConnaughey, N., "Evaluation of Outgassing of Candidate Insulation Materials for the Brayton Cycle Heat Receiver," GESP-321, July 23, 1969.
20. Cameron, H.M., Thermal Cycling Test on a 3 Inch Diameter Columbium - 1 Percent Zirconium to 316 Stainless Steel Transition Joint NASA TMX-2118.

APPENDIX A

DESIGN CRITERIA FOR LOW CYCLE FATIGUE OF Cb-1Zr

Page intentionally left blank

APPENDIX A
DESIGN CRITERIA FOR LOW CYCLE FATIGUE OF Cb-1Zr

INTRODUCTION

The rationale upon which the following fatigue criteria are based, is outlined by Coffin and Langer in a number of papers. The work of Manson, though resulting in a somewhat different formulation, is nevertheless based on essentially the same rationale. An excellent discussion of many aspects of low cycle fatigue is presented in the book by Manson.* Criteria are first developed here for low temperatures, at which creep or rate effects are not significant. The extension of the low temperature results into the elevated temperature regime, in which deformations are time dependent, is then discussed. It must be kept in mind throughout this development, that all formulas are empirical in nature, and can only be truly verified by comparison with sufficient fatigue test data in the form of σ_a - N_f curves.

LOW TEMPERATURE CRITERIA

At low temperatures, the imposition of cyclic straining results, after a finite number of cycles, in a hysteresis loop as given in Figure A1. The total strain range per cycle is split up into an elastic part and a plastic part, as shown. A relation is postulated between the plastic strain range $\Delta\epsilon_p$, and the number of cycles to failure N_f , such that

$$N_f^{1/2} \Delta\epsilon_p = C \quad (1)$$

where C is constant. Equating the plastic strain at one quarter cycle to the monotonic tensile fracture ductility ϵ_f , it is found that $C = \frac{1}{2} \epsilon_f$, and

$$N_f^{1/2} \Delta\epsilon_p = \frac{1}{2} \epsilon_f \quad (2)$$

*Manson, S. S., Thermal Stress and Low-Cycle Fatigue, McGraw Hill, Inc., New York, 1966.

The fracture ductility is defined in terms of the natural strain at fracture as

$$\epsilon_f = \ln \frac{100}{100-RA} \quad (3)$$

where RA is the percent reduction in area; i.e., $RA = 100 \frac{A_o - A}{A_o}$, where A_o is the original cross-sectional area of the tensile specimen, and A is the area at fracture.

For design purposes, it is not practical to state criteria in terms of quantities such as plastic strain. Normally, designs are based on elastic methods of analysis. The results of elastic analyses usually provide fairly reliable estimates of deformations, but result in stresses which may be much too conservative. It is therefore desirable to use strain, rather than stress, as the significant variable.

Referring again to Figure A1, the stress amplitude σ_a is defined as the elastically computed amplitude of stress evaluated from one-half the total strain range; i.e.,

$$\sigma_a = \frac{1}{2} E \Delta\epsilon \quad (4)$$

where E is the modulus of elasticity. In other words, σ_a is the amplitude (one-half the range) of the cyclic stress computed elastically. Dividing the total strain range

$$\Delta\epsilon = \Delta\epsilon_e + \Delta\epsilon_p \quad (5)$$

where

$$\Delta\epsilon_e = \frac{2\Delta S}{E} \quad (6)$$

$$\Delta\epsilon_p = \frac{C}{N_f^{1/2}} = \frac{1}{2 N_f^{1/2}} \ln \frac{100}{100-RA} \quad (7)$$

Substituting Equations (5), (6), and (7) into Equation (4),

$$\sigma_a = \frac{E}{4 N_f^{1/2}} \ln \frac{100}{100-RA} + \Delta S \quad (8)$$

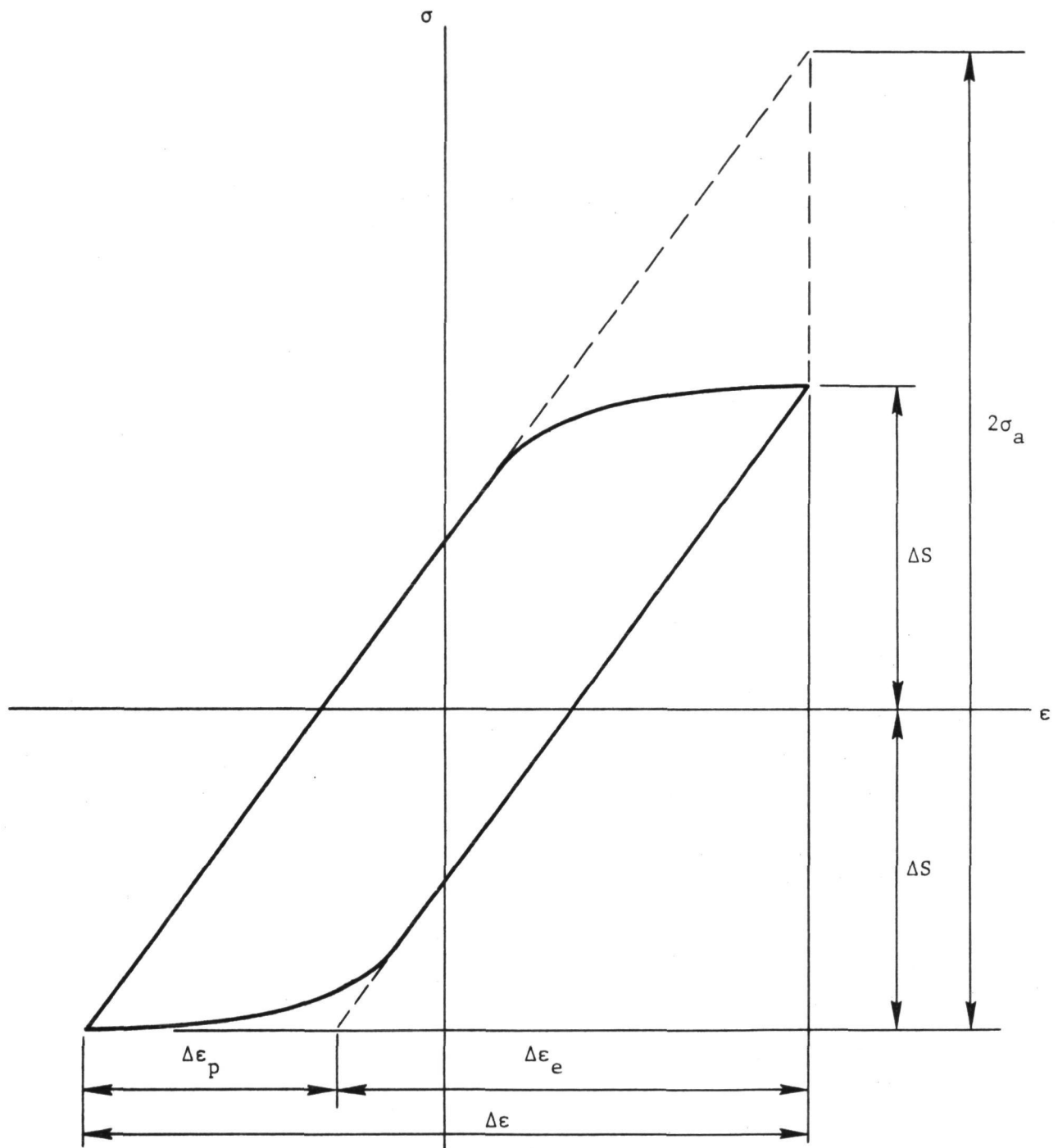


Figure A1. Hysteresis Loop of a Strain Cycle.

Though experimental data indicate that ΔS depends on the number of cycles, an approximation may be made by replacing ΔS by the endurance limit σ_e , which is the fatigue strength for a very large number (10^7) of cycles. We then have the following:

$$\sigma_a = \frac{E}{4 N_f^{1/2}} \ln \frac{100}{100-RA} + \sigma_e \quad (9)$$

This approximation introduces a small error in the low cycle region (10^2 - 10^3 cycles). Manson has avoided use of this approximation by proposing a more general equation for the total strain range:

$$\Delta \epsilon = M N_f^z + \frac{G}{E} N_f^v \quad (10)$$

It is felt at this time, however, that the present lack of fatigue data does not warrant a formulation more complex than that of Equation (9).

Equation (9) relates the elastically computed stress amplitude σ_a , to the number of cycles to failure N_f . E is a known material property, while RA and σ_e are to be evaluated by constructing a "best fit" curve from the available experimental data by using, for example, a least squares method. These curves are usually plotted on the log-log scale.

If no fatigue data are available, RA and σ_e must be estimated in some manner. For Cb-1Zr, data are available for percent elongation, rather than reduction of area, as a function of temperature. These data require, therefore, some adjustment to obtain the reduction in area. With l the length of the tensile specimen at fracture, and l_o the original length, the percent elongation, denoted by EL , is given by:

$$EL = 100 \frac{l - l_o}{l_o} \quad (11)$$

For our purposes, the material is idealized to be incompressible. Thus,

$$A l = A_o l_o \quad (12)$$

It can then easily be shown that

$$RA = \frac{100 EL}{100 + EL} \quad (13)$$

Substituting Equation (13) into Equation (3), the fracture ductility in terms of elongation at fracture is found to be:

$$\epsilon_f = \ln \left(1 + \frac{EL}{100} \right) \quad (14)$$

The endurance limit σ_e is estimated as one-half the ultimate tensile strength σ_u , i.e., $\sigma_e = \frac{1}{2} \sigma_u$.

Based on properties data at 1800°F ($E = 14 \times 10^6$ psi; $\epsilon_f = .1133$; $\sigma_e = 13$ ksi), the fatigue curve is plotted in Figure A2. In conjunction with this curve, the curves based on safety factors of $\frac{1}{20} N_f$ and $\frac{1}{2} \sigma_a$ are also shown. The lower of these curves in any particular region is used as the design curve. It must be kept in mind that, at this point, no account has been taken of the effects of (1), stress oscillating about a non-zero mean value, and (2), creep deformations at elevated temperature.

EFFECT OF MEAN STRESS

The reduction in allowable stress amplitude at a given number of cycles to failure, due to mean stress, is computed by constructing a modified Goodman diagram alongside the σ_a - N_f plot, as shown in Figure A3. The coordinates of such a diagram are stress amplitude and mean stress. The reduced allowable stress amplitude σ'_a is found by determining, from the σ_a - N_f curve, the stress amplitude σ_a , for zero mean stress at a given life N_f . A straight line is then drawn connecting σ_a on the vertical axis to a stress level on the horizontal axis corresponding to the allowable stress level in the absence of an alternating stress. For our purposes, this is taken as the ultimate tensile strength σ_u , which is 26,000 psi. The straight line shown in Figure A3 is then defined as the focus of combinations of mean stress σ_M , and stress amplitude σ'_a , which will yield a life N_f . σ'_a is then found to be given by:

$$\sigma'_a = \sigma_a \left(1 - \frac{\sigma_M}{\sigma_u} \right) \quad (15)$$

For the case presently being considered, the stress oscillates between zero and a maximum given by twice the stress amplitude. The mean stress,

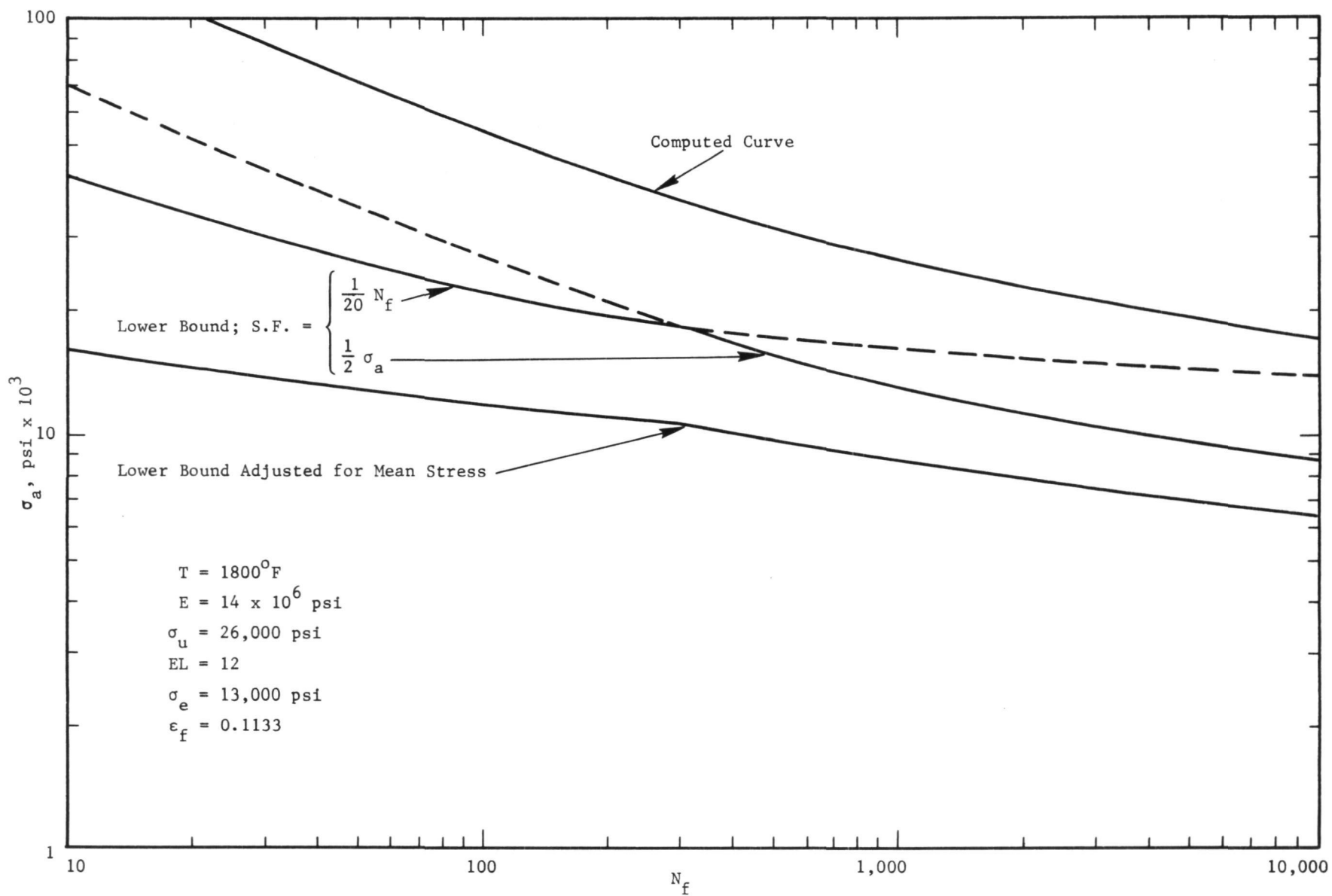


Figure A2. Fatigue Curves for Cb-1Zr Without Creep Effects.

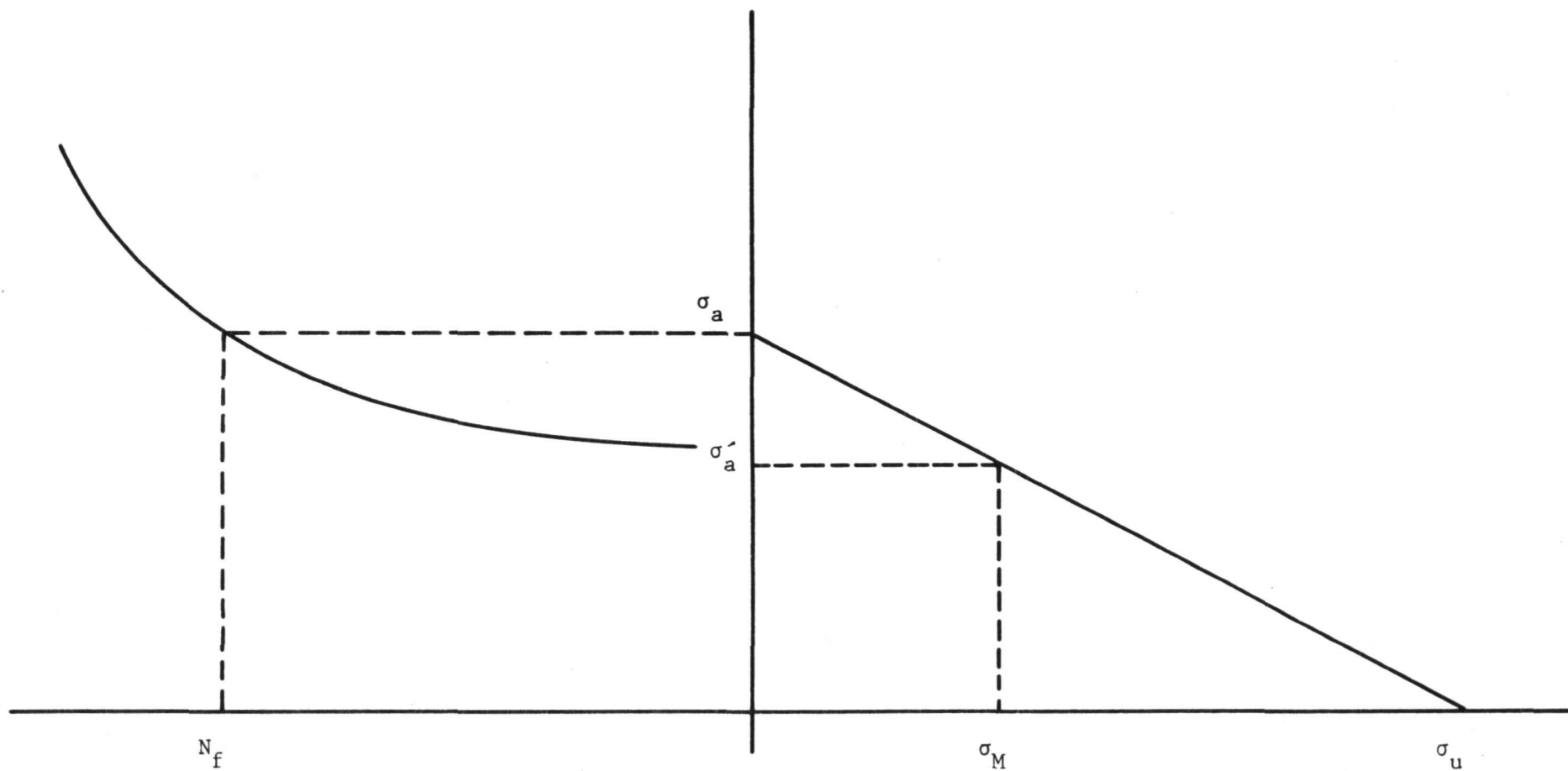


Figure A3. Modified Goodman Diagram.

therefore, is half the maximum, or equal to the allowable stress amplitude.*
Hence,

$$\sigma_M = \sigma'_a \quad (16)$$

The reduction in lower bound stress amplitude due to mean stress, is plotted in Figure A2.

DESIGN AT ELEVATED TEMPERATURES

Attention is now directed to a consideration of the effect on stress amplitude of creep deformations occurring at elevated temperatures and low frequencies. Creep deformations affect only the plastic part of the total strain range. For low temperature fatigue, the plastic strain is given by

$$\Delta \epsilon_p = \frac{\epsilon_f}{2 N_f^{1/2}} \quad (17)$$

For elevated temperatures this expression is generalized by either

$$\Delta \epsilon_p = \frac{\epsilon_f}{2 N_f^k} \quad (18)$$

where k is a temperature and rate dependent exponent greater than $\frac{1}{2}$, or

$$\Delta \epsilon_p = \frac{\epsilon'_f}{2 N_f^{1/2}} \quad (19)$$

where ϵ'_f is a reduced fracture ductility, also dependent on both temperature and time. A determination of k in Equation (18) can only be made by plotting fatigue test data. The reduced fracture ductility ϵ'_f , on the other hand, may be estimated from the reduction in area at fracture of monotonic tensile test specimens at various temperatures and strain rates. Coffin has shown that there is good correlation between ductility determined from monotonic tensile tests and ductility determined from cycle behavior, for molybdenum steel. It is therefore proposed that a series of monotonic tensile tests at various temperature and especially at various strain rates be carried out, and the results implemented in the

*This is conservative, since no yielding is assumed. As the stress amplitude increases and yielding occurs, the mean stress is decreased below this level. When the stress amplitude is equal to the yield stress, the mean stress is zero.

fatigue analysis by use of the reduced ductility. This appears to be a convenient means of avoiding a large series of cyclic tests at various frequencies and temperatures.

The reduced tensile fracture ductility is plotted against a parameter $P_1 = T (\beta_1 - \log \dot{\epsilon})$. This parameter, proposed by Coffin, implies an equivalency between temperature and strain rate; i.e., they are combined into a single parameter. The fracture ductility curve may then be applied to the cyclic loading case by interpreting $\dot{\epsilon}$ as the plastic strain rate determined by dividing the plastic strain range by one-half the average period. As an alternative, Coffin also plotted fracture ductility against the parameter $P_2 = T (\beta_2 + \log t)$, which is commonly used for plotting creep strength data. For Cb-1Zr, $\beta_2 = 15$ when t is measured in hours.

Unfortunately, no test data presently exists for Cb-1Zr which could be used to estimate the strain rate dependent stress amplitude. However, from the data that does exist for elongation vs. temperature, it appears that the variation of ductility with P_1 may not be significant. To provide some quantitative assessment of rate effects at elevated temperatures, let us consider, as an example, the case in which low cyclic frequency results in fracture ductility of one-half that obtained from the existing monotonic tensile elongation data. This is equivalent to saying that the stress amplitude in excess of the endurance limit (i.e., that part of the stress amplitude due to plastic strain) is reduced by one-half. This results in the set of theoretical fatigue curves plotted in Figure A4.

Use of this arbitrarily assumed reduction in fracture ductility at elevated temperatures yields reductions in stress amplitude (including the effect of a non-zero mean stress) in the neighborhood of 10-20%.

In conclusion, it cannot be overemphasized that the present formulation of design criteria for low cycle fatigue of Cb-1Zr, can be satisfactorily verified only upon correlation with sufficient fatigue test data.

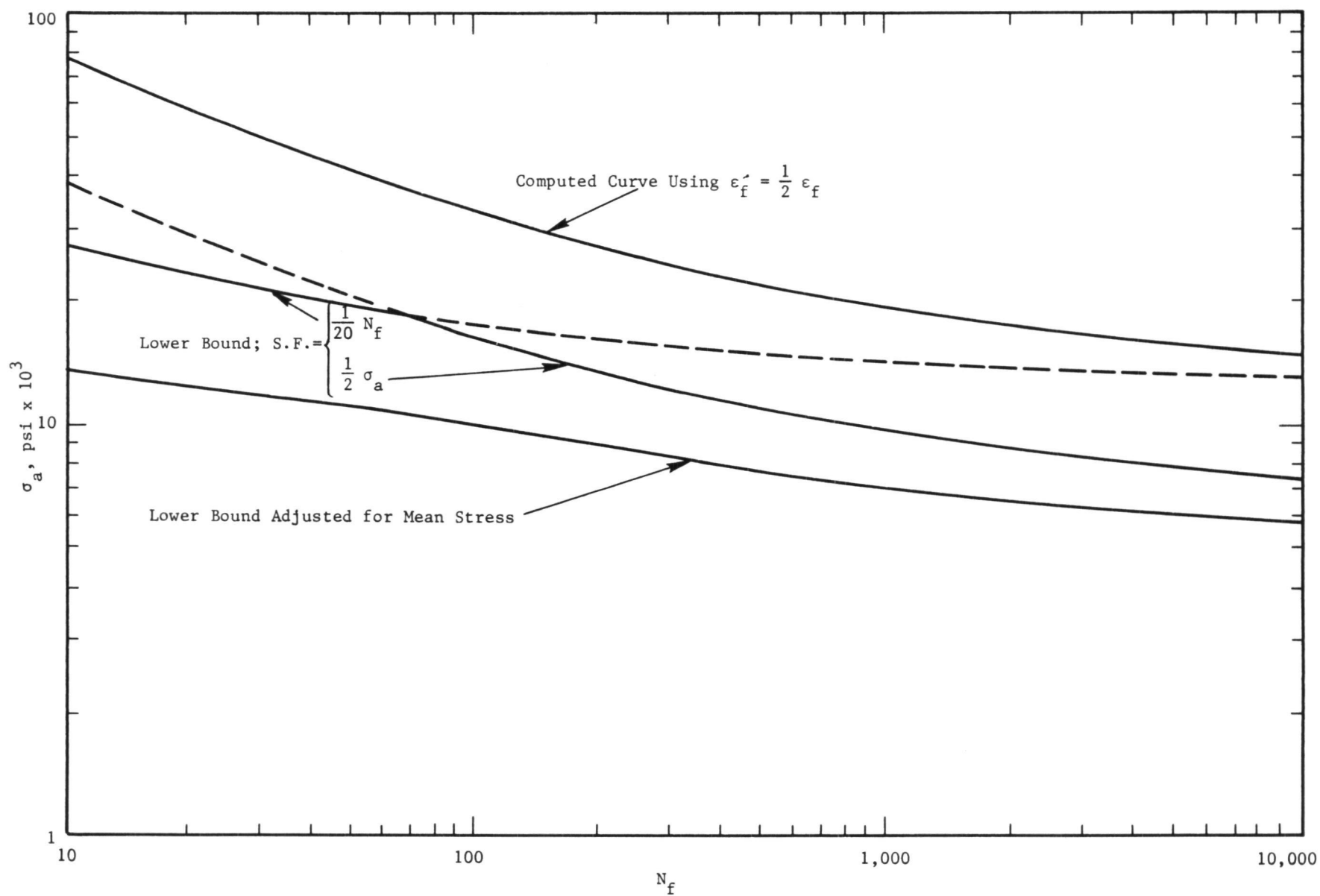


Figure A4. Fatigue Curves for Cb-1Zr Including Creep Effects.

APPENDIX B

DOOR ACTUATOR MAJOR COMPONENTS

Page intentionally left blank

APPENDIX B

DOOR ACTUATOR MAJOR COMPONENTS

General Description

The door actuator is designed to operate the heat receiver doors. The major components are described below and a summary of their temperature limitations are shown in Table B1.

Linear Actuator

The linear actuator is manufactured by Plessey Airborne Corp., Model designation: L 10-27-10. It is designed to meet requirements of MIL-A-8064-A. The power source is a permanent magnet reversible dc motor which meets the requirements of MIL-M-8609B.

Output shaft speed with the normal operating load of 150 lbs is 4.6 in/min. The maximum operating load is 300 lbs at 26 volts. The limiting static load is 500 lbs in tension or compression. Lubrication is per MIL-L-6880 for an estimated life of 10,000 cycles at the rated load and continuous duty cycle. The operating voltage range is 18 to 30 volts dc.

The linear actuator has two internal limit switches which may be adjusted to set the length of the stroke. The stroke was set within the limits of 1.490 to 1.560 inches. The extension or retraction of the actuator shaft can be controlled by a double pole, 3 position switch.

TABLE B1

ACTUATOR COMPONENT TEMPERATURE LIMITS

Linear actuator

Max. casing temperature	200°F
Rated ambient temperatures	-65 to 160°F

Potentiometer

Rated ambient temperature	-67 to 302°F
---------------------------	--------------

Teflon wire	-85 to 392°F
-------------	--------------

Polymide bearings	600°F
-------------------	-------

Connectors, external	800°F
----------------------	-------

Coolant temperature (exiting)	160°F Maximum
-------------------------------	---------------

Potentiometer

The position feed back potentiometer is a linear motion, infinite resolution, linear output device with the following specifications:

Source - Computer Instruments Corp., Model 116

Terminal resistance	5000 ohms \pm 10%
Electrical stroke	2.000 \pm .005 inch
Independent linearity	\pm 0.5% with 100 kohm load
Temperature range	-55°C to 150°C
Dielectric strength	500 VRMS
Maximum wiper current	10 ma
Life	1 million cycles

The purpose of the potentiometer is to sense the actuator shaft position and thus the door position. In addition to the indication function, the potentiometer signal can be used to control the linear actuator.

Double Bellows

The double bellows assembly seals the actuator output shaft and is arranged so that internal pressure of the door actuator is applied externally to the bellows. This arrangement achieves the largest possible differential pressure rating.

The bellows have a design life of 100,000 cycles in a 2.00-inch total stroke with a 30 psi pressure differential (external > internal) at 700°F. The nominal combined spring rate of the two bellows is 42 lb/in.

The hydroformed bellows capsule material is Inconel 718 which was selected to meet design life requirements. The end terminals are

Inconel 600, selected because of welding compatibility. All double bellows assemblies were X-rayed to assure clearance between moving parts.

Overtravel Device

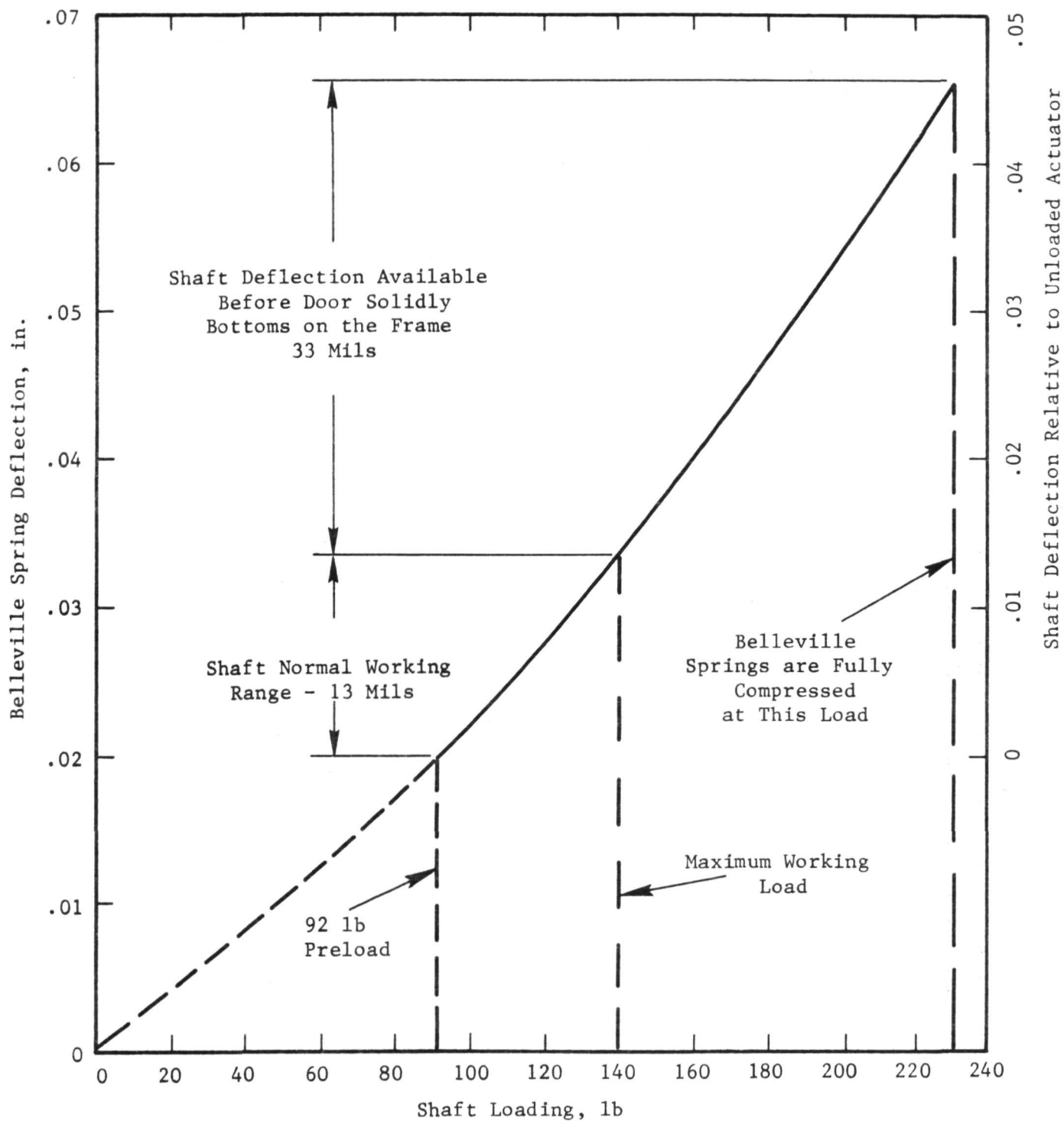
The output shaft of the door actuator is in series with the three Belleville springs which are preloaded so that they will not deflect until the compressive load in the shaft is 92 lbs. In the normal working condition, i.e., when the actuator internal pressure is 21.6 psia, vacuum is external to the actuator and the door is in the closed position, the linkage and the shaft will have 140 lbs compressive load. The Belleville springs will be compressed .033 inches from free length and will be capable of compressing an additional .033 inches. Figure B1 is a force-deflection plot showing these relationships. The additional compression capability allows the door and frame to have considerable thermal motion before the actuator door system solidly bottoms out.

Thermocouples

The thermocouples are chromel/alumel type, 16 gauge standard wire with fiberglass insulation rated for a maximum ambient temperature of 950°F. Thermocouples are attached to the linear actuator motor housing. As stated earlier, the maximum motor casing temperature allowed is 200°F.

Feedthroughs

The feedthrough connectors are manufactured by Physical Sciences Corp. of Arcadia, California. These hermetic connectors are weld mounted and rated vacuum tight to 2×10^{-8} cc/sec of helium, and operational for continuous service to 800°F. Internal to the door actuator, the six-pin connector has three wires connected to a



National Disc Spring - A1-753831
Load vs. Deflection, Three Springs in Series.

Figure B1. Door Actuator Overtravel Capability.

potentiometer and three wires to an actuator. External to the door actuator, the six-pin connector mates with a Physical Science Corp. T106-10-6S-F1 straight plug.

APPENDIX C

WELD QUALIFICATION RESULTS AND DOCUMENTATION

Page intentionally left blank

The qualification results are given in this Appendix for each weld item number listed in Table IX (See Page 112). Each unique joint configuration, welding parameters and test results are listed on the qualification form. In addition, weld process control records and applicable photomicrographs are presented.

WELDER PERFORMANCE QUALIFICATION TESTS ON GROOVE WELDS
ITEM 1

Welder Name Homer Mann Badge No. 5874
Program Name Brayton Cycle Heat Receiver Contract No. NAS 3-10944
Welding Process Manual TIG
Position (flat, horizontal, vertical, overhead) Horizontal
Welding Specification No. 03-0025-00-A
Material - Specification or MCN⁽¹⁾ Cb-1Zr Alloy Material Supplied by ORNL
Filler Material - Specification or MCN Cb-1Zr alloy - Spec. No. 01-0055-00-A
Diameter and Wall Thickness (if tube) or Joint Thickness 0.040-inch sheet
Filler Material - Diameter 0.062-inch
Fixture Description or Drawing No. Butt Weld Clamping Fixture
Weld Process Control Record No. (Exhibit I) Attach: 129
Radiographic Test Report (Form SP 1164) Attach: Acceptable

Bend Test Results

Bend No.	Results
1	<u>105° bend - no cracks observed</u>
2	<u>105° bend - no cracks observed</u>
3	<u>105° bend - no cracks observed</u>

Test Conducted by D. R. Caldwell
per Spec. No. 03-0025-00-A

We certify that the statements in this record are correct and that test welds were prepared, welded, and tested in accordance with Specification 03-0025-00-A

Date April 27, 1969 Signed William R. Young

(1) MCN Material Control Number

WELDER PERFORMANCE QUALIFICATION TESTS ON GROOVE WELDS
ITEM 1

Welder Name Carl Woodruff Badge No. 5873
Program Name Brayton Cycle Heat Receiver Contract No. NAS 3-10944
Welding Process Manual TIG
Position (flat, horizontal, vertical, overhead) Horizontal
Welding Specification No. 03-0025-00-A
Material - Specification or MCN⁽¹⁾ Cb-1Zr Alloy Material Supplied by ORNL
Filler Material - Specification or MCN Cb-1Zr Alloy - Spec. No. 01-0055-00-A
Diameter and Wall Thickness (if tube) or Joint Thickness 0.040-inch sheet
Filler Material - Diameter 0.062-inch
Fixture Description or Drawing No. Butt Weld Clamping Fixture
Weld Process Control Record No. (Exhibit I) Attach: 129
Radiographic Test Report (Form SP 1164) Attach: Acceptable

Bend Test Results

Bend No.	Results
1	<u>105° bend - no cracks observed</u>
2	<u>105° bend - no cracks observed</u>
3	<u>105° bend - no cracks observed</u>

Test Conducted by D. R. Caldwell
per Spec. No. 03-0025-00-A

We certify that the statements in this record are correct and that test welds were prepared, welded, and tested in accordance with Specification 03-0025-00-A

Date April 27, 1967 Signed W. R. Young

(1) MCN Material Control Number

WELDER PERFORMANCE QUALIFICATION TESTS ON GROOVE WELDS
ITEM 2

Welder Name Homer Mann Badge No. 5874
Program Name Brayton Cycle Heat Receiver Contract No. NAS 3-10944
Welding Process Manual TIG
Position (flat, horizontal, vertical, overhead) Horizontal
Welding Specification No. 03-0025-00-A
Material - Specification or MCN⁽¹⁾ Cb-1Zr Alloy Material Supplied by ORNL
Filler Material - Specification or MCN Cb-1Zr Alloy - Spec. No. 01-0055-00-A
Diameter and Wall Thickness (if tube) or Joint Thickness 0.250-inch plate
Filler Material - Diameter 0.093-inch
Fixture Description or Drawing No. Butt Weld Clamping Fixture
Weld Process Control Record No. (Exhibit I) Attach: 129
Radiographic Test Report (Form SP 1164) Attach: Acceptable

Bend Test Results

Bend No.	Results
1	<u>105° bend - no cracks observed</u>
2	<u>105° bend - no cracks observed</u>
3	<u>105° bend - no cracks observed</u>

Test Conducted by D. R. Caldwell
per Spec. No. 03-0025-00-A

We certify that the statements in this record are correct and that test welds were prepared, welded, and tested in accordance with Specification 03-0025-00-A

Date April 24, 1967 Signed W. R. Young

(1) MCN Material Control Number

WELDER PERFORMANCE QUALIFICATION TESTS ON GROOVE WELDS
ITEM 2

Welder Name Carl Woodruff Badge No. 5873
Program Name Brayton Cycle Heat Receiver Contract No. NAS 3-10944
Welding Process Manual TIG
Position (flat, horizontal, vertical, overhead) Horizontal
Welding Specification No. 03-0025-00-A
Material - Specification or MCN ⁽¹⁾ Cb-1Zr Alloy Material Supplied by ORNL.
Filler Material - Specification or MCN Cb-1Zr Alloy - Spec. No. 01-0055-00-A
Diameter and Wall Thickness (if tube) or Joint Thickness 0.250-inch plate
Filler Material - Diameter 0.093-inch
Fixture Description or Drawing No. Butt Weld Clamping Fixture
Weld Process Control Record No. (Exhibit I) Attach: 129
Radiographic Test Report (Form SP 1164) Attach: Acceptable

Bend Test Results

Bend No.	Results
1	<u>105° bend - no cracks observed</u>
2	<u>105° bend - no cracks observed</u>
3	<u>105° bend - no cracks observed</u>

Test Conducted by D. R. Caldwell
per Spec. No. 03-0025-00-A

We certify that the statements in this record are correct and that test welds were prepared, welded, and tested in accordance with Specification 03-0025-00-A

Date April 24, 1967 Signed W. R. Young

(1) MCN Material Control Number

PROCESS CONTROL RECORD

PROCESS CONTROL RECORD NO.

129

Page 1 of 2

DATE 11-25-68	SUBJECT Welding of Columbium, Tantalum, and Their Alloys by the Inert Gas Tungsten Arc Process-Specification SPPS 03-0025-00-A	
CONTRACT NO NAS 3-10944		
PART NAME	DRAWING NUMBER	WELD NUMBER
Brayton Cycle Weld	47D173046 Items 9-10	Large and Small Bosses
Qualification	Items 1 and 2	1/4" Plate and 0.040" Plate

A. WELDING CHAMBER

Mfgr. VASCO

Model No. 4-608

(1) Vacuum Gage	Mfgr. NRC	Model No. 507
(2) Readout Instrument	Mfgr. NRC	Model No. 0710G425
	Serial No.	Calibration Date
(3) Chamber Vacuum	Torr Before Bakeout	
	Torr After Bakeout (Hot)	Torr After Bakeout (Cold) 6 x 10 ⁻⁶
(4) Leak Rate	Minutes:	1 2 3 4 5 6
	Vacuum (10 ⁻³ Torr)	.01 .04 .06 .08 .10 .14 Overall Microns/Hr. 1.4

B. INERT GAS:

Type Helium

Supplier ~~XXXXX~~ AEC

(1) Inlet Analysis	H ₂ O 0.1 PPM	O ₂ 0.9 PPM
(2) Inlet Gas Analysis Equipment	Mfgr. Beckman O ₂ Trace Analyzer	Model 80
	Mfgr. Beckman Elect. Hygrometer	Model 27901

(3) Weld Chamber Analysis:

Equipment: Gas Chromatograph Mark III - MS 5A Column

SCAN NO.	TIME	ANALYSIS (PPM)				CONDITION	REMARKS
		H ₂ O	H ₂	O ₂ +Ar	N ₂		
229	10:48	0.4	-	2.7	19	Weld Chamber	Gloves Open
230	11:15	0.6	-	3.1	18		Welding
231	12:35	1.5	-	4.2	15	Weld Chamber	
232	2:05	5.8	-	1.8	8.2		
233	3:08	9.5	-	4.0	3.5	Weld Chamber	Stopped for Night
234	4:14	10.8	-	2.2	6.0		
237	9:40	0.3	-	3.3	3.5	Weld Chamber	11-26-68 Gloves Open
238	11:15	3.5	-	2.7	4.0	Weld Chamber	
239	12:34	5.8	-	2.9	5.0	Weld Chamber	Welding Resumed

PROCESS CONTROL RECORD (Continued)	PROCESS CONTROL RECORD NO.	
	129	Page 2 of 2

C. EQUIPMENT & PROCEDURES:

(1) Welding Equipment	Mfgr. Miller	Model No. ESR-400	
	Serial No. N318048		
(2) Tungsten Electrodes	AWS-ASTM Class EWT _h , B297-55T	Size 0.093 - 0.125	
(3) Fixtures	Material in Contact with Parts Molybdenum		
	Cleanliness Verification P.A.B.	Alignment Verification P.A.B.	
(4) Arc-Welding Torch	Type TEC Model 520		
	Installation Verification P.A.B.		
(5) Welding Power	DC Straight-Polarity Verification P.A.B.		
	JOINT TYPE		
	a	Butt	Manual
	b	Butt	Manual
	c		
	d		
(6) Filler Wire	SIZE	MCN	CLEANING DATE
	a 0.062	01-0055-00-A	11-13-68
	b 0.093	01-0055-00-A	11-13-68
(7) Cleaning & Handling	Applicable Specification 03-0010-00-C		
	Verification of Cleaning & Handling P.A.B.		
	Record Cleaning Process Control Record No(s). P-175		
(8) Removal of Parts from Chamber	Temperature Below 400°F by Surface Pyrometer (Temp. Recorded) P.A.B.		

D. QUALITY ASSURANCE:

	BADGE NO.	INITIALS	DATE
(1) Verification that "before & after" weld specimens are attached and this record is complete.	5885	D.R.C.	4-10-69
(2) Visual inspection per SPPS 03-0025-00-A	5871	P.A.B.	11-25-68
(3) Radiographic Inspection: (a) A report similar to the attached Radiographic Test Report (NS 1271) shall be prepared and submitted to NSP Quality Assurance along with the actual X-ray films and this Welding Process Control Record.	5885	D.R.C.	12-13-68
(b) If repair was required, record new Weld Process Control Number here.			
(4) Equipment & Process Qualification: Last Qualification Date Date of Last Weld to this Specification	VERIFICATION OF QUALIFICATION		
	BADGE NO.	INITIALS	DATE
	5871	P.A.B.	11-24-68
	5871	P.A.B.	11-24-68

**SPACE POWER & PROPULSION SECTION
CINCINNATI, OHIO 45215**

RADIOGRAPHIC TEST REPORT

(A) CONTRACT NO.	(B) ASSEMBLY NAME & DRAWING NO.
NAS 3-10944	Personnel Qualification
(C) WELDING PROCESS CONTROL NO.	(D) LAB PERFORMING INSPECTION
129	NSP Nondestructive Testing

(E) PROGRAM NAME	Brayton Cycle Heat Receiver
------------------	-----------------------------

(F) PERFORMING LAB NO.	(G) WELD NO.	(H) VIEW	(I) ORIG. REPAIR	(J) REMARKS (DISCREPANCY REPORT, ETC.)
	1 - 040"		Orig.	Welded by H. Mann
	2 - 040"		Orig.	Welded by C. Woodruff
	1 - 0.250"		Orig.	Welded by H. Mann
	2 - 0.250"		Orig.	Welded by C. Woodruff

The above radiographs have been reviewed and accepted per

Spec. No. 03-0025-00-A

W. D. Krumm
AUTHORIZED SIGNATURE

12-1-68
DATE

The above radiographs have been reviewed and accepted per except as noted in the remarks column.

AUTHORIZED SIGNATURE

DATE _____

WELDING PROCEDURE QUALIFICATION TESTS
ITEM 3

Specification No. 03-0025-00-A Date 1-14-69

Program Name Brayton Cycle Heat Receiver Contract No. NAS 3-10944

Welding Process Automatic TIG Manual or Machine Machine

Weld Joint Butt

Material: Spec or MCN Cb-1Zr Alloy Material to Spec or MCN Cb-1Zr Alloy Material
Supplied by ORNL Supplied by ORNL

Drawing No. None to Drawing No. None

Thickness 0.125-inch to Thickness 0.125-inch

Filler Metal - Spec or MCN and Diameter Cb-1Zr Alloy MCN 16A-008, 045-inch diameter

Welding Procedure:

Single or Multiple Pass Single

Fixturing Laboratory Butt Weld Clamping Fixture

Position of Groove Horizontal

Joint Dimensions per 03-0015-00-A

Welding Parameters Amps 270-275 Volts 20 IPM 9.63

Filler Metal Feed 44 IPM

Welding Atmosphere

Weld Process Control Record No. 153
(Exhibit I)

Inspection:

Radiographic Test Report (SP 1164) Acceptable

Metallographic Examination Result Acceptable

Section Weld 1 MB 559, MB 560, MB 561

Section Weld 2 MB 562, MB 563, MB 564

Section Weld 3

Welder's Name J. North Badge No. 2412

Test Conducted by D. R. Caldwell Lab No. 5885

per 03-0025-00-A

We certify that the statements in this record are correct and that all test welds were prepared, welded, and tested in accordance with Specification 03-0025-00-A

Date April 24, 1969 Signed W. R. Young

PROCESS CONTROL RECORD

PROCESS CONTROL RECORD NO.

153

Page 1 of 2

DATE 1-14-69	SUBJECT Welding of Columbium, Tantalum, and Their Alloys by the Inert Gas Tungsten Arc Process-Specification SPPS 03-0025-00-A
CONTRACT NO NAS 3-10944	

PART NAME	DRAWING NUMBER	WELD NUMBER
Brayton Cycle Weld Qualification	Item 3	

A. WELDING CHAMBER

Mfgr. VASCO

Model No. 4-608

(1) Vacuum Gage	Mfgr. NRC							Model No. 507	
(2) Readout Instrument	Mfgr. NRC							Model No. 0710G425	
	Serial No.							Calibration Date	
(3) Chamber Vacuum	Torr Before Bakeout								
	Torr After Bakeout (Hot)						Torr After Bakeout (Cold)		
(4) Leak Rate	Minutes:	1	2	3	4	5	6		
	Vacuum (10^{-3} Torr)	.03	.06	.08	.10	.13	.16	Overall Microns/Hr. 1.6	

B. INERT GAS:

Type Helium

Supplier ~~AMX~~ AEC

(1) Inlet Analysis	H ₂ O 0.2 PPM	O ₂ 0.9 PPM
(2) Inlet Gas Analysis Equipment	Mfgr. Beckman O ₂ Trace Analyzer	Model 80
	Mfgr. Beckman Elect. Hygrometer	Model 27901

(3) Weld Chamber Analysis:

Equipment: Gas Chromatograph Mark III - MS 5A Column

SCAN NO.	TIME	ANALYSIS (PPM)				CONDITION	REMARKS
		H ₂ O	H ₂	O ₂	N ₂		
422	10:50	0.1	14	0.27	1.1	Weld Chamber	Gloves Open
423	12:30	0.1	14	0.94	1.2	Weld Chamber	Welding
424	1:30	0.2	14	1.2	2.0	Weld Chamber	
425	2:45	0.6	14	1.6	3.5	Weld Chamber	
426	3:30	0.1	13	2.3	4.5	Weld Chamber	
427	4:00	1.2	14	1.3	4.9	Weld Chamber	Welding Completed

PROCESS CONTROL RECORD (Continued)	PROCESS CONTROL RECORD NO.	Page 2 of 2
	153	

C. EQUIPMENT & PROCEDURES:

(1) Welding Equipment.	Mfgr. Miller	Model No. ESR-400	
	Serial No. N318048		
(2) Tungsten Electrodes	AWS-ASTM Class EWT-2, B297-55T	Size 0.093	
(3) Fixtures	Material in Contact with Parts Molybdenum		
	Cleanliness Verification P.A.B.	Alignment Verification P.A.B.	
(4) Arc-Welding Torch	Type TEC Model 520		
	Installation Verification P.A.B.		
(5) Welding Power	DC Straight-Polarity Verification P.A.B.		
	JOINT TYPE		ARC VOLTS
	a	Butt	20
	b		
	c		
	d		
(6) Filler Wire	SIZE	MCN	CLEANING DATE
	a	0.045"	16A-008
	b		12-11-68
(7) Cleaning & Handling	Applicable Specification 03-0010-00-C		
	Verification of Cleaning & Handling P.A.B.		
	Record Cleaning Process Control Record No(s). P-180		
(8) Removal of Parts from Chamber ...	Temperature Below 400°F by Surface Pyrometer (Temp. Recorded) P.A.B.		

D. QUALITY ASSURANCE:

	BADGE NO.	INITIALS	DATE
(1) Verification that "before & after" weld specimens are attached and this record is complete.	5885	D.R.C.	4-10-69
(2) Visual inspection per SPPS 03-0025-00-A	5871	P.A.B.	1-14-69
(3) Radiographic Inspection: (a) A report similar to the attached Radiographic Test Report (NS 1271) shall be prepared and submitted to NSP Quality Assurance along with the actual X-ray films and this Welding Process Control Record.	5885	D.R.C.	2-20-69
(b) If repair was required, record new Weld Process Control Number here.			
(4) Equipment & Process Qualification:	VERIFICATION OF QUALIFICATION		
	BADGE NO.	INITIALS	DATE
Last Qualification Date	5871	P.A.B.	1-13-69
Date of Last Weld to this Specification	5871	P.A.B.	1-13-69

**SPACE POWER & PROPULSION SECTION
CINCINNATI, OHIO 45215**

(A) CONTRACT NO.

NAS 3-10944

(C) WELDING PROCESS CONTROL NO.

153

(B) ASSEMBLY NAME & DRAWING NO.

Weld Qualification 47D173030

(D) LAB PERFORMING INSPECTION

NSP Nondestructive Testing

(E) PROGRAM NAME

Brayton Cycle Heat Receiver

(F)
PERFORMING LAB NO.

(G) WELD NO.

(H) **VIEW**

(I) ORIG. REPAIR	
---------------------	--

(J) REMARKS (DISCREPANCY REPORT, ETC.)

Plate 1

Orig.

Plate 2

Orig.

The above radiographs have been reviewed and accepted per 03-0025-00-A

W H Kane
AUTHORIZED SIGNATURE

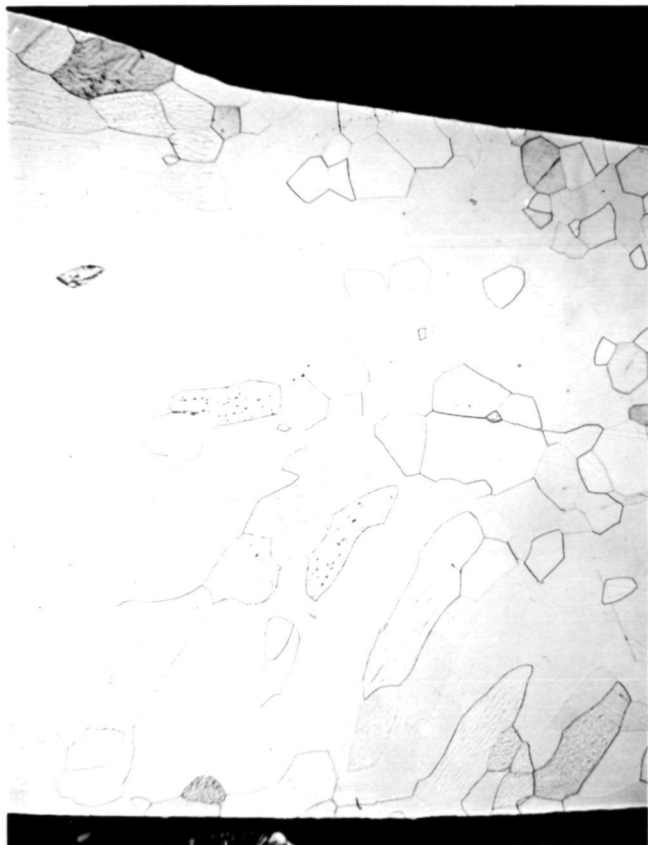
1-29-69
DATE

The above radiographs have been reviewed and accepted per except as noted in the remarks column.

AUTHORIZED SIGNATURE

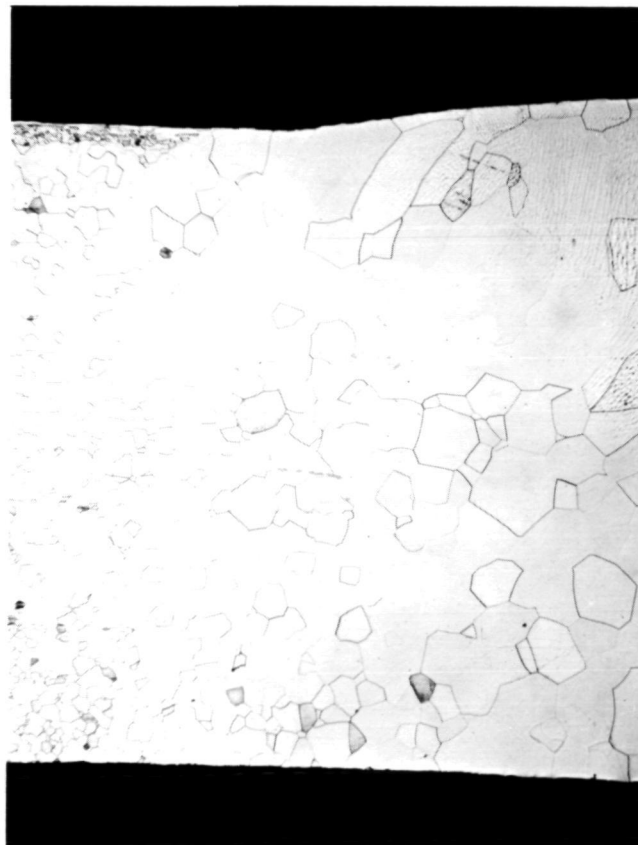
DATE _____

Typical Microstructure of Automatic TIG Weld with Filler Metal of 0.125-Inch Thick Cb-1Zr Alloy Plate.



(MB 560B)

Weld 1



(MB 564B)

Weld 2

Figure C-1. Transverse Sections Showing Part of Weld and HAZ.

Etchant: $\text{H}_2\text{SO}_4\text{-HF-H}_2\text{O}_2\text{-H}_2\text{O}$

Mag. 25x

WELDING PROCEDURE QUALIFICATION TESTS

Item 5 (4 & 6)

Specification No. 03-0025-00-A Date 2-13-69Program Name Brayton Cycle Heat Receiver Contract No. NAS 3-10944Welding Process Manual TIG Manual or Machine ManualWeld Joint ButtMaterial: Spec or MCN Cb-1Zr alloy material supplied by ORNL. to Spec or MCN Cb-1Zr alloy material supplied by ORNL.Drawing No. 47D173046 G1 to Drawing No. 47D173046 G1Thickness 0.125-inch to Thickness 0.125-inchFiller Metal - Spec or MCN and Diameter Cb-1Zr alloy, MCN 16A-007-01, 0.062-inch

Welding Procedure:

Single or Multiple Pass MultipleFixturing No fixture used - tacked.Position of Groove HorizontalJoint Dimensions per 03-0015-00-AWelding Parameters Amps Manual Volts Manual IPM ----Filler Metal Feed Manual

Welding Atmosphere

Weld Process Control Record No. 167
(Exhibit I)

Inspection:

Radiographic Test Report (SP 1164) AcceptableMetallographic Examination Result AcceptableSection Weld 1 MB 771Section Weld 2 MB 772Section Weld 3 MB 772Welder's Name H. Mann Badge No. 5874Test Conducted by D. Caldwell Lab No. 5885per 03-0025-00-AWe certify that the statements in this record are correct and that all test welds were prepared, welded, and tested in accordance with Specification 03-0025-00-ADate 6-13-69 Signed W. R. Young

PROCESS CONTROL RECORD

PROCESS CONTROL RECORD NO.

167

Page 1 of 2

DATE 2-13-69	SUBJECT Welding of Columbium, Tantalum, and Their Alloys by the Inert Gas Tungsten Arc Process-Specification SPPS 03-0025-00-A	
CONTRACT NO. NAS 3-10944		
PART NAME Brayton Cycle Weld Qualification	DRAWING NUMBER 47D173046	WELD NUMBER Items 2, 5 & 9

A. WELDING CHAMBER

Mfgr. VASCO Vertical

Model No. 4-608

(1) Vacuum Gage	Mfgr. NRC	Model No. 507
(2) Readout Instrument	Mfgr. NRC	Model No. 0710G425
	Serial No.	Calibration Date
(3) Chamber Vacuum	Torr Before Bakeout	
	Torr After Bakeout (Hot)	Torr After Bakeout (Cold) 2.3×10^{-5}
(4) Leak Rate	Minutes:	1 2 3 4 5 6
	Vacuum (10^{-3} Torr)	.12 .23 .40 .57 .73 .89 Overall Microns/Hr. 8.9

B. INERT GAS:

Type Helium

Supplier ~~WPA~~ AEC

(1) Inlet Analysis	H ₂ O 5.5 PPM	O ₂ 1.4 PPM
(2) Inlet Gas Analysis Equipment	Mfgr. Beckman O ₂ Trace Analyzer	Model 80
	Mfgr. Beckman Elect. Hygrometer	Model 27901

(3) Weld Chamber Analysis:

Equipment: Gas Chromatograph Mark III - MS 5A Column

SCAN NO.	TIME	ANALYSIS (PPM)				CONDITION	REMARKS
		H ₂ O	H ₂	O ₂	N ₂		
553	10:15	0.23	10	0.68	5.2	Vertical Chamber	Gloves Open
554-1	11:30	4.5	9.5	1.5	8.0	Vertical Chamber	Welding Complete

PROCESS CONTROL RECORD
(Continued)

PROCESS CONTROL RECORD NO.

167

Page 2 of 2

C. EQUIPMENT & PROCEDURES:

1) Welding Equipment	Mfr. Miller	Model No. ESR-400	
	Serial No. N318048		
2) Tungsten Electrodes	AWS-ASTM Class EWh, B297-55T	Size 0.093-inch	
3) Fixtures	Material in Contact with Parts Molybdenum		
	Cleanliness Verification P.A.B.	Alignment Verification P.A.B.	
4) Arc-Welding Torch	Type TEC Model 520		
	Installation Verification P.A.B.		
5) Welding Power	DC Straight-Polarity Verification P.A.B.		
	JOINT TYPE		ARC VOLTS
	a	Butt	Manual
	b	Butt	Manual
	c	Butt	Manual
6) Filler Wire	SIZE	MCN	CLEANING DATE
	a	0.062	16A-007-01
7) Cleaning & Handling	Applicable Specification 03-0010-00-C		
	Verification of Cleaning & Handling P.A.B.		
	Record Cleaning Process Control Record No(s). P-180		
8) Removal of Parts from Chamber	Temperature Below 400°F by Surface Pyrometer (Temp. Recorded) P.A.B.		

D. QUALITY ASSURANCE:

(1) Verification that "before & after" weld specimens are attached and this record is complete.	BADGE NO.	INITIALS	DATE
	5871	P.A.B.	2-14-69
(2) Visual inspection per SPPS 03-0025-00-A	5871	P.A.B.	2-13-69
(3) Radiographic Inspection: (a) A report similar to the attached Radiographic Test Report (NS 1271) shall be prepared and submitted to NSP Quality Assurance along with the actual X-ray films and this Welding Process Control Record.	5885	D.R.C.	5-15-69
(b) If repair was required, record new Weld Process Control Number here			
(4) Equipment & Process Qualification: Last Qualification Date Date of Last Weld to this Specification	VERIFICATION OF QUALIFICATION		
	BADGE NO.	INITIALS	DATE
	5871 5871	P.A.B. P.A.B.	2-12-69 2-12-69

GENERAL ELECTRICSPACE POWER & PROPULSION SECTION
CINCINNATI, OHIO 45215**RADIOGRAPHIC TEST REPORT**

(A) CONTRACT NO.

NAS 3-10944

(B) ASSEMBLY NAME & DRAWING NO.

Weld Qualification Test Piece 47D173046

(C) WELDING PROCESS CONTROL NO.

167

(D) LAB PERFORMING INSPECTION

NSP Nondestructive Testing

(E) PROGRAM NAME

Brayton Cycle Heat Receiver

(F) PERFORMING LAB NO.	(G) WELD NO.	(H) VIEW	(I) ORIG. REPAIR	(J) REMARKS (DISCREPANCY REPORT, ETC.)
	1	A	Orig	6-inch diameter girth weld
	1	B	Orig	6-inch diameter girth weld
	2	A	Orig	6-inch diameter girth weld
	2	B	Orig	6-inch diameter girth weld
	3	A	Orig	6-inch diameter girth weld
	3	B	Orig	6-inch diameter girth weld

The above radiographs have been reviewed and accepted per

03-0025-00-A

W. H. Kearns

AUTHORIZED SIGNATURE

5-20-69
DATEThe above radiographs have been reviewed and accepted per
except as noted in the remarks column.

AUTHORIZED SIGNATURE

DATE

Typical Microstructure of a Manual TIG Girth
Weld on a 6-Inch Dia. x 0.125-Inch Wall
Cb-1Zr Alloy Manifold Section.

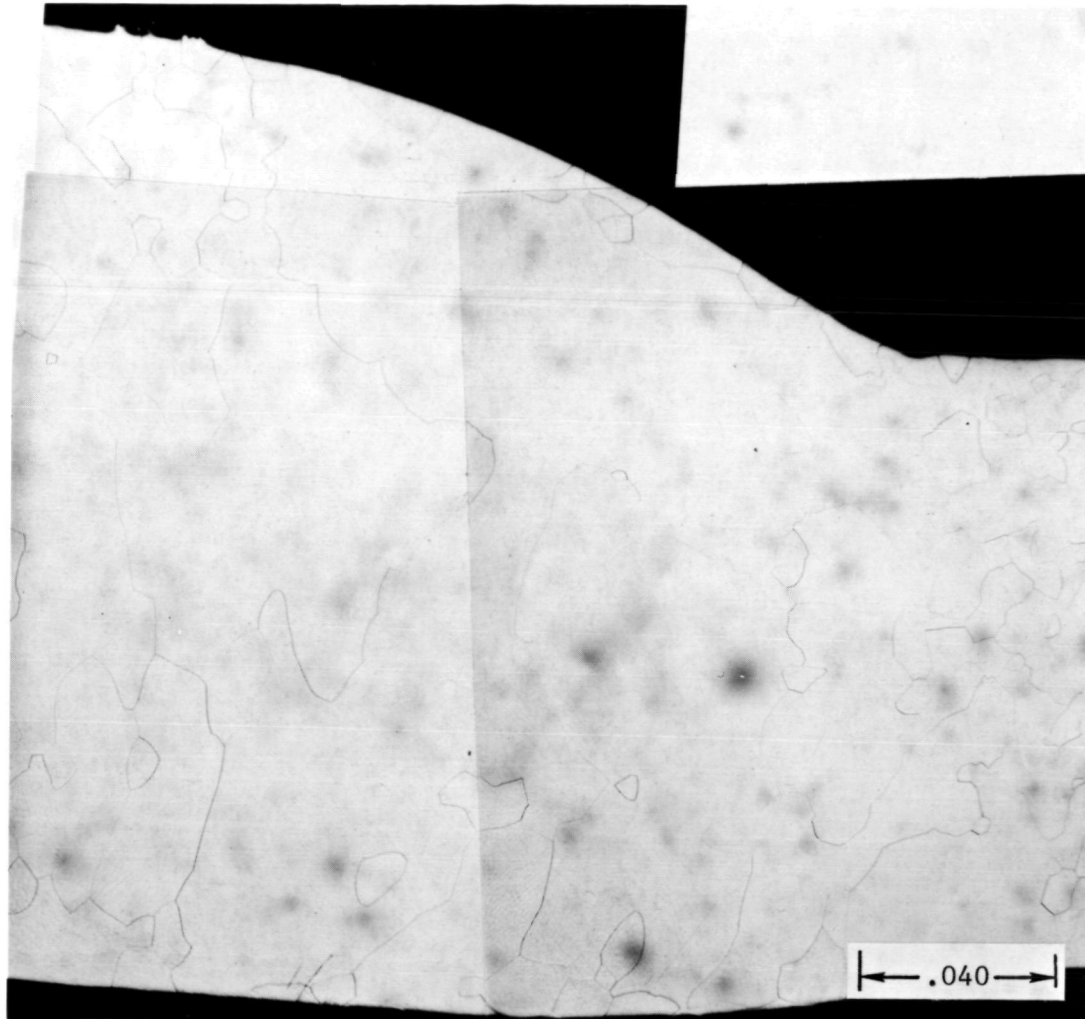


Figure C-2. Transverse Section Showing Parent Metal,
HAZ and Part of Weld. (MB 771)

Etchant: $\text{H}_2\text{SO}_4\text{-HF-H}_2\text{O}_2\text{-H}_2\text{O}$

WELDING PROCEDURE QUALIFICATION TESTS

Items 7 & 8

Specification No. 03-0025-00-A Date 11-12-68Program Name Brayton Cycle Heat Receiver Contract No. NAS 3-10944Welding Process Manual TIG Manual or Machine ManualWeld Joint ButtMaterial: Spec or MCN Cb-1Zr alloy material supplied by ORNL. to Spec or MCN Cb-1Zr alloy material supplied by ORNL.Drawing No. 47D173046 P8 to Drawing No. 47D173046 P8Thickness 0.125-inch to Thickness 0.125-inchFiller Metal - Spec or MCN and Diameter Cb-1Zr alloy, MCN 16A-007-01, 0.062-inch

Welding Procedure:

Single or Multiple Pass MultipleFixturing No fixture used - tacked.Position of Groove HorizontalJoint Dimensions per 03-0015-00-AWelding Parameters Amps Manual Volts Manual IPM ----Filler Metal Feed Manual

Welding Atmosphere

Weld Process Control Record No. 124
(Exhibit I)

Inspection:

Radiographic Test Report (SP 1164) AcceptableMetallographic Examination Result AcceptableSection Weld 1 MB 774Section Weld 2 MB 775Section Weld 3 MB 776Welder's Name H. Mann Badge No. 5874Test Conducted by D. Caldwell Lab No. 5885per 03-0025-00-AWe certify that the statements in this record are correct and that all test welds were prepared, welded, and tested in accordance with Specification 03-0025-00-ADate 6-13-69 Signed W. R. Young

PROCESS CONTROL RECORD

PROCESS CONTROL RECORD NO.

124

Page 1 of 2

DATE 11-12-68	SUBJECT Welding of Columbium, Tantalum, and Their Alloys by the Inert Gas Tungsten Arc Process-Specification SPPS 03-0025-00-A	
CONTRACT NO. NAS 3-10944		
PART NAME	DRAWING NUMBER	WELD NUMBER
Brayton Cycle Weld	47D173046	Items 7 & 8
Qualification		

A. WELDING CHAMBER		Mfr. VASCO	Model No. 4-608
(1) Vacuum Gage	Mfr. NRC	Model No. 507	
(2) Readout Instrument	Mfr. NRC	Model No. 0710G425	
	Serial No.	Calibration Date	
(3) Chamber Vacuum	Torr Before Bakeout		
	Torr After Bakeout (Hot)	Torr After Bakeout (Cold)	2.6 x 10 ⁻⁶
(4) Leak Rate	Minutes:	1 2 3 4 5 6	
	Vacuum (10 ⁻³ Torr)	.02 .03 .04 .05 .06 .07	Overall Microns/Hr. 0.7

B. INERT GAS:		Type Helium	Supplier AKKOS AEC
(1) Inlet Analysis	H ₂ O 0.15 PPM	O ₂ 0.85 PPM	
(2) Inlet Gas Analysis Equipment	Mfr. Beckman O ₂ Trace Analyzer	Model 80	
	Mfr. Beckman Elect. Hygrometer	Model 27901	

(3) Weld Chamber Analysis:		Equipment: Gas Chromatograph Mark III - MS 5A Column					
SCAN NO.	TIME	ANALYSIS (PPM)				CONDITION	REMARKS
		H ₂ O	H ₂	O ₂	N ₂		
202	10:15	0.2	-	1.2	2.9	Weld Chamber	Prior to Welding

PROCESS CONTROL RECORD

(Continued)

PROCESS CONTROL RECORD NO.

124

Page 2 of 2

C. EQUIPMENT & PROCEDURES:

(1) Welding Equipment	Mfgr. Miller	Model No. ESR-400
	Serial No. N318048	
(2) Tungsten Electrodes	AWS-ASTM Class EWT-2, B297-55T	Size 0.125-inch
(3) Fixtures	Material in Contact with Parts Molybdenum	
	Cleanliness Verification P.A.B.	Alignment Verification P.A.B.
(4) Arc-Welding Torch	Type TEC Model 520	
	Installation Verification P.A.B.	
(5) Welding Power	DC Straight-Polarity Verification P.A.B.	
	JOINT TYPE	ARC VOLTS INPUT AMPS
	a Butt	Manual Manual
	b Butt	Manual Manual
	c	
	d	
(6) Filler Wire	SIZE MCN	CLEANING DATE
	a 0.062 16A-007-01	10-17-68
	b	
(7) Cleaning & Handling	Applicable Specification 03-0010-00-C	
	Verification of Cleaning & Handling P.A.B.	
	Record Cleaning Process Control Record No(s). P-170	
(8) Removal of Parts from Chamber	Temperature Below 400°F by Surface Pyrometer (Temp. Recorded) P.A.B.	

D. QUALITY ASSURANCE:

(1) Verification that "before & after" weld specimens are attached and this record is complete.	BADGE NO.	INITIALS	DATE
	5871	P.A.B.	11-13-68
(2) Visual Inspection per SPPS 03-0025-00-A	5871	P.A.B.	11-12-68
(3) Radiographic Inspection:			
(a) A report similar to the attached Radiographic Test Report (NS 1271) shall be prepared and submitted to NSP Quality Assurance along with the actual X-ray films and this Welding Process Control Record.	5885	D.R.C.	5-15-69
(b) If repair was required, record new Weld Process Control Number here			
(4) Equipment & Process Qualification:	VERIFICATION OF QUALIFICATION		
	BADGE NO.	INITIALS	DATE
Last Qualification Date	5871	P.A.B.	11-11-68
Date of Last Weld to this Specification	5871	P.A.B.	11-11-68

SPACE POWER & PROPULSION SECTION
CINCINNATI, OHIO 45215

(A) CONTRACT NO. NAS 3-10944		(B) ASSEMBLY NAME & DRAWING NO. Weld Qualification Test Piece 47D173046		
(C) WELDING PROCESS CONTROL NO. 124		(D) LAB PERFORMING INSPECTION NSP Nondestructive Testing		
(E) PROGRAM NAME Brayton Cycle Heat Receiver				
(F) PERFORMING LAB NO.	(G) WELD NO.	(H) VIEW	(I) ORIG. REPAIR	(J) REMARKS (DISCREPANCY REPORT, ETC.)
	1	A	Orig.	47D173046 P8 Longitudinal Weld

03-0025-00-A

5-20-69
DATE

AUTHORIZED SIGNATURE

DATE _____

Typical Microstructure of a Manual TIG Seam
Weld on a 3-Inch Dia. x 0.125-Inch Wall
Cb-1Zr Alloy Diffuser Tube.



Figure C-3. Transverse Section Showing Parent Metal,
HAZ and Part of Weld. (MB 776)

Etchant: $\text{H}_2\text{SO}_4\text{-HF-H}_2\text{O}_2\text{-H}_2\text{O}$

WELDING PROCEDURE QUALIFICATION TESTS

Item 9

Specification No. 03-0025-00-A Date 2-19-69
Program Name Brayton Cycle Heat Receiver Contract No. NAS 3-10944
Welding Process Manual TIG Manual or Machine Manual
Weld Joint Fillet
Material: Spec or MCN NASA C-356336 to Spec or MCN Cb-1Zr Alloy Material Supplied by ORNL
Drawing No. 47B116898 P1 to Drawing No. 47D173046 G1
Thickness 0.22" to Thickness 0.125"
Filler Metal - Spec or MCN and Diameter 16A-035 -01 0.093" Diameter

Welding Procedure:

Single or Multiple Pass Multiple
Fixturing Tacked with Centering Fixture

Position of Groove Horizontal
Joint Dimensions per 03-0015-00-A
Welding Parameters Amps 200 Volts 20 IPM Manual
Filler Metal Feed Manual

Welding Atmosphere

Weld Process Control Record No. 172
(Exhibit I)

Inspection:

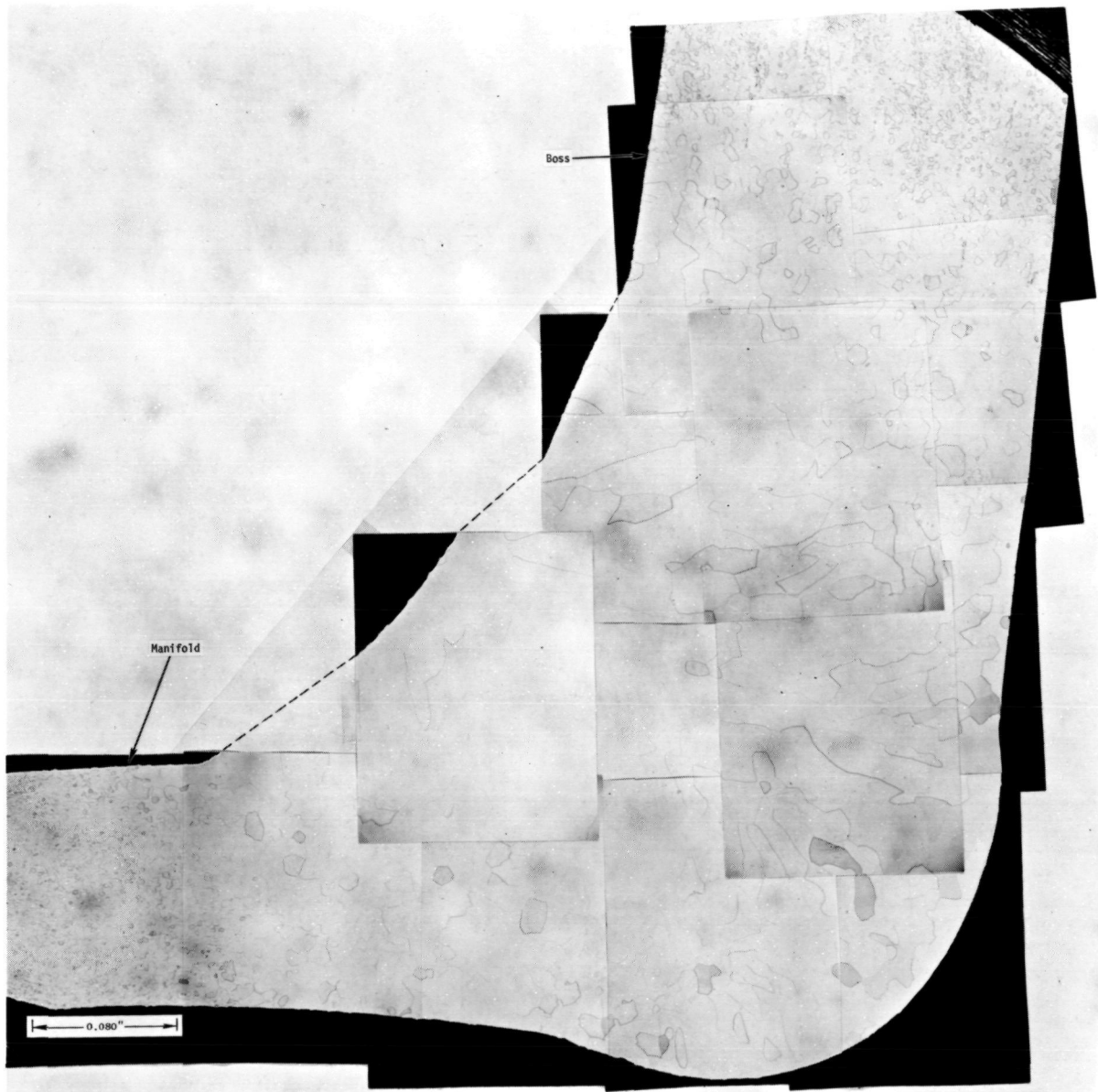
Radiographic Test Report (SP 1164) Radiographic Inspection Not Applicable To
These Welds
Metallographic Examination Result Acceptable
Section Weld 1 MB 1113
Section Weld 2 MB 1114
Section Weld 3 MB 1115

Welder's Name H. Mann Badge No. 5874
Test Conducted by D. Caldwell Lab No. 5885
per 03-0025-00-A

We certify that the statements in this record are correct and that all test welds were prepared, welded, and tested in accordance with Specification 03-0025-00-A

Date 2-2-69 Signed W. R. King

TYPICAL MICROSTRUCTURE OF A Cb-1Zr ALLOY BOSS TO INLET
MANIFOLD MANUAL TIG FILLET WELD



(MB 1113)

Figure C-4. Transverse Section Showing Parent Metal, HAZ and Weld.

Etchant: H_2SO_4 -HF- H_2O_2 - H_2O

WELDING PROCEDURE QUALIFICATION TESTS

Item 10

Specification No. 03-0025-00-A Date 2-19-69
Program Name Brayton Cycle Heat Receiver Contract No. NAS 3-10944
Welding Process Manual TIG Manual or Machine Manual
Weld Joint Fillet
Material: Spec or MCN NASA C-356336 to Spec or MCN Cb-1Zr Alloy Material
Supplied by ORNL
Drawing No. 47B116898 P2 to Drawing No. 47D173046 G1
Thickness 0.22" to Thickness 0.125"
Filler Metal - Spec or MCN and Diameter 16A-035-01 0.093" Diameter

Welding Procedure:

Single or Multiple Pass Multiple
Fixturing Tacked With Centering Fixture

Position of Groove Horizontal
Joint Dimensions per 03-0015-00-A
Welding Parameters Amps 200 Volts 20 IPM Manual
Filler Metal Feed Manual

Welding Atmosphere

Weld Process Control Record No. 172
(Exhibit I)

Inspection:

Radiographic Test Report (SP 1164) Radiographic Inspection Not Applicable To
These Welds.
Metallographic Examination Result Acceptable
Section Weld 1 MB 1116
Section Weld 2 MB 1117
Section Weld 3 MB 1118

Welder's Name H. Mann Badge No. 5874
Test Conducted by D. Caldwell Lab No. 5885
per 03-0025-00-A

We certify that the statements in this record are correct and that all test welds were prepared, welded, and tested in accordance with Specification 03-0025-00-A

Date 11-20-69 Signed W. R. Young

PROCESS CONTROL RECORD

PROCESS CONTROL RECORD NO.

172

Page 1 of 2

DATE 2-19-69	SUBJECT Welding of Columbium, Tantalum, and Their Alloys by the Inert Gas Tungsten Arc Process-Specification SPPS 03-0025-00-A
CONTRACT NO. NAS 3-10944	

PART NAME	DRAWING NUMBER	WELD NUMBER
Brayton Cycle Weld Qualification	47D173046	Items 9 and 10

A. WELDING CHAMBER		Mfgr. VASCO	Vertical	Model No. 4-608				
(1) Vacuum Cage	Mfgr. NRC	Model No. 507						
(2) Readout Instrument	Mfgr. NRC	Model No. 0710C425						
	Serial No.	Calibration Date						
(3) Chamber Vacuum	Torr Before Bakeout							
	Torr After Bakeout (Hot)		Torr After Bakeout (Cold) 1.3x10 ⁻⁵					
(4) Leak Rate	Minutes:	1	2	3	4	5	6	
	Vacuum (10 ⁻³ Torr)	08	16	25	33	41	49	Overall Microns/Hr. 4.9

B. INERT GAS:		Type Helium	Supplier Airco AEC
(1) Inlet Analysis	H ₂ O 1.3	PPM	O ₂ 2.0 PPM
(2) Inlet Gas Analysis Equipment	Mfgr. Beckman O ₂ Trace Analyzer		Model 80
	Mfgr. Beckman Elect. Hygrometer		Model 27901

(3) Weld Chamber Analysis:		Equipment: Gas Chromatograph Mark III - MS 5A Column					
SCAN NO.	TIME	ANALYSIS (PPM)				CONDITION	REMARKS
		H ₂ O	H ₂	O ₂	N ₂		
589	10:20	.32	9.7	.87	2.4	Vertical Chamber	Gloves Open
590	12:30	12.0	7.6	1.9	6.5	Vertical Chamber	Welding
591	12:55	14.0	-	2.9	3.8	Vertical Chamber	Welding
592	1:50	18.0	-	17	4.4	Vertical Chamber	Welding Complete

PROCESS CONTROL RECORD
(Continued)

PROCESS CONTROL RECORD NO.

172

Page 2 of 2

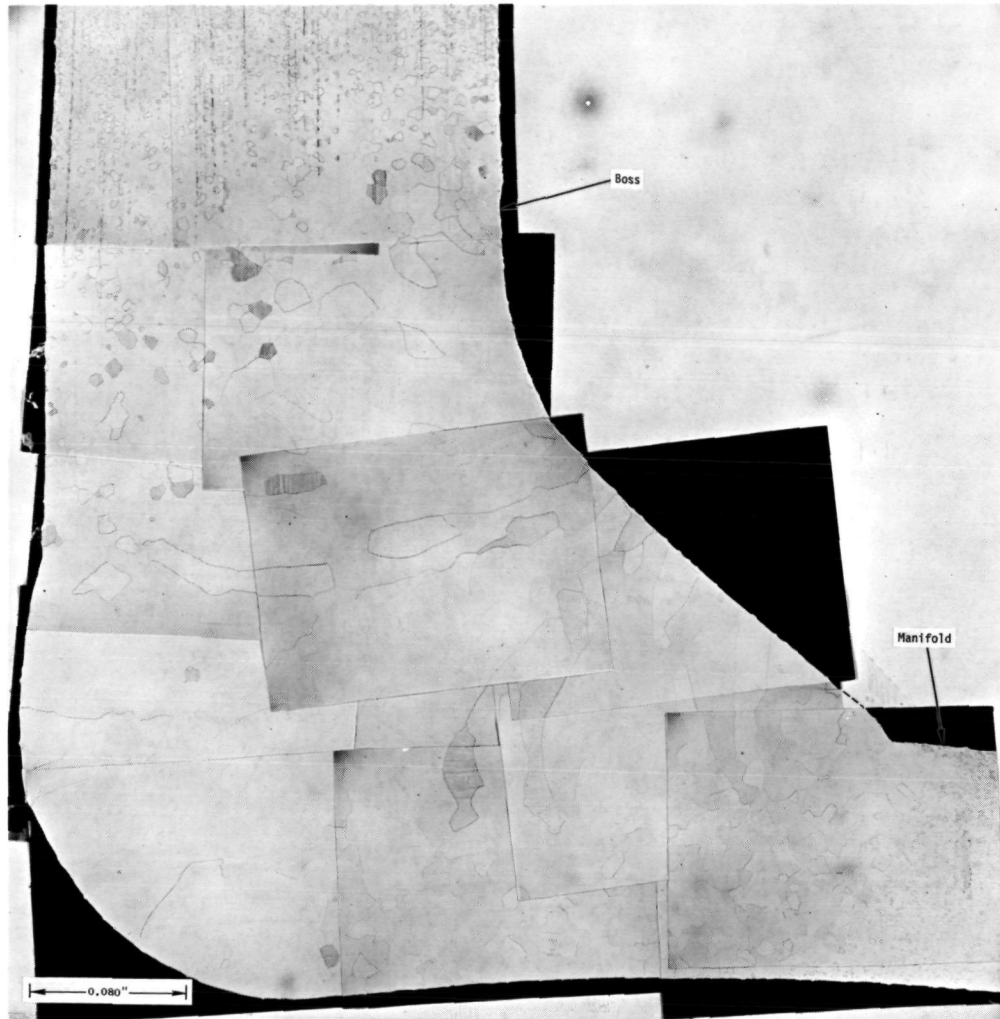
C. EQUIPMENT & PROCEDURES:

(1) Welding Equipment	Mfr. Miller Electric Co.		Model No. 330 A/BP	
	Serial No. M283288			
(2) Tungsten Electrodes	AWS-ASTM Class EWT-2		Size 3/32"	
(3) Fixtures	Material in Contact with Parts Mo			
	Cleanliness Verification xx		Alignment Verification xx	
(4) Arc-Welding Torch	Type TEC (Modified)			
	Installation Verification xx			
(5) Welding Power	DC Straight-Polarity Verification xx			
	JOINT TYPE		ARC VOLTS	INPUT AMPS
	a	Fillet	20	200
	b			
	c			
(6) Filler Wire	SIZE		MCN	CLEANING DATE
	a	0.093"	16A-035-01	2-12-69
(7) Cleaning & Handling	Applicable Specification		03-0010-00-C	
	Verification of Cleaning & Handling		xx	
	Record Cleaning Process Control Record No(s). P-175, P-180, P-188			
(8) Removal of Parts from Chamber	Temperature Below 400°F by Surface Pyrometer (Temp. Recorded) xx			

D. QUALITY ASSURANCE:

(1) Verification that "before & after" weld specimens are attached and this record is complete.	BADGE NO.	INITIALS	DATE
	5871	PAB	2-20-69
(2) Visual inspection per <u>SPPS 03-0025-00-A</u>	5871	PAB	2-19-69
(3) Radiographic Inspection: (a) A report similar to the attached Radiographic Test Report (NS 1271) shall be prepared and submitted to NSP Quality Assurance along with the actual X-ray films and this Welding Process Control Record.	Radiographic inspection not applicable to these welds.		
(b) If repair was required, record new Weld Process Control Number here.....			
(4) Equipment & Process Qualification: Last Qualification Date Date of Last Weld to this Specification	VERIFICATION OF QUALIFICATION		
	BADGE NO.	INITIALS	DATE
	5871	PAB	2-13-69
	5871	PAB	2-18-69

TYPICAL MICROSTRUCTURE OF A Cb-1Zr ALLOY BOSS TO OUTLET
MANIFOLD MANUAL TIG FILLET WELD



(MB 1116)

Figure C-5. Transverse Section Showing Parent Metal, HAZ and Weld.

Etchant: $\text{H}_2\text{SO}_4\text{-HF-H}_2\text{O}_2\text{-H}_2\text{O}$

WELDING PROCEDURE QUALIFICATION TESTS

Item 11

Specification No. 03-0025-00-A Date 2-18-69
Program Name Brayton Cycle Heat Receiver Contract No. NAS 3-10944
Welding Process Automatic TIG Manual or Machine Automatic
Weld Joint Socket
Material: Spec or MCN NASA C-356336 to Spec or MCN NASA C-356336
Drawing No. 47B116899 P1 to Drawing No. 47D173046 P7
Thickness 0.025" wall to Thickness 0.025" wall
Filler Metal - Spec or MCN and Diameter None Used

Welding Procedure:

Single or Multiple Pass Single
Fixturing Tacked - Manual. Rotated with Brad Thompson
Ind. Rotary Fixture
Position of Groove Tube Rotation on Horizontal Axis
Joint Dimensions per 03-0015-00-A
Welding Parameters Amps 70 Volts 17 RPM 3
Filler Metal Feed None Used

Welding Atmosphere

Weld Process Control Record No. 171
(Exhibit I)

Inspection:

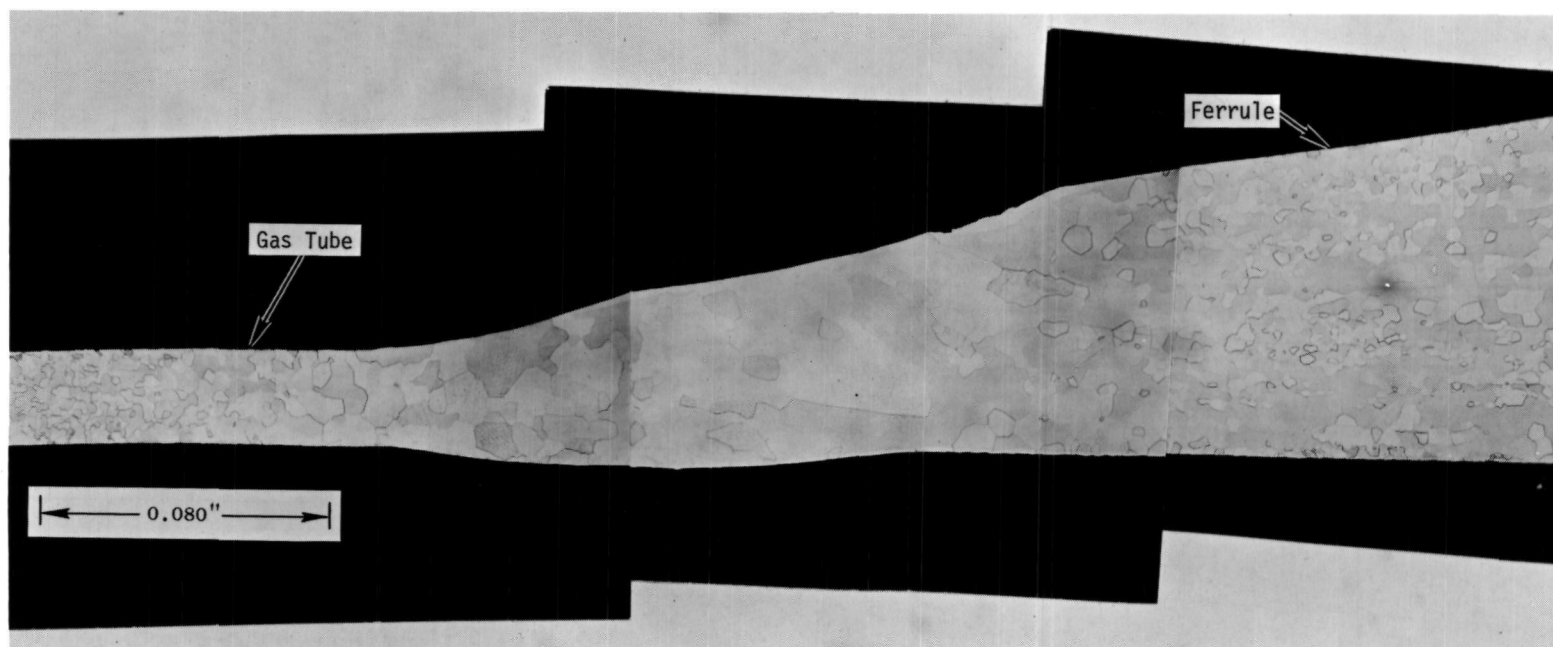
Radiographic Test Report (SP 1164) Acceptable
Metallographic Examination Result Acceptable
Section Weld 1 MB 1119
Section Weld 2 MB 1120
Section Weld 3 MB 1121

Welder's Name J. North Badge No. 2412
Test Conducted by D. Caldwell Lab No. 5885
per 03-0025-00-A

We certify that the statements in this record are correct and that all test welds were prepared, welded, and tested in accordance with Specification 03-0025-00-A

Date 2-20-69 Signed W. A. Young

TYPICAL MICROSTRUCTURE OF A Cb-1Zr ALLOY INLET FERRULE TO 0.025-INCH WALL
GAS TUBE AUTOMATIC TIG SOCKET WELD



(MB 1121)

Figure C-6. Transverse Section Showing Parent Metal, HAZ and Weld.

Etchant: H_2SO_4 -HF- H_2O_2 - H_2O

WELDING PROCEDURE QUALIFICATION TESTS
Item 12

Specification No. 03-0025-00-A Date 2-18-69

Program Name Brayton Cycle Heat Receiver Contract No. NAS 3-10944

Welding Process Automatic TIG Manual or Machine Automatic

Weld Joint Socket

Material: Spec or MCN NASA C-356336 to Spec or MCN NASA C-356336

Drawing No. 47B116899 P2 to Drawing No. 47D173046 P6

Thickness 0.025" Wall to Thickness 0.025" Wall

Filler Metal - Spec or MCN and Diameter None Used

Welding Procedure:

Single or Multiple Pass Single

Fixturing Tacked - Manual. Rotated With Brad Thompson

Ind. Rotary Fixture

Position of Groove Tube Rotation on Horizontal Axis

Joint Dimensions per 03-0015-00-A

Welding Parameters Amps 70 Volts 17 RPM 5

Filler Metal Feed None Used

Welding Atmosphere

Weld Process Control Record No. 171
(Exhibit I)

Inspection:

Radiographic Test Report (SP 1164) Acceptable

Metallographic Examination Result Acceptable

Section Weld 1 MB 1122

Section Weld 2 MB 1123

Section Weld 3 MB 1124

Welder's Name J. North Badge No. 2412

Test Conducted by D. Caldwell Lab No. 5885

per 03-0025-00-A

We certify that the statements in this record are correct and that all test welds were prepared, welded, and tested in accordance with Specification 03-0025-00-A

Date 11-20-69 Signed A R Young

PROCESS CONTROL RECORD	PROCESS CONTROL RECORD NO. <div style="text-align: center;">171</div>
Page 1 of 2	

DATE <div style="text-align: center;">2-18-69</div>	SUBJECT Welding of Columbium, Tantalum, and Their Alloys by the Inert Gas Tungsten Arc Process-Specification SPPS 03-0025-00-A
CONTRACT NO <div style="text-align: center;">NAS 3-10944</div>	

PART NAME	DRAWING NUMBER	WELD NUMBER
Brayton Cycle Weld	47D173046	Item 11
Qualification	47D173046	Item 12

A. WELDING CHAMBER	Mfr. VASCO	Horizontal	Model No. 4-608				
(1) Vacuum Gage	Mfr. NRC	Model No. 507					
(2) Readout Instrument	Mfr. NRC	Model No. 0710G425					
	Serial No.	Calibration Date					
(3) Chamber Vacuum	Torr Before Bakeout						
	Torr After Bakeout (Hot)		Torr After Bakeout (Cold) 9.5×10^{-6}				
(4) Leak Rate	Minutes:	1	2	3	4	5	6
	Vacuum (10^{-3} Torr)	06	14	21	28	36	43
		Overall Microns/Hr. 4.3					

B. INERT GAS:	Type Helium	Supplier Adco AEC
(1) Inlet Analysis	H ₂ O 1.6 PPM	O ₂ 1.8 PPM
(2) Inlet Gas Analysis Equipment	Mfr. Beckman O ₂ Trace Analyzer	Model 80
	Mfr. Beckman Elect. Hygrometer	Model 27901

(3) Weld Chamber Analysis:		Equipment: Gas Chromatograph Mark III - MS 5A Column					
SCAN NO.	TIME	ANALYSIS (PPM)				CONDITION	REMARKS
		H ₂ O	H ₂	O ₂	N ₂		
576	9:45	0.1	13.5	4.9	9.7	Welding Chamber	Gloves Open
577	11:26	0.4	--	2.3	4.9	Welding Chamber	
578	12:30	1.8	7.8	3.5	6.7	Welding Chamber	
579	1:45	2.3	8.5	3.7	4.6	Welding Chamber	Welding
580	2:30	2.6	8.0	5.5	9.9	Welding Chamber	Welding
581	3:30	3.4	--	6.4	10.1	Welding Chamber	Welding
582	4:30	4.3	--	6.8	13	Welding Chamber	Welding Complete

PROCESS CONTROL RECORD <i>(Continued)</i>	PROCESS CONTROL RECORD NO.	Page 2 of 2
	171	

C. EQUIPMENT & PROCEDURES:

(1) Welding Equipment	Mfgr. Miller Electric Company	Model No. ESR-400	
	Serial No. N318048		
(2) Tungsten Electrodes	AWS-ASTM Class EWT-2	Size 1/16"	
(3) Fixtures	Material in Contact with Parts Mo		
	Cleanliness Verification xx	Alignment Verification xx	
(4) Arc-Welding Torch	Type TEC (Modified)		
	Installation Verification xx		
(5) Welding Power	DC Straight-Polarity Verification xx		
	JOINT TYPE		ARC VOLTS
	a	Socket	17
	b		
	c		
	d		
(6) Filler Wire	SIZE	MCN	CLEANING DATE
	a	None Used	
	b		
(7) Cleaning & Handling	Applicable Specification 03-0010-00-C		
	Verification of Cleaning & Handling xx		
	Record Cleaning Process Control Record No(s). P-175, P-180		
(8) Removal of Parts from Chamber	Temperature Below 400°F by Surface Pyrometer (Temp. Recorded) xx		

D. QUALITY ASSURANCE:

(1) Verification that "before & after" weld specimens are attached and this record is complete.	BADGE NO.	INITIALS	DATE
	5871	PAB	2-21-69
(2) Visual inspection per SPPS 03-0025-00-A	5871	PAB	2-18-69
(3) Radiographic Inspection: (a) A report similar to the attached Radiographic Test Report (NS 1271) shall be prepared and submitted to NSP Quality Assurance along with the actual X-ray films and this Welding Process Control Record.	5871	PAB	2-21-69
(b) If repair was required, record new Weld Process Control Number here			
(4) Equipment & Process Qualification: Last Qualification Date Date of Last Weld to this Specification	VERIFICATION OF QUALIFICATION		
	BADGE NO.	INITIALS	DATE
	5871	PAB	2-17-69
	5871	PAB	2-17-69

GENERAL ELECTRICSPACE POWER & PROPULSION SECTION
CINCINNATI, OHIO 45215**RADIOGRAPHIC TEST REPORT**

(A) CONTRACT NO.

NAS 3-10944

(B) ASSEMBLY NAME & DRAWING NO.

Weld Qualification Test Piece 47D173046

(C) WELDING PROCESS CONTROL NO.

171

(D) LAB PERFORMING INSPECTION

NSP Nondestructive Testing

(E) PROGRAM NAME

Brayton Cycle Heat Receiver

(F) PERFORMING LAB NO.	(G) WELD NO.	(H) VIEW	(I) ORIG. REPAIR	(J) REMARKS (DISCREPANCY REPORT, ETC.)
	1	A	Orig.	Item 11 - Inlet ferrule to tube
	1	B	Orig.	Item 11 - Inlet ferrule to tube
	2	A	Orig.	Item 11 - Inlet ferrule to tube
	2	B	Orig.	Item 11 - Inlet ferrule to tube
	3	A	Orig.	Item 11 - Inlet ferrule to tube
	3	B	Orig.	Item 11 - Inlet ferrule to tube
	4	A	Orig.	Item 12 - Outlet ferrule to tube
	4	B	Orig.	Item 12 - Outlet ferrule to tube
	5	A	Orig.	Item 12 - Outlet ferrule to tube
	5	B	Orig.	Item 12 - Outlet ferrule to tube
	6	A	Orig.	Item 12 - Outlet ferrule to tube
	6	B	Orig.	Item 12 - Outlet ferrule to tube

The above radiographs have been reviewed and accepted per

03-0025-00-A

AUTHORIZED SIGNATURE

2/21/69

DATE

The above radiographs have been reviewed and accepted per
except as noted in the remarks column.

AUTHORIZED SIGNATURE

DATE

TYPICAL MICROSTRUCTURE OF A Cb-1Zr ALLOY OUTLET FERRULE TO 0.025-INCH WALL
GAS TUBE AUTOMATIC TIG SOCKET WELD



(MB 1124)

Figure C-7. Transverse Section Showing Parent Metal, HAZ and Weld.

Etchant: H_2SO_4 -HF- H_2O_2 - H_2O

WELDING PROCEDURE QUALIFICATION TESTS
ITEM 13

Specification No. 03-0025-00-A Date 12-21-68

Program Name Brayton Cycle Heat Receiver Contract No. NAS 3-10944

Welding Process Automatic TIG Manual or Machine Machine

Weld Joint Butt

Material: Spec or MCN NASA C-356336 to Spec or MCN NASA C-356336

Drawing No. 47B174876P1 to Drawing No. 47B116901P1

Thickness 0.025-inch wall to Thickness 0.025-inch wall

Filler Metal - Spec or MCN and Diameter None Used.

Welding Procedure:

Single or Multiple Pass Single

Fixturing Tacked - Manual, Rotated with Brad Thompson Ind. Rotary Fixture

Position of Groove Horizontal

Joint Dimensions per 03-0015-00-A

Welding Parameters Amps 30 Volts 16-17 ~~IPM~~ 3 rpm

Filler Metal Feed None

Welding Atmosphere

Weld Process Control Record No. 141
(Exhibit I)

Inspection:

Radiographic Test Report (SP 1164) Acceptable

Metallographic Examination Result Acceptable

Section Weld 1 MB 571, MB 573

Section Weld 2 MB 575, MB 577

Section Weld 3 MB 579, MB 581

Welder's Name J. North Badge No. 2412

Test Conducted by D. R. Caldwell Lab No. 5885

per 03-0025-00-A

We certify that the statements in this record are correct and that all test welds were prepared, welded, and tested in accordance with Specification 03-0025-00-A

Date April 24, 1969 Signed W. R. Young

PROCESS CONTROL RECORD

PROCESS CONTROL RECORD NO.

141

Page 1 of 2

DATE 12-21-68
CONTRACT NO NAS 3-10944
SUBJECT Welding of Columbium, Tantalum, and Their Alloys by the Inert Gas Tungsten Arc Process-Specification SPPS 03-0025-00-A

PART NAME	DRAWING NUMBER	WELD NUMBER
Brayton Cycle Weld Qualification Items 11, 12, 13 and 14		

A. WELDING CHAMBER

Mfgr. VASCO

Model No. 4-608

(1) Vacuum Gage	Mfgr. NRC	Model No. 507
(2) Readout Instrument	Mfgr. NRC	Model No. 0710G425
	Serial No.	Calibration Date
(3) Chamber Vacuum	Torr Before Bakeout	
	Torr After Bakeout (Hot)	Torr After Bakeout (Cold) 8.0×10^{-6}
(4) Leak Rate	Minutes:	1 2 3 4 5 6
	Vacuum (10^{-3} Torr)	.02 .05 .08 .11 .14 .17 Overall Microns/Hr. 1.7

B. INERT GAS:

Type Helium

Supplier ~~AEC~~ AEC

(1) Inlet Analysis	H ₂ O 0.1 PPM	O ₂ 0.9 PPM
(2) Inlet Gas Analysis Equipment	Mfgr. Beckman O ₂ Trace Analyzer	Model 80
	Mfgr. Beckman Elect. Hygrometer	Model 27901

(3) Weld Chamber Analysis:

Equipment: Gas Chromatograph Mark III - MS 5A Column

SCAN NO.	TIME	ANALYSIS (PPM)				CONDITION	REMARKS
		H ₂ O	H ₂	O ₂	N ₂		
330	8:53	0.20	6.0	0.2	7.6	Weld Chamber	Prior to Weld
331	10:03	0.30	7.5	0.4	8.1	Weld Chamber	
332	11:13	0.30	8.6	0.5	10.2	Weld Chamber	
333	12:04	0.55	6.5	0.7	14.1	Weld Chamber	
334	1:18	1.30	6.2	1.0	15.3	Weld Chamber	Analysis Stopped for Day

PROCESS CONTROL RECORD (Continued)	PROCESS CONTROL RECORD NO.	
	141	Page 2 of 2

C. EQUIPMENT & PROCEDURES:

(1) Welding Equipment	Mfgr. Miller	Model No. ESR-400
	Serial No. N318048	
(2) Tungsten Electrodes	AWS-ASTM Class EWT-2, B297-55T	Size 0.062
(3) Fixtures	Material in Contact with Parts None	
	Cleanliness Verification P.A.B.	Alignment Verification P.A.B.
(4) Arc-Welding Torch	Type TEC Model 520	
	Installation Verification P.A.B.	
(5) Welding Power	DC Straight-Polarity Verification P.A.B.	
	JOINT TYPE	ARC VOLTS
	a Butt	16-17
	b Butt	16-17
	c	
	d	
(6) Filler Wire	SIZE	MCN
	a None Used	
	b None Used	
(7) Cleaning & Handling	Applicable Specification 03-0010-00-C	
	Verification of Cleaning & Handling P.A.B.	
	Record Cleaning Process Control Record No(s). P-175	
(8) Removal of Parts from Chamber	Temperature Below 400°F by Surface Pyrometer (Temp. Recorded) P.A.B.	

D. QUALITY ASSURANCE:

	BADGE NO.	INITIALS	DATE
(1) Verification that "before & after" weld specimens are attached and this record is complete.	5885	D.R.C.	4-10-67
(2) Visual inspection per SPPS 03-0025-00-A	5871	P.A.B.	12-21-68
(3) Radiographic Inspection: (a) A report similar to the attached Radiographic Test Report (NS 1271) shall be prepared and submitted to NSP Quality Assurance along with the actual X-ray films and this Welding Process Control Record.	5885	D.R.C.	2-7-67
(b) If repair was required, record new Weld Process Control Number here			
(4) Equipment & Process Qualification:	VERIFICATION OF QUALIFICATION		
Last Qualification Date	BADGE NO.	INITIALS	DATE
	5871	P.A.B.	12-20-68
Date of Last Weld to this Specification	5871	P.A.B.	12-20-68

GENERAL ELECTRICSPACE POWER & PROPULSION SECTION
CINCINNATI, OHIO 45215**RADIOGRAPHIC TEST REPORT**

(A) CONTRACT NO.

NAS 3-10944

(B) ASSEMBLY NAME & DRAWING NO.

Weld Qualification Test Piece 47D173046

(C) WELDING PROCESS CONTROL NO.

141

(D) LAB PERFORMING INSPECTION

NSP Nondestructive Testing

(E) PROGRAM NAME

Brayton Cycle Heat Receiver

(F) PERFORMING LAB NO.	(G) WELD NO.	(H) VIEW	(I) ORIG. REPAIR	(J) REMARKS (DISCREPANCY REPORT, ETC.)
	1	A	Orig.	1.25-inch OD tube
	1	B	Orig.	1.25-inch OD tube
	2	A	Orig.	1.25-inch OD tube
	2	B	Orig.	1.25-inch OD tube
	3	A	Orig.	1.25-inch OD tube
	3	B	Orig.	1.25-inch OD tube
	4	A	Orig.	0.75-inch OD tube
	4	B	Orig.	0.75-inch OD tube
	5	A	Orig.	0.75-inch OD tube
	5	B	Orig.	0.75-inch OD tube
	6	A	Orig.	0.75-inch OD tube
	6	B	Orig.	0.75-inch OD tube

The above radiographs have been reviewed and accepted per

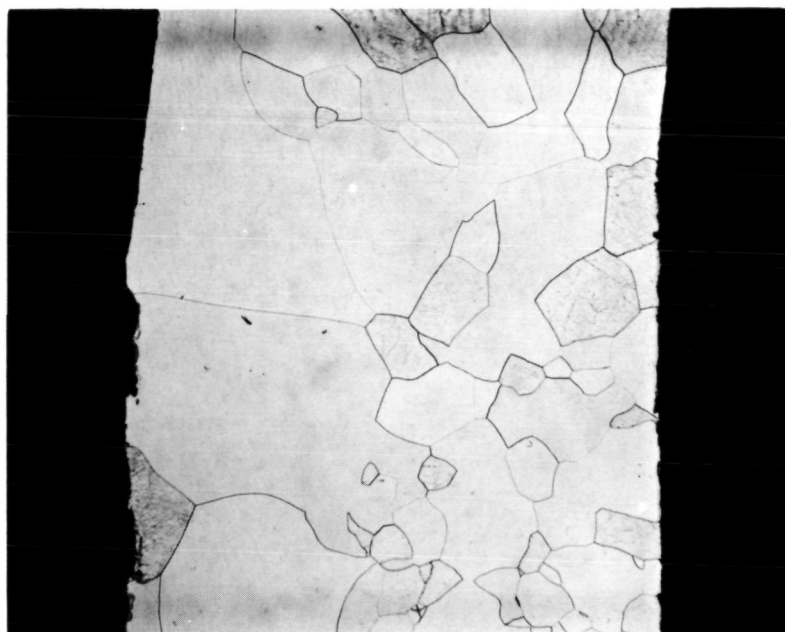
03-0025-00-A

W.H. Keane
AUTHORIZED SIGNATURE1-3-69
DATEThe above radiographs have been reviewed and accepted per
except as noted in the remarks column.

AUTHORIZED SIGNATURE

DATE

Typical Microstructure of Automatic TIG Weld of 1.25-Inch OD x
0.025-Inch Wall Cb-1Zr Alloy Tube to Reducer.



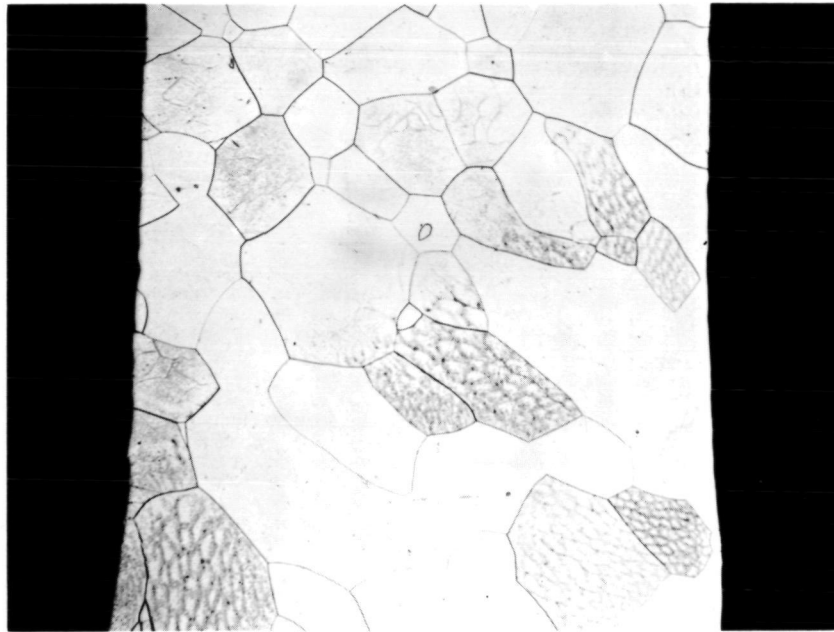
(MB 571A)

Figure C-8. Transverse Section Showing Part of Weld and HAZ of the Reducer.

Etchant: H_2SO_4 -HF- H_2O_2 - H_2O

Mag. 100x

Typical Microstructure of Automatic TIG Weld of 0.75-Inch OD x
0.025-Inch Wall Cb-1Zr Alloy Tube to Reducer.



(MB 576A)

Figure C-9. Transverse Section Showing HAZ and Parent Metal of Tube.

Etchant: H_2SO_4 -HF- H_2O_2 - H_2O

Mag. 100x

WELDING PROCEDURE QUALIFICATION TESTS

ITEM 14

Specification No. 03-0025-00-A Date 12-21-68Program Name Brayton Cycle Heat Receiver Contract No. NAS 3-10944Welding Process Automatic TIG Manual or Machine MachineWeld Joint ButtMaterial: Spec or MCN NASA C-356336 to Spec or MCN NASA C-356336Drawing No. 47R199365 P6 to Drawing No. 47B116901P1Thickness 0.025-inch wall to Thickness 0.025-inch wallFiller Metal - Spec or MCN and Diameter None Used

Welding Procedure:

Single or Multiple Pass SingleFixturing Tacked - Manual. Rotated with Brad Thompson Ind. Rotary FixturePosition of Groove HorizontalJoint Dimensions per 03-0015-00-AWelding Parameters Amps 30 Volts 16-17 RPM 5 rpmFiller Metal Feed None

Welding Atmosphere

Weld Process Control Record No. 141
(Exhibit I)

Inspection:

Radiographic Test Report (SP 1164) AcceptableMetallographic Examination Result AcceptableSection Weld 1 MB 572, MB 574Section Weld 2 MB 576, MB 578Section Weld 3 MB 580, MB 582Welder's Name J. North Badge No. 2412Test Conducted by D. R. Caldwell Lab No. 5885per 03-0025-00-AWe certify that the statements in this record are correct and that all test welds were prepared, welded, and tested in accordance with Specification 03-0025-00-ADate April 24, 1969 Signed W. R. Yew

WELDING PROCEDURE QUALIFICATION TESTS

Item 15

Specification No. 03-0025-00-A Date 6-3-69Program Name Brayton Cycle Heat Receiver Contract No. NAS 3-10944Welding Process Manual TIG Manual or Machine ManualWeld Joint SocketMaterial: Spec or MCN NASA C-356336 to Spec or MCN NASA C-356336Drawing No. 47B116899 P1 to Drawing No. 47B116898 P1Thickness 0.065" Wall to Thickness 0.065" WallFiller Metal - Spec or MCN and Diameter None Used

Welding Procedure:

Single or Multiple Pass SingleFixturing Self Aligning JointPosition of Groove HorizontalJoint Dimensions per 03-0015-00-AWelding Parameters Amps 90 Volts 18 IPM ManualFiller Metal Feed None Used

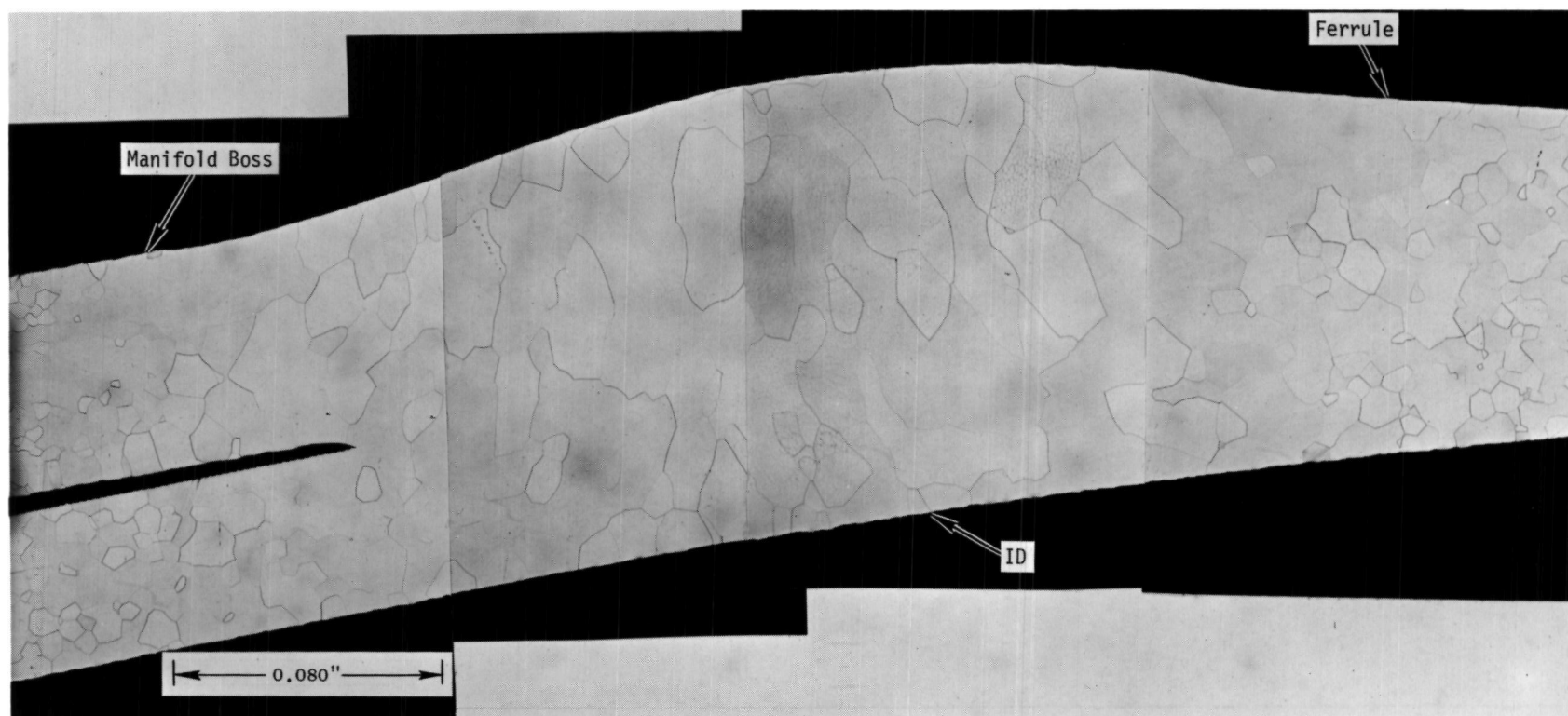
Welding Atmosphere

Weld Process Control Record No. 252
(Exhibit I)

Inspection:

Radiographic Test Report (SP 1164) AcceptableMetallographic Examination Result AcceptableSection Weld 1 MB 1125Section Weld 2 MB 1126Section Weld 3 MB 1127Welder's Name J. North Badge No. 2412Test Conducted by D. Caldwell Lab No. 5885per 03-0025-00-AWe certify that the statements in this record are correct and that all test welds were prepared, welded, and tested in accordance with Specification 03-0025-00-ADate 11-2-69 Signed W. A. Young

TYPICAL MICROSTRUCTURE OF A Cb-1Zr ALLOY GAS TUBE FERRULE TO
MANIFOLD BOSS MANUAL TIG SOCKET WELD



(MB 1127)

Figure C-10. Transverse Section Showing HAZ and Weld.

Etchant: $\text{H}_2\text{SO}_4\text{-HF-H}_2\text{O}_2\text{-H}_2\text{O}$

WELDING PROCEDURE QUALIFICATION TESTS

Item 16

Specification No. 03-0025-00-A Date 6-3-69
Program Name Brayton Cycle Heat Receiver Contract No. NAS 3-10944
Welding Process Manual TIG Manual or Machine Manual
Weld Joint Socket
Material: Spec or MCN NASA C-356336 to Spec or MCN NASA C-356336
Drawing No. 47B116900 P1 to Drawing No. 47B116898 P2
Thickness 0.062" Wall to Thickness 0.062" Wall
Filler Metal - Spec or MCN and Diameter None Used

Welding Procedure:

Single or Multiple Pass Single
Fixturing Self Aligning Joint

Position of Groove Horizontal
Joint Dimensions per 03-0015-00-A
Welding Parameters Amps 90 Volts 18 IPM Manual
Filler Metal Feed None Used

Welding Atmosphere

Weld Process Control Record No. 252
(Exhibit I)

Inspection:

Radiographic Test Report (SP 1164) Acceptable
Metallographic Examination Result Acceptable
Section Weld 1 MB 1128
Section Weld 2 MB 1129
Section Weld 3 MB 1130

Welder's Name J. North Badge No. 2412
Test Conducted by D. Caldwell Lab No. 5885
per 03-0025-00-A

We certify that the statements in this record are correct and that all test welds were prepared, welded, and tested in accordance with Specification 03-0025-00-A

Date 11-20-69 Signed W. R. Young

PROCESS CONTROL RECORD	PROCESS CONTROL RECORD NO. 252
	Page 1 of 2

DATE <div style="text-align: center;">6-3-69</div>	SUBJECT Welding of Columbium, Tantalum, and Their Alloys by the Inert Gas Tungsten Arc Process-Specification SPPS 03-0025-00-A
CONTRACT NO. <div style="text-align: center;">NAS 3-10944</div>	

PART NAME	DRAWING NUMBER	WELD NUMBER
Brayton Cycle Weld	47D173046	Items 15 and 16
Qualification		

A. WELDING CHAMBER	Mfgr. VASCO Vertical	Model No. 4-608
--------------------	---------------------------	-----------------

(1) Vacuum Gage	Mfgr. NRC	Model No. 507												
(2) Readout Instrument	Mfgr. NRC	Model No. 0710G425												
	Serial No.	Calibration Date												
(3) Chamber Vacuum	Torr Before Bakeout													
	Torr After Bakeout (Hot)	Torr After Bakeout (Cold) 6.3×10^{-6}												
(4) Leak Rate	Minutes:	<table style="display: inline-table; border-collapse: collapse;"> <tr> <td style="border: 1px solid black; width: 20px; text-align: center;">1</td> <td style="border: 1px solid black; width: 20px; text-align: center;">2</td> <td style="border: 1px solid black; width: 20px; text-align: center;">3</td> <td style="border: 1px solid black; width: 20px; text-align: center;">4</td> <td style="border: 1px solid black; width: 20px; text-align: center;">5</td> <td style="border: 1px solid black; width: 20px; text-align: center;">6</td> </tr> <tr> <td style="border: 1px solid black; text-align: center;">02</td> <td style="border: 1px solid black; text-align: center;">04</td> <td style="border: 1px solid black; text-align: center;">.06</td> <td style="border: 1px solid black; text-align: center;">08</td> <td style="border: 1px solid black; text-align: center;">10</td> <td style="border: 1px solid black; text-align: center;">.12</td> </tr> </table>	1	2	3	4	5	6	02	04	.06	08	10	.12
1	2	3	4	5	6									
02	04	.06	08	10	.12									
	Vacuum (10^{-3} Torr)	Overall Microns/Hr. 1.2												

B. INERT GAS:	Type Helium	Supplier Airco NCG
---------------	-------------	-------------------------------

(1) Inlet Analysis	H ₂ O .02 PPM	O ₂ .75 PPM
(2) Inlet Gas Analysis Equipment	Mfgr. Beckman O ₂ Trace Analyzer	Model 80
	Mfgr. Beckman Elect. Hygrometer	Model 27901

(3) Weld Chamber Analysis:	Equipment: Gas Chromatograph Mark III - MS 5A Column
----------------------------	--

SCAN NO.	TIME	ANALYSIS (PPM)				CONDITION	REMARKS
		H ₂ O	H ₂	O ₂	N ₂		
1193	9:10	0.1	3.0	2.0	4.8	Vertical Chamber	Prior to Welding
1194	9:25	1.2	3.4	1.1	2.3	Vertical Chamber	Welding
1197	12:45	1.2	9.7	1.1	2.7	Vertical Chamber	Welding Completed

PROCESS CONTROL RECORD (Continued)	PROCESS CONTROL RECORD NO.	
	252	Page 2 of 2

C. EQUIPMENT & PROCEDURES:

(1) Welding Equipment	Mfgr. Miller Electric Co.	Model No. 330 A/BP	
	Serial No. M283288		
(2) Tungsten Electrodes	AWS-ASTM Class EWT-2	Size 1/16"	
(3) Fixtures	Material in Contact with Parts Mo		
	Cleanliness Verification xx	Alignment Verification xx	
(4) Arc-Welding Torch	Type TEC (Modified)		
	Installation Verification xx		
(5) Welding Power	DC Straight-Polarity Verification xx		
	JOINT TYPE	ARC VOLTS	INPUT AMPS
	a Socket	18	90
	b		
	c		
(6) Filler Wire	SIZE	MCN	CLEANING DATE
	a None Used		
	b		
(7) Cleaning & Handling	Applicable Specification 03-0010-00-C		
	Verification of Cleaning & Handling xx		
	Record Cleaning Process Control Record No(s). P-175, P-180, P-188, P-192		
(8) Removal of Parts from Chamber	Temperature Below 400°F by Surface Pyrometer (Temp. Recorded) xx		

D. QUALITY ASSURANCE:

	BADGE NO.	INITIALS	DATE
(1) Verification that "before & after" weld specimens are attached and this record is complete.	5871	PAB	6-5-69
(2) Visual Inspection per SPPS 03-0025-00-A	5871	PAB	6-3-69
(3) Radiographic Inspection:	5871	PAB	6-5-69
(a) A report similar to the attached Radiographic Test Report (NS 1271) shall be prepared and submitted to NSP Quality Assurance along with the actual X-ray films and this Welding Process Control Record.			
(b) If repair was required, record new Weld Process Control Number here.			
(4) Equipment & Process Qualification:	VERIFICATION OF QUALIFICATION		
	BADGE NO.	INITIALS	DATE
Last Qualification Date	5871	PAB	5-27-69
Date of Last Weld to this Specification	5871	PAB	5-29-69

GENERAL ELECTRICSPACE POWER & PROPULSION SECTION
CINCINNATI, OHIO 45215**RADIOGRAPHIC TEST REPORT**

(A) CONTRACT NO.

NAS 3-10944

(B) ASSEMBLY NAME & DRAWING NO.

Weld Qualification Test Piece 47D173046

(C) WELDING PROCESS CONTROL NO.

252

(D) LAB PERFORMING INSPECTION

NSP Nondestructive Testing

(E) PROGRAM NAME

Brayton Cycle Heat Receiver

(F) PERFORMING LAB NO.	(G) WELD NO.	(H) VIEW	(I) ORIG. REPAIR	(J) REMARKS (DISCREPANCY REPORT, ETC.)
	1	A	Orig.	Item 15 - Inlet ferrule to boss
	1	B	Orig.	Item 15 - Inlet ferrule to boss
	2	A	Orig.	Item 15 - Inlet ferrule to boss
	2	B	Orig.	Item 15 - Inlet ferrule to boss
	3	A	Orig.	Item 15 - Inlet ferrule to boss
	3	B	Orig.	Item 15 - Inlet ferrule to boss
	4	A	Orig.	Item 16 - Outlet ferrule to boss
	4	B	Orig.	Item 16 - Outlet ferrule to boss
	5	A	Orig.	Item 16 - Outlet ferrule to boss
	5	B	Orig.	Item 16 - Outlet ferrule to boss
	6	A	Orig.	Item 16 - Outlet ferrule to boss
	6	B	Orig.	Item 16 - Outlet ferrule to boss

The above radiographs have been reviewed and accepted per

03-0025-00-A

AUTHORIZED SIGNATURE

6-5-69

DATE

The above radiographs have been reviewed and accepted per
except as noted in the remarks column.

AUTHORIZED SIGNATURE

DATE

WELDING PROCEDURE QUALIFICATION TESTS

Item 17

Specification No. 03-0025-00-A Date 2-12-69Program Name Brayton Cycle Heat Receiver Contract No. NAS 3-10944Welding Process Manual TIG Manual or Machine ManualWeld Joint FilletMaterial: Spec or MCN Cb-1Zr alloy material supplied by ORNL. to Spec or MCN Cb-1Zr alloy material supplied by ORNL.Drawing No. 47D173046 G1 to Drawing No. 47D173046 P8Thickness 0.125-inch to Thickness 0.125-inchFiller Metal - Spec or MCN and Diameter Cb-1Zr alloy, MCN 16A-007-01, 0.062-inch

Welding Procedure:

Single or Multiple Pass MultipleFixturing No fixture used - tacked.Position of Groove HorizontalJoint Dimensions per 03-0015-00-AWelding Parameters Amps Manual Volts Manual IPM ----Filler Metal Feed Manual

Welding Atmosphere

Weld Process Control Record No. 165
(Exhibit I)

Inspection:

Radiographic Test Report (SP 1164) Not ApplicableMetallographic Examination Result AcceptableSection Weld 1 MB 777Section Weld 2 MB 778Section Weld 3 MB 779J. North 2412Welder's Name H. Mann Badge No. 5874Test Conducted by D. Caldwell Lab No. 5885per 03-0025-00-AWe certify that the statements in this record are correct and that all test welds were prepared, welded, and tested in accordance with Specification 03-0025-00-ADate 6-13-69 Signed W. R. Young

PROCESS CONTROL RECORD

PROCESS CONTROL RECORD NO.

165

Page 1 of 2

DATE 2-12-69	SUBJECT Welding of Columbium, Tantalum, and Their Alloys by the Inert Gas Tungsten Arc Process-Specification SPPS 03-0025-00-A	
CONTRACT NO. NAS 3-10944		
PART NAME Brayton Cycle Weld	DRAWING NUMBER 47D173046	WELD NUMBER Items 17 & 18
Qualification		

A. WELDING CHAMBER

Mfgr. VASCO Verticle

Model No. 4-608

(1) Vacuum Gage	Mfgr. NRC	Model No. 507
(2) Readout Instrument	Mfgr. NRC	Model No. 0710G425
	Serial No.	Calibration Date
(3) Chamber Vacuum	Torr Before Bakeout	
	Torr After Bakeout (Hot)	Torr After Bakeout (Cold)
(4) Leak Rate	Minutes:	1 2 3 4 5 6
	Vacuum (10^{-3} Torr)	.03 .06 .08 .10 .13 .15 Overall Microns/Hr. 1.5

B. INERT GAS:

Type Helium

Supplier ~~Airco~~ AEC

(1) Inlet Analysis	H ₂ O 5.5 PPM	O ₂ 2.2 PPM
(2) Inlet Gas Analysis Equipment	Mfgr. Beckman O ₂ Trace Analyzer	Model 80
	Mfgr. Beckman Elect. Hygrometer	Model 27901

(3) Weld Chamber Analysis:

Equipment: Gas Chromatograph Mark III - MS 5A Column

SCAN NO.	TIME	ANALYSIS (PPM)				CONDITION	REMARKS
		H ₂ O	H ₂	O ₂	N ₂		
544	10:50	0.11	11	0.62	4.4	Vertical Chamber	Gloves Open
545	12:30	0.86	8.8	1.1	5.7	Vertical Chamber	Welding
546	1:20	2.95	8.7	0.73	0.96	Vertical Chamber	Welding
547	2:25	5.30	8.1	0.97	0.96	Vertical Chamber	Welding
548	3:30	7.00	7.5	1.3	9.2	Vertical Chamber	Welding
549	4:35	8.30	7.8	2.5	14	Vertical Chamber	Welding
550	5:40	9.20	7.3	2.4	17	Vertical Chamber	Welding Complete

PROCESS CONTROL RECORD (Continued)	PROCESS CONTROL RECORD NO.	
	165	Page 2 of 2

C. EQUIPMENT & PROCEDURES:

(1) Welding Equipment	Mfgr. Miller	Model No. ESR-400	
	Serial No. N318048		
(2) Tungsten Electrodes	AWS-ASTM Class EWT _h , B297-55T		Size 0.093-inch
(3) Fixtures	Material in Contact with Parts Molybdenum		
	Cleanliness Verification P.A.B.	Alignment Verification P.A.B.	
(4) Arc-Welding Torch	Type TEC Model 520		
	Installation Verification P.A.B.		
(5) Welding Power	DC Straight-Polarity Verification P.A.B.		
	JOINT TYPE		ARC VOLTS
	a	Fillet	Manual
	b	Fillet	Manual
	c		
	d		
(6) Filler Wire	SIZE		MCN
	a	0.062	16A-007-01
	b		
(7) Cleaning & Handling	Applicable Specification 03-0010-00-C		
	Verification of Cleaning & Handling P.A.B.		
	Record Cleaning Process Control Record No(s). P-180		
(8) Removal of Parts from Chamber	Temperature Below 400°F by Surface Pyrometer (Temp. Recorded) P.A.B.		

D. QUALITY ASSURANCE:

(1) Verification that "before & after" weld specimens are attached and this record is complete.	BADGE NO.	INITIALS	DATE
	5871	P.A.B.	2-13-69
(2) Visual inspection per SPPS 03-0025-00-A	5871	P.A.B.	2-12-69
(3) Radiographic Inspection. (a) A report similar to the attached Radiographic Test Report (NS 1271) shall be prepared and submitted to NSP Quality Assurance along with the actual X-ray films and this Welding Process Control Record.	Radiographic Inspection Not Applicable to These Welds.		
(b) If repair was required, record new Weld Process Control Number here.			
(4) Equipment & Process Qualification: Last Qualification Date Date of Last Weld to this Specification	VERIFICATION OF QUALIFICATION		
	BADGE NO.	INITIALS	DATE
	5871	P.A.B.	2-11-69
	5871	P.A.B.	2-11-69

Typical Microstructure of a Manual TIG Fillet
Weld of a 3-Inch Dia. x 0.125-Inch Wall
Cb-1Zr Alloy Tube to a 6-Inch Dia. x 0.125-
Inch Wall Cb-1Zr Alloy Manifold.

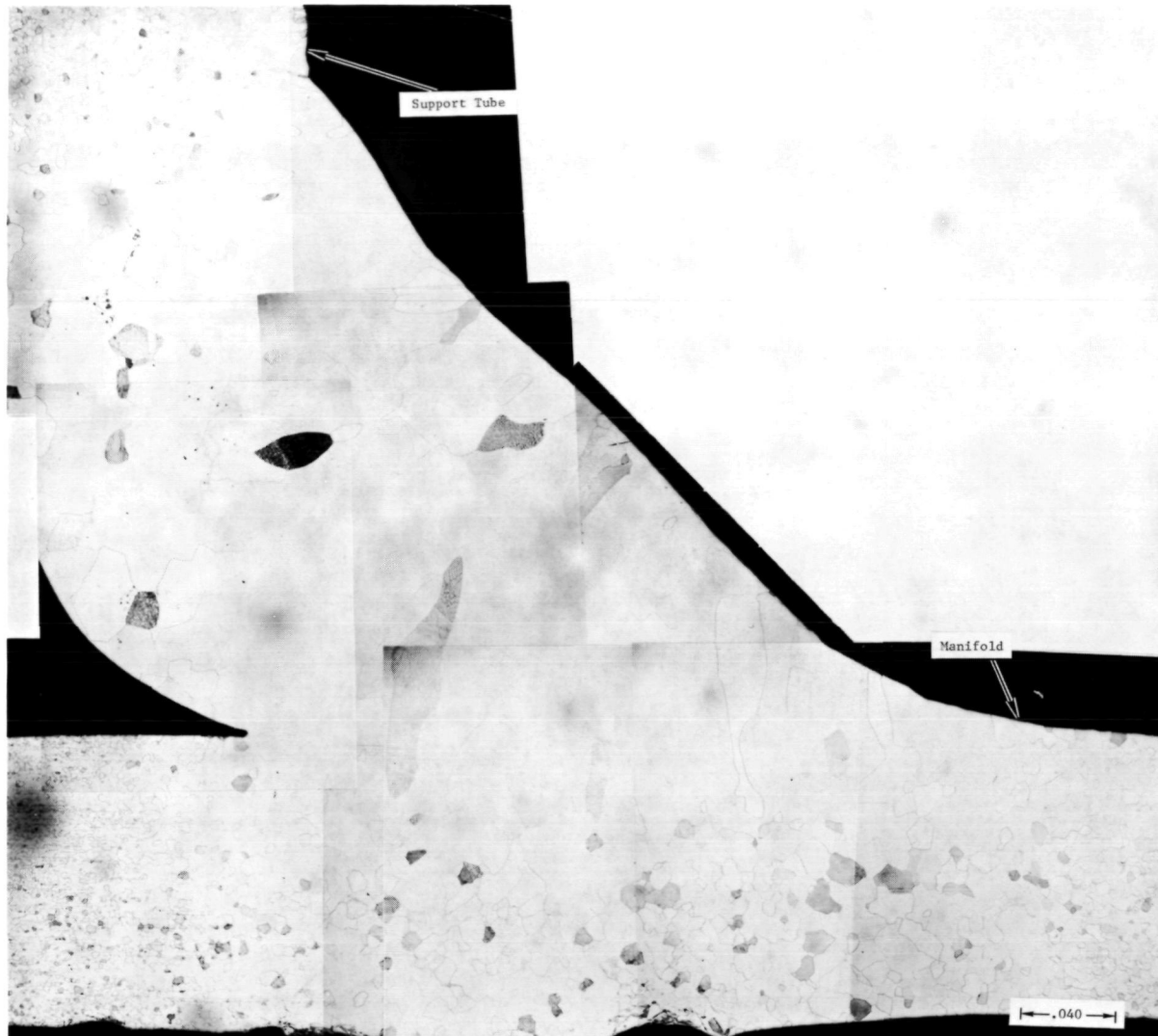


Figure C-11. Transverse Section of Weld. (MB 779)

Etchant: $\text{H}_2\text{SO}_4\text{-HF-H}_2\text{O}_2\text{-H}_2\text{O}$

WELDING PROCEDURE QUALIFICATION TESTS

Item 18 (Flange to Tube)

Specification No. 03-0025-00-A Date 2-12-69Program Name Brayton Cycle Heat Receiver Contract No. NAS 3-10944Welding Process Manual TIG Manual or Machine ManualWeld Joint FilletMaterial: Spec or MCN Cb-1Zr Alloy Material to Spec or MCN Cb-1Zr Alloy Material
Supplied by ORNL Supplied by ORNLDrawing No. 47D173046 P9 to Drawing No. 47B116945 P1Thickness 0.250" to Thickness 0.125" WallFiller Metal - Spec or MCN and Diameter 16A-007-01 0.062" Diameter

Welding Procedure:

Single or Multiple Pass MultipleFixturing Self Aligning JointPosition of Groove HorizontalJoint Dimensions per 03-0015-00-AWelding Parameters Amps 240 Volts 20 IPM ManualFiller Metal Feed Manual

Welding Atmosphere

Weld Process Control Record No. 165
(Exhibit I)

Inspection:

Radiographic Test Report (SP 1164) Radiographic Inspection Not Applicable toMetallographic Examination These Welds
Result AcceptableSection Weld 1 MB 1131Section Weld 2 MB 1132Section Weld 3 MB 1133Welder's Name H. Mann Badge No. 5874Test Conducted by D. Caldwell Lab No. 5885per 03-0025-00-AWe certify that the statements in this record are correct and that all test welds were prepared, welded, and tested in accordance with Specification 03-0025-00-ADate 11-20-69 Signed H. R. Young

PROCESS CONTROL RECORD							PROCESS CONTROL RECORD NO.		
							165		
							Page 1 of 2		
DATE 2-12-69			SUBJECT Welding of Columbium, Tantalum, and Their Alloys by the Inert Gas Tungsten Arc Process-Specification SPPS 03-0025-00-A						
CONTRACT NO NAS 3-10944									
PART NAME			DRAWING NUMBER				WELD NUMBER		
Brayton Cycle Weld			47D 173046				Items 17 & 18		
Qualification									
A. WELDING CHAMBER			Mfgr. VASCO Vertical				Model No. 4-608		
(1) Vacuum Gage			Mfgr. NRC				Model No. 507		
(2) Readout Instrument			Mfgr. NRC				Model No. 0710G425		
			Serial No.				Calibration Date		
(3) Chamber Vacuum			Torr Before Bakeout						
			Torr After Bakeout (Hot)				Torr After Bakeout (Cold) 7×10^{-6}		
(4) Leak Rate			Minutes:	1	2	3	4	5	6
			Vacuum (10^{-3} Torr)	.03	.06	.08	.10	.13	.15
							Overall Microns/Hr. 1.5		
B. INERT GAS:			Type Helium				Supplier APC AEC		
(1) Inlet Analysis			H ₂ O 5.5 PPM				O ₂ 2.2 PPM		
(2) Inlet Gas Analysis Equipment			Mfgr. Beckman O ₂ Trace Analyzer				Model 80		
			Mfgr. Beckman Elect. Hygrometer				Model 27901		
(3) Weld Chamber Analysis:			Equipment: Gas Chromatograph Mark III - MS 5A Column						
SCAN NO.	TIME	ANALYSIS (PPM)				CONDITION	REMARKS		
		H ₂ O	H ₂	O ₂	N ₂				
544	10:50	0.11	11	0.62	4.4	Vertical Chamber	Gloves Open		
545	12:30	0.86	8.8	1.1	5.7	Vertical Chamber	Welding		
546	1:20	2.95	8.7	0.73	9.6	Vertical Chamber	Welding		
547	2:25	5.30	8.1	0.97	9.6	Vertical Chamber	Welding		
548	3:30	7.00	7.5	1.3	9.2	Vertical Chamber	Welding		
549	4:35	8.30	7.8	2.5	14	Vertical Chamber	Welding		
550	5:40	9.20	7.3	2.4	17	Vertical Chamber	Welding Completed		

PROCESS CONTROL RECORD (Continued)	PROCESS CONTROL RECORD NO.	
	165	Page 2 of 2

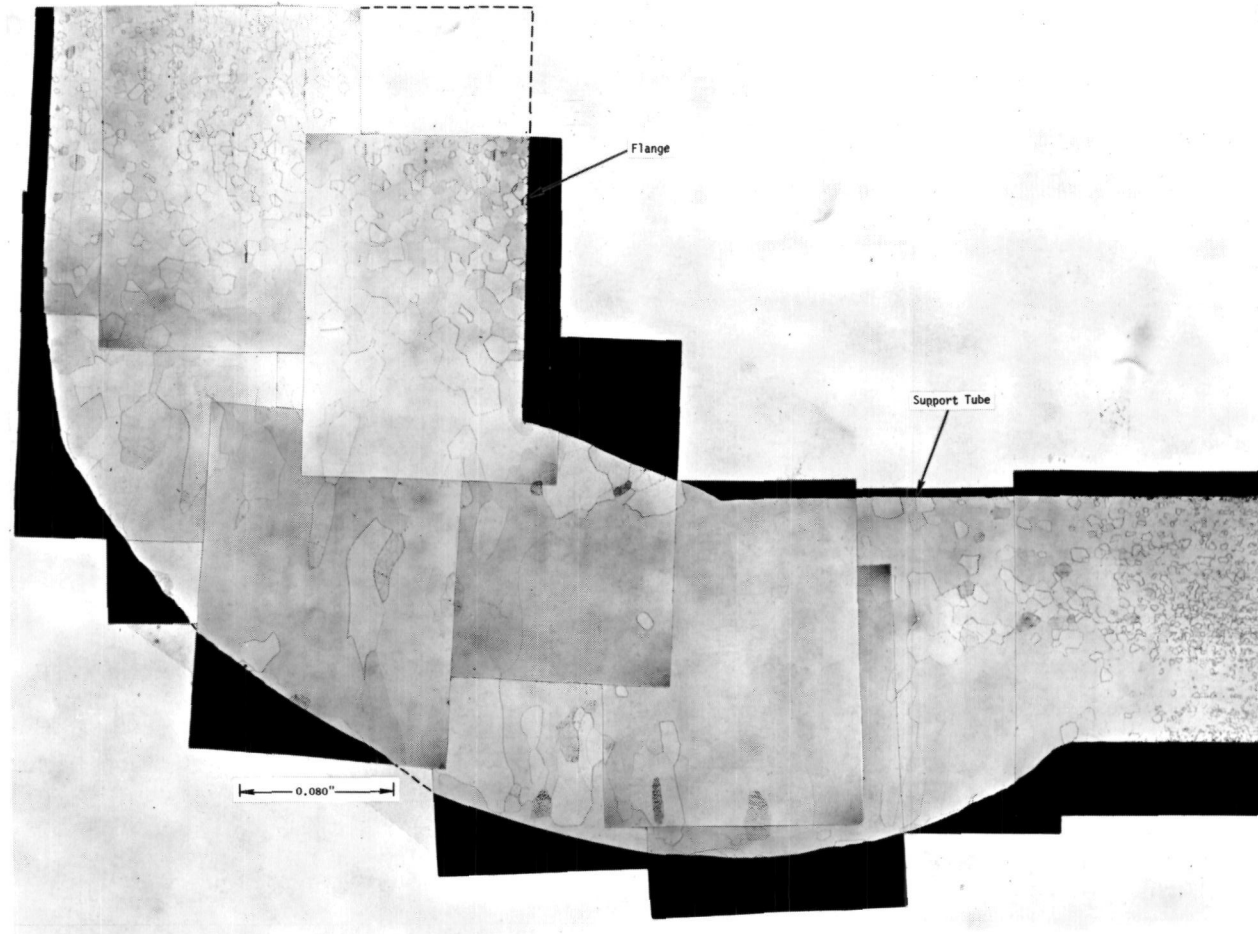
C. EQUIPMENT & PROCEDURES:

(1) Welding Equipment	Mfgr. Miller	Model No. ESR-400	
	Serial No. N 318048		
(2) Tungsten Electrodes	AWS-ASTM Class EWT-2	Size 3/32"	
(3) Fixtures	Material in Contact with Parts Mo		
	Cleanliness Verification xx	Alignment Verification xx	
(4) Arc-Welding Torch	Type TEC (Modified)		
	Installation Verification xx		
(5) Welding Power	DC Straight-Polarity Verification		
	JOINT TYPE		ARC VOLTS
			INPUT AMPS
	a	Fillet	20
	b		240
	c		
	d		
(6) Filler Wire	SIZE	MCN	CLEANING DATE
	a 0.062	16A-007-01	12-10-68
	b		
(7) Cleaning & Handling	Applicable Specification 03-0010-00-C		
	Verification of Cleaning & Handling xx		
	Record Cleaning Process Control Record No(s). P-175, P-180		
(8) Removal of Parts from Chamber	Temperature Below 400°F by Surface Pyrometer (Temp. Recorded) xx		

D. QUALITY ASSURANCE:

(1) Verification that "before & after" weld specimens are attached and this record is complete.	BADGE NO.	INITIALS	DATE
	5871	PAB	2-13-69
(2) Visual inspection per SPPS 03-0025-00-A	5871	PAB	2-12-69
(3) Radiographic Inspection: (a) A report similar to the attached Radiographic Test Report (NS 1271) shall be prepared and submitted to NSP Quality Assurance along with the actual X-ray films and this Welding Process Control Record.	Radiographic Inspection Not Applicable To These Welds		
(b) If repair was required, record new Weld Process Control Number here.			
(4) Equipment & Process Qualification: Last Qualification Date Date of Last Weld to this Specification	VERIFICATION OF QUALIFICATION		
	BADGE NO.	INITIALS	DATE
	5871	PAB	2-11-69
	5871	PAB	2-11-69

TYPICAL MICROSTRUCTURE OF A Cb-1Zr ALLOY FLANGE TO SUPPORT
TUBE MANUAL TIG FILLET WELD



(MB 1131)

Figure C-12. Transverse Section Showing Parent Metal, HAZ and Weld.

Etchant: $\text{H}_2\text{SO}_4\text{-HF-H}_2\text{O}_2\text{-H}_2\text{O}$

WELDING PROCEDURE QUALIFICATION TESTS

Item 18A

Specification No. 03-0025-00-A Date 2-12-69Program Name Brayton Cycle Heat Receiver Contract No. NAS 3-10944Welding Process Manual TIG Manual or Machine ManualWeld Joint FilletMaterial: Spec or MCN Cb-1Zr alloy material supplied by ORNL. to Spec or MCN Cb-1Zr alloy material supplied by ORNL.Drawing No. 47D173046 G1 to Drawing No. 47B116945 P1Thickness 0.125-inch to Thickness 0.125-inchFiller Metal - Spec or MCN and Diameter Cb-1Zr alloy, MCN 16A-007-01, 0.062-inch

Welding Procedure:

Single or Multiple Pass MultipleFixturing No fixture used - tackPosition of Groove HorizontalJoint Dimensions per 03-0015-00-AWelding Parameters Amps Manual Volts Manual IPM ----Filler Metal Feed Manual

Welding Atmosphere

Weld Process Control Record No. 165
(Exhibit I)

Inspection:

Radiographic Test Report (SP 1164) Not ApplicableMetallographic Examination Result AcceptableSection Weld 1 MB 780Section Weld 2 MB 781Section Weld 3 MB 782Welder's Name J. North Badge No. 2412
H. Mann 5874Test Conducted by D. Caldwell Lab No. 5885per 03-0025-00-AWe certify that the statements in this record are correct and that all test welds were prepared, welded, and tested in accordance with Specification 03-0025-00-ADate 6-13-69 Signed W.R. Young

Typical Microstructure of a Manual TIG Fillet
Weld of a 3-Inch Dia. x 0.125-Inch Wall
Cb-1Zr Alloy Support Tube to a 6-Inch
Dia. x 0.125-Inch Wall Cb-1Zr Alloy Manifold



Figure C-13. **Transverse Section of Weld.** (MB 781)

Etchant: $\text{H}_2\text{SO}_4\text{-HF-H}_2\text{O}_2\text{-H}_2\text{O}$

WELDING PROCEDURE QUALIFICATION TESTS

Item 19

Specification No. 03-0025-00-A Date 5-27-69
Program Name Brayton Cycle Heat Receiver Contract No. NAS 3-10944
Welding Process Manual TIG Manual or Machine Manual
Weld Joint Lap
Material: Spec or MCN Spec. 01-0052-00-C to Spec or MCN Cb-12r Alloy Material Supplied by ORNL
Drawing No. P47D174871 to Drawing No. 47D173046 G1
Thickness 0.125" to Thickness 0.125"
Filler Metal - Spec or MCN and Diameter None Used

Welding Procedure:

Single or Multiple Pass Single
Fixturing Tacked - Manual
Position of Groove Horizontal
Joint Dimensions per 03-0015-00-A
Welding Parameters Amps 225-275 Volts 20-22 IPM Manual
Filler Metal Feed None Used

Welding Atmosphere

Weld Process Control Record No. 248
(Exhibit I)

Inspection:

Radiographic Test Report (SP 1164) Radiographic Inspection Not Applicable To
Metallographic Examination These Welds Result Acceptable
Section Weld 1 MB 1134
Section Weld 2 MB 1135
Section Weld 3 MB 1136

Welder's Name H. Mann Badge No. 5874
Test Conducted by D. Caldwell Lab No. 5885
per 03-0025-00-A

We certify that the statements in this record are correct and that all test welds were prepared, welded, and tested in accordance with Specification 03-0025-00-A

Date 5-26-69 Signed [Signature]

PROCESS CONTROL RECORD	PROCESS CONTROL RECORD NO. 248
	Page 1 of 2

DATE 5-27-69	SUBJECT Welding of Columbium, Tantalum, and Their Alloys by the Inert Gas Tungsten Arc Process-Specification SPPS 03-0025-00-A
CONTRACT NO NAS 3-10944	

PART NAME	DRAWING NUMBER	WELD NUMBER
Brayton Cycle Weld	47D 173046	Item 19 - Support
Qualification		Ring

A. WELDING CHAMBER		Mfr. VASCO	Vertical	Model No. 4-608				
(1) Vacuum Gage	Mfr. NRC	Model No. 507						
(2) Readout Instrument	Mfr. NRC	Model No. 0710G425						
	Serial No.	Calibration Date						
(3) Chamber Vacuum	Torr Before Bakeout							
	Torr After Bakeout (Hot)		Torr After Bakeout (Cold) 3×10^{-6}					
(4) Leak Rate	Minutes:	1	2	3	4	5	6	
	Vacuum (10^{-3} Torr)	.03	.06	.08	.10	.13	.15	Overall Microns/Hr. 1.5

B. INERT GAS:		Type Helium	Supplier WATCO NCG
(1) Inlet Analysis	H ₂ O 0.2 PPM	O ₂ 0.75 PPM	
(2) Inlet Gas Analysis Equipment	Mfr. Beckman O ₂ Trace Analyzer	Model 80	
	Mfr. Beckman Elect. Hygrometer	Model 27901	

(3) Weld Chamber Analysis:		Equipment: Gas Chromatograph Mark III - MS 5A Column					
SCAN NO.	TIME	ANALYSIS (PPM)				CONDITION	REMARKS
		H ₂ O	H ₂	O ₂	N ₂		
1167	1:15		9.7	3.2	8.1	Vertical Chamber	Prior to Welding
1168	1:30		9.7	0.9	1.5	Vertical Chamber	Welding
1169	3:00		9.4	0.9	1.9	Vertical Chamber	Welding
1170	3:45		8.6	0.4	1.5	Vertical Chamber	Welding Complete

PROCESS CONTROL RECORD <i>(Continued)</i>	PROCESS CONTROL RECORD NO. 248	Page 2 of 2
---	---------------------------------------	-------------

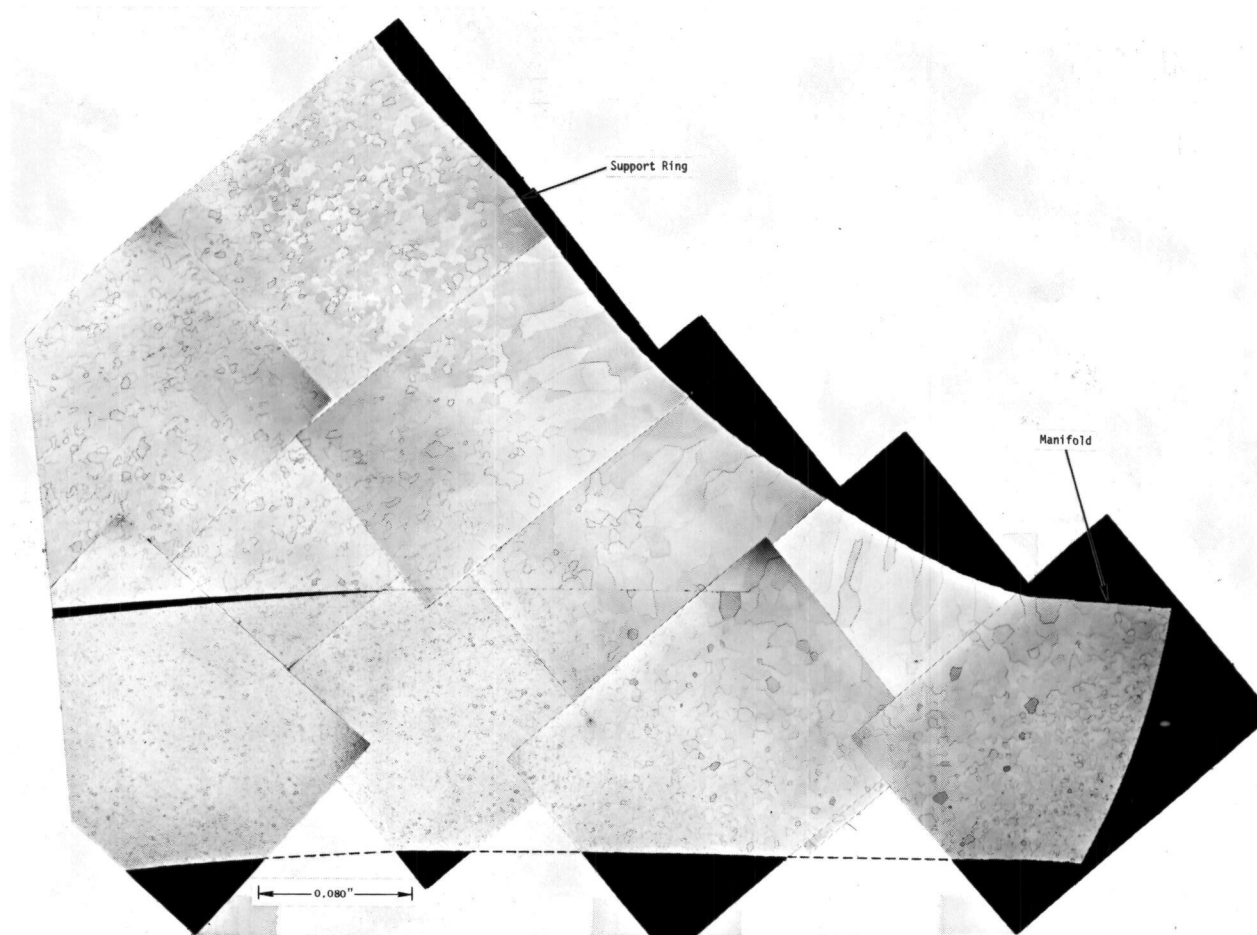
C. EQUIPMENT & PROCEDURES:

(1) Welding Equipment	Mfr. Miller Electric Company	Model No. ESR-400
	Serial No. N 318048	
(2) Tungsten Electrodes	AWS-ASTM Class EWT-2	Size 1/8"
(3) Fixtures	Material in Contact with Parts Mo	
	Cleanliness Verification xx	Alignment Verification xx
(4) Arc-Welding Torch	Type TEC (Modified)	
	Installation Verification xx	
(5) Welding Power	DC Straight-Polarity Verification xx	
	JOINT TYPE	ARC VOLTS
	a Lap	20-22
	b	
	c	
	d	
(6) Filler Wire	SIZE	MCN
	a None Used	
	b	
(7) Cleaning & Handling	Applicable Specification 03-0010-00-C	
	Verification of Cleaning & Handling xx	
	Record Cleaning Process Control Record No(s). P-175, P-180, P-188	
(8) Removal of Parts from Chamber	Temperature Below 400°F by Surface Pyrometer (Temp. Recorded) xx	

D. QUALITY ASSURANCE:

(1) Verification that "before & after" weld specimens are attached and this record is complete.	BADGE NO.	INITIALS	DATE
	5871	PAB	5-28-69
(2) Visual inspection per SPPS 03-0025-00-A	5871	PAB	5-27-69
(3) Radiographic Inspection:	Radiographic Inspection Not Applicable To This Weld		
(a) A report similar to the attached Radiographic Test Report (NS 1271) shall be prepared and submitted to NSP Quality Assurance along with the actual X-ray films and this Welding Process Control Record.			
(b) If repair was required, record new Weld Process Control Number here			
(4) Equipment & Process Qualification:	VERIFICATION OF QUALIFICATION		
	BADGE NO.	INITIALS	DATE
Last Qualification Date	5871	PAB	5-7-69
Date of Last Weld to this Specification	5871	PAB	5-26-69

TYPICAL MICROSTRUCTURE OF A Cb-1Zr ALLOY SHELL SUPPORT RING TO
MANIFOLD MANUAL TIG LAP WELD



(MB 1134)

Figure C-14. Transverse Section Showing Parent Metal, HAZ and Weld.

Etchant: H_2SO_4 -HF- H_2O_2 - H_2O

Page intentionally left blank

APPENDIX D

DISCREPANCY REPORT - POSTWELD ANNEAL OF
BRAYTON CYCLE OUTLET MANIFOLD, GIRTH WELD NO. 1

Page intentionally left blank

SUBJECT: DISCREPANCY REPORT
POSTWELD ANNEAL OF BRAYTON CYCLE
OUTLET MANIFOLD, GIRTH WELD NO. 1

August 11, 1969

At approximately 11:25 am on 7-29-69, the subject vacuum anneal was aborted when a pressure surge was noted. At that time, the weld area of the manifold had been at 2200°F for 55 minutes of the 60-minute anneal cycle.

The operator immediately shut off all electrical power to the heater. One to two minutes later the leak had been detected and sealed. After this temporary seal pressure, readout was 2×10^{-4} torr, and the part temperature had dropped to approximately 1600°F. Two minutes later, pressure had increased to 0.1 torr and temperature decreased to 1250°F. Six minutes later at a temperature of 900°F, helium was introduced into the chamber cooling the part to below 400°F in 20 minutes.

Cause of Failure

The air leak occurred in plastic tubing which is used to connect the sealed motor housing on the weld fixture to a vacuum feedthrough. Apparently this tubing, although over four feet away from the annealing furnace, was softened and failed as a result of the radiant heat from the annealing furnace.

Corrective Action

The entire motor housing and associated tubing were removed from the vacuum chamber, a practice to be followed on all future anneals.

Postanneal Evaluation

The results of the various tests and analyses performed to determine the condition of the manifold after Anneal No. 1 indicated that the amount of contamination was at most superficial. Apparently the protective tantalum foil wrapped over the manifold had intercepted much of the atmospheric contamination.

Visual inspection of the manifold after exposure revealed that the area in the optical path of the gas (girth weld inner) had a brown-black continuous scale. The ID of the manifold as indicated by borescope inspection did not contain the brown-black scale as noted on the OD except on the ID surfaces of the bosses which will be subsequently machined. Also, the 30-mil (0.030") thick control specimen which was in the furnace at the same temperature of the manifold at the time of exposure contained the brown-black scale. This specimen was available for chemical analysis, microhardness, and metallographic evaluation. The depth of penetration of contaminants in the control specimen should be the same as the manifold.

The results of the comparative impurity analyses of the exposed Cb-1Zr control 30-mil (0.030") sheet specimen and the impurity analysis of the control specimen in the as-received condition are summarized in Table D1. The significant fact is that upon removal of one mil (0.001") of material from both surfaces of the exposed specimen the oxygen and nitrogen content dropped almost to their original "as-received" values.

To completely document the hardness of the control specimen near the surface a very light microhardness load (10 gm) was used, and the specimen was mounted with a 30° tilt. A hardness of DPH 125 was found one-half mil (0.0005") below the surface. The hardness numbers between one and ten mils (0.001"-0.010") ranged between 52 and 90 DPH which was representative of the bulk hardness. The scatter in the data is attributed to the light microhardness load used which is quite sensitive to surface condition of the specimen, the difficulty in reading the small penetrations accurately, and the microstructure, i.e., the interception of grain boundaries.

Examination of the microstructure of the exposed control specimen at magnification up to 500x revealed no continuous surface oxide formation and evidence of grain boundary penetration only one grain deep (0.0004"). Figure D1 shows the microstructure at 100x; the quality of higher magnification photomicrographs was questionable due to the slightly rounded edge of the specimen.

The results of the comparative hardness evaluation of the actual manifold after Anneal No. 1 and Anneal No. 2 are summarized in Table D2. Anneal No. 2 was successfully performed without incident. The hardness data represents impressions made in the discolored areas in the region of the girth weld annealed in Anneal No. 1 (inner surface of the manifold and shell ring) and the outer surface of the manifold which was not in the optical path of the gas leak. These results are compared to data obtained from similar areas in the region of the girth weld in Anneal No. 2. There is essentially no difference in the hardness levels in these two areas; probably, the minimal differences seen can be attributed


to scatter. The hardness tests were performed with a portable Wilson hardness test machine with a 60 Kg load (Rockwell A scale), the lightest load available. Apparently, even this light load makes an impression that is too deep in the soft Cb-1Zr to be sensitive to the minimal amount of contamination of the surface.

As can be seen from Table D2, the data indicated uniform hardness of the shell ring in the discolored area; 3 mils (0.003") of material was removed with hardness impressions made at mil (0.001") intervals.

Review of the various results given above indicated that the contamination of the manifold is confined less than 1/2 mil (0.0005") below the surface. The discolored areas are probably associated with deposits from the tungsten elements since the microstructure shows no oxide film and no significant depth of penetration beneath these areas.

Manifold Rework

Based on the above results, it was recommended that mechanical removal of the surface contamination, followed by acid cleaning be employed. With NASA concurrence, belt sanders were used to remove most of the contaminated surface area. Hand polishing with abrasive paper was used to complete the mechanical cleaning. The outside of the manifold was then acid cleaned and rinsed. Careful visual inspection indicated complete removal of the contaminated surface.


W. R. Young, Manager
Advanced Joining

cak

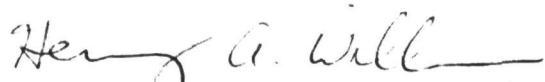

Postanneal Evaluation Performed
by Hervey A. Williams

TABLE D1
 IMPURITY ANALYSES OF Cb-1Zr SHEET SPECIMENS*
 FROM MANIFOLD ANNEAL NO. 1

	Chemical Analysis, ppm		
	<u>As Received</u>	<u>Annealed, Foil Wrapped</u>	<u>Annealed, Foil Wrapped, 1 Mil Removed from Each Surface</u>
O	160, 164	237, 274	176
N	27, 28	192, 219	54
H	< 1	< 1	
C	80, 81	100	

* Specimen thickness, 0.030"

TABLE D2

HARDNESS EVALUATION OF Cb-1Zr MANIFOLD
AND CONTROL SHEET SPECIMEN AFTER ANNEALS NOS. 1 & 2

Girth Weld Anneal No. 1			Girth Weld Anneal No. 2	
Manifold (ID)	Manifold (OD)	Shell Ring (ID)	Manifold (ID)	Shell Ring (ID)
R_A^*	R_A	R_A	R_A	R_A
32	34	30	30	31
33	32	29	32	33

Shell Ring (Anneal No. 1)

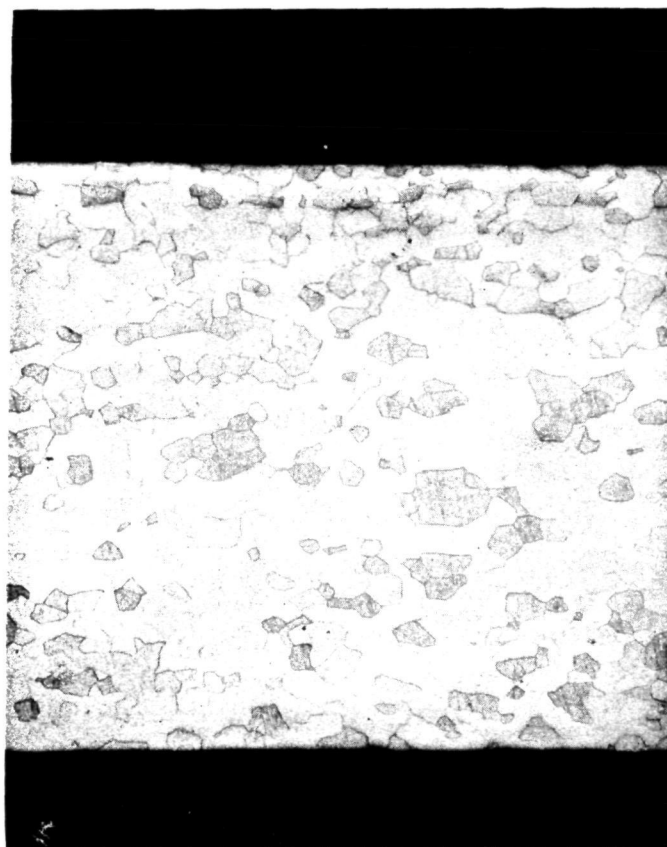
<u>Amount of Material Removed from Surface</u>	<u>Hardness R_A</u>
-0-	30
0.001	30
0.002	31.5
0.003	30

Cb-1Zr Control Sheet Specimen (0.030")

<u>As Received</u>		<u>Annealed</u>
#1	#2	<u>Manifold (Anneal No. 1)</u>
R_A	R_A	R_A
31	29	32
30	29.5	35

* R_A 29 = 79 DPH

R_A 34 = 89 DPH



(MB 1157)

Figure D1. Microstructure of Cb-1Zr Exposed Control Sheet (0.030") Specimen. Note No Significant Oxide Film or Penetration.

Etched: 1 part H_2O + 1 part H_2SO_4
1 part 30% H_2O_2 + 1 part Hf

Mag.: 100x

FINAL REPORT DISTRIBUTION LIST

NAS 3-10944

NASA
Lewis Research Center
21000 Brookpark Road
Cleveland, Ohio 44135
Attn: H. M. Cameron, MS 500-201
(5 + Repro)

NASA
Lewis Research Center
21000 Brookpark Road
Cleveland, Ohio 44135
Attn: Brayton Project Office, (25)
MS 500-201

NASA
Lewis Research Center
21000 Brookpark Road
Cleveland, Ohio 44135
Attn: H. O. Slone, MS 500-201

NASA
Lewis Research Center
21000 Brookpark Road
Cleveland, Ohio 44135
Attn: D. R. Packe, MS 500-201

NASA
Lewis Research Center
21000 Brookpark Road
Cleveland, Ohio 44135
Attn: R. E. English, MS 500-201

NASA
Lewis Research Center
21000 Brookpark Road
Cleveland, Ohio 44135
Attn: G. M. Ault, MS 3-13

NASA
Lewis Research Center
21000 Brookpark Road
Cleveland, Ohio 44135
Attn: H. Hinckley, MS 500-309

NASA
Lewis Research Center
21000 Brookpark Road
Cleveland, Ohio 44135
Attn: D. G. Beremand, MS 500-201

NASA
Lewis Research Center
21000 Brookpark Road
Cleveland, Ohio 44135
Attn: W. T. Wintucky, MS 500-201

NASA
Lewis Research Center
21000 Brookpark Road
Cleveland, Ohio 44135
Attn: P. A. Thollot, MS 500-201

NASA
Lewis Research Center
21000 Brookpark Road
Cleveland, Ohio 44135
Attn: A. S. Valerino, MS 500-202

NASA
Lewis Research Center
21000 Brookpark Road
Cleveland, Ohio 44135
Attn: V. Hlavin, MS 3-10

NASA
Lewis Research Center
21000 Brookpark Road
Cleveland, Ohio 44135
Attn: W. L. Stewart, MS 77-2

NASA
Lewis Research Center
21000 Brookpark Road
Cleveland, Ohio 44135
Attn: Library, MS 60-3

NASA
Lewis Research Center
21000 Brookpark Road
Cleveland, Ohio 44135
Attn: Report Control Office, MS 5-5

NASA
Lewis Research Center
21000 Brookpark Road
Cleveland, Ohio 44135
Attn: Reliability & Quality
Assurance Office, MS 500-111

FINAL REPORT DISTRIBUTION LIST - NAS 3-10944 - Page 2

NASA
Lewis Research Center
21000 Brookpark Road
Cleveland, Ohio 44135
Attn: Technology Utilization
Office, MS 3-19

NASA
Lewis Research Center
Plum Brook Station
Taylor Road
Sandusky, Ohio 44870
Attn: J. C. Nettles, MS 1441-1 (2)

NASA
Washington, D.C. 20546
Attn: P. R. Miller, Code RNP

NASA
Washington, D.C. 20546
Attn: H. D. Rothen, Code RNP

NASA
Scientific & Tech. Info. Facility
Post Office Box 5700
College Park, Maryland 20740
Attn: Acquisitions Branch
(SQT-34054)

NASA
Ames Research Center
Moffett Field, California 94035
Attn: Library

NASA
Flight Research Center
Post Office Box 273
Edwards, California 93523
Attn: Library

NASA
Goddard Space Flight Center
Greenbelt, Maryland 20771
Attn: Library

Jet Propulsion Laboratory
4800 Oak Grove Drive
Pasadena, California 91103
Attn: Library

NASA
Langley Research Center
Langley Station
Hampton, Virginia 23365
Attn: Library

NASA
Manned Spacecraft Center
Houston, Texas 77058
Attn: Library

NASA
Manned Spacecraft Center
Houston, Texas 77058
Attn: A. Redding, EP-5

NASA
Marshall Space Flight Center
Marshall Space Flight Center, Alabama 35812
Attn: Library

Aerojet-General Corporation
1100 West Hollyvale
Azusa, California 91702
Attn: Library

Aerospace Corporation
Post Office Box 95085
Los Angeles, California 91745
Attn: Library

AiResearch Manufacturing Company
402 South 36 Street
Phoenix, Arizona 85034
Attn: Library

AiResearch Manufacturing Company
402 South 36 Street
Phoenix, Arizona 85034
Attn: Lyle Six

AiResearch Manufacturing Company
9851 Sepulveda Boulevard
Los Angeles, California 90009
Attn: Library

AiResearch Manufacturing Company
2525 W. 190 Street
Torrance, California 90509
Attn: Library

FINAL REPORT DISTRIBUTION LIST - NAS 3-10944 - Page 3

Battelle Memorial Institute
505 King Avenue
Columbus, Ohio 43201
Attn: Library

Bendix Research Labs Division
Detroit, Michigan 48232
Attn: Library

Boeing Company
Aerospace Division
Post Office Box 3707
Seattle, Washington 98124
Attn: Library

Borg-Warner Corporation
Pesco Products Division
24700 North Miles Road
Bedford, Ohio 44146
Attn: Library

Bureau of Naval Weapons
Department of the Navy
Washington, D.C. 20025
Attn: Code RAPP

Continental Aviation and
Engineering Corporation
12700 Kercheval Avenue
Detroit, Michigan 48215
Attn: Library

Curtiss-Wright Corporation
Wright Aero Division
Main & Passaic Streets
Woodridge, New Jersey 07075
Attn: Library

General Dynamics Corporation
16501 Brookpark Road
Cleveland, Ohio 44142
Attn: Library

General Electric Company
Mechanical Technology Laboratory
R&D Center
Schenectady, New York 12301
Attn: Library

General Electric Company
Space Division
Cincinnati, Ohio 45215
Attn: Library

General Electric Company
Re-entry & Environmental Sys. Div.
3198 Chestnut Street
Philadelphia, Pennsylvania 19104
Attn: Library

General Motors Corporation
Indianapolis, Indiana 46206
Attn: Library

Hughes Aircraft Corporation
Centinda & Teale Avenue
Culver City, California 90230
Attn: Library

Institute for Defense Analyses
400 Army-Navy Drive
Arlington, Virginia 22202
Attn: Library

Lear Siegler, Inc.
3171 S. Bundy Drive
Santa Monica, California 90406
Attn: Library

Lockheed Missiles & Space Co.
Post Office Box 504
Sunnyvale, California 94088
Attn: Library

McDonnell Douglas Astronautics Co.
5301 Bolsa Avenue
Huntington Beach, California 92647
Attn: Library

McDonnell Douglas Astronautics Co.
3000 Ocean Park Boulevard
Santa Monica, California 90406
Attn: Library

Massachusetts Institute of Technology
Cambridge, Massachusetts 02139
Attn: Library

Mechanical Technology Incorporated
968 Albany-Shaker Road
Latham, New York 12110
Attn: Library

North American Rockwell Corporation
Space Division
12214 Lakewood Boulevard
Downey, California 90241
Attn: Library

FINAL REPORT DISTRIBUTION LIST - NAS 3-10944 - Page 4

Northern Research & Engineering Co.
219 Vassar Street
Cambridge, Massachusetts 02139
Attn: Library

Power Information Center
University of Pennsylvania
3401 Market Street, Room 2107
Philadelphia, Pennsylvania 19104

Solar
Div. of International Harvester
2200 Pacific Highway
San Diego, California 92112
Attn: Library

Space Systems Division
Los Angeles Air Force Station
Los Angeles, California 90045
Attn: Library

Sunstrand Denver
2480 West 70 Avenue
Denver, Colorado 80221
Attn: Library

TRW Systems
One Space Park
Redondo Beach, California 90278
Attn: Library

U.S. Army Engineer R&D Labs
Gas Turbine Test Facility
Fort Belvoir, Virginia 22060
Attn: W. Crim

United Aircraft Corporation
Pratt & Whitney Aircraft Div.
400 Main Street
East Hartford, Connecticut 06108
Attn: Library

United Aircraft Research Lab
East Hartford, Connecticut 06108
Attn: Library

Westinghouse Electric Corporation
Astronuclear Laboratory
Post Office Box 10864
Pittsburgh, Pennsylvania 15236
Attn: Library

Williams Research
Walled Lake, Michigan 48088
Attn: Library

Oak Ridge National Laboratory
Post Office Box Y
Oak Ridge, Tennessee 37830
Attn: Mr. Paul Gnadt

Oak Ridge National Laboratory
Post Office Box Y
Oak Ridge, Tennessee 37830
Attn: Dr. Art Miller

Energy Research Corporation
15 Durant Avenue
Bethel, Connecticut 06801
Attn: Mr. Richard Engdahl